

Dynamical modeling of the network controlling meiotic divisions

Dissertation zur Erlangung
des Doktorgrades der Naturwissenschaften (Dr. rer. nat.)
an der Fakultät für Biologie
der Ludwig-Maximilians-Universität München



Vorgelegt von

Katarzyna Jonak

Geboren am 18.05.1989 in Tychy, Polen

München, 2019

Eidesstattliche Erklärung

Hiermit erkläre ich an Eides statt, dass ich die vorliegende Dissertation selbstständig und ohne unerlaubte Hilfe angefertigt habe. Ich habe weder anderweitig versucht, eine Dissertation einzureichen oder eine Doktorprüfung durchzuführen, noch habe ich diese Dissertation oder Teile derselben einer anderen Prüfungskommission vorgelegt.

München den 01.09.2019

Katarzyna Jonak (Unterschrift)

Erstgutachter: Prof. Dr. Nicolas Gompel
Zweitgutachter: Prof. Dr. Christof Osman

Tag der Einreichung: 10.09.2019
Tag der mündlichen Prüfung: 27.01.2020

Diese Dissertation wurde angefertigt unter der Leitung von Dr. Wolfgang Zachariae in der Arbeitsgruppe Chromosomenbiologie am Max-Planck-Institut für Biochemie in Martinsried, Deutschland.

Abstract

Mitosis and meiosis are both controlled by oscillations in the activities of cyclin-dependent kinase 1 (Cdk1) and the anaphase-promoting complex/cyclosome (APC/C). Nevertheless, these types of cell division differ in fundamental aspects. In mitosis, Cdk1 and APC/C^{Cdc20} form a cyclical system whereby each cycle recreates the starting conditions for the next one. As a result, chromosome duplication during S-phase alternates with chromosome segregation during M-phase. By contrast, meiosis is a linear pathway of precisely two waves of Cdk1 and APC/C^{Cdc20} activity that govern the progression through one S-phase followed by two M-phases and a differentiation program dedicated to the formation of gametes or spores. Despite recent advances in our understanding of meiosis, it is unclear how the mitotic cell cycle engine is modified to regulate the two meiotic divisions. Therefore, we combined mathematical modeling with experimental studies on budding yeast to describe the general mechanism of progression through meiotic divisions with special emphasis on the regulation of the exit from meiosis II. We showed that progression through meiotic divisions is driven by a well conserved Cdk1-APC/C^{Cdc20} oscillator complemented by a set of meiotic regulators in order to perform two, and only two, meiotic divisions. The machinery that terminates the oscillations after completion of meiosis II consists of a meiosis I-specific mechanism that unleashes the irreversible inactivation of M-phase regulators after the second wave of APC/C^{Cdc20} activity, thereby preventing cells from undergoing an additional third division. Here, we describe the roles of the two main APC/C co-activators, Ama1 and Cdc20, in triggering the exit from meiosis and in terminating the oscillations. We show that Ama1 acts as a terminator of the meiotic oscillations, while Cdc20 is important for the proper timing of the exit from meiosis II. We propose that in the absence of Ama1, the properties of the system change, allowing Cdc20 to adopt the function of the terminator precisely after meiosis II. In addition, we evaluate APC/C-independent mechanisms, which might be important for preventing a third meiotic division.

Table of Contents

Eidesstattliche Erklärung.....	iii
Abstract.....	v
1. Introduction.....	1
1.1. General principles of meiosis	1
1.2. Control of cell division by the Cdk1-APC/C oscillator.....	4
1.3. Regulation of the progression through meiosis.....	6
1.4. Regulation of the exit from meiotic divisions	10
1.5. Mathematical modeling as a tool to describe biological systems	13
1.6. Mathematical models of cell cycle	21
1.7. Mathematical models of meiosis.....	24
1.8. Aim of the study	27
1.9. Contributions	28
2. Results	29
2.1. Strategy of the development of the mathematical model	29
2.2. The core of meiotic divisions is based on a Cdk1-APC/C oscillator supplemented with meiotic regulators.....	31
2.3. The properties of Cdk1-APC/C oscillator in meiosis	41
2.4. Role of meiosis II-specific APC/C co-activators in meiotic exit.....	46
2.5. Regulation of meiotic exit by Cdc20.....	57
2.6. Role of phosphatases in termination of meiotic oscillations.....	79
3. Discussion.....	87
3.1. Meiosis consists of two waves of Cdk1-APC/C activity.....	87
3.2. Mathematical modeling allows to study the multi-component network driving meiotic divisions	88
3.3. The Cdk1-APC/C oscillator modulates progression through divisions in meiosis	92
3.4. Exit from meiosis II and termination of meiotic oscillations are driven by APC/C	95
3.5. APC/C-independent mechanisms that regulate meiotic exit.....	99
3.6. Regulation of meiosis II-specific terminator by meiosis I-specific inhibitor	101
3.7. Is the exit from meiosis II irreversible?	102

3.8. On studying processes of meiosis II in high resolution	104
3.9. Concluding remarks	105
4. Materials and Methods	107
4.1. Construction of yeast strains	107
4.2. Induction of meiosis	110
4.3. Meiotic time course experiments	110
4.4. TCA protein extraction and SDS-PAGE analysis	111
4.5. Immunoblot detection of proteins in whole-cell extracts	111
4.6. Indirect immunofluorescence microscopy	112
4.7. Quantification of signal intensity from immunofluorescence staining	113
4.8. Quantification of ECL signals	114
4.9. Mathematical modeling	114
4.10. Statistical analysis	115
Abbreviations	117
References.....	119
Acknowledgments	133
Curriculum Vitae.....	135

1. Introduction

One of the most fundamental aspects of eukaryotic life is the capability of a cell to replicate and divide its genetic material, ensuring the survival and perpetuation of species. For this purpose, cells of sexually reproducing organisms encode molecular machineries that govern chromosome segregation in two types of cell division: mitosis and meiosis. Although the core of the regulation of both types of cell division is based on the same key mechanisms, mitosis and meiosis differ in fundamental aspects. Mitosis is adopted by cells in order to multiply, creating genetically identical daughter cells during one round of DNA replication followed by one round of nuclear division. By contrast, meiosis halves the content of the genetic material, generating haploid gametes, such as eggs and sperms, from a diploid germ cell. This is a result of cells performing one round of DNA replication followed by exactly two nuclear divisions. Failure in the molecular control of the divisions may lead to changes in chromosome content and as a result to conditions such as Down syndrome and infertility (Hassold and Hunt, 2001; Sherman et al., 2007). To ensure the production of healthy and viable gametes, the meiotic machinery has to promote precise and robust regulation of the consecutive divisions. Despite recent advances in studying meiosis, our molecular understanding of this type of cell division still remains incomplete. In this work, I have investigated the regulatory network that controls two meiotic divisions using mathematical modeling in combination with biological experiments. I have studied how budding yeast orchestrates meiotic divisions and what are the essential components contributing to the proper completion of meiosis resulting in formation of four haploid spores.

1.1. General principles of meiosis

Meiosis has to ensure the maintenance of proper ploidy (number of chromosomes) in the daughter cells by promoting a specific set of cell cycle events that differs from mitosis (**Figure 1**). The general principles of both types of cell division are similar: the genetic material has to be duplicated during S-phase and segregated into new nuclei during M-phase. However, unlike during proliferation that alternates between these two phases, meiosis is a linear pathway, which consists of two consecutive nuclear divisions that follow one event of DNA replication (Petronczki et al., 2003). Successful

completion of meiotic divisions is followed by a differentiation program dedicated to generation of gametes or spores encapsulating haploid nuclei. This process is called gametogenesis or sporulation, respectively.

Meiosis evolved as means for rapid evolution, by bringing variation to a genetic pool of sexually reproducing eukaryotes (Kerr et al., 2012). This is a result of combining the genetic material of maternal and paternal cells during recombination. Recombination of homologous chromosomes allows the exchange of genetic material and the establishment of a physical link (chiasma) during the crossing over. During the first meiotic division sister chromatids clamp together providing mono-orientation (Petronczki et al., 2006; Tóth et al., 2000). The mono-orientation is essential to reduce the number of chromosomes and maintain ploidy. It is a unique feature of the first meiotic division absent from mitosis, which is characterized by bi-orientation. In budding yeast, mono-orientation during meiosis I is mediated by a protein complex, called monopolin, that clamps the sister kinetochores together (Tóth et al., 2000). Properly attached homologous chromosomes can be resolved during meiosis I by destruction of the molecules that are holding them together (Buonomo et al., 2000). These molecules, called cohesins, create a complex that entraps sister chromatids by forming a ring around them (Gruber et al., 2003; Klein et al., 1999). The complex consists of three subunits, called Smc1, Smc3 and an α -klesin subunit: Scc1 in mitosis or Rec8 in meiosis. During mitosis, cohesin is cleaved entirely at the onset of anaphase, resulting in segregation of chromosomes to opposite poles (Uhlmann et al., 1999). However, in meiosis, cohesin is removed in a stepwise manner. During meiosis I only the fraction of Rec8 molecules along chromosome arms (arm Rec8) is cleaved, culminating in the segregation of homologous chromosomes. The fraction of Rec8 residing at the centromeres (centromeric Rec8) that holds the sister chromatids together is protected from cleavage by a complex molecular machinery (Kiburz et al., 2005; Nasmyth and Haering, 2005). Following segregation of homologous chromosomes, cells enter the second meiotic division. Unlike in meiosis I, sister kinetochores attach to microtubules from the opposite spindle poles ensuring bi-orientation of chromatids. The protection machinery of the centromeric Rec8 is removed, allowing cleavage of the remaining pool of cohesin and segregation of sister chromatids. These events ensure formation of haploid daughter cells.

1.2. Control of cell division by the Cdk1-APC/C oscillator

Chromosome segregation is controlled by two main regulators: a serine/threonine cyclin-dependent kinase (Cdk) and an E3 ubiquitin ligase anaphase-promoting complex/cyclosome (APC/C) (Nasmyth, 1996; Nigg, 2001; Zachariae and Nasmyth, 1999). They provide a mechanism that ensures the progression through different stages of both mitosis and meiosis (**Figure 2**). Budding yeast encodes a single Cdk that drives the cell cycle, Cdk1/Cdc28, which exhibits constant levels though the cell division (Mendenhall and Hodge, 1998). Its activity depends on its regulatory subunits, cyclins, which are synthesized at specific stages of cell division. In budding yeast, G1 cyclins, Cln1-Cln3, are required for the transition to S-phase. B-type cyclins, Clb1-Clb6, drive the progression through later stages of cell division (Bloom and Cross, 2007; Murray, 2004). Four of the B-type cyclins, Clb1-Clb4, are involved in the spindle assembly and chromosome segregation during M-phase. Changes in Cdk1 activity levels depend not only on the synthesis of cyclins, but also on their degradation, which is essential to establish the cell cycle oscillator. Levels of cyclins increase during metaphase and decrease during anaphase, as they are targeted for proteolysis to the 26S proteasome by addition of ubiquitin chains by the APC/C (Irniger, 1995; Sudakin, 1995).

The activity of APC/C rises during anaphase, allowing cells to enter a low Cdk1 state and divide the nuclei. APC/C activity depends on its co-activators, namely Cdc20, Cdh1, and Ama1 (Pesin and Orr-Weaver, 2008). They dictate the substrate specificity at a defined time of cell division. Cdh1 plays a crucial role during the exit from mitosis, maintaining cells in the subsequent G1-phase (Yeong et al., 2000). In meiosis it has been shown that Cdh1 activity is restricted to pre-meiotic G1-phase (Oelschlaegel et al., 2005). On the other hand, Ama1 is present only during meiosis. It is required for inhibition of M-phase proteins at prophase I (Okaz et al., 2012). Cdc20 is present in both mitosis and meiosis and it triggers the two main M-phase events. Firstly, it targets cyclins for degradation, resulting in inactivation of Cdk1 and spindle disassembly. Secondly, it provokes cohesin cleavage by a caspase-like cysteine protease, called separase/Esp1 (Uhlmann et al., 1999). Esp1 activity is inhibited during metaphase through the complex formation with securin/Pds1 (Buonomo et al., 2003; Ciosk et al., 1998), which is targeted for degradation by APC/C^{Cdc20} (Cohen-Fix et al., 1996). As a result, Esp1 is freed from the inhibitory complex with Pds1. This event allows the cleavage of cohesin and segregation of chromosomes.

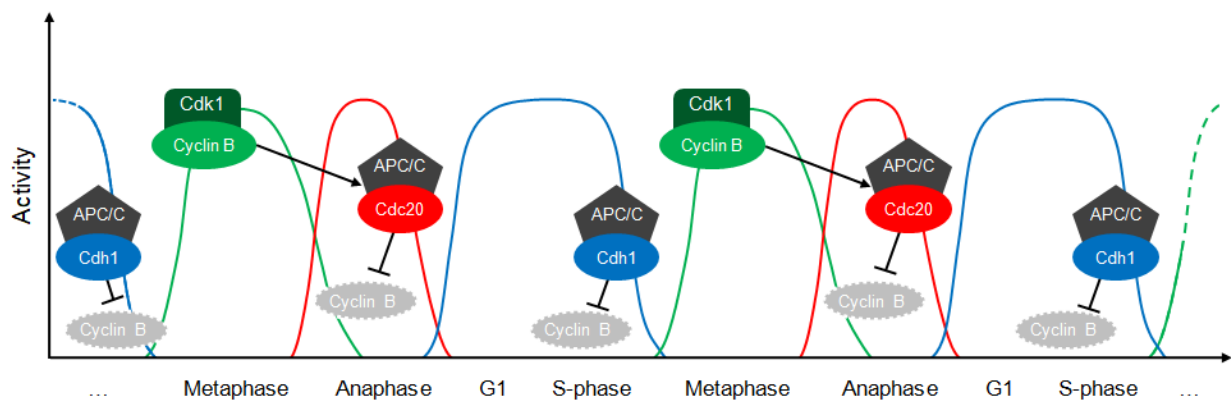
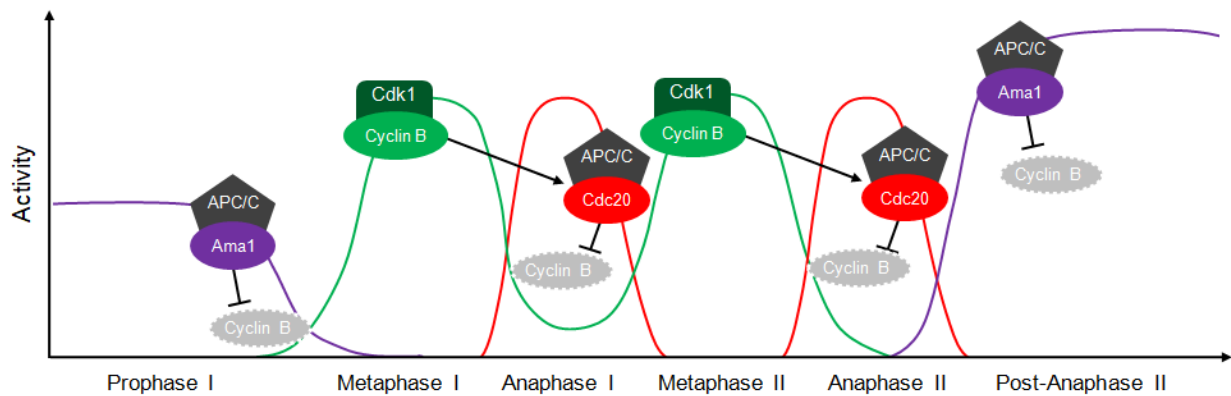
A Mitotic cell cycle**B Meiotic linear pathway**

Figure 2. Cdk1 and APC/C drive progression through mitosis and meiosis. (A) In mitosis, B-type cyclins activate Cdk1 that phosphorylates the APC/C core, allowing binding of Cdc20. APC/C^{Cdc20} targets cyclins for degradation at anaphase, inhibiting Cdk1 and activating APC/C^{Cdh1}. APC/C^{Cdh1} triggers the exit from the M-phase and the entry into the next cycle. **(B)** During prophase I of meiosis, APC/C^{Ama1} prevents accumulation of M-phase cyclins until completion of recombination. At metaphase I, highly synthesized cyclins activate Cdk1 that inhibits activities of APC/C^{Ama1} and APC/C^{Cdh1}. On the other hand, Cdk1 activates APC/C^{Cdc20}, which triggers degradation of cyclins and entry into anaphase I. Unlike in mitosis, in meiosis cells inactivate APC/C^{Cdc20} and re-accumulate cyclins for the second division without an intervening S-phase. At the onset of anaphase II cells activate APC/C^{Cdc20} that triggers degradation of cyclins and APC/C^{Ama1} that triggers degradation of other M-phase regulators.

Cdk1 has different roles in regulating the APC/C activity. It inhibits APC/C^{Cdh1} by phosphorylating the Cdh1 protein, preventing its binding to the APC/C core (Zachariae et al., 1998; Jaspersen et al., 1999). Similarly, it has been shown that Cdk1-Clb1 inhibits the activity of APC/C^{Ama1} in meiosis (Okaz et al., 2012). Thus, both co-activators are able to activate APC/C only during the stage of low Cdk1 activity. On the other hand, Cdk1-Clb phosphorylates the APC/C core, allowing binding of Cdc20 (Kramer et al., 2000; Rudner and Murray, 2000). The consequence is formation of an oscillatory mechanism that drives the events of the cell cycle. In mitosis, APC/C^{Cdc20} is activated

only once, triggering cleavage of cohesin in a single step. The single wave of Cdk1-Clbs and APC/C^{Cdc20} activities is recreated in the next cycle of a new cell (Kapuy et al., 2009; Novák et al., 2010). As mitotic cells exit M-phase, they maintain low Cdk1 activity by the activation of APC/C^{Cdh1} and assembly of inhibitory complex with an stoichiometric inhibitor of Cdk1, namely Sic1 (Schwob et al., 1994). This mitotic oscillatory engine of Cdk1-APC/C is modified to generate a two-division meiosis. Unlike in mitosis, in meiosis APC/C^{Cdc20} is activated precisely twice after DNA replication, generating a system of two consecutive divisions that allows stepwise elimination of cohesin. Only after the second division, cells maintain low activity of Cdk1. It has been proposed that the meiosis-specific APC/C co-activator, Ama1, is involved in this process, similar to Cdh1 in mitosis (Okaz et al., 2012).

1.3. Regulation of the progression through meiosis

The Cdk1-APC/C^{Cdc20} oscillator is complemented by a large number of proteins, forming a complex regulatory network regulating cell division. This network directs the production of healthy daughter cells with remarkable robustness and precision. It ensures that all events happen in the right order and time, preventing errors that may cause unsuccessful completion of meiosis (Hartwell and Weinert, 1989; Musacchio, 2015; Novák et al., 2010; Shonn et al., 2000).

1.3.1. Commitment to meiosis and pre-meiotic S-phase

In higher eukaryotes, meiosis is provoked by a hormonal signal that directs germ cells to perform meiotic divisions (Bowles and Koopman, 2010). In budding yeast, *Saccharomyces cerevisiae*, entry into meiosis is initiated in diploid cells in response to poor nutrient conditions during G1-phase (Roeder, 1995). Under these conditions, budding yeast produce a meiosis-specific transcription factor, Ime1, which ensures the synthesis of several early-meiotic genes (Mitchell et al., 1990). One of these proteins is a serine/threonine protein kinase, named Ime2. It is required for pre-meiotic S-phase and serves as a substitute of mitotic Cdk1-Cln2 in promoting DNA replication (Smith and Mitchell, 1989; Szwarcwort-Cohen et al., 2009) along with Dbf4-dependent Cdc7 kinase and Cdk1-Clb5/6 (Benjamin et al., 2003; Dirick et al., 1998; Sclafani, 2000). At this time, the maternal and paternal chromosomes are duplicated, Rec8 is synthesized and cohesin is loaded onto the chromosomes, binding sister chromatids together (Nasmyth and Haering, 2009).

1.3.2. Prophase I and DNA recombination

As cells finish DNA replication, they enter low Cdk1 state and start the process of recombination after the deliberate introduction of DNA double-strand breaks (DSBs) in the homologous chromosomes (Klapholz et al., 1985). The DSBs are being sensed by the DNA damage response machinery that provokes the activation of the Dmc1 recombinase and, as a result, formation of the synaptonemal complex (SC) (Busygina et al., 2013). The SC is a railway-like structure that binds chromosomes together and helps maintaining the pairing during the DNA repair (Page and Hawley, 2004). Until after DNA breaks are repaired, cells are prevented from further progression through meiosis by the activity of the meiotic recombination checkpoint (RC) that senses the unrepaired DNA on the chromosomes (Malone et al., 2004). The main target of the RC is the meiosis-specific transcription factor Ndt80 (Tung et al., 2000). It regulates the synthesis of more than 200 meiotic genes, among them M-phase cyclins: Clb1, Clb3, and Clb4 (**Figure 3**) (Chu and Herskowitz, 1998). Synthesis of Ndt80 is prevented by its transcriptional repressor Sum1, which is active during prophase I (Lindgren et al., 2000). It has been proposed that this repression depends on the activity of the RC (Corbi et al., 2014; Pak and Segall, 2002). However, the exact regulation of Ndt80 by the RC remains unclear.

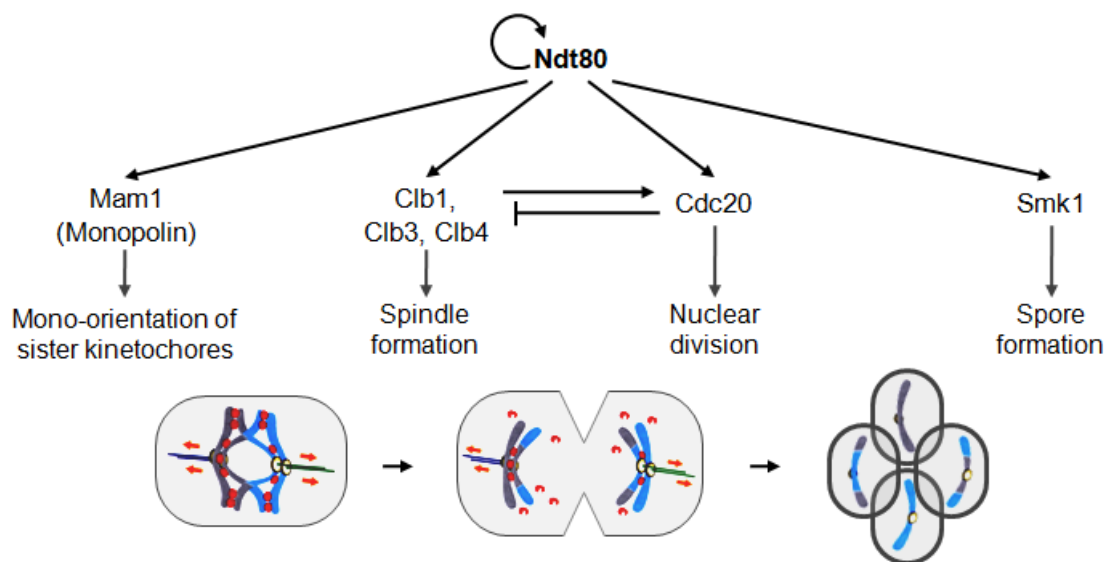


Figure 3. Regulation of progression through meiosis by Ndt80-dependent synthesis. Ndt80 is activated after silencing of the recombination checkpoint. By an auto-regulatory positive feedback loop, it amplifies its own synthesis and triggers progression to the first division. Ndt80 coordinates meiotic progression through regulation of the synthesis of more than 200 meiotic genes, among others Mam1 (monopolin), M-phase cyclins, Cdc20 and Smk1 (MAPK kinase). Arrows in the graph indicate activation of a protein or a process, while bar-headed lines indicate inactivation of a protein. Modified from (Winter, 2012).

The repression of Ndt80 synthesis prevents premature activation of Cdk1 by M-phase cyclins and formation of meiotic bipolar spindle. Cdk1 activity is further suppressed by the protein kinase Swe1 (Leu and Roeder, 1999). It has been reported that the deletion of this kinase in meiosis has little effect on the checkpoint arrest (Pak and Segall, 2002). A more pronounced effect is observed by eliminating Ama1 (Okaz et al., 2012). In the absence of Ama1, cells enter the first meiotic division before the completion of DNA repair. The consequences of the premature exit from prophase I are recombination defects and chromosome missegregation. It has been shown that APC/C^{Ama1} controls the prolonged prophase I by targeting for degradation the key M-phase regulators, such as cyclins and polo-like kinase Cdc5 (Okaz et al., 2012).

1.3.3. Progression through two meiotic divisions

The transition from prophase I to metaphase I is marked by three main events: the destruction of the SC, the silencing of the RC and the rapid accumulation of M-phase cyclins resulting in the formation of a bipolar metaphase I spindle (Okaz et al., 2012). The silencing of the RC leads to the suppression of Sum1 and elevation of Ndt80 levels due to auto-regulation of its transcription (Chu et al., 1998). The activity of Ndt80 depends on M-phase kinases, Cdk1 and Ime2, which inhibit the activity of Sum1 through its phosphorylation (Ahmed et al., 2009; Shin et al., 2010). Moreover, it has been proposed that Ime2, and possibly Cdc5, promote activation of Ndt80 through its direct phosphorylation (Acosta et al., 2011; Schindler and Winter, 2006; Sopko et al., 2002). Upon entry into metaphase I with high activity of Cdk1, Ndt80 becomes active and APC/C^{Ama1} becomes inactive due to the inhibitory phosphorylation of Ama1 protein (Okaz et al., 2012). This mutual inhibition between APC/C^{Ama1} and Cdk1-Clb1 ensures the irreversibility of the transition (Okaz et al., 2012).

During metaphase I, only two B-type cyclins are transcribed: Clb1 and Clb4. Clb3 accumulates only during the time of meiosis II. The importance of limiting the activity of Clb3 to meiosis II is not yet understood (Berchowitz, 2013; Carlile and Amon, 2008). Active Cdk1-Clb1/4 promotes the formation of the metaphase I spindle required for the segregation of homologous chromosomes. Sister kinetochores mono-orient due to the activity of the monopolin complex, which is restricted to the first division. The meiosis I-specificity of monopolin complex has been found to be regulated by a protein produced exclusively during the first division, namely Spo13 (Katis et al., 2004; Lee et al., 2004). Spo13 promotes monopolin function by recruiting it to kinetochores and enhancing its activity through Cdc5-dependent phosphorylation.

The proper attachment of homologous kinetochores to microtubules is sensed by a machinery called the spindle assembly checkpoint (SAC). The SAC restrains the activity of APC/C^{Cdc20} during metaphase, thereby inhibiting the cleavage of cohesin (Hwang et al., 1998; Musacchio and Salmon, 2007). The activity of the SAC depends on the proteins that are conserved among all eukaryotes, such as Mad2, Bub3 and Mps1 (Hoyt et al., 1991; Li and Murray, 1991). The Mad2-Cdc20 complex interacts with Bub3 and forms an inhibitory complex of APC/C^{Cdc20}, named the mitotic checkpoint complex (MCC) (Sudakin et al., 2001). It has been reported that the loss of the SAC activity in meiosis I shortens the duration of metaphase I and accelerates anaphase I onset in vertebrates oocytes (Homer et al., 2005). This leads to an increase of aneuploid gametes caused by unstable connections of homologs with microtubules and consequent missegregation. Once all chromosomes are properly attached, the SAC is silenced and the inhibition of APC/C^{Cdc20} is relieved, leading to degradation of cyclins and securin/Pds1. It has been proposed that cyclins are not completely degraded and therefore some basal activity of Cdk remains to prevent additional DNA replication between the two divisions (Dahmann et al., 1995; Phizicky et al., 2018; Strich et al., 2004). Degradation of Pds1 results in activation of separase/Esp1 and cleavage of cohesin. Only the phosphorylated fraction of Rec8 may be cleaved. In budding yeast, this phosphorylation is ensured by the activities of two kinases: Cdc7-Dbf4 and the casein kinase 1 δ , Hrr25 (Katis et al., 2010). While Rec8 molecules distributed along the chromosome arms are susceptible to phosphorylation, the centromeric fraction of Rec8 remains unphosphorylated and protected from cleavage. The protection mechanism involves a protein called shugoshin/Sgo1, which recruits to the centromeres a protein phosphatase 2A regulated by a subunit Rts1 (PP2A^{Rts1}) (Riedel et al., 2006). PP2A^{Rts1} counterbalances the phosphorylation, thus protecting the centromeric pool of Rec8 from Esp1-mediated destruction (Riedel et al., 2006). Centromeric Rec8 remains to hold the sister chromatids together until the onset anaphase II.

Following the cleavage of arm Rec8 and the first nuclear division, cells enter a second round of high Cdk1 activity. During meiosis II, cyclins re-accumulate and reactivate Cdk1, allowing the assembly of bipolar metaphase II spindles. The sister chromatids attach to microtubules emerging from opposite poles of the spindle, in so-called bi-oriented fashion. The SAC senses unattached kinetochores and inhibits the activity of APC/C^{Cdc20} until after all chromosomes are properly oriented on the metaphase II spindles. APC/C^{Cdc20} is activated for the second time triggering degradation of B-type cyclins and activation of Esp1. As PP2A^{Rts1} is removed from the centromeres,

centromeric pool of Rec8 is phosphorylated and cleaved. At the onset of anaphase II, Cdk1 is inactivated due to complete degradation of cyclins, which leads to activation of APC/C^{Ama1} and degradation of other meiotic regulators. With the destruction of cyclins and Cdc5, elongated anaphase II spindles disassemble. Cells exit the second division and enter a developmental pathway of differentiation that involves a set of proteins required for spore formation (Argüello-Miranda et al., 2017).

1.4. Regulation of the exit from meiotic divisions

During the exit from a cell division, APC/C activity raises, leading to a decrease in Cdk1 activity and entry into a low Cdk1/kinase state. On the protein regulatory level, the exit from a cell division can be defined as a decline in the concentrations of nuclear M-phase cyclins and Pds1 followed by cleavage of Rec8. On the level of chromosome organization, it leads to chromosome segregation into separate nuclei and disassembly of spindles. These two levels of regulation are coupled with each other during both mitosis and meiosis, allowing for robust control of progression through the exit from a cell division (Zachariae and Nasmyth, 1999). During the exit from mitosis and meiosis II, cells prepare for the next event characterized by a low activity of Cdk1: re-entry into the G1-phase of the next cycle and differentiation program, respectively. By contrast, at the exit from meiosis I, cells do not cleave all of cohesin and do not completely inactivate Cdk1. They prepare for re-accumulation of cyclins and entry into the second meiotic division.

1.4.1. Preventing complete inactivation of Cdk1 at the exit from meiosis I

Preventing DNA re-replication and enabling the re-accumulation of cyclins is a unique characteristic of the exit from meiosis I. Studies in fission yeast and budding yeast have shown that significant portion of cyclin B remains in the nuclei during anaphase I (Izawa et al., 2005; Strich et al., 2004). Reduced, but not completely abolished activity of Cdk in *Xenopus* oocytes is required for preventing DNA replication after meiosis I and for timely transition to meiosis II (Gerhart et al., 1984; Iwabuchi et al., 2000). It has been proposed that destruction of cyclin B between meiosis I and -II is antagonized by different factors. Firstly, the APC/C^{Cdc20}-dependent degradation of cyclin B is reduced during anaphase I (Gross et al., 2000). Secondly, the synthesis of cyclins increases between meiosis I and -II, thus counterbalancing the APC/C-dependent degradation (Hochegger et al., 2001). In budding yeast, during the transition from meiosis I to meiosis II, the activity of Ndt80 is maintained until the exit from meiosis II (Argüello-

Miranda et al., 2017). Lastly, Cdk1 activity may not be completely abolished due to down-regulation of its inhibitors, such as Sic1 and Cdh1 (Holt et al., 2007). Inhibitors of Cdk1 are inactivated by Cdk1-dependent phosphorylation. This phosphorylation is reversed by the activity of phosphatases, such as Cdc14. It has been speculated that during the exit from meiosis I, the ability of Cdc14 to remove Cdk1-phosphorylation may be reduced due to the activity of Cdc5 and Ime2 (Holt et al., 2007).

1.4.2. Regulation of the APC/C activity at the exit from meiosis II

Two strategies to regulate the exit from meiosis I and meiosis II by the APC/C have been suggested (Irniger, 2006; Tyson and Novak, 2008). The first one assumes that APC/C^{Cdc20} activity is partially inhibited during anaphase I, thus preventing complete degradation of cyclins and other regulators. In fission yeast, the APC/C^{Cdc20} activity is inhibited at anaphase I by the meiosis I-specific inhibitor, called Mes1 (Izawa et al., 2005; Kimata et al., 2011). Mes1 binds to the same domain of Cdc20, called Slp1 in fission yeast, as the M-phase cyclin Cdc13 in a competitive manner, thus inhibiting the activity of the ligase. In budding yeast, no inhibitor of a similar activity has been found to date. In vertebrates oocytes, hyperactive APC/C^{Cdc20} is used to trigger the exit from meiosis II. Cells arrest in metaphase II (cytostatic factor arrest) by inhibiting APC/C^{Cdc20} activity with Emi2 to prevent the entry into developmental process without fertilization (Irniger, 2006; Schindler and Schultz, 2009). Upon fertilization Ca²⁺ signal is introduced that activates APC/C^{Cdc20} and triggers the completion of meiosis.

The second strategy of regulating the exit by the APC/C activity implies the existence of an additional meiosis II-specific co-activator that carries out the exit from meiosis II. In fission yeast, meiosis is completed by the activation of a meiosis-specific Cdh1 paralogue, Mfr1/Fzr1 (Kimata et al., 2011). In *Drosophila*, the exit from meiosis is executed by meiosis-specific APC/C activators: Fzr2 during spermatogenesis and Cortex during oogenesis (Chu et al., 2001; Jacobs et al., 2002). Likewise, budding yeast express a meiosis-specific APC/C co-activator, Ama1, that is up-regulated during the exit from meiosis II, implying a similar role to fission yeast Mfr1/Fzr1 (Cooper et al., 2000; Diamond et al., 2009). Regulation of APC/C^{Ama1} in meiosis II is not well understood. Ama1 shows a similar transcriptional and translational pattern as the meiosis II-specific protein Clb3 (Berchowitz et al., 2013; Brar et al., 2012). Clb3 translation is coordinated by the activity of Ime2 kinase, which inhibits the repressor of Clb3 translation, a meiosis-specific RNA-binding protein called Rim4 (Berchowitz et al., 2013). Whether a similar machinery is required for the meiosis II-specific up-regulation and activation of Ama1 is unknown.

1.4.3. Regulation of meiotic divisions by phosphatases

Progression through two meiotic divisions is strictly coordinated by the kinases and counteracting phosphatases that regulate activities of the substrates of the cell cycle kinases. Among the key phosphatases that direct the cell division in both mitosis and meiosis in budding yeast are Cdc14, protein phosphatase 2A (PP2A) and protein phosphatase 1 (PP1). Cdc14 is required for reduplication of spindle pole bodies (SPBs) and spindle disassembly (Buonomo et al., 2003; Jaspersen and Morgan, 2000). While Cdc14 is highly conserved among eukaryotes, its exact role during meiosis is unclear (Mocciaro and Schiebel, 2010). In budding yeast, Cdc14 is sequestered in the nucleolus during most of the cell cycle and meiosis. It is activated upon release through the Cdc14 early anaphase release (FEAR) pathway and mitotic exit network (MEN) to counteract Cdk1 substrates (Stegmeier and Amon, 2004; Sullivan and Morgan, 2007). In meiosis, the FEAR pathway is required to activate Cdc14 during anaphases of meiosis I and -II (Marston et al., 2003). Inhibition of Cdc14 activity leads to the inability to reduplicate SPBs and thus to form meiosis II spindles (Buonomo et al., 2003). Despite the importance of Cdc14 activity at the exit from meiosis I, the inactivation of the phosphatase in meiosis II does not affect the disassembly of anaphase II spindles and the exit from meiosis II (Argüello-Miranda et al., 2017).

Other phosphatases may be involved in regulation of the meiotic divisions and the exit from meiosis II. PP1 is a highly conserved serine/threonine phosphatase involved in several events during cell cycle and meiosis. In budding yeast, PP1 regulates the activity of the SAC (Sassoon et al., 1999) and progression through early meiosis (Bailis and Roeder, 2000; Sarkar et al., 2014). Moreover, while regulated by a meiosis-specific subunit Gip1, it appears to be required for spore wall formation and its nuclear import (Tachikawa et al., 2001). PP2A is another conserved serine/threonine phosphatase that consists of a catalytic subunit (Pph21/Pph22), a scaffold subunit (Tpd3) and a regulatory subunit (Cdc55 or Rts1) that directs the substrate specificity (Sneddon et al., 1990; Healy et al., 1991; Shu et al., 1997). PP2A^{Cdc55} has been shown to counterbalance Cdk1 and Ime2-dependent phosphorylations during meiosis (Holt et al., 2007). It coordinates spindle assembly and chromosome segregation (Bizzari and Marston, 2011; Kerr et al., 2016). It regulates the entry and the exit from mitosis (Queralt et al., 2006; Sarkar et al., 2014). Moreover, it has been shown that PP2A^{Cdc55} dephosphorylates the APC/C subunits, Cdc16 and Cdc27, thus preventing Cdc20 from binding to the APC/C core (Rossio et al., 2013). In vertebrates oocytes, PP2A^{B55} (PP2A^{Cdc55} in yeast) is required for timely entry into meiosis II (Adhikari et al., 2014), targeting for dephosphorylation Cdk1 and Cdc5 sites (Cundell et al., 2013).

1.5. Mathematical modeling as a tool to describe biological systems

Protein networks that regulate biological processes, such as meiosis, usually consist of multiple molecules interacting with each other in a complex manner. The complexity of the biological system is also a consequence of nonlinear characteristics of the response to stimuli, meaning that the amount of the reaction product is not proportional to the amount of the starting material (Fischer, 2008). Thus, analysis of such processes often requires a simplification by mathematical description, achieved by using an approach called mathematical modeling. Mathematical modeling allows to capture the main properties of the studied system and to understand how the system responds to the stimuli, perturbations and changes in the regulatory network (Fischer, 2008; Sible and Tyson, 2007). It is often used to generate testable hypotheses and allows the integration of data coming from different levels of biological description. Mathematical modeling allows formalizing the relations between the most essential elements of the studied system and formulating novel conceptual questions (Fischer, 2008; Kohl et al., 2010).

1.5.1. Development of mathematical models of dynamical biological processes

A dynamical biological system is a system of interacting components that undergoes changes in time. In mathematical modeling language such components are called variables. The change may refer to the modification in molecular concentration of a protein within a cell. The goal of mathematical modeling is to describe, analyze, and predict the behavior of the individual variables and the emergent properties of the studied system (Tyson et al., 2001). To build a mathematical model of biological system, a knowledge from biological experiments is required to define the basic regulation of the system and the key components of the regulatory network. After defining the basic players, a wiring diagram of interactions between system components is constructed. Such diagram is a graphical representation of the connections between all key variables. Mathematical models present these interactions based on the wiring diagram with mathematical equations that define the rules of the time-dependent changes using the laws of biochemical reaction kinetics. The interactions are described with parameters, which are constants used to specify the reaction speed (rate constants). Mathematical functions contain collection of parameters defining biophysical or biochemical interactions between molecules. Importantly, mathematical model describing the same interactions with the same set of equations may result in different solutions depending on the values of the parameters used to define the interactions. Therefore, a crucial step during development of a model is estimation of the parameters. This step requires

running the computational simulation, which solves the mathematical equations and present the result of the model in form of a change of the variable over time. The values of the parameters can be adjusted by comparing the numerical solution to experimental data and biological phenotypes. The model can be readjusted by changing the basic assumptions and components of the network depicted by the wiring diagram, as well as by changing the form of equations or the parameter values. The adjusted model can be used to test hypotheses and to make predictions regarding the phenotype of biological mutants. **Figure 4** presents simplified process scheme of development of a typical mathematical model.

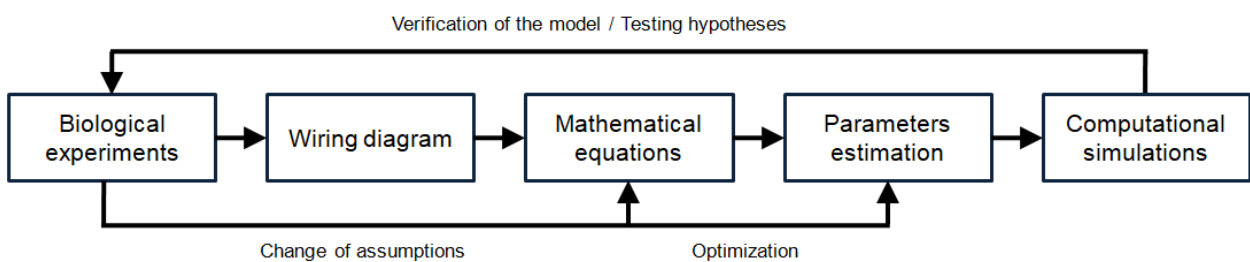


Figure 4. Process scheme of developing a mathematical model of biological system. Knowledge from biological observations is necessary for the description of key regulators of the studied process. Based on a wiring diagram depicting the relevant interactions between the components of the system (network) mathematical equations are constructed. After estimation of parameter values, the simulation is run to solve the equations. The solutions are verified by biological experiments.

1.5.2. Mathematical description of the protein dynamics

There are two main approaches to describe a dynamical system (Alon, 2006; Sauro, 2018). The first one is called a deterministic approach, in which the variable value defines its exact state at the next time point. The second one is called a stochastic approach, in which the variable value defines the probability of a particular state at the next time point. Deterministic modeling is used to study the behavior of a cell without considering biological perturbations, such as gene expression level. Often it is assumed that a large number of studied molecules does not affect the probability of a particular interaction and response of the system. If the system consists of a small number of random effects that become relevant to the outcome, the individual reactions are calculated with the stochastic approach. Systems with a high number of molecules that exhibit stochastic effects are often well approximated by deterministic models that describe the average behavior within the cell (Sauro, 2018). The deterministic approach is widely used in the studies of cell cycle in various organisms, from prokaryotes and unicellular eukaryotes, to vertebrates (Sible and Tyson, 2007).

The biochemical reactions described in a deterministic manner are often based on a mathematical representation in the form of ordinary differential equations (ODEs) (Sauro, 2018; Tyson et al., 2001). With defined ODEs and initial values of the variables (at time point zero), the future behavior of the biological system can be characterized. A set of ODEs is solved numerically during the process called computer simulation and is often referred to as *in silico* experimentation.

The change of the studied biological variable over time due to interactions with other variables is usually described using five general types of biological processes (Alon, 2006; Szallasi et al., 2006):

$$\frac{dx_i}{dt} = \text{synthesis} - \text{degradation} \pm \text{chemical modification} \pm \text{complex formation} \pm \text{transport} \quad (1)$$

In **Equation 1**, x_i describes a subsequent time-dependent variable presented in the form of differential equation $\frac{d}{dt}$. The value of the variable at a given time t forms the state of the system at this particular time. Different terms describing the model component refer to the active or inactive states of the variable presented with a positive or negative sign. A positive sign indicates a reaction resulting in gain of the product. A negative sign describes a reaction resulting in loss of the product. The positive term *synthesis* defines the formation of the molecule in the form of transcription/translation, while the negative term *degradation* describes its destruction. Other processes can be described as having both positive or negative effects. The *chemical modification* indicates activation or inactivation processes, such as phosphorylation of a protein. The term *complex formation* refers to the assembly or disassembly of a molecular complex. The term *transport* defines the import and export of the molecule within the cell, such as transport between the nucleus and cytoplasm. When the positive and negative reactions are balanced, the variable does not change over time. In the protein regulatory networks, the variables describing the components of the network are coupled with each other, forming a set of multiple ODEs.

1.5.3. Approximation of biochemical interactions between molecules

A mathematical model has to be as close to reality as possible in the description of the biological system, but also as simple as possible for the computational analysis (Tyson et al., 2003; Sible and Tyson, 2007). For simplification, biochemical reactions are approximated by mathematical equations that are based on known biochemical laws (Alon, 2006; Szallasi et al., 2006). Approximation of the biochemical reaction is used in

ODEs models with an assumption of homogenous environment of the studied system. The commonly used biochemical law is the law of mass action, stating that the rate of a chemical reaction is proportional to the product of the concentrations of the reagents, such as constant synthesis of a protein:

$$\frac{d[X]}{dt} = k_s \quad (2)$$

In **Equation 2**, X is the concentration of the protein produced at a constant rate k_s . The concentration depends only on the initial value of the protein. The more complex reactions describe the processes affected by the components of the system, such as the 1st order reaction, as in the example of protein degradation:

$$\frac{d[X]}{dt} = -k_d[X] \quad (3)$$

In **Equation 3**, k_d is a constant rate of degradation of the protein. The concentration depends on the protein itself and changes linearly. More complex kinetics is described with the 2nd order reactions, in which the activity of the protein depends on at least one additional component. An example is formation of a protein complex:

$$\frac{d[XY]}{dt} = k_{as}[X][Y] = k_{as}(X_T - [XY])(Y_T - [XY]) \quad (4)$$

Proteins X and Y form a heterodimer XY . The formation of the complex proceeds with a constant rate of the assembly k_{as} . The total concentrations of the proteins used in the reaction are indicated by X_T and Y_T .

Many reactions described in the mathematical models have high activation energy and do not occur spontaneously, for example enzymatic reactions (Sauro, 2018). They are described with Michaelis-Menten kinetics. The enzyme E binds to the substrate S and let the substrate turn into a product P :

$$\frac{d[P]}{dt} = \frac{v_{max}[S]}{K_m + [S]} \quad (5)$$

In **Equation 5**, v_{max} is a maximal speed of the reaction and K_m is a Michaelis-Menten constant. When the change in the substrate concentration is slow, Hill kinetics is often used as an approximation (Gonze and Abou-Jaoudé, 2013). It describes biochemical processes, in which the binding of the ligand to the molecule is higher or lower in the presence of other ligands:

$$\frac{d[P]}{dt} = \frac{v_{max}[S]^n}{K_m^n + [S]^n} \quad (6)$$

In **Equation 6**, K_m describes a Hill constant and n is a Hill coefficient that determines the steepness of the response. If $n > 1$, the binding of the ligand to the protein increases in the presence of other ligands. If $n < 1$, this binding decreases. If $n = 1$, the binding does not affect the steepness of the response. A specific type of enzymatic reaction is a competitive inhibition, during which the ligand prevents the occurrence of the reaction (Schäuble et al., 2013). An inhibitor I binds to the active site of an enzyme and compete with a substrate S with the dissociation constant K_I :

$$\frac{d[P]}{dt} = \frac{v_{max}[S]}{[S] + K_m(1 + \frac{[I]}{K_I})} \quad (7)$$

When biological system consists of two states derived by the actions of two different enzymes with opposing effects, a modified form of Michaelis-Menten kinetics is used, called Goldbeter-Koschland kinetics (Goldbeter and Koschland, 1981):

$$\frac{d[X_p]}{dt} = -\frac{d[X_d]}{dt} = k_{ph} \frac{X_T - [X_p]}{K_{mph} + X_T - [X_p]} - k_{deph} \frac{[X_p]}{K_{mdph} + [X_p]} \quad (8)$$

For the variable X_p that describes the phosphorylated form of a protein, the opposite X_d characterizes the dephosphorylated form of the same protein. Parameters k_{ph} and k_{deph} define maximal speed of the phosphorylation and dephosphorylation reactions, respectively. K_{mph} and K_{mdph} are the Michaelis-Menten constants of the reactions.

1.5.4. Common patterns of interactions between proteins

Biological dynamical systems show a wide range of responses resulting from interactions between the molecules. Often the interactions generate a particular behavior of the components of the network and the whole system. Examples are switches and oscillations of proteins regulating transitions between various stages of the cell cycle (Ingolia and Murray, 2004; Tyson and Novak, 2008). Regulatory control of biological system is based on the patterns of interactions, called motifs. The common motifs in biology are feed forward and feedback loops (**Figure 5**). Feed forward loops are used to transmit the signal in a cascade from the input stimuli. They are responsible for noise rejection and nonlinear amplification of the signal (Sauro, 2018). Feed forward loop with positively interacting components consisting of at least two different

pathways is called coherent. It can rapidly shut down when the starting protein that transmit the signal is inactivated. When a component X has different roles in regulating the output of the system, the incoherent feed forward loop is involved.

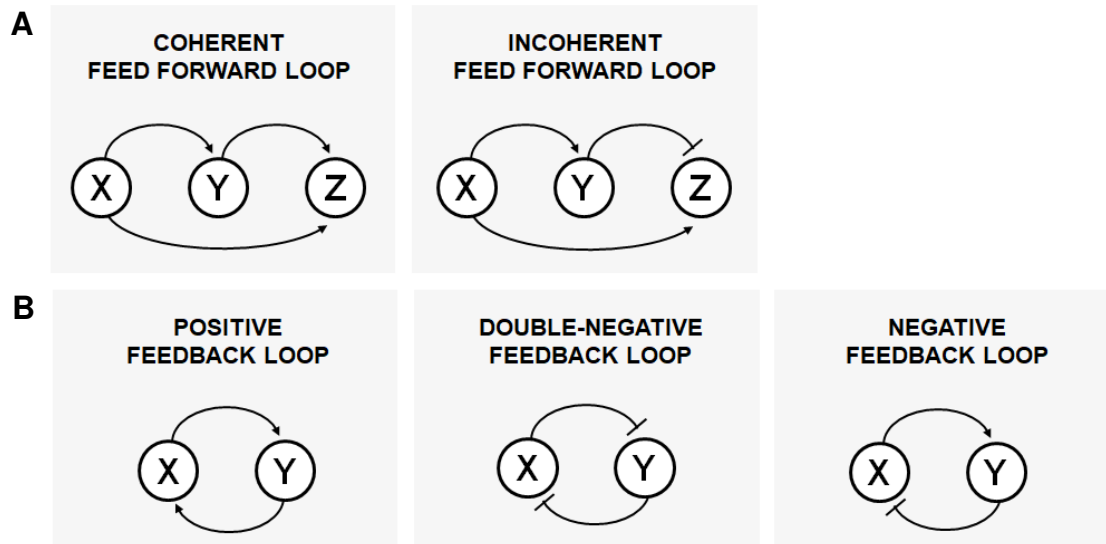


Figure 5. Schemes of common motifs. Each panel presents general description of the feed forward (**A**) or the feedback (**B**) loop with interactions between components of the studied system named X , Y and Z . Positive interactions are presented with arrow-headed lines, while negative with bar-headed lines.

Feedback loops base the response of the system on how it affects itself. Cellular regulatory networks commonly contain multiple feedback loops allowing the existence of many back-up mechanisms (Ferrell et al., 2009). A positive feedback loop occurs when the product of a reaction leads to the increase in that reaction due to mutual activation of the system components. An example is a meiotic transcription factor Ndt80, which positively regulates its own synthesis. A special type of a positive feedback loop is a double-negative feedback loop that is based on a mutual inhibition. This pattern of interaction ensures the existence of two states of the system, in which one protein cannot exist in the presence of another. This type of interaction is crucial during the cell cycle, in which Cdk1 inhibits the activity of APC/C^{Cdh1} through phosphorylation of Cdh1 protein, while APC/C^{Cdh1} inhibits the activity of Cdk1 through degradation of cyclins. The opposite effect on a system has a negative feedback loop, which is formed when the system components are antagonistic towards each other. In this case, one protein stimulates another, which in turn inhibits the activity of its own activator. The product of the reaction leads to a decrease in that reaction. A common example of a negative feedback loop is the interaction between Cdk1 and APC/C^{Cdc20} during mitosis and meiosis.

1.5.5. Types of dynamical behavior of biological system

Nonlinear dynamical systems are characterized by steady states in which the variables are constant in time in spite of ongoing processes. Steady states can be stable or unstable depending on whether they recover or not after small perturbations. The behavior of the dynamical system and transitions between different states is called bifurcation. It is represented by a signal-response curve, also called bifurcation diagram (Ferrell, 2013; Tyson et al., 2001). The bifurcation diagram describes the modification of the studied variable depending on a change of the particular parameter value of the signal. **Figure 6** presents different types of dynamical system behaviors on the bifurcation diagrams based on the type of interaction between molecules and the motifs. The basic type of behavior of the biological system is linear, like for the protein degradation, or hyperbolic, like for the protein phosphorylation described with the 2nd order kinetics (Tyson et al., 2003).

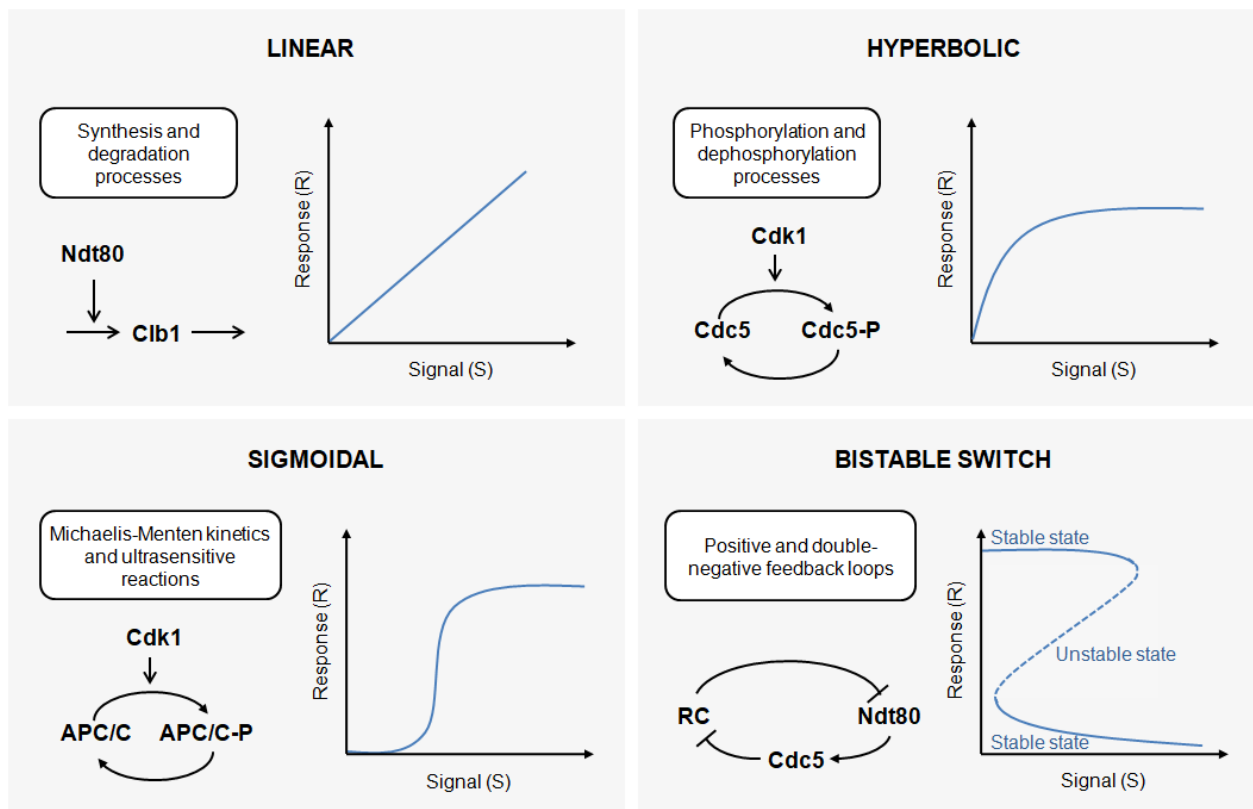


Figure 6. Behavior of biological system described with a signal-response curves. Different types of responses (R) to a signal (S) are presented. S is the parameter that describes the effect of one component of the network on the other. Blue curves indicate the response in term of value of the system component dependent on the value of the bifurcation parameter S. Stable regions in bistable switch are indicated with solid lines, while unstable with dashed lines.

Many biochemical reactions work as a switch between different states of the system that exhibit ultrasensitivity. Ultrasensitive reactions respond with a higher sensitivity to a signal than Michaelis-Menten kinetics (Tyson et al., 2003). Ultrasensitivity appears when a system reacts to small changes in the input signal producing a larger nonlinear response with a sigmoidal behavior. It can be reached by series of multi-step mechanisms, such as multisite phosphorylation, and can be described with Goldbeter-Koshland or Hill kinetics (Ferrell and Ha, 2014). An example is activation and inactivation of the APC/C^{Cdc20} by Cdk1-cyclin B complex during M-phase. APC/C^{Cdc20} reacts abruptly when the concentration of active Cdk1 is high, which allows multisite phosphorylation of the APC/C.

The ultrasensitivity is often generated by a positive or a double-negative feedback loop, which forms a switch-like response (Ferrell, 2013). The switch changes abruptly as the signal crosses a critical value (threshold). In a bifurcation diagram, it is presented as a bistable response (Tyson et al., 2001). Bistability is a property of the system that exhibits two stable steady states coexisting at a certain concentration of a signal (bifurcation parameter). In the bistable region, two stable steady states are separated by unstable region than can be described as a mountain ridge separating two valleys (Tyson et al., 2001). The switch from low to high response occurs with a change of the signal concentration by jumping through the unstable state. An example is a bistable switch that occurs at the entry into metaphase I of meiosis, during which the RC inhibits the synthesis of Ndt80, which in turns produces the inhibitor of the RC, namely Cdc5 (Okaz et al., 2012).

Negative feedback loop may result in two types of responses: homeostasis or oscillations. Oscillatory behavior is common in biological systems, from cell cycle and to control of gene expression in DNA damage response pathways. Oscillations can occur in the system when four general conditions are met (Ferrell et al., 2011). Firstly, oscillations require a negative feedback loop of at least two components. Secondly, an oscillatory response requires a sufficient time delay between the activities of the components of the oscillator. Moreover, the system has to exhibit non-linearity. Lastly, appropriate rate constants of the reactions are necessary. Depending on the values of the parameters, the system may oscillate or stabilize at intermediate levels. Depending on the type of the oscillations, the number of interacting components may be also an additional requirement. A two-component system may exhibit oscillations with decreased amplitude over time leading to the appearance of stable steady states of interacting components creating damped oscillations (**Figure 7A**) (Griffith, 1968).

Sustained oscillations, like the oscillations of the cell cycle, usually require at least three components in the negative feedback loop in order to achieve a sufficient time delay (Figure 7B). In the three-component system, protein X activates protein Z through the activation of an intermediate enzyme Y; then, protein Z inhibits X directly. In this condition, protein Y creates a necessary time delay and a sharp response causing the system to repeatedly overshoot and undershoot the steady state, preventing it from entering an intermediate level (Ferrell et al., 2011; Tyson and Novak, 2008).

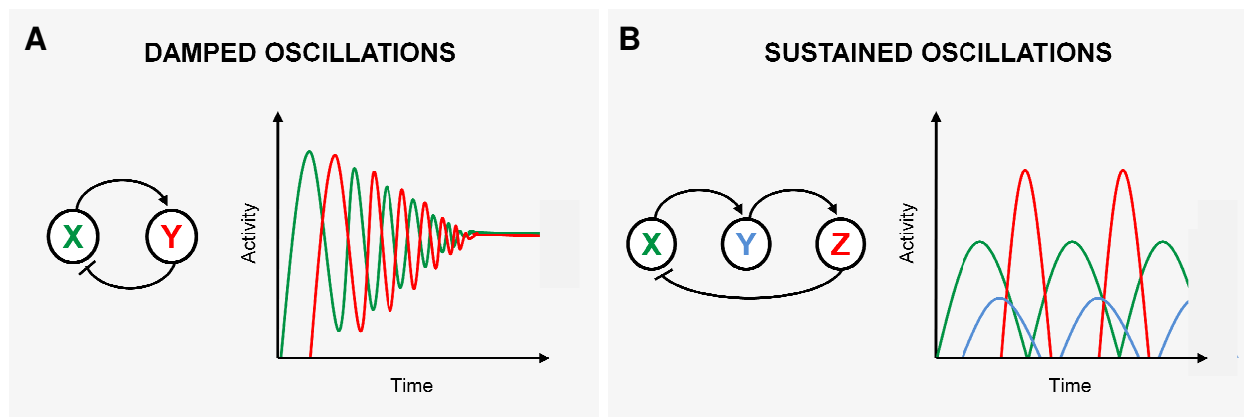


Figure 7. Types of oscillations created by a negative feedback loop. (A) Damped oscillations are often created in two-component systems. In this scenario, the amplitude of the oscillations decreases in time leading to decay of the oscillations. The components of such system enter intermediate steady state. (B) Sustained oscillations are often created in three-component systems. In this scenario, the amplitude of the oscillations is stable.

1.6. Mathematical models of cell cycle

Progression through a cell division is strictly regulated by the activity of Cdk1 and its regulators. Together, they create a complex network of interactions, forming feedback and feed forward loops that direct cell fate (Tyson and Novak, 2008). Mathematical models of the mitotic cell cycle help to understand mechanisms driving the divisions and the importance of particular elements of the network required for the proper regulation of mitosis (Tyson, 1999).

Mathematical models have been used for decades to understand the processes of the cell cycle in different organisms. The first models focused on defined phases of the cell cycle and its relation to cell growth (Brooks et al., 1980; Shields and Smith, 1977). With more knowledge gained from biological experiments and first descriptions of Cdk1-based regulation of the cell division (Nurse, 1990; Pines, 1995), models were developed that included essential Cdk1 regulation (Goldbeter, 1991). More detailed experimental descriptions helped to develop models explaining control of cell division with different

genetic mutants in yeast and in mammalian embryos (Hatzimanikatis et al., 1999; Novak and Tyson, 1993; Thron et al., 1996). Various levels of regulation of cell division, such as physiology, biochemistry, and genetics, started to be incorporated in more details, for example in the model of cell cycle in budding yeast (Chen et al., 2000) that included such regulatory mechanisms as DNA synthesis machinery, spindle formation and cell separation. This model was the first one to be tested against a big set of experimental data. It has been later extended with additional modules, such as checkpoints and phosphatases (Chen et al., 2004). It has been tested on more than 120 mutants based on experiments provided by Cross et al. (Cross et al., 2002). The model anticipated the existence of a phosphatase opposing Cdk1 activity that was later identified (Queralt et al., 2006). The latest version of the model (Kraikivski et al., 2015) has been used to predict the phenotypes of more than 30 novel mutant alleles. It has been proposed that due to similarities of the cell cycle control among species (Nurse, 1990), the principles of the models developed for budding yeast can be extended to higher organisms (Csikász-Nagy et al., 2006).

1.6.1. Mathematical modeling of Cdk1-APC/C oscillator

Despite the complexity and variety of biological oscillators, the main core design includes an essential negative feedback loop between Cdk1 and the APC/C^{Cdc20}. The general principle of the mitotic oscillator is that Cdk1 activates APC/C^{Cdc20} that inhibits Cdk1 through cyclins degradation. APC/C^{Cdc20} is activated at the onset of anaphase and requires phosphorylation of the APC/C core. This phosphorylation is triggered by Cdk1 and Cdc5 that increases the binding of Cdc20 to the APC/C (Golan et al., 2002; Rudner and Murray, 2000). The phosphorylation on more than 100 sites of the APC/C (Kraft et al., 2003; Zhang et al., 2016) gives a required time delay between the activity of Cdk1 and the degradation of cyclins, necessary for the oscillations to occur (Yang and Ferrell, 2013). Different approaches are used to model this delay, for example ultrasensitivity introduced with the Hill function based on the assumed multi-step phosphorylation of the APC/C (Yang and Ferrell, 2013). Models that consist of two components of the oscillator create damped oscillations that approach a steady state with intermediate levels of both Cdk1 and Cdc20 (Ferrell et al., 2011). Sustained oscillations are modeled by including a signaling cascade into the negative feedback loop. Ferrell et al. describes an intermediate protein acting as an enzyme to transmit the positive signal that generates a delay in response to APC/C activity (Ferrell et al., 2011). This approach is used in models of the cell cycle in *Xenopus* oocytes, budding yeast and fission yeast (Chen et al., 2000; Novak et al., 2001; Novak and Tyson, 1993). The

intermediate protein that introduces the delay has been proposed to be the polo-like kinase (Ferrell et al., 2011) or the phosphorylated form of APC/C (Chen et al., 2004). It has been reported that binding of Cdc20 to APC/C is inhibited by the Cdk1-dependent phosphorylation of the Cdc20 protein (Chung and Chen, 2003; Labit et al., 2012; Yudkovsky et al., 2000). This possibility is introduced in some of the models to create a delay in the two-component systems based on the additional double-negative feedback loop (Ciliberto et al., 2005; Vinod et al., 2013). The APC/C core can be included as a binding partner of Cdc20 (Kraikivski et al., 2015). Through phosphorylation of the APC/C, Cdk1 acts as an activator providing a necessary negative feedback loop. At the same time, it has the opposite effect on the Cdc20 protein. Faster events of phosphorylation and dephosphorylation for Cdc20 and slower for the APC/C core ensure a sufficient time delay for sustained oscillations.

1.6.2. Mathematical modeling of irreversible switches

The bistable switches are common properties of various transitions during the mitotic cell cycle. They are characterized by positive or double-negative feedback loops and nonlinearity of the reactions that create irreversible transitions (Tyson and Othmer, 1978). Irreversibility has been firstly introduced in a model of cell division in *Xenopus* oocytes (Borisuk and Tyson, 1998). The transition is triggered by the concentration of active Cdk-cyclin complex, called MPF (maturation-promoting factor), after exceeding a certain threshold. The model predicted the existence of two steady states that explained how cells remain in M-phase even when the MPF activity drops in anaphase. Later it has been shown that other transitions in cell cycle are controlled by bistable switches, such as the G1/S-phase transition (Cappell et al., 2018; Charvin et al., 2010; Zhang et al., 2011) and the entry into M-phase (Mochida et al., 2016; Rata et al., 2018).

It has been proposed that the mitotic exit is irreversible due to degradation of M-phase cyclins by APC/C^{Cdc20} (Potapova et al., 2006; Reed et al., 2003). However, later it has been shown that APC/C^{Cdc20}-dependent inactivation of Cdk1 is not sufficient to make the system exit irreversibly from mitosis due to the continues synthesis of cyclins (Novak et al., 2007). Therefore, it has been suggested that a positive feedback loop may provide the irreversibility of the transition to low Cdk1 state of the next cycle (Ferrell, 2002). The positive feedback loop was based on the activation of Cdk1 inhibitor Sic1 that allowed the maintenance of low Cdk1 activity after the initial cyclin proteolysis, similarly as during the G1/S-phase transition (**Figure 8A**) (López-Avilés et al., 2009).

Irreversibility during the exit may occur due to the action of other regulators. Cdc14 phosphatase may be involved in triggering the exit from mitosis through

dephosphorylation of Cdk1 inhibitors at the onset of anaphase (Vinod et al., 2011). Additionally, PP2A^{Cdc55} is required for general regulation of mitotic exit in eukaryotes (Figure 8B). The irreversible switch at the exit from mitosis is triggered by the Greatwall pathway that results in activation of the phosphatase, dephosphorylation of key mitotic regulators and the exit from the cycle (Baro et al., 2013; Hégarat et al., 2014; Queralt et al., 2006).

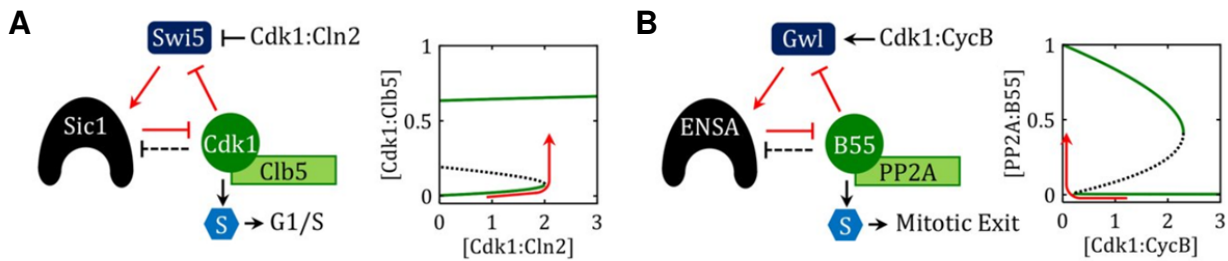


Figure 8. Bistable switches in cell cycle transitions. The motifs (left panels) and bifurcation diagrams (right panels). Green solid lines of bifurcation diagrams represent steady states, while dashed lines unstable states. Red arrows describe the transition from the starting state to a new state. **(A)** Transition from G1- to S-phase. Sic1 and Cdk1-Cln5 create a double-negative feedback loop that results in a bistable switch. A new cell is at a low steady state during G1 with low activity of Cdk1 and highly accumulated Sic1. The increase in Cdk1-Cln2 activity in late G1 triggers the entry into the high Cdk1 state of S-phase. **(B)** Exit from mitosis. ENSA enzyme is a direct inhibitor of PP2A^{B55}, which in turns inhibit ENSA through dephosphorylation. Additionally, PP2A^{B55} inhibits the activity of Gwl (Greatwall) kinase. During anaphase cells wait for reduced activity of Cdk1-Clbs to allow inactivation of Gwl and activation of PP2A^{B55}, which dephosphorylates M-phase regulators and returns the cell to a low Cdk1 state of G1. Taken from (Hopkins et al., 2017).

1.7. Mathematical models of meiosis

Although mathematical models are commonly used to describe the control of cell cycle in several organisms, not many models describing meiosis have been developed to date. Studies have been carried out in *Xenopus* oocytes to understand the activation of the maturation process and completion of meiotic divisions (Ferrell and Machleder, 1998; Pfeuty et al., 2012). Nevertheless, a principle of the two meiotic divisions has not been formulated. Notwithstanding, partial models of meiosis exist.

1.7.1. Modeling the entry into meiosis

One of the most studied subjects in meiosis is the meiotic commitment. The meiotic entry in budding yeast occurs due to the dynamics of the regulatory network after nutrients deprivation. The transition to meiosis strongly depends on initiators of cell division, such as Ime1 and Ime2, described in more details using ODEs (Ray et al., 2013). The network of meiotic entry consists of a set of positive and negative feedback loops allowing the irreversible entry into meiosis and commitment to the pre-meiotic S-

phase. Another model describing this switch incorporates the regulation of initiators of both meiosis and mitosis: Ime1/Ime2 and Cdk1-Cln3 (Wannige et al., 2015). The study shows that the entry into cell division is based on an all-or-none type of bistable switch that explains mutually exclusive existence of the initiation pathway of both types of cell division. Similar conclusions of bistability of the entry into meiosis were driven from the mathematical model based on fission yeast (Bhola et al., 2018).

1.7.2. The model of the entry into metaphase I

It has been found that the entry into metaphase I is based on a bistable switch (Okaz et al., 2012). The model of the prophase I-to-metaphase I transition explains this irreversibility as a consequence of a mutual inhibition between APC/C^{Ama1} and Cdk1. **Figure 9A** presents a wiring diagram of the main interactions in the model. The initial conditions of the model start with prophase I levels of meiotic regulators, during which DSBs are under repair and the RC is active (**Figure 9B**). The RC inhibits the synthesis of Ndt80 by activating its transcriptional repressor Sum1. Sum1 can be inactivated by two kinases: Ime2 and Cdk1. With the checkpoint satisfied, Sum1 frees the *NDT80* promoter and allows the synthesis of Ndt80 and other M-phase regulators. Proteins that are not specific to meiosis, like cyclins and Cdc5, can be synthesized during prophase I in Ndd1-dependent manner in the mutant lacking Ama1. The activities of APC/C^{Ama1} and the RC keep the system in check for entering metaphase I prematurely by inhibiting the activity of key M-phase regulators. In the model APC/C^{Ama1} is regulated in a complex manner. Cdk1-Clb1 inhibits its activity by phosphorylating Ama1. Additionally, the model predicts the existence of Ndt80-dependent stoichiometric inhibitor of Ama1, named additional inhibitor (AI).

The model explains the irreversible switch that governs the transition from prophase I to metaphase I upon repair of DSBs (**Figure 9C**). It presents the response of the kinase activity to different concentration of Ama1. At the wild-type level of Ama1, the system coexists at two states: high and low activity of Cdk1/Cdc5/kinase in metaphase I and prophase I, respectively. In the presence of DSBs cells maintain a low kinase state until after the repair is completed and the RC is silenced. The bistable region becomes narrower with the DSBs repair due to removal of the positive feedback loop between Ndt80, Cdc5 and the RC. The narrow range forces the system to jump to the higher branch of the bifurcation diagram (metaphase I). Additionally, the model describes the effect of the increased concentration of Ama1 that prevents the transition to the high kinase state. Thus, cells are unable to enter metaphase I and remain in prophase I arrest (Okaz et al., 2012).

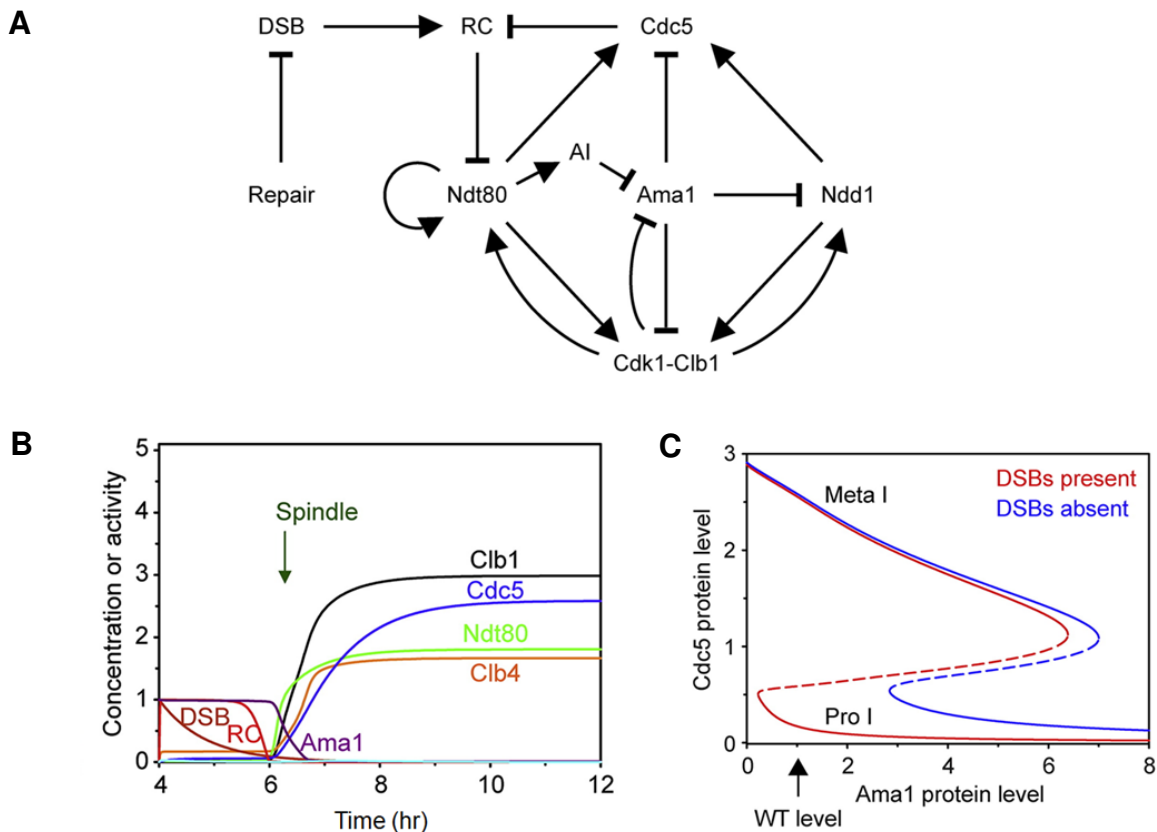


Figure 9. The model of prophase I-to-metaphase I transition. (A) Wiring diagram of interactions between main components of the model. DSB is double-strand break, RC is the recombination checkpoint and AI is an additional inhibitor of Aml1. Arrow-headed and bar-headed lines indicate positive and negative interactions, respectively. (B) Computational simulation of meiotic time course. Graph presents change in the proteins concentration or activity in time in wild-type cells. Simulation mimics the biological time course starting at prophase I at 4 hr. Green arrow indicates start of the process of formation of metaphase I spindle. (C) Bifurcation diagram describing response in the Cdc5 protein level on a signal in form of the parameter defining total concentration of Aml1. WT indicates wild-type levels of Aml1 assumed in the model. Pro I is prophase I, while Meta I is metaphase I. Red line describes the response in the presence of DSBs, while blue line describes the response when DSBs are repaired. Solid lines indicate stable states, while dashed lines unstable states. Taken from (Okaz et al., 2012).

1.8. Aim of the study

Despite the recent advances in studying meiosis, the exact mechanism of its regulation is still unclear. It has been proposed that the two meiotic divisions may be based on a modified mitotic regulatory machinery (Tyson and Novak, 2008). However, how this mitotic engine is modified to create precisely two consecutive divisions in meiosis is not fully understood. Thus, the major aim of this work is to elucidate the dynamics of the protein network controlling the progression through meiotic divisions, with special emphasis on the exit from meiosis II, using mathematical modeling in combination with biological experiments on budding yeast.

Mathematical modeling allows testing various hypotheses about the regulation of meiosis leading to exactly two divisions. It allows determining the sensitivities of the studied dynamical system and identifying its key regulators. Nevertheless, despite these advantages a functional mathematical model of meiotic two divisions has not been published to date. One of the challenges of developing the mathematical model of meiosis includes poor understanding of the complex protein network regulating the divisions. Experimental support for the model design is demanding, since the manipulation of the meiotic genes must not disrupt the earlier phases of mitotic cell cycle and the entry into meiosis.

In this work, I present the first mathematical model describing regulation of two meiotic divisions. The model is based on the knowledge of cell cycle control of meiosis and biological experiments performed in our lab on budding yeast. Budding yeast are used to study meiosis due to the ability of each cell to undergo meiosis and differentiation, ease in manipulation of genetic background and well-studied control of cell cycle events. In order to study meiosis in a large scale and with high resolution, I used our newly developed synchronization technique of meiotic cell culture (Argüello-Miranda et al., 2017). I modified the method to study in more details the exit from meiosis II and post-anaphase II events. Furthermore, I used various approaches to test the importance of different regulators in meiosis II. I developed a model based on these experiments and tested hypotheses about possible mechanisms of the control of meiotic exit.

1.9. Contributions

The experiment presented in Figure 22 was conducted by Dr. Orlando Argüello-Miranda and described in his doctoral thesis (Argüello-Miranda, 2015). The rest of the work presented in this thesis is my own.

2. Results

To shed light on the control of progression through the meiotic divisions and the exit from meiosis, we studied the dynamics of the main regulators contributing to the two waves of Cdk1 and APC/C activities. For this purpose, we developed a mathematical model characterizing the regulatory network driving two meiotic divisions. First three subchapters describe studies on the transitions required for entry and progression through the meiotic divisions. Later subchapters characterize possible mechanisms of the exit from meiosis after precisely two waves of Cdk1 and APC/C activities, resulting in the completion of meiotic divisions and entry into the differentiation program of sporulation.

2.1. Strategy of the development of the mathematical model

To address the question of the molecular mechanism that guarantees two meiotic divisions, we defined the main biological events of meiosis that contribute to the progression through the divisions. We omitted early and late phases of meiosis, such as DNA replication and sporulation. Based on biological observations, we constructed a wiring diagram of interactions between regulators of meiotic divisions. We considered that interactions depicted in the diagram depend on the molecular concentration or activity of the participants of the reaction (variables) and on fixed rate constants (parameters). All the variables in the model, which describe the components of the meiotic network, are dimensionless and represent the relative concentrations and activities of proteins or regulatory process. We used a deterministic approach and developed a set of nonlinear ordinary differential equations (ODEs) formulated according to biochemical reaction laws based on the wiring diagram. The background synthesis of the proteins included in the model is approximated by the zero order kinetics. The background degradation is based on the 1st order kinetics and the processes of activation and inactivation are described by the 1st and the 2nd order kinetics. Background degradation and inactivation are included to avoid unlimited increase in protein level and activity. The ultrasensitive responses are described with Goldbeter-Koshland kinetics and a Hill function. The parameters are designated as k and Michaelis-Menten constants as J . Subscripts indicate the type of the reaction: k_s stands for synthesis, k_d for degradation, k_a for activation, k_i for inactivation, k_{as} and k_{ds}

for association and dissociation of the complex, respectively. These parameters are given in a dimension of min^{-1} . Michaelis-Menten constants and other parameters are dimensionless. The same conventions apply for all models presented in this work.

To solve the set of ODEs, we performed computational simulations. We integrated the equations and determined the starting conditions for the simulation. We specified the preliminary values of the parameters using the previous work (Okaz et al., 2012) and our guesses based on our knowledge of biological processes. Values of the parameters of protein degradation (degradation rates) were derived from biological observations. The solution for each component of the model was plotted in the simulation window that displays the changes of the variables over time.

We optimized the values of parameters by adopting a commonly used approach called “guess-and-check” method, in which the parameter values are estimated by fitting them to the observed phenotypes “by hand” (Sible and Tyson, 2007). We fitted the parameters to wild-type observations and the phenotypes of some mutant strains. Deletion of a gene or depletion of a protein was simulated by setting the synthesis rate of a relevant protein and/or its total concentration to zero at the beginning of the simulation. Inactivation or inhibition of a protein activity was simulated by setting the parameter of activation to zero at a specified time of the simulation. The aim of the parameter optimization was to find a single set of parameter values, which could recreate meiosis of the wild-type strain and various mutant strains *in silico*. The initial parameter values were revised by comparing numerical solutions to experimental data with respect to protein appearance at different stages of meiosis and the time of spindle formation. It is important to note that the chosen values of the model parameters are not optimal and different sets of the values may give comparable solutions.

2.2. The core of meiotic divisions is based on a Cdk1-APC/C oscillator supplemented with meiotic regulators

The two meiotic divisions could be generated by a mitotic Cdk1-APC/C oscillator with addition of meiosis-specific regulators that trigger the entry into the first division and possibly limit the number of divisions to two (**Figure 11**). To create a mathematical model of the regulation of meiosis, we incorporated an oscillator into the existing model of the prophase I-to-metaphase I transition (Okaz et al., 2012).

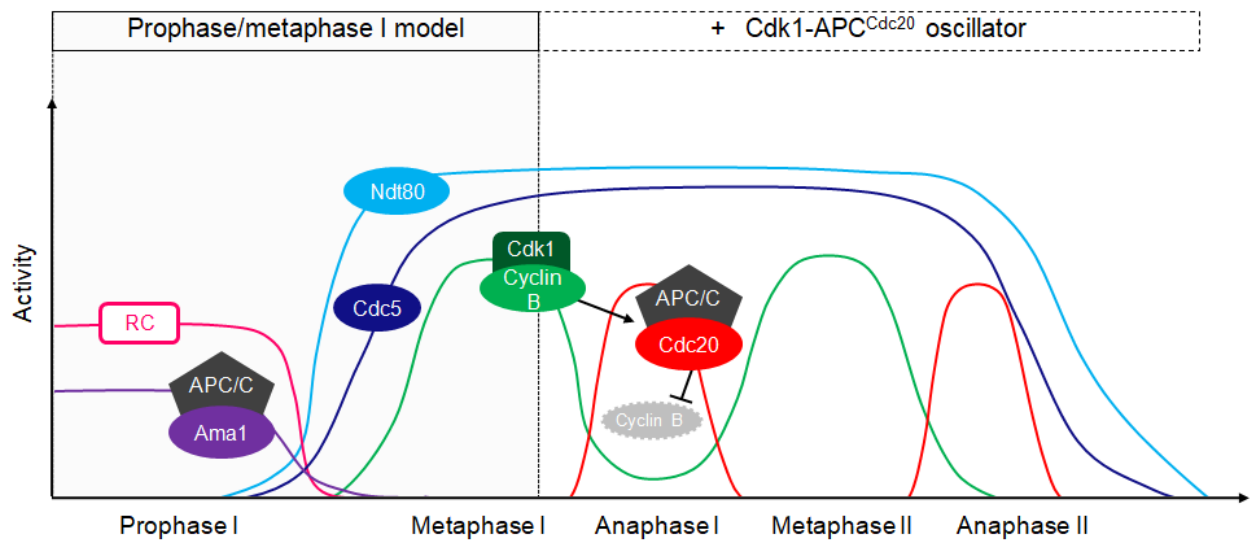


Figure 11. The core of the mathematical model of meiotic divisions is based on Cdk1-APC/C oscillations and the model of meiotic entry. The scheme presents stages of meiosis regulated by machineries described by the model of the prophase I-to-metaphase I transition (Okaz et al., 2012) and the Cdk1-APC/C oscillator. The entry into high kinase state of metaphase I and meiosis-specific regulators, such as Ndt80, are provided by the Okaz et al. model. The oscillator is incorporated to provide the progression through meiotic divisions. RC indicates the recombination checkpoint.

2.2.1. The modified model of prophase I-to-metaphase I transition provides the regulatory network that controls the entry into metaphase I

To create a model of two meiotic divisions, we used as a basis an existing model of the prophase I-to-metaphase I transition developed by Okaz et al. (Okaz et al., 2012). The model describes the irreversible exit from prophase I and the entry into metaphase I, which is regulated by a complex network of meiosis-specific proteins, such as Ama1 and Ndt80, and proteins common to both meiosis and mitosis, such as Clb1 and Cdc5 (**Figure 11**). We simplified the model by omitting the modules not necessary to understand the progression through two meiotic divisions, creating a modified version of the prophase I-to-metaphase I model, as presented by the wiring diagram in **Figure 12A**.

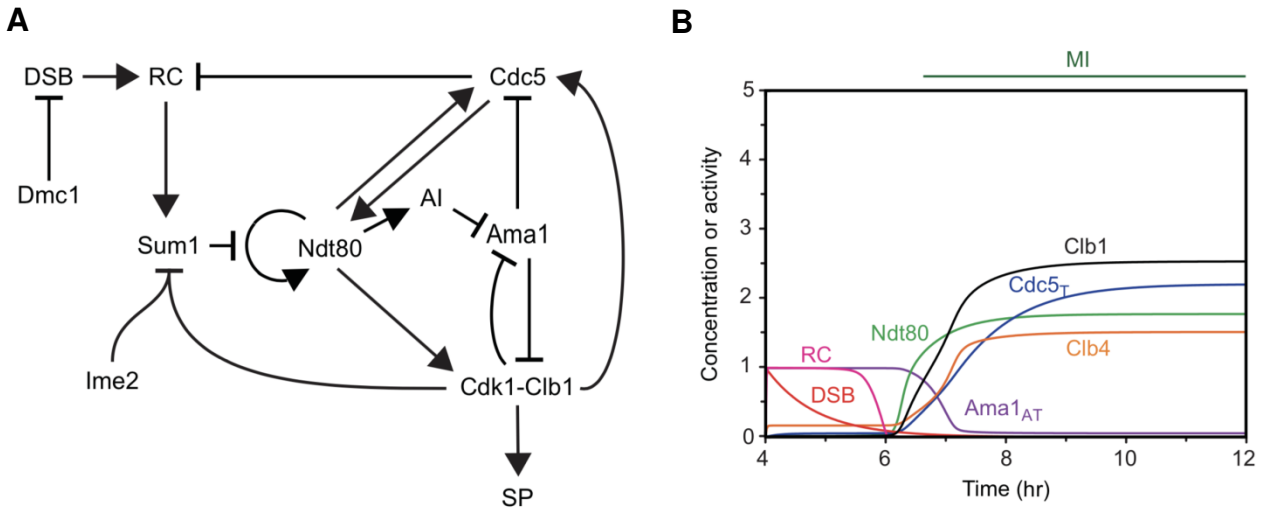


Figure 12. The modified mathematical model of prophase I-to-metaphase I transition provides the entry into meiotic divisions. (A) Detailed wiring diagram of the modified model. For simplification, Cdk1-Clb4 and Ama1:AI complex are omitted in the diagram. Each interaction is depicted by an arrow \downarrow or bar-headed line \perp indicating positive or negative regulation, respectively. (B) Computational simulation presenting concentration or activity of the key meiotic regulators in WT cells. Simulation starts with DSB formation, which corresponds to $t = 4$ hr in a WT meiotic culture. Green line above the graph depicts the time of the formation and the persistence of metaphase I spindle (MI).

We performed computational simulations that recreated a biological 12 hr time course in wild-type (WT) cells using the modified model (Figure 12B). We started simulations at the time of formation of DSBs, which corresponds to 4 hr in a WT meiotic time course. At this time, cells exhibit the activity of the RC due to unrepaired DSBs. At 6 hr cells accumulate Ndt80, which is followed by accumulation of Cdc5 and cyclins. Cdk1 is activated leading to formation of metaphase I spindles (MI) and inhibition of Ama1 activity. Due to inactivation of Ama1 and lack of another Cdk1 inhibitor, cells arrest in metaphase I with constant levels of M-phase regulators and stabilized spindle. The observed metaphase I-arrest phenotype is caused by the lack of Cdc20 in the model that provides the transition from metaphase I to anaphase I, as studying the progression through divisions was not a subject of the model developed by Okaz et al.

The following equations describing the biological events of the prophase I-to-metaphase I transition in the modified version of the model used to build the model of two divisions are derived from the model described in Okaz et al. In this model, the entry into metaphase I is triggered by silencing of the RC. The activity of the RC is modeled as an ultrasensitive switch (Equation 9) dependent on the activity of Cdc5 and the exponential decrease in DSBs. The decrease in DSBs is proportional to the level of the DNA repair mechanisms represented by Dmc1 (Equation 10), which is the meiosis-specific recombinase required for DSBs repair (Busygina et al., 2013).

$$[RC] \frac{d}{dt} = k_{RCa1} \cdot [DSB] \cdot \frac{1 - [RC]}{J_{RC} + 1 - [RC]} - (k_{RCi1} + k_{RCi2} \cdot [Cdc5]) \cdot \frac{[RC]}{J_{RC} + [RC]} \quad (9)$$

$$[DSB] \frac{d}{dt} = -k_{DSBi1} \cdot [DSB] \cdot [Dmc1] \quad (10)$$

After the repair of DSBs, cells activate Ndt80. In the model of the prophase I-to-metaphase I transition, Ndt80 is presented as total nuclear protein, which corresponds to the active form of this protein. *NDT80* expression is activated by Ndt80 itself, which competes for the binding to its promoter with the transcriptional repressor Sum1 (Pak and Segall, 2002). In the model, it is presented by an algebraic equation (**Equation 13**) that complements the competitive inhibition reaction. We modified this version of Ndt80 by including an additional form of the protein regulated by Ime2 or Cdc5 (Schindler and Winter, 2006; Sopko et al., 2002). We assumed that the active form of total Ndt80, which has been developed by Okaz et al., is now an inactive version, referred to as Ndt80_T (**Equation 11**). The newly added form with regulated activity corresponds to the fully active Ndt80 (**Equation 12**) that triggers its own synthesis.

$$[Ndt80_T] \frac{d}{dt} = k_{Ndt80s1} + k_{Ndt80s2} \cdot \frac{[Ndt80]}{J_N + [Ndt80]} - k_{Ndt80d1} \cdot [Ndt80_T] \quad (11)$$

$$[Ndt80] \frac{d}{dt} = (k_{Ndt80a1} + k_{Ndt80a2} \cdot [Cdc5]) \cdot ([Ndt80_T] - [Ndt80]) - k_{Ndt80i1} \cdot [Ndt80] - k_{Ndt80d1} \cdot [Ndt80] \quad (12)$$

$$J_N = J_{Ndt80} \cdot \left(1 + \frac{\alpha \cdot ([Sum1_T] - [Sum1_{Ime2}^i]) + \beta \cdot ([Sum1_{Ime2}^i] - [Sum1_I])}{k_i} \right) \quad (13)$$

The model of the prophase I-to-metaphase I transition uses three forms of Sum1 that control Ndt80 expression. Regulation of Sum1 depends on the activities of the RC, Ime2 and Cdk1 (**Equation 17**). Sum1 is inactivated by Ime2-dependent phosphorylation in prophase I (Sum1_{Ime2}ⁱ) (**Equation 14**). Additionally, Sum1 is inactivated by Cdk1 (Sum1_{Cdk1}ⁱ) (**Equation 15**). For this inhibition, Ndt80 activity needs to synthesize M-phase cyclins. Thus, the Cdk1-dependent inhibition of Sum1 requires prior inhibition of Sum1 by Ime2 (Ahmed et al., 2009; Shin et al., 2010). The activation of Sum1 by the RC (Sum1_{RC}ⁱ) counteracts this inactivation (**Equation 16**). The total concentration of Sum1 (Sum1_T) is constant throughout meiosis (Pak and Segall, 2002; Okaz et al., 2012).

$$[Sum1_{Ime2}^i] \frac{d}{dt} = k_{Sum1i1} \cdot ([Sum1_T] - [Sum1_{Ime2}^i]) - k_{Sum1a1} \cdot [Sum1_{Ime2}^i] \quad (14)$$

$$[Sum1_{Cdk1}^i] \frac{d}{dt} = (k_{Sum1i2} + k_{Sum1i3} \cdot ([Clb1] + [Clb4])) \cdot ([Sum1_T] - [Sum1_{Cdk1}^i]) - k_{Sum1a2} \cdot [Sum1_{Cdk1}^i] \quad (15)$$

$$[Sum1_{RC}^i] \frac{d}{dt} = k_{Sum1i4} \cdot ([Sum1_T] - [Sum1_{RC}^i]) - k_{Sum1a3} \cdot [RC] \cdot [Sum1_{RC}^i] \quad (16)$$

$$[Sum1_I] = [Sum1_{me2}^i] \cdot \frac{[Sum1_{RC}^i]}{[Sum1_T]} \cdot \frac{[Sum1_{Cdk1}^i]}{[Sum1_T]} \quad (17)$$

The initial activation of Ndt80 leads to the production of Cdc5 and, in turn, inhibition of the RC. This double-negative feedback loop boosts the activity of Ndt80 and production of cyclins. In the model, the total concentration of Clb1 and Clb4 is assumed to be equal to the active form of Cdk1-Clb1 and Cdk1-Clb4, respectively (**Equations 18-19**). The synthesis of Clb1 and Clb4 depends on Ndt80, while their proteolysis depends on APC/C^{Ama1} (Okaz et al., 2012). The model of the prophase I-to-metaphase I transition introduces an additional synthesis of Clb1 that depends on the activity of Ndd1, a subunit of a mitotic transcription factor (Breedon, 2000; Loy et al., 1999). Ndd1 triggers premature synthesis of Clb1 in the absence of Ama1, which suppresses mitotic cell-cycle control during prophase I. This process is essential for proper segregation of homologs during meiosis I. For simplification of the model used as a basis of the model of two meiotic divisions, we omitted the module of Ndd1 and the Ndd1-dependent synthesis of meiotic regulators, as we do not investigate the premature entry into metaphase I caused by this transcription factor and the return to growth phenomena.

$$[Clb1] \frac{d}{dt} = k_{Clb1s1} + k_{Clb1s2} \cdot [Ndt80] - (k_{Clb1d1} + k_{Clb1d2} \cdot [Ama1] + k_{Clb1d3} \cdot [Ama1_T]) \cdot [Clb1] \quad (18)$$

$$[Clb4] \frac{d}{dt} = k_{Clb4s1} + k_{Clb4s2} \cdot [Ndt80] - (k_{Clb4d1} + k_{Clb4d2} \cdot [Ama1] + k_{Clb4d3} \cdot [Ama1_T]) \cdot [Clb4] \quad (19)$$

Active Cdk1 is required for the formation of a metaphase I spindle (Haase et al., 2001). In the model, spindle formation is controlled by a generic Cdk1 substrate SP activated through multi-site phosphorylation by Cdk1 (**Equation 20**). The activity of the SP varies between 0 and 1, and the spindle is assembled when the value raises above 0.5 (Okaz et al., 2012).

$$[SP] \frac{d}{dt} = k_{SPa1} \cdot ([Clb1] + [Clb4]) \cdot \frac{1 - [SP]}{J_{SP} + 1 - [SP]} - k_{SPi1} \cdot \frac{[SP]}{J_{SP} + [SP]} \quad (20)$$

Cdc5 is presented in two forms: as a total level, referred to as Cdc5_T (**Equation 21**), and as an active form (**Equation 22**) which depends on the activity of Cdk1, similarly as

during mitosis (Mortensen et al., 2005). Cdc5 is synthesized by Ndt80 and targeted for degradation by APC/C^{Ama1} (Okaz et al., 2012). Similar to Clb1, Cdc5 synthesis is additionally controlled by Ndd1. However, in a modified version of the model, we omitted this regulation. Thus, the equation describing the total levels of Cdc5 in Okaz et al. was modified to **Equation 21**.

$$[Cdc5_T] \frac{d}{dt} = k_{Cdc5s1} + k_{Cdc5s2} \cdot [Ndt80] - (k_{Cdc5d1} + k_{Cdc5d2} \cdot [Ama1] + k_{Cdc5d3} \cdot [Ama1_T]) \cdot [Cdc5_T] \quad (21)$$

$$[Cdc5] \frac{d}{dt} = (k_{Cdc5a1} + k_{Cdc5a2} \cdot [Clb1] + k_{Cdc5a3} \cdot [Clb4]) \cdot ([Cdc5_T] - [Cdc5]) - (k_{Cdc5i1} + k_{Cdc5d1} + k_{Cdc5d2} \cdot [Ama1] + k_{Cdc5d3} \cdot [Ama1_T]) \cdot [Cdc5] \quad (22)$$

The APC/C core is omitted in the model, as the concentration of APC/C subunits are constant throughout meiosis and not limiting for the activity of the ligase. The total level of Ama1, referred to as Ama1_T, is assumed to be constant. The activity of Ama1 is inhibited by Cdk1-Clb1 through multi-site phosphorylation, creating a double-negative feedback loop that suppresses the activity of Cdk1 and Ama1 at the same time (Okaz et al., 2012). The active form of Ama1, referred to as Ama1_{AT}, is modeled as an ultrasensitive switch with Goldbeter-Koshland kinetics (**Equation 23**).

$$[Ama1_{AT}] \frac{d}{dt} = k_{Ama1a1} \cdot \frac{[Ama1_T] - [Ama1_{AT}]}{J_{Ama1} + [Ama1_T] - [Ama1_{AT}]} - (k_{Ama1i1} + k_{Ama1i2} \cdot [Clb1]) \cdot \frac{[Ama1_{AT}]}{J_{Ama1} + [Ama1_{AT}]} \quad (23)$$

Additionally, in the model of the prophase I-to-metaphase I transition it has been assumed that Ama1 forms a complex with an additional inhibitor (AI), which represses the activity of APC/C^{Ama1}. The inhibitor is synthesized by Ndt80 (**Equation 24**). The AI forms a complex with both phosphorylated and unphosphorylated forms of Ama1, referred to as Ama1:AI (**Equation 25**). The most active form of Ama1 that triggers the degradation of cyclins and Cdc5 is unphosphorylated and free of AI (**Equation 26**). However, it has been proposed by Okaz et al. that both phosphorylation and binding to the AI reduce the activity of the APC/C^{Ama1}, but do not completely suppress it. Therefore, the proteolysis of Cdc5 and cyclins is proportional to both Ama1_T and unbound Ama1 described with **Equation 26**.

$$[AI_T] \frac{d}{dt} = k_{AITs1} \cdot [Ndt80] - k_{AITd1} \cdot [AI_T] \quad (24)$$

$$[Ama1:AI] \frac{d}{dt} = k_{AIs1} \cdot ([Ama1_T] - [Ama1:AI]) \cdot ([AI_T] - [Ama1:AI]) - k_{AId1} \cdot [Ama1:AI] \quad (25)$$

$$[Ama1] = [Ama1_{AT}] - \frac{[Ama1:AI] \cdot [Ama1_{AT}]}{[Ama1_T]} \quad (26)$$

Initial values describing the concentration or activity of the RC, DSB and Ama1_{AT} at the beginning of the simulation were set to 1, as these components of the model are present at prophase I. Initial values of other variables were set to 0, as they appear only when DSBs are repaired. The values of the model parameters are depicted in **Table 1**.

In summary, in the modified version of the model of the prophase I-to-metaphase I transition, which we used as a core for the model of the meiotic two divisions, we adopted the majority of the equations and parameters described in Okaz et al. We modified **Equation 11** describing Ndt80 synthesis and added an additional form of the protein with regulated activity (**Equation 12**). We simplified the system by excluding the Ndd1-dependent synthesis of Clb1 and Cdc5 (**Equations 18** and **21**). We excluded the Ndd1-regulatory module that is triggering the early synthesis of M-phase proteins in the absence of Ama1 during prophase I.

Table 1. Parameter values of the simplified model of prophase I-to-metaphase I transition.

Equation number	Parameters and their values
9	$k_{RCa1} = 1, k_{RCi1} = 0.1, k_{RCi2} = 2, J_{RC} = 0.01$
10	$Dmc1 = 1, k_{DSBi1} = 0.02$
11, 12, 13	$k_{Ndt80s1} = 0.01, k_{Ndt80s2} = 2, k_{Ndt80d1} = 1, k_{Ndt80a1} = 4, k_{Ndt80a2} = 2, k_{Ndt80i1} = 0.2, J_{Ndt80} = 0.2, \alpha = 1, \beta = 0.1, k_i = 0.01$
14, 15, 16	$Sum1_T = 1, k_{Sum1i1} = 0.025, k_{Sum1a1} = 0.1^{-5}, k_{Sum1i2} = 0.1, k_{Sum1i3} = 1, k_{Sum1a2} = 0.01, k_{Sum1i4} = 0.25, k_{Sum1a3} = 1$
18	$k_{Clb1s1} = 0.002, k_{Clb1s2} = 0.2, k_{Clb1d1} = 0.1, k_{Clb1d2} = 0.2, k_{Clb1d3} = 0.02$
19	$k_{Clb4s1} = 0.2, k_{Clb4s2} = 0.1, k_{Clb4d1} = 0.2, k_{Clb4d2} = 1, k_{Clb4d3} = 0.02$
20	$k_{SPa1} = 2, k_{SPi1} = 2, J_{SP} = 0.01$
21, 22	$k_{Cdc5s1} = 0.004, k_{Cdc5s2} = 0.03, k_{Cdc5d1} = 0.02, k_{Cdc5d2} = 0.06, k_{Cdc5d3} = 0.002, k_{Cdc5a1} = 0.1, k_{Cdc5a2} = 0.4, k_{Cdc5a3} = 0.3, k_{Cdc5i1} = 0.1$
23	$Ama1_T = 1, k_{Ama1a1} = 0.1, k_{Ama1i1} = 0.005, k_{Ama1i2} = 0.1, J_{Ama1} = 0.1$
24	$k_{AIs1} = 0.1, k_{AId1} = 0.15$
25	$k_{AIs1} = 10, k_{AId1} = 1$

2.2.2. Combining the model of the entry into metaphase I with the Cdk1-APC/C oscillator provides the necessary transitions for the meiotic progression

To describe the entry into the second division, we studied a mechanism that is required for the transition from metaphase to anaphase. The minimal Cdk1-APC/C oscillator was based on the existing models of the cell cycle (Chen et al., 2004; Tyson and Novak, 2008). The oscillator is depicted in a simplified form in **Figure 13A**. The negative feedback loop providing the oscillatory behavior of the system is based on the activation of APC/C^{Cdc20} by Cdk1 and inactivation of Cdk1 by APC/C^{Cdc20}. Additionally, a Cdc5-dependent activation of APC/C^{Cdc20} is included, which provides an additional connection between the mitotic and the meiotic machineries.

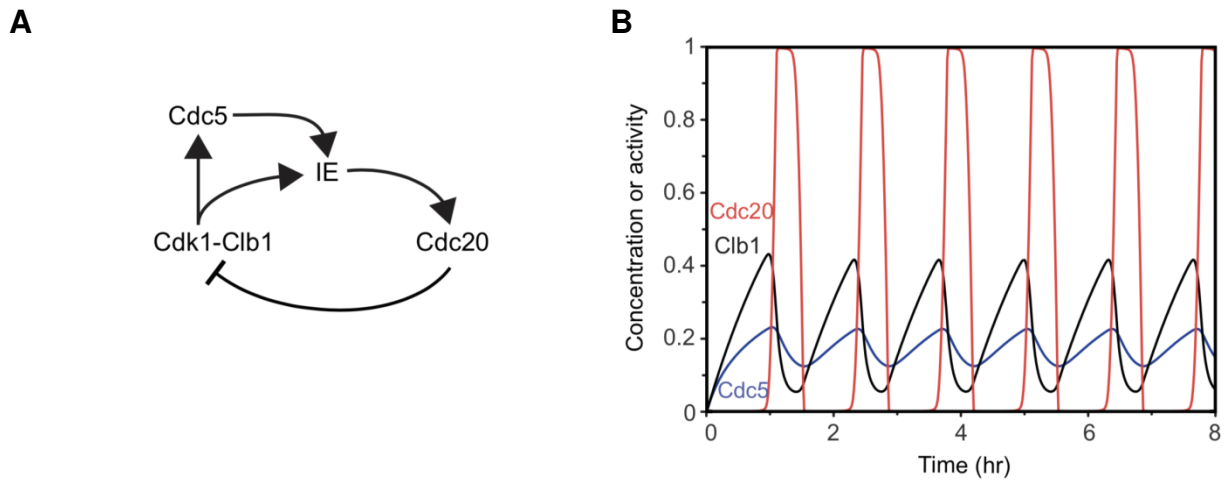


Figure 13. The minimal model of a Cdk1-APC/C oscillator provides the transition from metaphase to anaphase. The oscillator is based on two main components: Cdk1-cyclin B and APC/C^{Cdc20}, depicted in the model as Clb1 and Cdc20, respectively. The time delay between the activity of Clb1 and Cdc20 is achieved by the introduction of nonlinearity and an intermediate enzyme (IE) transmitting the signal. (A) Wiring diagram of the minimal oscillator. ↓, positive interaction; ⊥, negative interaction. (B) Simulation of the minimal oscillator showing concentration or activity of Clb1, Cdc20 and Cdc5.

In the model, Cdk1 is activated by the M-phase cyclins, depicted in form of Clb1 (**Equation 27**). Cdk1-Clb1 phosphorylates the APC/C core, which allows binding of Cdc20 and activation of the ligase. Additionally, we extended the minimal oscillator by including the Cdc5 kinase, which has been proposed to phosphorylate and activate the APC/C core along with Cdk1 (Golan et al., 2002; Rudner and Murray, 2000). The activity of Cdc5 depends on Cdk1-dependent activation (**Equation 28**).

$$[Clb1] \frac{d}{dt} = k_{Clb1s1} - (k_{Clb1a1} + k_{Clb1a2} \cdot [Cdc20]) \cdot [Clb1] \quad (27)$$

$$[Cdc5] \frac{d}{dt} = (k_{Cdc5a1} + k_{Cdc5a2} \cdot [Clb1]) \cdot (1 - [Cdc5]) - k_{Cdc5i1} \cdot [Cdc5] \quad (28)$$

In order for the system to oscillate, a time delay was introduced in form of an additional intermediate enzyme (IE) that mediates between Cdk1 and Cdc20 (Ferrell et al., 2011; Pomerening et al., 2005; Tyson et al., 2003) (**Equation 28**). We incorporated the IE into the model, in which Cdk1 and Cdc5 activate the enzyme triggering activation of Cdc20 (**Equation 29**). The activation and inactivation of Cdc20 is faster than the activation and inactivation of the IE, ensuring that the decline in Clb1 does not affect Cdc20 activity immediately.

$$[IE] \frac{d}{dt} = (k_{IEa1} \cdot [Clb1] + k_{IEa2} \cdot [Cdc5]) \cdot \frac{1 - [IE]}{J_{IE} + 1 - [IE]} - k_{IEi1} \cdot \frac{[IE]}{J_{IE} + [IE]} \quad (29)$$

$$[Cdc20] \frac{d}{dt} = k_{Cdc20a1} \cdot [IE] \cdot \frac{1 - [Cdc20]}{J_{Cdc20} + 1 - [Cdc20]} - k_{Cdc20i1} \cdot \frac{[Cdc20]}{J_{Cdc20} + [Cdc20]} \quad (30)$$

The system starts in the low Cdk1 state, during which cells do not synthesize M-phase regulators. Thus, the initial values of all the variables were set to 0. The parameters of the minimal model of Cdk1-APC/C oscillator are presented in **Table 2**.

Table 2. Parameter values of the minimal model of Cdk1-APC/C oscillations.

Equation number	Parameters and their values
27	$k_{Clb1s1} = 0.01, k_{Clb1d1} = 0.01, k_{Clb1d2} = 0.2$
28	$k_{Cdc5a1} = 0.01, k_{Cdc5a2} = 0.05, k_{Cdc5i1} = 0.1$
29	$k_{IEa1} = 0.1, k_{IEa2} = 0.1, k_{IEi1} = 0.04, J_{IE} = 0.01$
30	$k_{Cdc20a1} = 1, k_{Cdc20i1} = 0.5, J_{Cdc20} = 0.001$

We simulated the behavior of cells in the four-component system (**Figure 13B**). Clb1 and Cdc5 activate the IE, which results in activation of Cdc20 with a time delay. This leads to abrupt degradation of Clb1. Cdc20 follows the decline of the IE after Clb1 degradation and allows re-accumulation of cyclins for the next division. Cdc5 does not depend directly on the activity of Cdc20, but is regulated by Cdk1, which provides a time delay for Cdc5 inactivation.

To study the progression through the meiotic divisions, we expanded the modified model of the prophase I-to-metaphase I transition that provides the entry into the first division and the key meiotic regulators (**Equations 9-26**). We incorporated the Cdk1-APC/C^{Cdc20} oscillator (**Equations 27-30**). The interactions between the components of the combined model are presented in **Figure 14A**. **Equations 18-19** describing Clb1 and Clb4, respectively, were substituted by **Equations 31-32**, which incorporate Cdc20-dependent degradation of cyclins.

$$[Clb1] \frac{d}{dt} = k_{Clb1s1} + k_{Clb1s2} \cdot [Ndt80] - (k_{Clb1d1} + k_{Clb1d2} \cdot [Ama1] + k_{Clb1d3} \cdot [Ama1_T] + k_{Clb1d4} \cdot [Cdc20]) \cdot [Clb1] \quad (31)$$

$$[Clb4] \frac{d}{dt} = k_{Clb4s1} + k_{Clb4s2} \cdot [Ndt80] - (k_{Clb4d1} + k_{Clb4d2} \cdot [Ama1] + k_{Clb4d3} \cdot [Ama1_T] + k_{Clb4d4} \cdot [Cdc20]) \cdot [Clb4] \quad (32)$$

The IE is activated by Cdc5 and the combined activity of Clb1 and Clb4. Thus, **Equation 29** was substituted by **Equation 33**. Cdc20 is synthesized in a Ndt80-dependent manner. Thus we added an additional form of total level of Cdc20 protein, referred to as Cdc20_T (**Equation 34**). We modified the active form of Cdc20 (**Equation 35**) by including the background degradation. The initial values of the newly described components were set to 0. The new and modified parameters of the model are presented in **Table 3**.

$$[IE] \frac{d}{dt} = (k_{IEa1} \cdot ([Clb] + [Clb4]) + k_{IEa2} \cdot [Cdc5]) \cdot \frac{1 - [IE]}{J_{IE} + 1 - [IE]} - k_{IEi1} \cdot \frac{[IE]}{J_{IE} + [IE]} \quad (33)$$

$$[Cdc20_T] \frac{d}{dt} = k_{Cdc20s1} + k_{Cdc20s2} \cdot [Ndt80] - k_{Cdc20d1} \cdot [Cdc20_T] \quad (34)$$

$$[Cdc20] \frac{d}{dt} = k_{Cdc20a1} \cdot [IE] \cdot \frac{[Cdc20_T] - [Cdc20]}{J_{Cdc20} + [Cdc20_T] - [Cdc20]} - k_{Cdc20i1} \cdot \frac{[Cdc20]}{J_{Cdc20} + [Cdc20]} - k_{Cdc20d1} \cdot [Cdc20] \quad (35)$$

Table 3. Parameter values of modified equations in the combined model.

Equation number	Parameters and their values
31	$k_{Clb1s1} = 0.002, k_{Clb1s2} = 0.02, k_{Clb1d1} = 0.02, k_{Clb1d2} = 0.2, k_{Clb1d3} = 0.02,$ $k_{Clb1d4} = 0.2$
32	$k_{Clb4s1} = 0.05, k_{Clb4s2} = 0.1, k_{Clb4d1} = 0.2, k_{Clb4d2} = 1, k_{Clb4d3} = 0.02, k_{Clb4d4} = 1$
33	$k_{IEa1} = 0.02, k_{IEa2} = 0.01, k_{IEi1} = 0.05, J_{IE} = 0.0001$
34, 35	$k_{Cdc20s1} = 0.001, k_{Cdc20s2} = 0.2, k_{Cdc20d1} = 0.1, k_{Cdc20a1} = 1, k_{Cdc20i1} = 0.5,$ $J_{Cdc20} = 0.01$

We performed simulations of the combined model, starting from the time of DSB formation, which corresponds to 4 hr in a WT meiotic time course (**Figure 14B**). Ndt80 accumulates at 6 hr, after inhibition of the Ndt80 repressor Sum1. It is followed by Cdc5, Clb1 and Clb4. Due to the introduction of the Cdk1-APC/C oscillator, cyclins accumulate periodically. Cdc20 total protein appears at the same time as cyclins, unlike its active version (**Figure 14C**). Interestingly, due to the stable behavior of Ndt80, Cdc20_T persists at high levels in contrast to its periodic activity.

With the introduction of the Cdk1-APC/ C^{Cdc20} oscillations, the system recreates the transition from metaphase, with high activity of Cdk1, to anaphase, with high activity of APC/ C^{Cdc20} . The combined model successfully recapitulates key events that drive the meiotic divisions, such as: (i) the entry into the first meiotic division with accumulation of Ndt80 and M-phase cyclins; (ii) the transition from metaphase I to anaphase I with degradation of cyclins; (iii) the transition from anaphase I to metaphase II with re-accumulation of cyclins. However, the model fails to terminate at meiosis II. Instead of complete degradation of cyclins, the oscillations of Cdk1-APC/ C^{Cdc20} continue after the second wave of their activities, creating additional divisions.

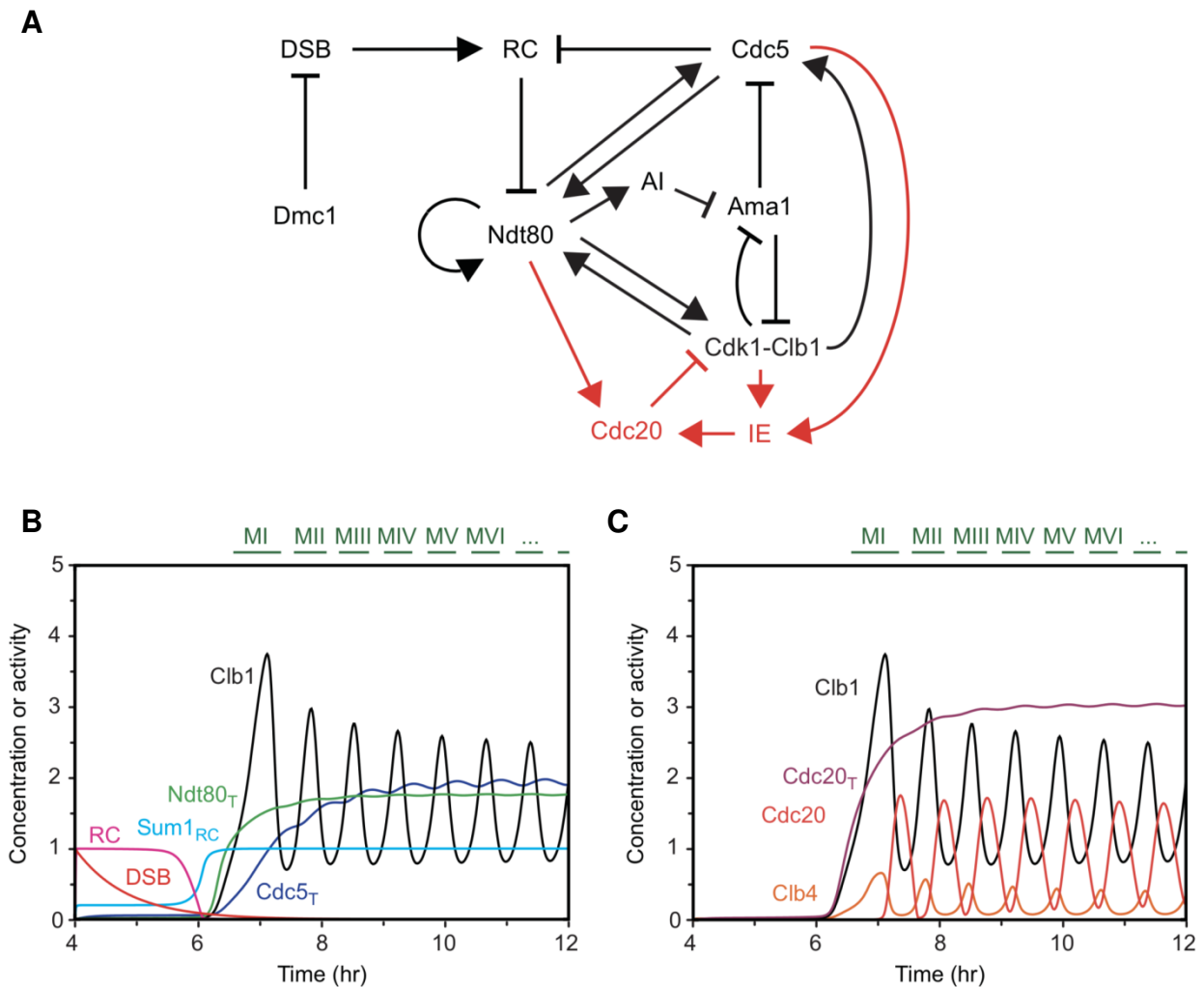


Figure 14. Combining the model of metaphase I entry with the Cdk1-APC/C oscillator provides metaphase-to-anaphase transitions. (A) Simplified wiring diagram of the combined model. Interactions provided by the oscillator are depicted in red. For simplification Cdk1-Clb4, Ama1:AI, SP and Sum1 are omitted in the diagram. ↓, positive interaction; ⊥, negative interaction. (B-C) Simulation of the model showing concentration or activity of: the RC, Ndt80 and their regulators (B); cyclins and Cdc20 (C). MI, MII, ... are metaphase I, -II, ... spindles indicating the consecutive divisions.

2.3. The properties of Cdk1-APC/C oscillator in meiosis

Periodic activation of Cdk1 counteracted by APC/C ensures that all the events of the cell cycle happen in the right order and time. In mitotic cells, during the low Cdk1 state of interphase and anaphase, APC/C activity is dominant, cyclins are poorly transcribed and constantly destroyed. Once cells enter the high Cdk1 state of metaphase, these mechanisms are reversed (Kapuy et al., 2009). Meiosis consists of a similar machinery. However, unlike during proliferation, there are only two waves of Cdk1 activity. It has been proposed that the complex regulation of cyclins may be the key to unravel how meiotic divisions are orchestrated (Carlie and Amon, 2008; Futcher, 2008). Thus, we asked whether the biological properties of cyclins may be relevant for cells to perform precisely two divisions.

2.3.1. The components of the meiotic oscillator exhibit different dynamical patterns

During meiotic divisions three M-phase cyclins are expressed: Clb1, Clb3 and Clb4. We asked which cyclins are necessary for proper activation of the oscillator and, as a consequence, for progression through two meiotic divisions. For this purpose we performed an experiment on a synchronized meiotic cell culture in cells containing deletions of different cyclins: *clb1Δ*, *clb3Δ* and *clb4Δ*. We collected immunofluorescence (IF) samples in a conventional meiotic time course, during which cells were sporulated in sporulation medium (SPM). We used Pds1 tagged at the C-terminus with 18 Myc epitopes (Pds1-myc18) as a protein marker of the progression through meiosis (Shirayama et al., 1999). We used DAPI to visualize the nuclear divisions by staining the DNA content and α -tubulin antibodies to visualize spindles. The number of the bipolar spindle indicates the progression through meiosis, which is a consequence of activity of the Cdk1-APC/C oscillator. We consider formation of one and two spindles as landmarks for meiosis I and -II, respectively. All tested mutant strains exhibit similar meiotic progression as the WT cells for the first 8 hr in SPM (**Figure 15A**). At later stages, a visible difference is observed between the tested strains. Unlike *clb3Δ* cells, which divide nuclei twice and disassemble bipolar spindles with similar kinetics as WT cells, *clb1Δ* and *clb4Δ* mutants are defective in completion of two meiotic divisions. These cells are delayed in degradation of Pds1 and disassembly of meiotic spindles. After 24 hr, half of cells are tetra-nucleated in comparison to ~90% of WT and *clb3Δ* cells (**Figure 15B**). The majority of cells abolish the activity of the oscillator, possibly due to deficiency in cyclin levels. Thus, both Clb1 and Clb4 are important for proper function of the meiotic oscillator and progression through two meiotic divisions.

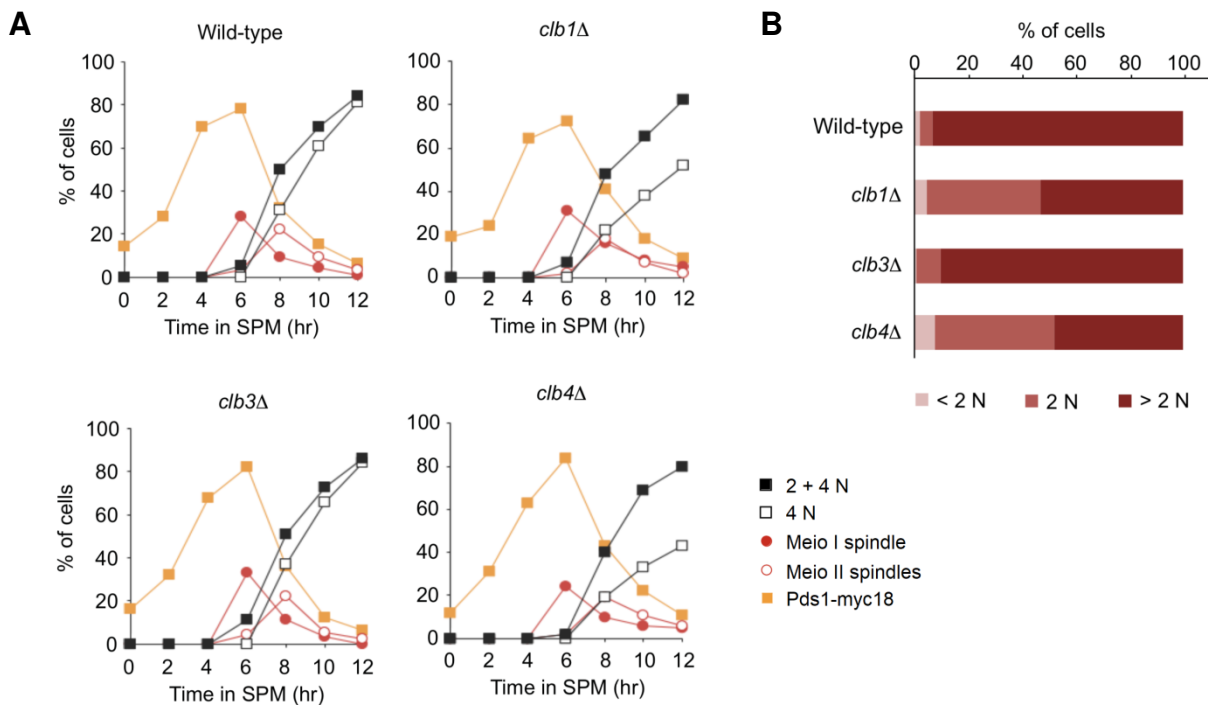


Figure 15. Clb1 and Clb4 are required for the proper activity of the meiotic oscillator. A conventional meiotic time course was performed on WT (Z30291), *clb1Δ* (Z22156), *clb3Δ* (Z30292) and *clb4Δ* (Z30293) strains expressing Pds1-myc18. **(A)** Quantification of meiotic progression by IF detection. Fixed cells were stained to detect nuclear division (2+4N is at least one division, 4N is two divisions), nuclear Pds1-myc18 signal and meiosis I (Meio I) and -II (Meio II) spindles. Plots indicate percentage of cells at each time point. **(B)** Quantification of percentage of nuclear division after 24 hr. Bar plots indicate percentage of cells with one nucleus (<2N), two nuclei (2N) and more than two nuclei (>2N).

Next, we asked about the properties of Clb1 and Clb4 during meiotic divisions that may contribute to the specific two-division model of meiosis. We quantified the nuclear signal of Clb1 and Clb4 at defined stages of meiosis. The quantification of the cyclin levels provided us with a possibility to identify the differences in the levels at meiosis I and -II. We performed a conventional meiotic time course with strains containing Clb1 and Clb4 tagged at the C-terminus with 9 Myc epitopes (Clb1-myc9 and Clb4-myc9), as well as untagged control serving as a correction for the background signal. The nuclear signal was measured at different stages of meiosis based on the morphology of the spindle and number of nuclei. Clb1 and Clb4 accumulate during metaphase I and -II. Clb1-myc9 exhibits similar average intensities during both divisions (**Figure 16A**), in contrast to Clb4-myc9 (**Figure 16B**). The signal of the latter is at least twice lower at metaphase II than at metaphase I. Unlike Clb1, Clb4 is completely degraded between meiosis I and -II. The nuclear signal of Clb1-myc9 is still detectable during anaphase I, but significantly reduced. Additionally, some portion of Clb1 diffuses to the cytoplasm (Buonomo et al., 2003). As cells progress through divisions, cyclins level do not exceed the level at metaphase I, suggesting a possible activity of the degradation during metaphase II or insufficient time for stronger accumulation at later stages of meiosis.

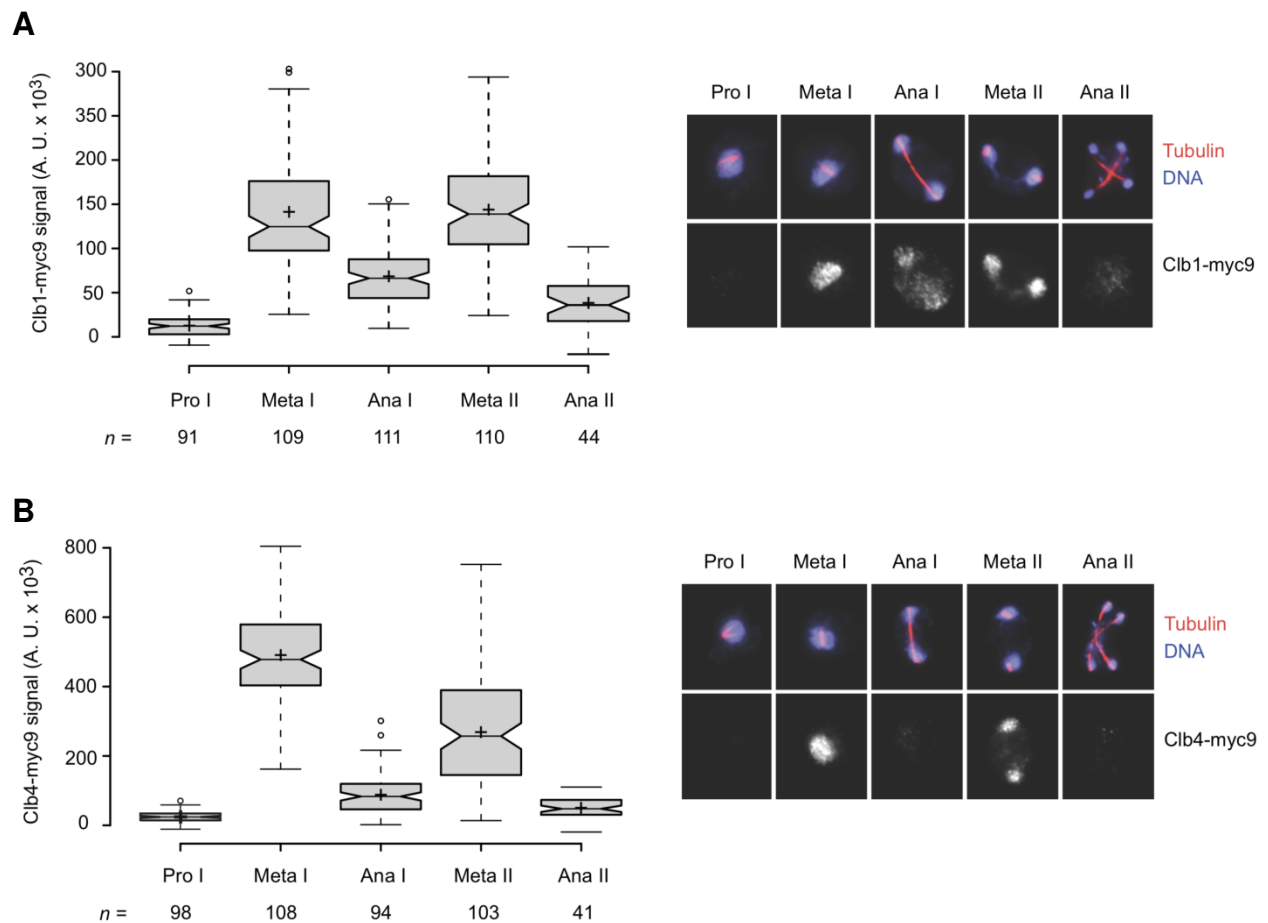


Figure 16. Clb1 and Clb4 exhibit different dynamical pattern during meiosis. Intensity of nuclear Myc signal was measured for Clb1-myc9 (Z29974) **(A)** and Clb4-myc9 (Z5157) **(B)** at different stages of meiosis. Left panels show box plots displaying quantified signal intensity of Myc-tagged proteins after subtraction of the background signal from untagged control (Z29971). Right panels show representative pictures of cells at different stages of meiosis stained for spindles (red tubulin), nuclear division (blue DNA) and Myc signal (grayscale panel). Pro I is prophase I, Meta I and Meta II are metaphase I and -II, respectively, Ana I and Ana II are anaphase I and -II, respectively. n is the number of quantified cells.

Differences in the levels of cyclins throughout meiosis prompted us to ask whether the dynamical pattern of another component of the oscillator, namely Cdc20, is different at meiosis I and -II. We quantified intensity of Cdc20 tagged at the N-terminus with 18 Myc epitopes (Myc18-Cdc20). We observed that Cdc20 protein accumulates gradually reaching the highest peak around anaphase I (**Figure 17A**). At metaphase I, we observed almost twice lower average intensity of Myc18-Cdc20 signal in comparison to subsequent stages of meiotic divisions. It has been previously proposed (Salah and Nasmyth, 2000) that Cdc20 protein forms two peaks of accumulation, which follow Cdc20 activity. However, our quantification and mathematical model presented in the previous chapter indicate that Cdc20 levels and activity exhibit a different dynamical pattern. Cdc20 protein persists at high level during meiotic divisions showing one peak of its total nuclear concentration. Cdc20 total nuclear protein gradually rises during metaphase I and is maintained until metaphase II.

To study the difference between the total nuclear level of Cdc20 and its activity, we tested the intensity of the Pds1-myc18 nuclear signal at different stages of meiosis, as Pds1 is a well-known substrate of Cdc20 (Shirayama et al., 1999). Pds1-myc18 accumulate strongly during prophase I (**Figure 17B**), due to the synthesis dependent on the Mbp1 transcription factor, but not Ndt80 (MacIsaac et al., 2006). Similar levels of Pds1-myc18 are present at metaphase I, indicating the absence of its degradation machinery. At anaphase I, the signal decreases visibly indicating high activity of APC/C^{Cdc20}. Similar to Clb4, Pds1 is completely degraded at this stage of meiosis. During the second division, cells re-accumulate Pds1, pointing to inactivation of APC/C^{Cdc20}. However, an inability to re-accumulate metaphase I-like levels of Pds1 and high levels of Cdc20 protein at the same stage prompted us to speculate about a possible basal activity of APC/C^{Cdc20} during metaphase II.

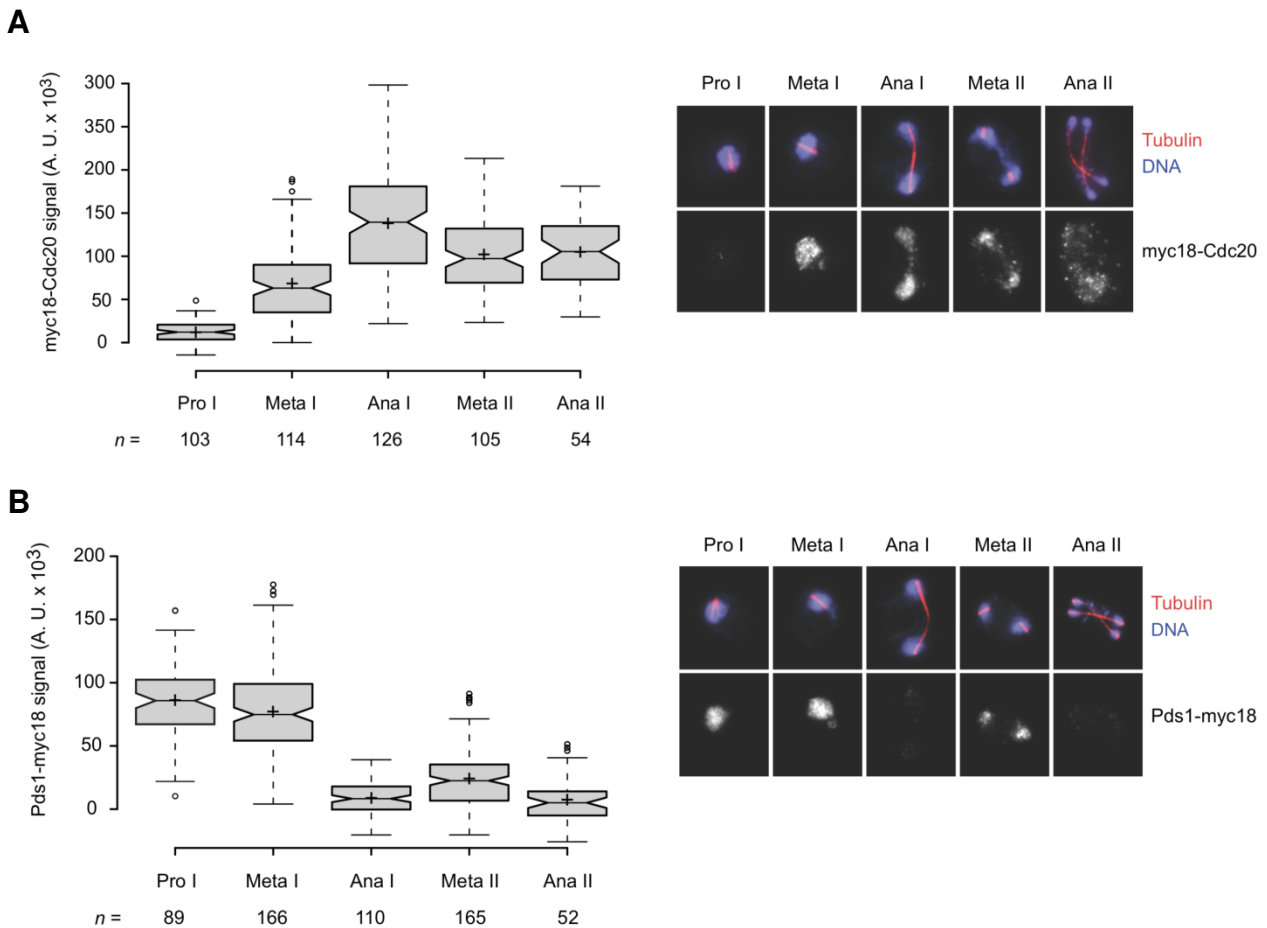


Figure 17. The dynamical pattern of Cdc20 level and activity is different throughout meiosis. Intensity of nuclear Myc signal was measured for Myc18-Cdc20 (Z29973) (**A**) and Pds1-myc18 (Z19647) (**B**) at different stages of meiosis. Left panels show box plots displaying quantified signal intensity of Myc-tagged proteins after subtraction of the background signal from untagged control (Z29971). Right panels show representative pictures of cells at different stages of meiosis stained for spindles (red tubulin), nuclear division (blue DNA) and Myc signal (grayscale panel). Pro I is prophase I, Meta I and Meta II are metaphase I and -II, respectively, Ana I and Ana II are anaphase I and -II, respectively. *n* is the number of quantified cells.

2.3.2. Recreating dynamical pattern of the components of the oscillator does not explain the two-division meiosis

We asked whether recreating the observed properties of the Cdk1-APC/C oscillator in the mathematical model is sufficient to answer the question how meiosis makes precisely two divisions. We used the combined model of the prophase I-to-metaphase I transition and the oscillator. We refitted the parameters (**Table 4**) to achieve similar dynamical pattern of Clb1, Clb4 and Cdc20 as observed experimentally during the first two divisions. These patterns include: (i) gradual accumulation of Cdc20 and persistence of the protein between meiosis I and -II; (ii) similar levels of Clb1 during metaphase I and II; (iii) half decrease in the level of Clb4 during metaphase II; (iv) incomplete degradation of Clb1 during anaphase I; (v) complete degradation of Clb4 during anaphase I.

Table 4. Parameter values of the readjusted model.¹

Equation number	Parameters and their values
13	$J_{Ndt80} = 0.1$
20	$k_{SPa} = 1$
31, 32	$k_{Clb1d4} = 0.08, k_{Clb4s2} = 0.2, k_{Clb4d1} = 0.1$
33, 35	$k_{IEa1} = 0.015, k_{Cdc20a1} = 1.5$

¹Only parameters with changed values are shown

We performed a computational simulation of the combined model with readjusted parameters. The model recreates the levels of the relevant proteins as depicted in **Figure 18**. However, the system is unable to stop the oscillations after the second division. It creates damped oscillations that stabilize at intermediate levels of cyclins and Cdc20.

The results of simulation and quantification of the nuclear signals of the main M-phase cyclins prompted us to speculate that Cdc20 substrates are regulated differently between meiosis I and -II. In the model, Clb1 degradation is slower than degradation of Clb4, which ensures a basal activity of Cdk1 during anaphase I, recreating the biologically observed pattern. Additionally, the model explains that the inability to re-accumulate metaphase I-like levels of Clb4 and Pds1 at meiosis II is due to two factors: the basal activity of Cdc20 at metaphase II and the short period of lowered activity of APC/C during the second division. Cdc20 itself exhibits an interesting dynamical pattern which is different between its total levels and activity. It is mostly caused by persistent activity of its transcription factor Ndt80, while its main activator Cdk1 exhibits an oscillatory behavior.

Although our combined model recreated physiological levels of cyclins and Cdc20, as well as Cdc20 activity, it did not result in recapitulating the exit from meiosis II. Therefore, recreating the exact levels of the components of the oscillator is not sufficient for the explanation of the progression through meiotic divisions and the exit from meiosis II. We conclude that another mechanism exists apart from the oscillator that terminates the waves of Cdk1-APC/C activities after meiosis II.

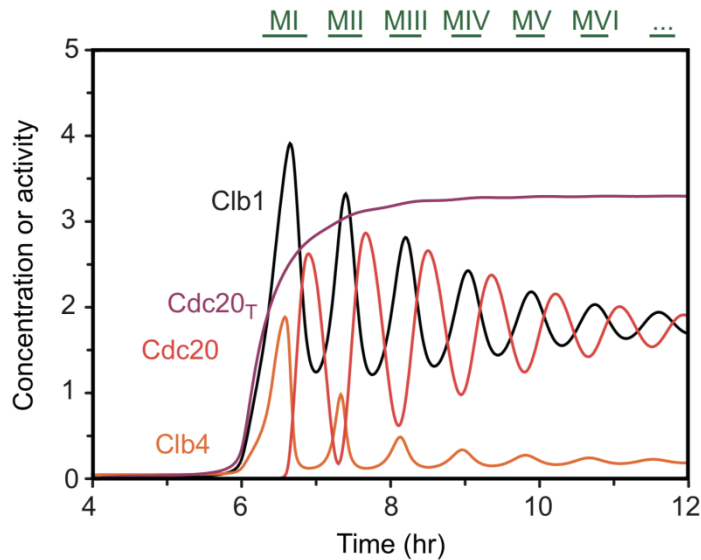


Figure 18. Model with readjusted parameters recreates the general levels of cyclins and Cdc20 in meiosis I and II. Simulation shows concentration or activity of Clb1, Clb4, Cdc20 (active form) and Cdc20_T (total levels). MI, MII, ... are metaphase I, -II, ... spindles indicating the consecutive divisions.

2.4. Role of meiosis II-specific APC/C co-activators in meiotic exit

2.4.1. A meiosis II-specific mechanism ensures termination of meiotic oscillations after completion of meiosis II

We asked whether a hypothetical mechanism for terminating the oscillations may prevent additional divisions after the exit from meiosis II. Firstly, we specified the minimal requirements of the hypothetical terminator, called Term. In order to terminate the oscillations precisely after meiosis II, accumulation and activity of the Term has to be inhibited at earlier stages of meiosis by a meiosis I-specific inhibitor, referred to as Inh (**Figure 19A**). The Inh prevents premature accumulation of the terminator, which would result in cutting-off the meiotic divisions before the completion of the second one. Thus, the initial value of the Inh is equal to 1. The inhibitor is degraded in a Cdc20-dependent manner at anaphase I (**Equation 36**). Due to the strong degradation and the synthesis independent of M-phase proteins, the inhibitor is present only during the first

division and does not re-accumulate for meiosis II. Along with its degradation, the terminator is synthesized at the exit of meiosis II. The terminator is modeled with an introduction of nonlinearity and a Hill function resulting in an ultrasensitive response (**Equation 37**). Initial value of the Term is set to 0.

$$[Inh] \frac{d}{dt} = -(k_{Inhd1} + k_{Inhd2} \cdot [Cdc20]) \cdot [Inh] \quad (36)$$

$$[Term] \frac{d}{dt} = k_{Terms1} \cdot \frac{J_{Term}^n}{J_{Term}^n + [Inh]^n} - k_{Termd1} \cdot [Term] \quad (37)$$

In order to terminate the oscillations, the terminator has to inactivate key meiotic regulators. We assumed that it stops the oscillations through degradation of Clb1 and Clb4, and, additionally, Ndt80 and Cdc5. Degradation of Ndt80 results in the inability to re-synthesize cyclins, as well as in decline in Cdc20 levels and activity. Equations describing these components of the model were modified with introduction of the Term-dependent degradation. **Equations 38-39** for regulation of Clb1 and Clb4 were based on previous **Equations 31-32**. **Equations 40-43** for regulation of Ndt80 and Cdc5 were based on previous **Equations 11-12, 21-22**. New parameter values are presented in **Table 5**.

$$[Clb1] \frac{d}{dt} = k_{Clb1s1} + k_{Clb1s2} \cdot [Ndt80] - (k_{Clb1d1} + k_{Clb1d2} \cdot [Ama1] + k_{Clb1d3} \cdot [Ama1_T] + k_{Clb1d4} \cdot [Cdc20] + k_{Clb1d5} \cdot [Term]) \cdot [Clb1] \quad (38)$$

$$[Clb4] \frac{d}{dt} = k_{Clb4s1} + k_{Clb4s2} \cdot [Ndt80] - (k_{Clb4d1} + k_{Clb4d2} \cdot [Ama1] + k_{Clb4d3} \cdot [Ama1_T] + k_{Clb4d4} \cdot [Cdc20] + k_{Clb4d5} \cdot [Term]) \cdot [Clb4] \quad (39)$$

$$[Ndt80_T] \frac{d}{dt} = k_{Ndt80s1} + k_{Ndt80s2} \cdot \frac{[Ndt80]}{J_N + [Ndt80]} - (k_{Ndt80d1} + k_{Ndt80d2} \cdot [Term]) \cdot [Ndt80_T] \quad (40)$$

$$[Ndt80] \frac{d}{dt} = (k_{Ndt80a1} + k_{Ndt80a2} \cdot [Cdc5]) \cdot ([Ndt80_T] - [Ndt80]) - (k_{Ndt80i1} + k_{Ndt80d1} + k_{Ndt80d2} \cdot [Term]) \cdot [Ndt80] \quad (41)$$

$$[Cdc5_T] \frac{d}{dt} = k_{Cdc5s1} + k_{Cdc5s2} \cdot [Ndt80] - (k_{Cdc5d1} + k_{Cdc5d2} \cdot [Ama1] + k_{Cdc5d3} \cdot [Ama1_T] + k_{Cdc5d4} \cdot [Term]) \cdot [Cdc5_T] \quad (42)$$

$$[Cdc5] \frac{d}{dt} = (k_{Cdc5a1} + k_{Cdc5a2} \cdot [Clb1] + k_{Cdc5a3} \cdot [Clb4]) \cdot ([Cdc5_T] - [Cdc5]) - (k_{Cdc5i1} + k_{Cdc5d1} + k_{Cdc5d2} \cdot [Ama1] + k_{Cdc5d3} \cdot [Ama1_T] + k_{Cdc5d4} \cdot [Term]) \cdot [Cdc5] \quad (43)$$

Table 5. Parameter values of the readjusted model with introduction of hypothetical terminator.¹

Equation number	Parameters and their values
36	$k_{Inh1} = 0.002, k_{Inh2} = 0.1$
37	$k_{Terms1} = 1, k_{Termd1} = 0.1, J_{Term} = 0.1^{-4}, n = 2$
38, 39	$k_{Clb1d5} = 0.5, k_{Clb4d5} = 1$
40-43	$k_{Ndt80d2} = 0.4, k_{Cdc5d4} = 0.1$

¹Only newly introduced parameters are presented.

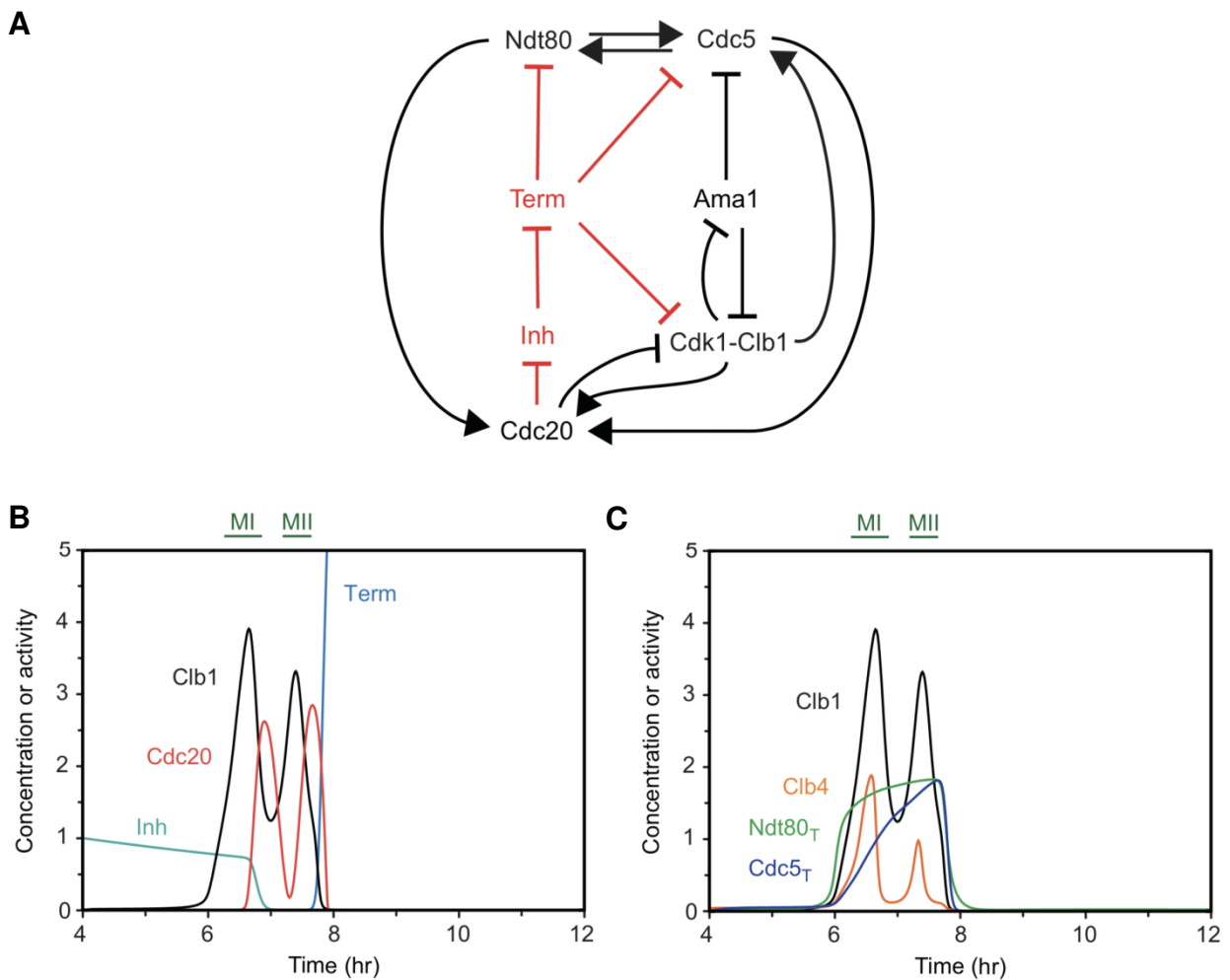


Figure 19. Meiosis II-specific hypothetical terminator of meiotic oscillations limit the number of divisions. The readjusted model was extended by inclusion of the hypothetical terminator (Term), which degrades cyclins, Ndt80 and Cdc5, and its meiosis I-specific inhibitor (Inh). **(A)** Simplified wiring diagram with inclusion of the Term module depicted in red. For simplification some interactions are omitted from the diagram. ↓, positive interaction; ⊥, negative interaction. **(B-C)** Simulation of the model with Term-dependent degradation of cyclins, Ndt80 and Cdc5 showing concentration or activity of Clb1, Cdc20, the terminator and its inhibitor **(B)** or Clb1, Clb4, Ndt80_T, Cdc5_T and Cdc20_T **(C)**. MI and MII are metaphase I and -II spindles indicating the consecutive divisions.

We asked whether degradation of key meiotic regulators introduced in the combined model is sufficient to stop the oscillations precisely after the second division and to recreate the WT phenotype. We performed simulations of the model with introduced Term-dependent degradation of cyclins, Ndt80 and Cdc5 in meiosis II. The hypothetical terminator appears at the exit from meiosis II after degradation of its inhibitor at anaphase I (**Figure 19B**). It triggers degradation of Clb1 and Clb4, therefore completely inactivating Cdk1 at the onset of anaphase II (**Figure 19C**). The terminator triggers abrupt degradation of Ndt80 and Cdc5 at around 8 hr. With degradation of Ndt80, all major regulators of meiosis that do not depend on the hypothetical terminator, such as Cdc20_T, follow the decline of Ndt80_T. This decline is a result of the strong dependence of the synthesis regulated by Ndt80 and the fast background degradation of the protein. The oscillator stops after the second division with disassembly of meiosis II spindles and degradation of the major M-phase regulators. We conclude that in order to complete meiosis precisely after the second division, cells need to activate a meiosis II-specific machinery exhibiting the properties of the hypothetical terminator. Thus, the minimal requirements of the terminator of the oscillations are: (i) meiosis I-specific inhibition of its accumulation and activity; (ii) meiosis II-specific dynamical pattern; (iii) direct or indirect degradation of Ndt80 and cyclins.

2.4.2. Cdh1 does not regulate two meiotic divisions

We hypothesized that the oscillations of Cdk1 and APC/C activities during meiosis are limited by a meiosis II-specific mechanism involved in degradation of key meiotic regulators. The importance of this mechanism prompted us to seek the biological identity of the terminator and its meiosis I-specific inhibitor.

In mitosis, the exit from a division is triggered by activity of APC/C^{Cdc20} and APC/C^{Cdh1} (Visintin et al., 1997). Both, Cdc20 and Cdh1, are present also in meiosis. Due to the fact that Cdc20 is a component of the oscillator, it is unlikely that it plays a role in the termination of meiotic oscillations. Thus, we focused on examining the role of other APC/C co-activators, such as Cdh1 and Ama1. Firstly, we focused on studying the relevance of Cdh1 for the progression through meiosis and meiotic exit. In meiosis, Cdh1 activity is regulated by two kinases: Ime2 and Cdk1 (Bolte et al., 2002; Jaspersen et al., 1999; Visintin et al., 1998). They phosphorylate Cdh1 during both divisions leading to its inability to bind and activate APC/C. Therefore, Cdh1 is active only in the absence of the kinases: during entry into meiosis and possibly after the exit from meiosis II. This pattern of Cdh1 activity creates the possibility of Cdh1 being involved

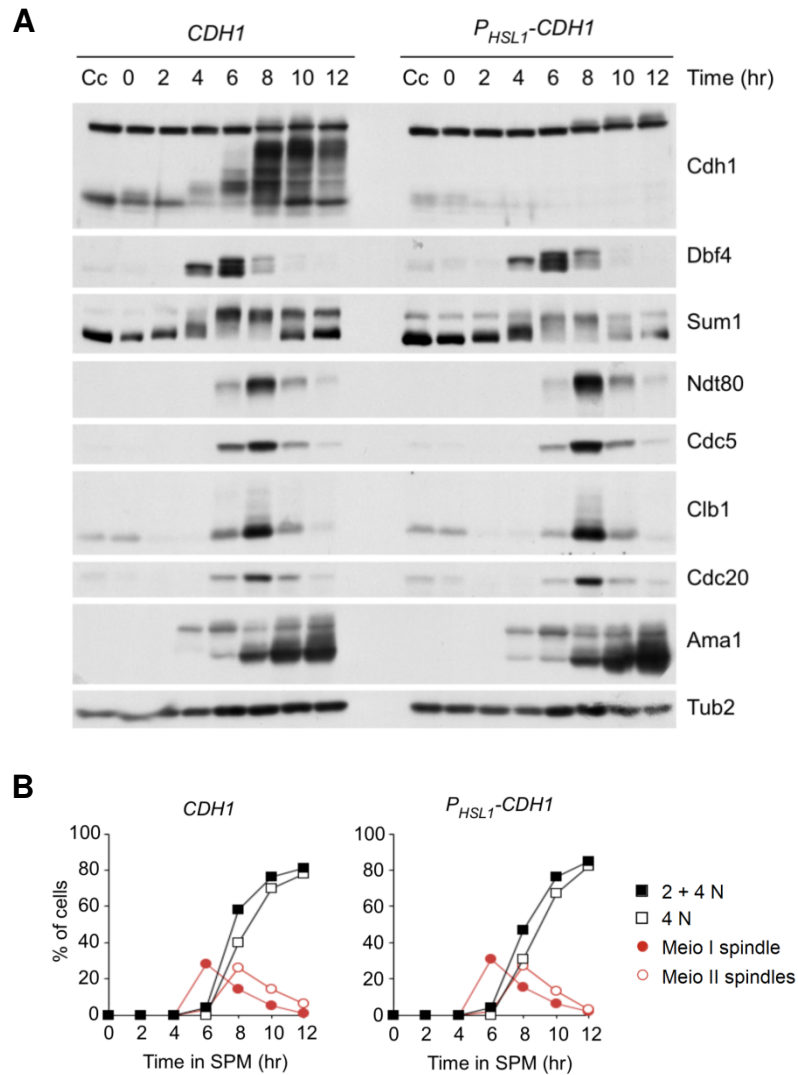


Figure 20. Cdh1 depletion from meiosis does not affect the progression through meiotic divisions and the exit from meiosis II. A conventional meiotic time course was performed with *CDH1* (Z29971) and *P_{HSL1}-CDH1* (Z27965) strains. **(A)** Immunoblot detection of proteins. Cc indicates sample taken from proliferating cells. **(B)** Quantification of meiotic progression by IF detection of nuclear division (2+4N is at least one division, 4N is two divisions) and meiosis I (Meio I) and -II (Meio II) spindles.

in the termination of meiotic oscillations after completion of meiosis II in a similar way as the hypothetical terminator. To test this hypothesis, we performed a conventional meiotic time course on cells lacking Cdh1 in meiosis. We placed *CDH1* under a mitosis-specific *HSL1* promoter in order to not disrupt the preceding mitotic divisions. *P_{HSL1}-CDH1* cells accumulate M-phase proteins at 8 hr and form bipolar spindle with similar kinetics as the control *CDH1* cells. In both strains the meiosis I-specific protein Dbf4 is degraded at the same time, indicating the exit from meiosis I (**Figure 20A**). WT cells accumulate unphosphorylated form of Cdh1 at 10 hr (the fastest migrating band), indicating its activation at the late stage of meiosis. Cells depleted of Cdh1 lose the protein during first hours in meiosis. Both strains dephosphorylate other substrate of Cdk1 and Ime2, namely Sum1, at 10 hr, indicating the complete inactivation of these

kinases. At this time, majority of cells degrade M-phase proteins, disassemble bipolar spindles and complete two divisions (**Figure 20B**). Degradation of Cdc5 and Ndt80 is triggered by the activity of strongly accumulated Ama1 in both strains. These results indicate that Cdh1 activity does not regulate the exit from meiosis and does not terminate meiotic oscillations. Additionally, depletion of Cdh1 does not cause defects in meiotic progression. It is possible that strong accumulation of Cdh1 protein during meiosis in WT cells is important for late events of meiosis associated with sporulation or G1-phase arrest.

2.4.3. Ama1 exhibits properties of the hypothetical terminator of meiotic oscillations

Ama1 is a meiosis-specific activator of APC/C that exhibits similar properties to the hypothetical terminator of meiotic oscillations. It is not expressed during mitosis, thus it does not affect the cell cycle oscillator during proliferation. Furthermore, it has been shown that it targets for degradation M-phase cyclins, such as Clb1 and Clb4, as well as Cdc5 (Okaz et al., 2012). Ndt80 appears to be indirectly affected by the Ama1 activity. Although it has been suggested that strong accumulation of Ama1 protein at the exit from meiosis II may play a role in the completion of meiosis, Ama1 is known to exhibit additional functions during meiosis, being required for proper transition from prophase I to metaphase I.

Unlike the hypothetical terminator, Ama1 is present during prophase I and its activity prevents premature accumulation of M-phase cyclins. Furthermore, Ama1 is regulated by Clb1-dependent inhibition. Additionally, Ama1 is inhibited through binding to an Ndt80-dependent stoichiometric inhibitor of unknown identity, called an additional inhibitor (AI). Mutual inhibition between Ama1, Clb1 and AI creates a double-negative feedback loop, which is a property that allows irreversible exit from prophase I. We asked whether this specific dynamical pattern of Ama1 activity and accumulation allows the termination of meiotic oscillations after completion of meiosis II.

We developed a model, in which we replaced the hypothetical terminator by Ama1, as presented in wiring diagram in **Figure 21A**. We incorporated into the combined model an additional form of regulated total levels of Ama1, referred to as Ama1_T. High accumulation of Ama1 is inhibited in early stages of meiosis by a meiosis I-specific mechanism. We assumed that the inhibitor of Ama1 synthesis is based on the same principles as the hypothetical inhibitor, which is present during prophase I (initial value set to 1), preventing premature accumulation of Ama1. The inhibitor of the synthesis is degraded during anaphase I in a Cdc20-dependent manner. To avoid re-accumulation

of the inhibitor after the exit from meiosis II, we added its Ama1-dependent degradation (**Equation 44**).

$$[Inh] \frac{d}{dt} = -(k_{Inhd1} + k_{Inhd2} \cdot [Cdc20] + k_{Inhd3} \cdot [Ama1] + k_{Inhd4} \cdot [Ama1_T]) \cdot [Inh] \quad (44)$$

Ama1 synthesis is inhibited with a Hill kinetics (**Equation 45**). Due to the fact that Ama1 is synthesized in lower levels in prophase I and metaphase I, we assumed additional inhibitor-independent synthesis of the protein, which was introduced in the model with the initial value of Ama1_T equal to 1. Degradation of Ama1 depends on unknown mechanism and was also included in a modified version of the equation depicting unphosphorylated form of Ama1 (**Equation 46**). As Ama1 basal activity is required for prophase I, the initial value of Ama1_{AT} was set to 1.

$$[Ama1_T] \frac{d}{dt} = k_{Ama1s1} \cdot \frac{J_{Inh}^n}{J_{Inh}^n + [Inh]^n} - k_{Ama1d1} \cdot [Ama1_T] \quad (45)$$

$$[Ama1_{AT}] \frac{d}{dt} = k_{Ama1a1} \cdot \frac{[Ama1_T] - [Ama1_{AT}]}{J_{Ama1} + [Ama1_T] - [Ama1_{AT}]} - (k_{Ama1i1} + k_{Ama1i2} \cdot [Cib1]) \cdot \frac{[Ama1_{AT}]}{J_{Ama1} + [Ama1_{AT}]} - k_{Ama1d1} \cdot [Ama1_{AT}] \quad (46)$$

Ama1 triggers degradation of Cdc5 and cyclins, as described with **Equations 21-22, 31-32**. Additionally, we included Ama1-dependent degradation of Ndt80 (**Equations 47-48**), as indicated by simulations of the hypothetical terminator. Newly introduced parameters or parameters with readjusted values are given in **Table 6**.

$$[Ndt80_T] \frac{d}{dt} = k_{Ndt80s1} + k_{Ndt80s2} \cdot \frac{[Ndt80]}{J_N + [Ndt80]} - (k_{Ndt80d1} + k_{Ndt80d2} \cdot [Ama1] + k_{Ndt80d3} \cdot [Ama1_T]) \cdot [Ndt80_T] \quad (47)$$

$$[Ndt80] \frac{d}{dt} = (k_{Ndt80a1} + k_{Ndt80a2} \cdot [Cdc5]) \cdot ([Ndt80_T] - [Ndt80]) - k_{Ndt80i1} \cdot [Ndt80] - (k_{Ndt80d1} + k_{Ndt80d2} \cdot [Ama1] + k_{Ndt80d3} \cdot [Ama1_T]) \cdot [Ndt80] \quad (48)$$

Table 6. Parameter values of the model with Ama1 as a terminator of the oscillations.¹

Equation number	Parameters and their values
31, 32	$k_{Cib1s2} = 0.08, k_{Cib1d4} = 0.035, k_{Cib4s2} = 0.1, k_{Cib4d1} = 0.2$
35	$k_{Cdc20a1} = 2$
44	$k_{Inhd3} = 0.005, k_{Inhd4} = 0.002$
45, 46	$k_{Ama1s1} = 1, k_{Ama1d1} = 0.015, J_{Inh} = 0.0002, n = 2$
47, 48	$k_{Ndt80d2} = 0.2, k_{Ndt80d3} = 0.15$

¹Only newly introduced or modified parameters are presented.

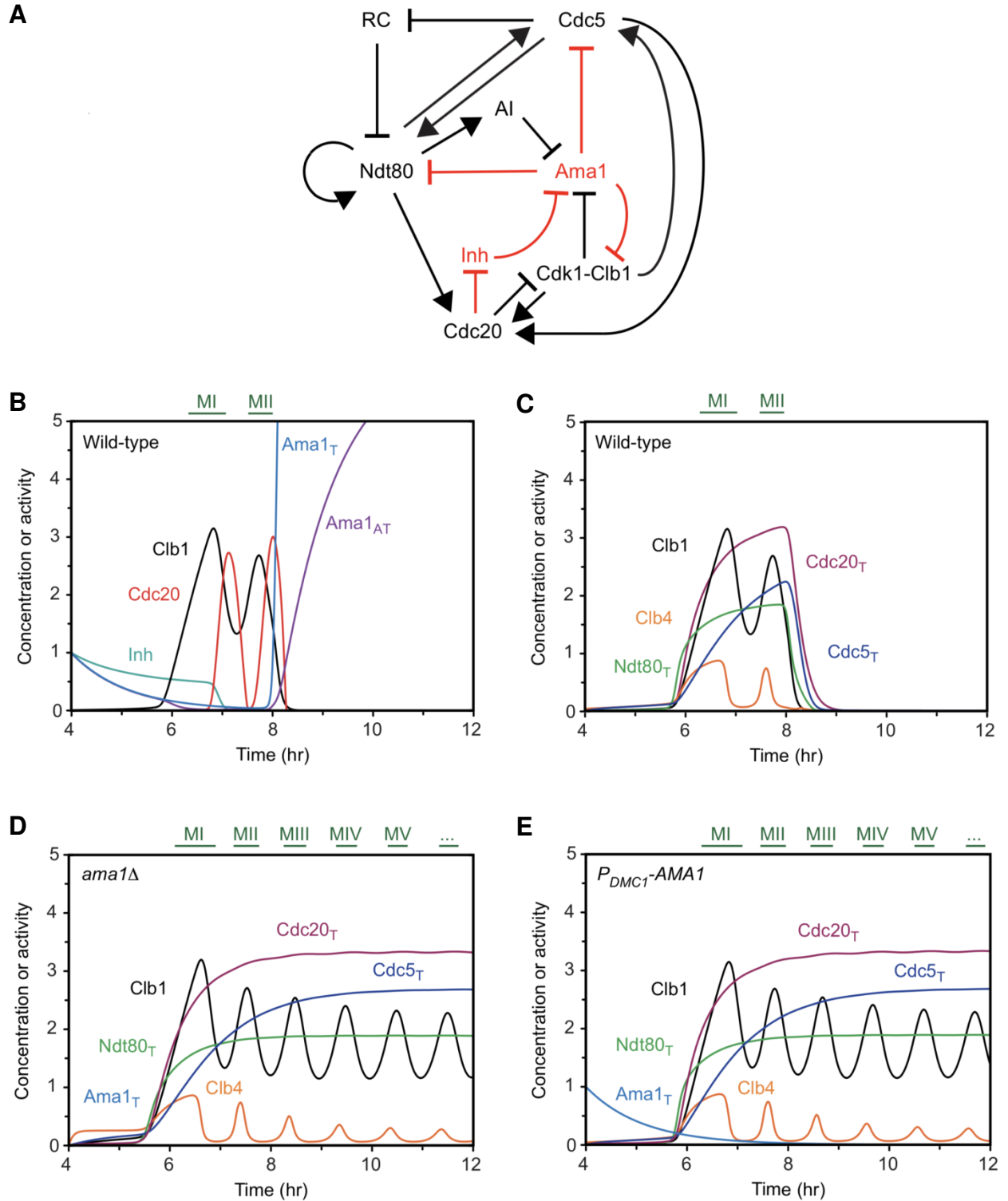


Figure 21. Ama1 exhibits the properties of hypothetical terminator. The hypothetical terminator module was replaced by Ama1-dependent degradation of cyclins, Ndt80 and Cdc5. Additionally, meiosis I-specific inhibitor of Ama1 synthesis, Inh, was included. **(A)** Simplified wiring diagram with Ama1 module depicted in red. For simplification some interactions are omitted from the diagram. \downarrow , positive interaction; \perp , negative interaction. **(B-D)** Simulation of the model depicting concentration or activity of different forms of Ama1, Inh, Clb1 and Cdc20 **(B)** or Ama1 substrates **(C-E)** in the presence of Ama1 **(B-C)**, in the absence of Ama1 ($Ama1_T = Ama1_{AT} = 0$, $k_{Ama1s1} = 0$) **(D)** or in the absence of Ama1 from meiosis II but not prophase I ($Ama1_T = Ama1_{AT} = 1$, $k_{Ama1s1} = 0$) **(E)**. MI, MII, ... are metaphase I, -II, ... spindles indicating the consecutive divisions.

We simulated a time course recreating a conventional biological experiment. Simulation of the model assuming Ama1 taking the role of the hypothetical terminator shows strong accumulation of Ama1 at meiosis II (**Figure 21B**). Ama1 accumulates at prophase I, where it inhibits premature accumulation of M-phase proteins. Ama1 level decreases exponentially as cells progress to metaphase I. At the exit from meiosis II Ama1_T rises abruptly as its inhibitor is degraded by Cdc20. With degradation of Clb1 at meiosis II, Ama1 activity rises following increase in its total level. This creates an irreversible switch, leading to a complete degradation of cyclins, Ndt80 and Cdc5, as well as indirect substrates such as Cdc20 (**Figure 21C**). We modeled Ama1 as a terminator mechanism, thus its exclusion from meiosis results in repetitive events of high and low Cdk1 activity that mimic multiple divisions (**Figure 21D**). Due to the fact that deletion of *AMA1* causes failure in proper completion of meiotic recombination and premature entry into metaphase I (Okaz et al., 2012), we tested a reduction of Ama1 levels only during meiosis II (**Figure 21E**). For this purpose we mimicked expression of *AMA1* from the *DMC1* promoter active during recombination. We observed that the activity of Ama1 in prophase I does not affect the exit from meiosis II. Cells perform multiple oscillations after the exit from meiosis II. Thus, the model predicts that the meiosis II-specific high accumulation and high activity of Ama1 is required for terminating Cdk1-APC/ C^{Cdc20} oscillations after the exit from meiosis II.

To verify the results obtained by the model, we performed biological experiment. To test the importance of Ama1 during later stages of meiosis without disrupting the entry into meiosis I, we made use of a depletion that expresses *AMA1* from the *DMC1* promoter. The experiment was performed by Dr. Orlando Argüello-Miranda (Argüello-Miranda, 2015). We performed a conventional meiotic time course using *ama1Δ P_{DMC1}-AMA1* strain. Pds1-myc18 was stained as a protein marker of progression through meiotic divisions. In this setup, WT cells accumulate high level of Ama1 after 10 hr, while *ama1Δ P_{DMC1}-AMA1* cells synthesize the protein only until 6 hr (**Figure 22A**). Cells from both strains progress through two divisions normally and exit around 10 hr degrading cyclins. At this time ~80% of cells disassemble meiotic spindles and complete two divisions (**Figure 22B**). Nonetheless, *ama1Δ P_{DMC1}-AMA1* cells are unsuccessful in degradation of Ndt80, Cdc5 and Cdc20, as predicted by the model. Furthermore, usually dephosphorylated proteins, such as Sum1 and Cdh1, exhibit persistent phosphorylation, resulting in their inactivity and suggesting continuous activity of M-phase kinases, such as Ime2.

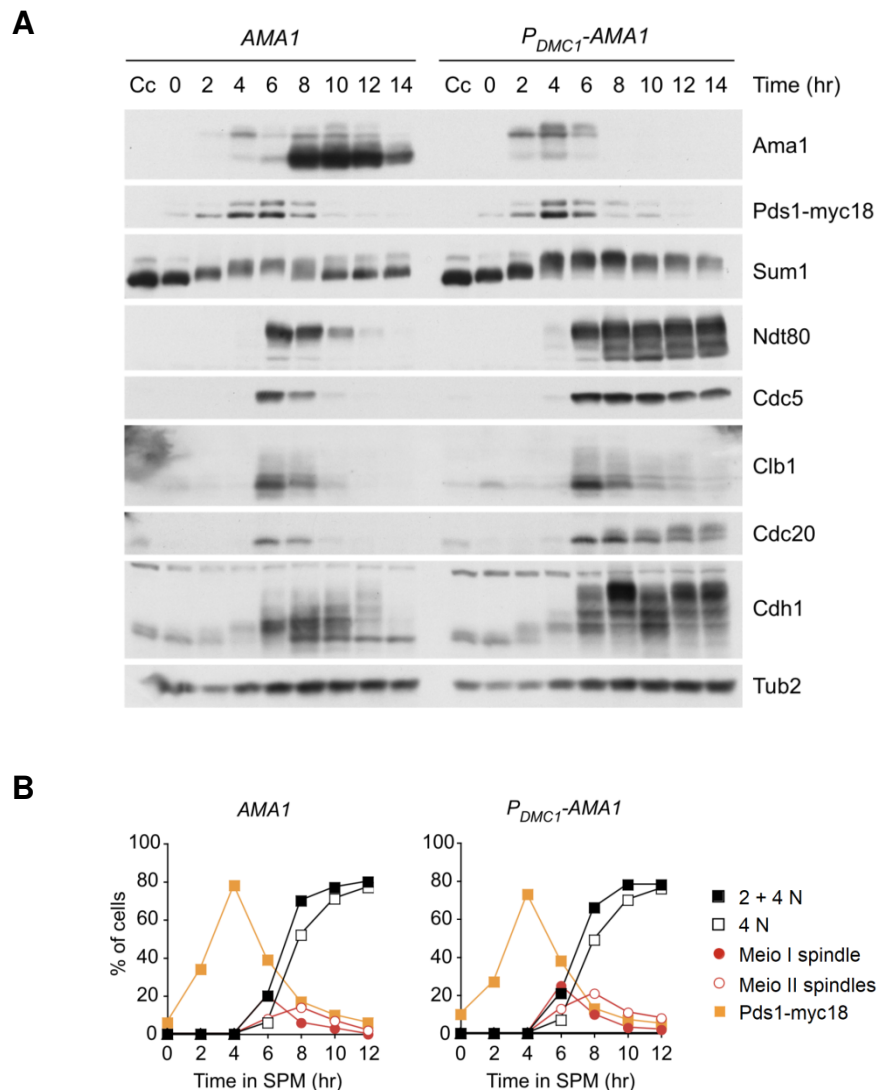


Figure 22. Ama1 depletion from meiosis II affects the exit from meiosis. A conventional meiotic time course was performed with *AMA1* (Z20217) and *ama1Δ P_{DMC1}-AMA1* (Z20219) cells. **(A)** Immunoblot detection of proteins. Cc means proliferating cells. **(B)** Quantification of meiotic progression by IF detection of nuclear division (2+4N is at least one division, 4N is two divisions), meiosis I (Meio I) and -II (Meio II) spindles, and nuclear Pds1-myc18. Taken from (Argüello-Miranda, 2015).

Unlike predicted by the model, cells without Ama1 in meiosis II do not perform additional divisions but exit from meiosis with complete degradation of cyclins and disassembly of meiotic spindles. These discrepancies between the results of computational experiment and biological experiment indicate incorrect assumptions in the model. Although both types of experiments show significant difference in the exit from meiosis in the absence of Ama1 with maintenance of the key meiotic regulators, the mathematical model incorrectly predicts the appearance of multiple Cdk1 oscillations after meiosis II. We speculate that *ama1Δ* does not show a typical phenotype of gene deletion with loss of function. It rather causes significant changes in the regulatory network, resulting in a robust regulation of termination of meiotic oscillations. In the absence of Ama1, usually degraded Ndt80 and Cdc20 proteins

persist longer after the exit from meiosis II. Moreover, other proteins, such as Cdh1, show modifications that differs from the WT situation. Due to the fact that even with the persistence of the transcription factor of cyclins, Ndt80, they are not present for meiosis III, we speculated that additional APC/C-dependent mechanism is involved in inhibition of their re-accumulation and thus in stopping the meiotic oscillations. Therefore, we suggest that deletion of *AMA1* may cause other proteins to acquire the function of Ama1 in the termination of the oscillations by keeping strong degradation of cyclins and thus inhibition of Cdk1 activity after meiosis II.

2.4.4. Cdh1 does not take the role of Ama1 in termination of the oscillations

We asked whether another mechanism apart from Ama1 is involved in terminating the oscillations. Due to the fact that Cdh1 is modified after the exit from meiosis II, we tested whether it takes the role of Ama1 in limiting the number of divisions in meiosis. We performed a conventional meiotic time course comparing *CDH1* and *P_{HSL1}-CDH1* in *ama1Δ P_{DMC1}-AMA1* genetic background. Both strains progress through meiosis with similar kinetics, as indicated by the accumulation of M-phase proteins (**Figure 23A**) and IF counting of Pds1-myc18 signals, bipolar spindles and nuclear division (**Figure 23B**). Depletion of Cdh1 does not affect degradation of cyclins and Pds1-myc18 and does not cause re-accumulation of these proteins after completion of meiotic divisions. Cells degrade Pds1-myc18, disassemble bipolar spindles and complete two divisions within 12 hr. Thus, Cdh1 is not important for termination of meiotic oscillations, as well as general progression through meiotic divisions. In the absence of Ama1, Cdh1 does not take its role as a terminator of the oscillations and does not influence the reduction of cyclin accumulation after the exit from meiosis II. However, in both strains containing WT or depleted Cdh1, we observed strong accumulation and persistence of Cdc20. Therefore, we speculated that not Cdh1, but rather Cdc20 may be relevant in termination of the oscillations. Normally, Cdc20 functions as a component of the oscillator. However, in the absence of Ama1 the properties of the network controlling two divisions may result in Cdc20 taking the usual role of Ama1 as the terminator of the oscillations. Stabilized Cdc20 after the exit from meiosis II may continuously degrade cyclins preventing the entry into meiosis III.

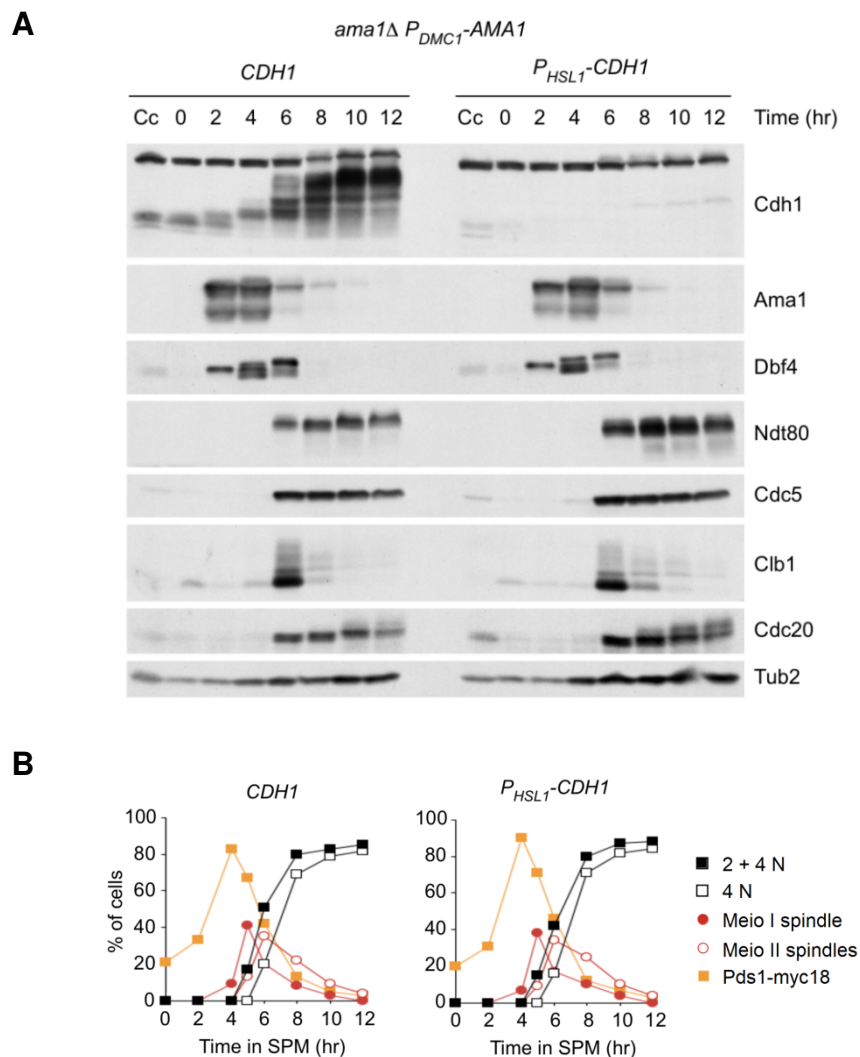


Figure 23. Depletion of Cdh1 in the absence of Ama1 in meiosis II does not cause defects in the exit from meiosis. A conventional meiotic time course was performed in *ama1Δ P_{DMC1}-AMA1* strains containing *CDH1* (Z22388) or *P_{HSL1}-CDH1* (Z28157). **(A)** Immunoblot detection of proteins. Cc means proliferating cells. **(B)** Quantification of meiotic progression by IF detection of nuclear division (2+4N is at least one division, 4N is two divisions), meiosis I (Meio I) and -II (Meio II) spindles, and nuclear Pds1-myc18.

2.5. Regulation of meiotic exit by Cdc20

We demonstrated that Ama1 is involved in the control of some of the events of the exit from meiosis II. It may take a role of the terminator of the meiotic oscillations in WT cells. However, the absence of the activity of this protein in meiosis II does not cause the predicted phenotype of multiple oscillations. Thus, we speculated that the loss of Ama1 function leads to the modification of the entire meiotic network and the gain of function by another APC/C co-activator. Since we excluded Cdh1 as a possible regulator of meiotic exit, we focused on the role of a component of meiotic oscillator, Cdc20. Indeed, Cdc20 exhibits modification at the exit from meiosis II in the absence of Ama1, suggesting its possible function as the terminator of the oscillations.

2.5.1. The model predicts that Cdc20 acts as the terminator of the oscillations in the absence of Ama1

To test the possibility of Cdc20 taking the role of the terminator, we first performed computational simulations. We revised the previous model describing Ama1 as a terminator, to be able to create more realistic dynamical patterns of proteins and recapitulate the *ama1Δ* phenotype with persisting Cdc20 in meiosis II. First, we readjusted the model parameters to fit the WT and *ama1Δ* phenotypes, as well as biological observations regarding the dynamics of the components of the oscillator. For better description of reality, we readjusted the model using parameters derived from experiments. We measured parameter values of protein degradation by performing a protein degradation assay (Baliga et al., 1969; Chou and Deshaies, 2011). It is used to measure half-lives of studied proteins by inactivating the translational elongation by the addition of cycloheximide (CHX) (Schneider-Poetsch et al., 2009). We divided cell cultures into a DMSO culture, serving as a control of meiotic progression, and a CHX culture. We studied three forms of degradation introduced in the model: background degradation, Cdc20-dependent degradation and Ama1-dependent degradation. First, we studied protein degradation triggered by Cdc20 and compared it to the background degradation to identify the effect of Cdc20. We performed experiments in metaphase I-arrested cells in the absence of Cdc20 and in anaphase I cells in the presence of Cdc20. To achieve high level of synchrony and resolution allowing manipulation of cells at a precise stage of meiosis, we used a system of *CDC20*-meiotic-arrest/release, *CDC20-mAR*, developed recently in our laboratory (Argüello-Miranda et al., 2017). In this system, cells are arrested at metaphase I by expressing *CDC20* from the mitotic *CLB2* promoter (*P_{CLB2}-CDC20*). At 8 hr, cells are released from the arrest to progress synchronously through meiotic divisions. This is achieved by the activation of an additional copy of *CDC20* placed under the inducible *CUP1* promoter (*P_{CUP1}-CDC20*) by addition of CuSO_4 . After the release from the arrest, cells enter anaphase I synchronously and complete divisions within 120 min.

To study the background degradation of M-phase proteins ("Meta I"), cells were arrested in metaphase I and treated with DMSO or CHX. DMSO culture exhibit increase of protein level (**Figure 24A**). The majority of detected proteins stabilize in CHX culture, indicating the absence of a degradation machinery. Ama1 is the only unstable protein. To test Cdc20-dependent degradation, we released cells from the metaphase I-arrest at 8 hr ("Ana I") and added DMSO or CHX to the cultures 40 min later. At this time, most of the cells enter anaphase I, as indicated by the disappearance of the meiosis I-specific

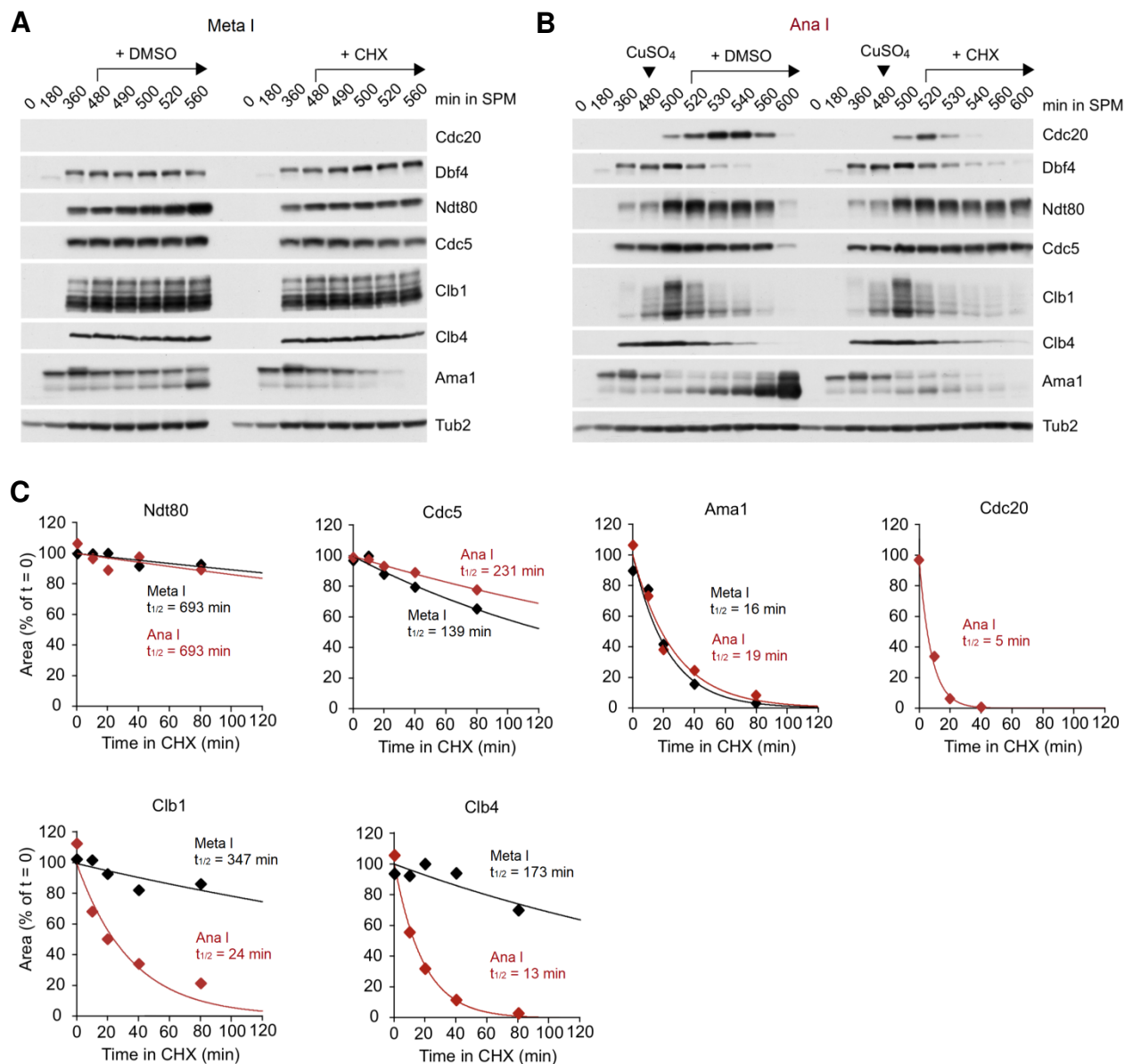


Figure 24. Levels and stability of meiotic regulators in the presence and absence of Cdc20 in meiosis I. *CDC20-mAR* cells (Z29418) were transferred to SPM ($t = 0$) and treated with solvent (DMSO, 0.5%) or cycloheximide (CHX, 0.5 mg/ml) at the indicated times. Proteins were detected in whole-cell extracts by immunoblotting. **(A)** Immunoblot detection of proteins in metaphase I-arrested cells (Meta I). DMSO/CHX was added at $t = 480$ min. **(B)** Immunoblot detection of proteins at anaphase I cells (Ana I) after release from metaphase I-arrest. Cells were treated with 10 μ M of CuSO₄ at $t = 480$ min and with DMSO/CHX at $t = 520$ min. **(C)** Graphs show half-lives ($t_{1/2}$) of proteins measured from CHX-treated cultures. Signal intensity was compared between metaphase I cells (Meta I) in the absence of Cdc20 and anaphase I cells (Ana I) in the presence of Cdc20. Data points are mean values from 2 gels.

protein Dbf4 (**Figure 24B**). Cells from the DMSO culture progress through meiosis normally, accumulating high amounts of Ama1 and degrading M-phase proteins. By contrast, the addition of CHX at anaphase I does not allow accumulation of Ama1, resulting in stabilization of Ndt80 and Cdc5, but not cyclins. Clb1 and Clb4 are stable in the absence of Cdc20 (half-lives >2 hr) similarly to Ndt80 and Cdc5 and are degraded abruptly during anaphase I (half-lives ~24 and 13 min, respectively) (**Figure 24C**). Interestingly, we observed slower degradation of Clb1, which is in agreement with previous quantification of Clb1 and Clb4 levels at different stages of meiosis. Slower degradation of Clb1 may be important for keeping a basal activity of Cdk1 during anaphase I and thus allowing fast re-accumulation of cyclins for metaphase II.

Next, we studied the stability of Ndt80 and Cdc5 in meiosis II to obtain Ama1-dependent degradation rates. We treated *AMA1* cells ("AMA1") and *ama1Δ P_{DMC1}-AMA1* cells ("no AMA1") with DMSO or CHX 60 min after the release from metaphase I-arrest. At this time, cells enter meiosis II. DMSO-treated cells degrade cyclins and exit meiosis in the presence and absence of Ama1 (**Figure 25A-B**). As expected, *ama1Δ P_{DMC1}-AMA1* cells have low levels of Ama1 protein that leads to persistence of Ndt80 and Cdc5. CHX-treated cells from a culture expressing *AMA1* show degradation of Ama1 substrates (**Figure 25A**) in contrast to cells with inactive Ama1 (**Figure 25B**). Both Ndt80 and Cdc5 are degraded with similar kinetics by Ama1, as indicated from measurements of their half-lives (**Figure 25C**). Interestingly, Ama1 shows similar half-life (<20 min) as in earlier stages of meiosis. Thus, Ama1 degradation does not depend on the stage of meiosis. Similar pattern is observed for Cdc20, whose half-life is ~5 min in the presence or absence of Ama1 and in meiosis I and -II. We did not measure half-lives of cyclins due to the low intensity of the signal in meiosis II.

We calculated degradation rates based on the half-lives and used them as new values of parameters describing Cdc20- and Ama1-dependent degradation. We refitted other parameters to recreate the known phenotypes of WT and *ama1Δ* cells. We selected a single set of parameter values that resulted in two meiotic divisions (**Table 7**).

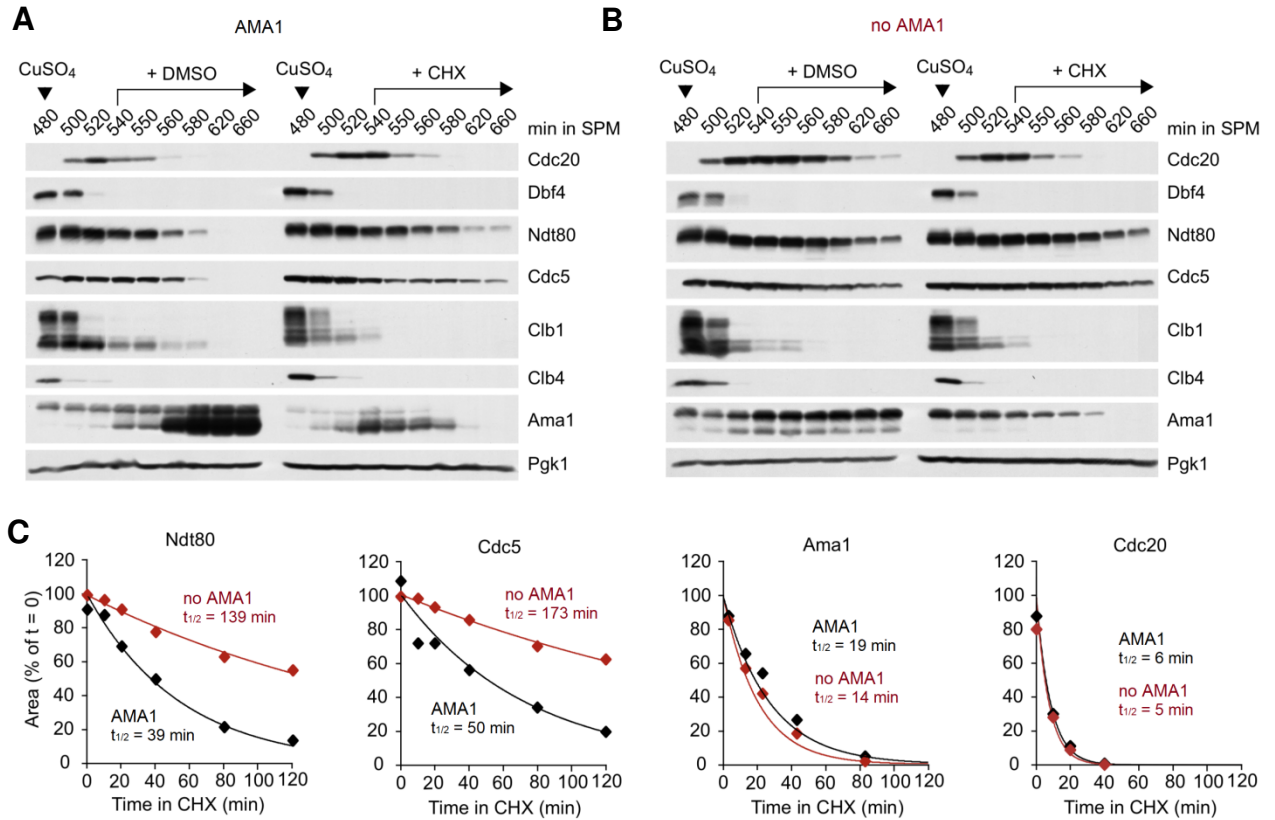


Figure 25. Levels and stability of meiotic regulators in the presence and absence of Ama1 in meiosis II. *CDC20-mAR* cells expressing *AMA1* (Z31284) or *ama1Δ P_{DMCI}-AMA1* (Z31285) were transferred to SPM ($t = 0$) and treated with 10 μ M of CuSO₄ at $t = 480$ min. Cells were treated with solvent (DMSO, 0.5%) or cycloheximide (CHX, 0.5 mg/ml) at $t = 540$ min. Proteins were detected in whole-cell extracts by immunoblotting. **(A)** Immunoblot detection of proteins in *AMA1* cells (*AMA1*). **(B)** Immunoblot detection of proteins in *ama1Δ P_{DMCI}-AMA1* cells (no *AMA1*). **(C)** Graphs show half-lives ($t_{1/2}$) of proteins measured from CHX-treated cell cultures. Signal intensity was compared between cells expressing *AMA1* and *ama1Δ P_{DMCI}-AMA1*. Data points are mean values from 2 gels.

Table 7. Parameter values of the model with Ama1 and Cdc20 as terminators of oscillations.¹

Equation number	Parameters and their values
9	$k_{RCa1} = 2, k_{RCi1} = 0.5, J_{RC} = 1$
13, 47, 48	$k_{Ndt80s1} = 0.002, k_{Ndt80s2} = 0.25, k_{Ndt80d1} = 0.01, k_{Ndt80d2} = 0.02,$ $k_{Ndt80d3} = 0.008, k_{Ndt80a1} = 1, k_{Ndt80a2} = 0.8, k_{Ndt80i1} = 0.4, k_i = 0.02$
14-16	$k_{Sum1i1} = 0.1, k_{Sum1a1} = 0.05, k_{Sum1i3} = 0.5, k_{Sum1a2} = 0.2, k_{Sum1i4} = 0.05,$ $k_{Sum1a3} = 0.3$
20	$k_{SPa1} = 0.3, k_{SPi1} = 3, J_{SP} = 0.001$
21, 22	$k_{Cdc5s1} = 0.001, k_{Cdc5s2} = 0.05, k_{Cdc5d1} = 0.01, k_{Cdc5d2} = 0.03, k_{Cdc5d3} = 0.001,$ $k_{Cdc5a1} = 0.2, k_{Cdc5a2} = 2, k_{Cdc5a3} = 1, k_{Cdc5i1} = 0.4$
31, 32	$k_{Clb1s1} = 0.001, k_{Clb1s2} = 0.04, k_{Clb1d1} = 0.01, k_{Clb1d2} = 0.02, k_{Clb1d3} = 0.0035,$ $k_{Clb1d4} = 0.05, k_{Clb4s1} = 0.002, k_{Clb4s2} = 0.03, k_{Clb4d1} = 0.01, k_{Clb4d2} = 0.03,$ $k_{Clb4d3} = 0.008, k_{Clb4d4} = 0.12$
33	$k_{IEa1} = 0.0004, k_{IEa2} = 0.0002, k_{IEi1} = 0.01$
34, 35	$k_{Cdc20s2} = 0.13, k_{Cdc20d1} = 0.15, k_{Cdc20a1} = 20, k_{Cdc20i1} = 1, J_{Cdc20} = 0.1$
44	$k_{Inhd1} = 0.01, k_{Inhd2} = 0.032$
45, 46	$k_{Ama1s1} = 2, k_{Ama1d1} = 0.06, k_{Ama1a1} = 1, J_{Inh} = 0.001, n = 1$

¹Only modified parameters are presented.

We simulated different conditions based on the readjusted model. In WT cells, Ama1 takes a role of the terminator of meiotic oscillations (**Figure 26A**). Initially, cyclins are degraded by Cdc20 at anaphase I and anaphase II. With gradual degradation of Clb1 and complete degradation of Inh, Ama1_T accumulates abruptly, triggering degradation of Cdc5 and Ndt80. Cells disassemble meiotic spindle and complete two divisions. Even lowered accumulation of Ama1 in meiosis II (half reduction of level mimicking heterozygous deletion of *AMA1*) causes irreversible exit from meiosis (**Figure 26B**), which is in agreement with biological observations (data not shown). Further reduction of Ama1 accumulation is still sufficient to exit from meiosis II with Ama1 functioning as a terminator (**Figure 26C**). However, expression of Ama1 from a constitutive promoter, which leads to similar levels of the protein in meiosis I and -II, results in inability of cells to properly activate Ama1 for the exit from meiosis II (**Figure 26D**). To simulate persistence of Ama1 protein at prophase I, we modified **Equation 45** describing Ama1_T. We introduced a background Inh-independent synthesis of Ama1 protein (parameters are $k_{Ama1s1} = 0$, $k_{Ama1s2} = 0.015$) (**Equation 49**).

$$[Ama1_T] \frac{d}{dt} = k_{Ama1s1} \cdot \frac{J_{Inh}^n}{J_{Inh}^n + [Inh]^n} + k_{Ama1s2} - k_{Ama1d1} \cdot [Ama1_T] \quad (49)$$

Under this condition, Ndt80 persists longer along with Cdc5 and Cdc20. Strong accumulation and activity of Cdc20 leads to complete degradation of cyclins, similar as in the absence of Ama1 in meiosis II, mimicking *ama1Δ P_{DMC1}-AMA1* cells (**Figure 26E**) and similar as in *ama1Δ* cells (**Figure 26F**). In all these scenarios, Cdc20 takes a role of the terminator of the meiotic oscillations. In cells lacking appropriate levels of Ama1 in meiosis II, Cdc20 is highly active to prevent any additional divisions. Its strong accumulation results from stable Ndt80, while its strong activity results from persistence of one of its activator, Cdc5. As Ndt80 is also responsible for the synthesis of cyclins, Cdc20-dependent degradation of Clb1 and Clb4 is stronger than the synthesis, leading to the prevention of their re-accumulation for the third division. In the revised model, a meiosis II-specific activity of Cdc20 is achieved by gradual accumulation of the protein and gradual increase of its activators. The kinetics of the activation and inactivation of IE and Cdc20 is crucial for maintaining a stable activity of Cdc20. It is important to note that Cdc20 cannot gain the function of the terminator before the exit from meiosis II in order to prevent the premature exit from meiosis after anaphase I. Thus, in the absence of Ama1, Cdc20 gains a meiosis II-specific function that is different from its function at the exit from meiosis I.

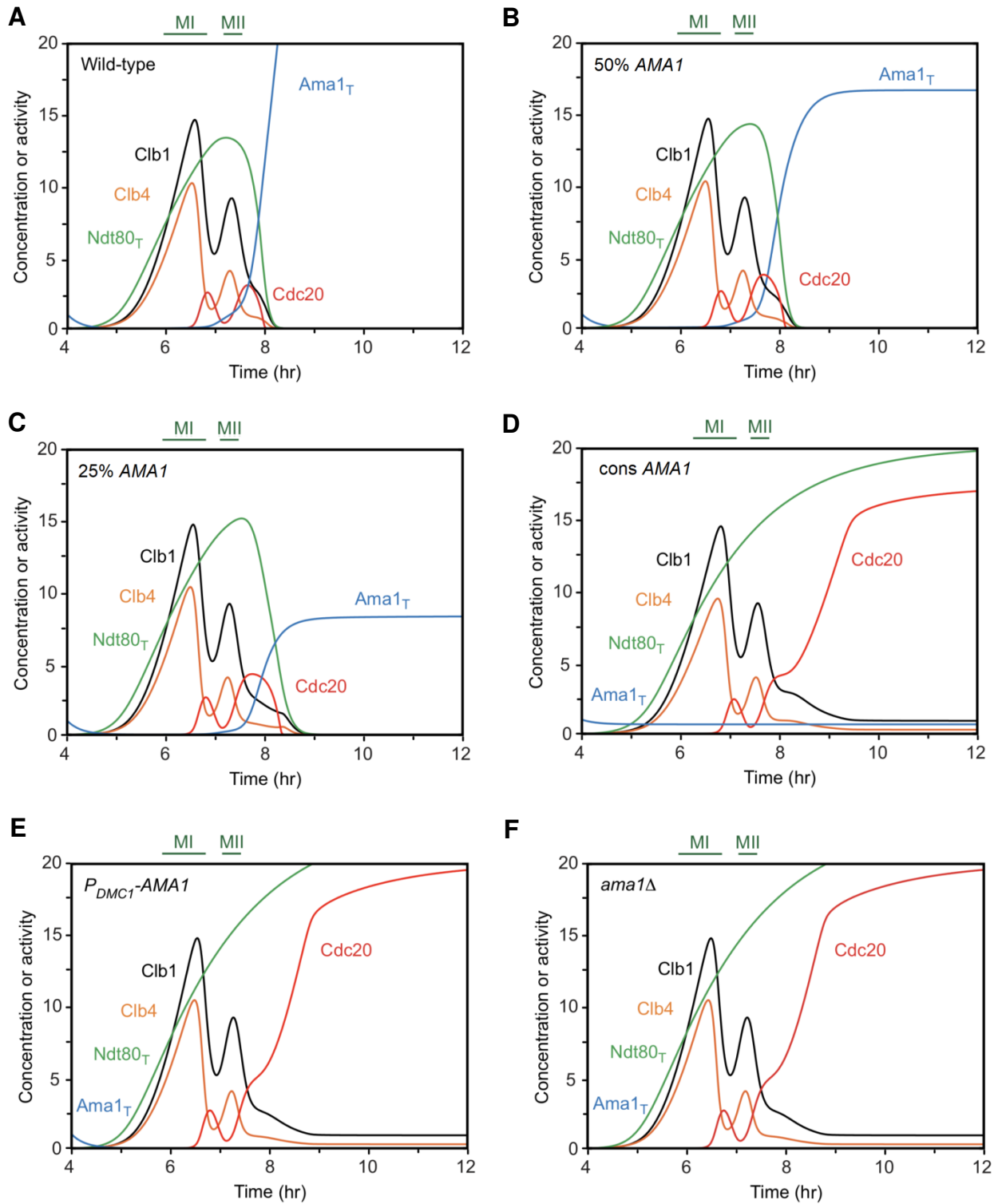


Figure 26. Cdc20 takes a role of Ama1 in termination of meiotic oscillations after meiosis II. Simulations were performed on the adjusted model with Ama1 serving as the terminator in WT cells (A), cells with 50% reduction ($k_{Ama1s1} = 1$) (B) or 75% reduction ($k_{Ama1s1} = 0.5$) (C) of *AMA1* expression and with Cdc20 serving as the terminator in cells with *AMA1* expressed from a constitutive (cons) promoter ($k_{Ama1s1} = 0$, $k_{Ama1s2} = 0.015$) (D), *AMA1* expressed from prophase I *DMC1* promoter ($Ama1_T = Ama1_{AT} = 1$, $k_{Ama1s1} = 0$) (E) or in *ama1\Delta* ($Ama1_T = Ama1_{AT} = 0$, $k_{Ama1s1} = 0$) (F). Parameters of the combined model were readjusted to fit the measured half-lives and phenotypes of WT cells and *ama1\Delta* mutant cells. Simulations show concentration or activity of key meiotic regulators. MI and MII are metaphase I and -II spindles indicating the consecutive divisions.

In order for Cdc20 to gain the function of the terminator in meiosis II, but not meiosis I, Cdc20 activity must be regulated differently between meiosis I and -II, leading to the increase of the activity during the exit from the second division. Our previous experiments and simulations showed that Cdc20 protein levels are lower at metaphase I than at metaphase II. We asked whether this time delay in accumulation of Cdc20 may provide an explanation of its meiosis II-specificity in the absence of Ama1. We tested computationally two scenarios: decrease in Ndt80-dependent synthesis of Cdc20 in meiosis II to the levels of meiosis I and increase in Ndt80-independent synthesis of Cdc20, mimicking equal levels of the protein in both meiosis I and -II. Additionally, we tested a scenario of abrupt but not gradual accumulation of the transcription factor of

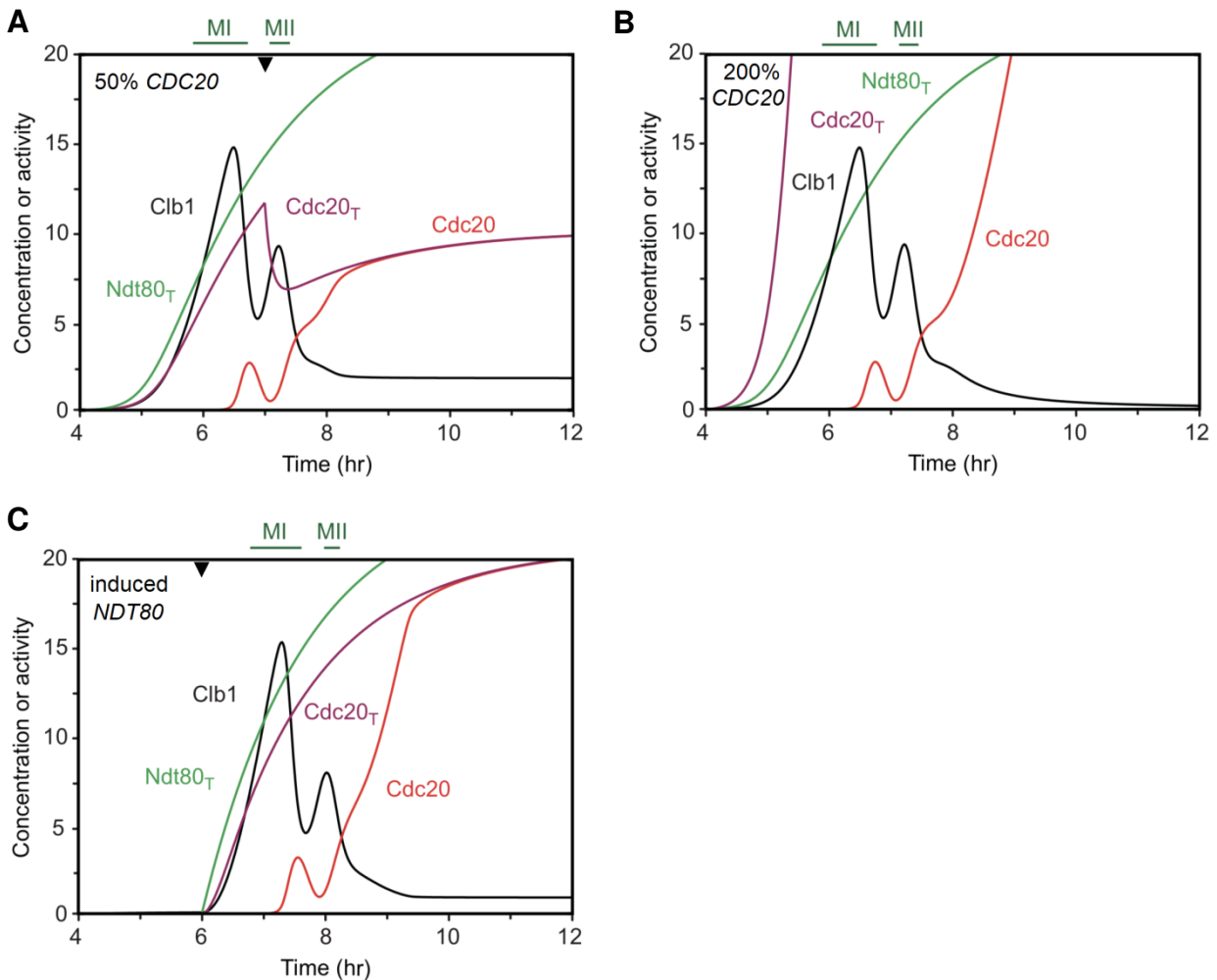


Figure 27. Difference in Cdc20 protein level between the two divisions is not sufficient to explain a possible meiosis II-specific activity of Cdc20. Simulations of the model present concentration or activity of Clb1, Cdc20, Cdc20_T and Ndt80_T in the absence of Ama1 ($Ama1_T = Ama1_{AT} = 0$, $k_{Ama1s1} = 0$). **(A)** 50% decrease in Cdc20 levels in meiosis II ($k_{Cdc20s2} = 0.065$ at $t = 7$ hr) does not affect the exit from meiosis II. **(B)** Two-fold increase in Ndt80-dependent synthesis of Cdc20 in meiosis I ($k_{Cdc20s2} = 1.3$ at $t = 4$ hr) does not affect the exit from meiosis II. **(C)** Increase of Cdc20 level in meiosis I by induction of Ndt80 in early meiosis ($k_{Ndt80s1} = 0.24$ at $t = 6$ hr, $k_{Ndt80s2} = 0$) does not cause defects in the meiotic exit. Black arrowheads indicate change of the parameters. **MI** and **MII** are metaphase I and -II spindles indicating the consecutive divisions.

Cdc20, namely Ndt80. Both decrease of the synthesis in meiosis II (**Figure 27A**) and increase of the synthesis in meiosis I (**Figure 27B**) result in robust progression through two meiotic divisions and the exit after meiosis II in the absence of Ama1. Similarly, simulations that mimic inducible expression of *NDT80* with the abrupt accumulation of Ndt80_T, leads to proper progression through meiosis (**Figure 27C**). In conclusion, gradual accumulation of Cdc20 is not required for proper progression through meiotic divisions. It is more likely that the kinetics of activation and inactivation of APC/C^{Cdc20} plays a crucial role in its meiosis II-specific activity in the absence of Ama1. Moreover, an inhibitor of APC/C^{Cdc20} activity may be present in between meiosis I and -II that prevents the exit from meiosis after only one division.

2.5.2. Cdc20 activity is required for timely exit from meiosis II

Ama1 and Cdc20 are both active during the exit from meiosis II in WT cells. Due to the change in the properties of the network regulating meiotic divisions in the absence of Ama1, Cdc20 terminates the oscillations after the exit from meiosis II. Thus, Cdc20 takes the role of Ama1. We asked whether the reverse is also true, and whether Ama1 can take the role of Cdc20 during meiosis. Firstly, we investigated a theoretical problem of Ama1 activity at the exit from meiosis I. In WT cells, anaphase I is triggered by the activity of Cdc20, which depends on the activity of Cdk1. Cdc20 and Cdk1 create an oscillator, which along with partial inhibition of Cdc20 in meiosis I allows the re-accumulation of cyclins for the second division. We simulated a scenario, in which cells lack Cdc20 activity in meiosis I and instead accumulate high levels of Ama1, similar to the levels at the exit from meiosis II in WT cells. For simulated induction of Ama1, we used a combined model with Ama1_T described with **Equation 49**, depicting additional background synthesis of the protein. In addition, we readjusted the parameters describing degradation of the inhibitor of Ama1 synthesis Inh, in order to prevent premature appearance of Ama1. **Table 8** presents changed parameter values that substitute the parameters used in previous versions of the model.

Table 8. Parameter values of the model with Ama1 and Cdc20 as terminators of oscillations.¹

Equation number	Parameters and their values
44	$k_{Inhd1} = 0.003, k_{Inhd2} = 0.05, k_{Inhd3} = 0.05, k_{Inhd4} = 0.02$

¹Only changed parameters are presented.

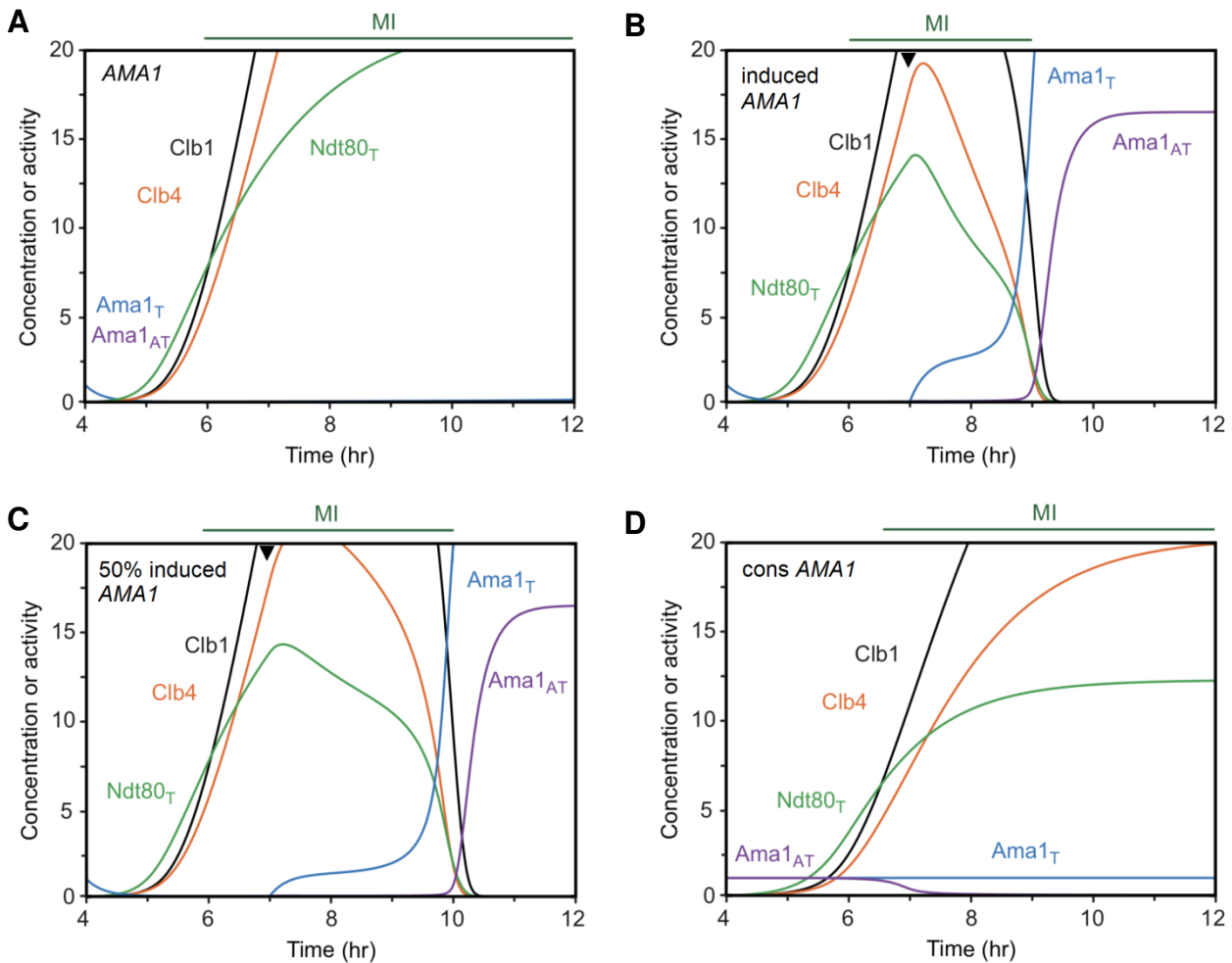


Figure 28. Ama1 does not take a role of Cdc20 in the exit from meiosis I. Simulation presents concentration or activity of proteins in metaphase I-arrest in the absence of Cdc20 ($k_{Cdc20s1} = k_{Cdc20s2} = 0$). **(A)** Cells with WT expression of *AMA1* ($k_{Ama1s1} = 2$). **(B-D)** Cells with induced expression of *AMA1* with meiosis II-like level ($k_{Ama1s2} = 0.15$ at $t = 7$ hr) **(B)**, 50% decrease ($k_{Ama1s2} = 0.075$ at $t = 7$ hr) **(C)** and prophase I-like level (*AMA1* expressed from consecutive promoter, cons) ($k_{Ama1s1} = 0$, $k_{Ama1s2} = 0.06$ at $t = 4$ hr) **(D)**. Black arrowheads indicate change of the parameters. **MI** is metaphase I spindle.

Cells depleted of Cdc20 arrest in metaphase I for long period (>6 hr *in silico*) (**Figure 28A**). Simulated induction of Ama1 around 7 hr leads to slow accumulation of the protein within next 2 hr (**Figure 28B**). At 9 hr, Ama1 activity slowly rises triggering degradation of its inhibitor Clb1. Degradation of Clb1 happens within next 30 min, leading to the full activation of highly synthesized Ama1 and degradation of its substrates, such as Cdc5 and Ndt80. Although cells degrade cyclins and disassemble meiotic spindle, they are unable to enter the second meiotic division with complete degradation of Ndt80 and stable activity of Ama1. Thus, cells exit irreversibly without entering meiosis II, which indicates the inability of Ama1 to take the role of Cdc20 in its absence. Even reduction of the levels of Ama1 leads to an inability to perform meiosis II (**Figure 28C**). Notwithstanding, prophase I-like levels of Ama1 are not able to trigger the exit from a metaphase I-arrest, possibly to due predominant inhibition by Clb1, which can only be overcome by strong accumulation of Ama1 (**Figure 28D**).

We verified the prediction of Ama1 inhibiting the entry into meiosis II in cells arrested in metaphase I by expression of *CDC20* from the mitotic promoter *HSL1* (P_{HSL1} -*CDC20*). We expressed high levels of Ama1 protein by introducing an additional copy of *AMA1* under inducible *GAL* promoter (P_{EST} -*AMA1*). This system takes advantage of the Gal4-estrogen receptor fusion for the induction of a gene under the *GAL* promoter with estradiol (Okaz et al., 2012). We induced *AMA1* at 7 hr. After induction, cells accumulate high level of Ama1 protein and degrade M-phase regulators within next 3 hr (**Figure 29**). As predicted by the model, cells exit from the high Cdk1 state, but do not re-accumulate cyclins for the second division. Thus, in the absence of Cdc20, Ama1 does not take its role in performing the exit from meiosis I and allowing the entry into the second division. Unlike Cdc20, Ama1 threatens the two-division meiosis and has to be inhibited robustly at meiosis I to allow the entry into meiosis II.

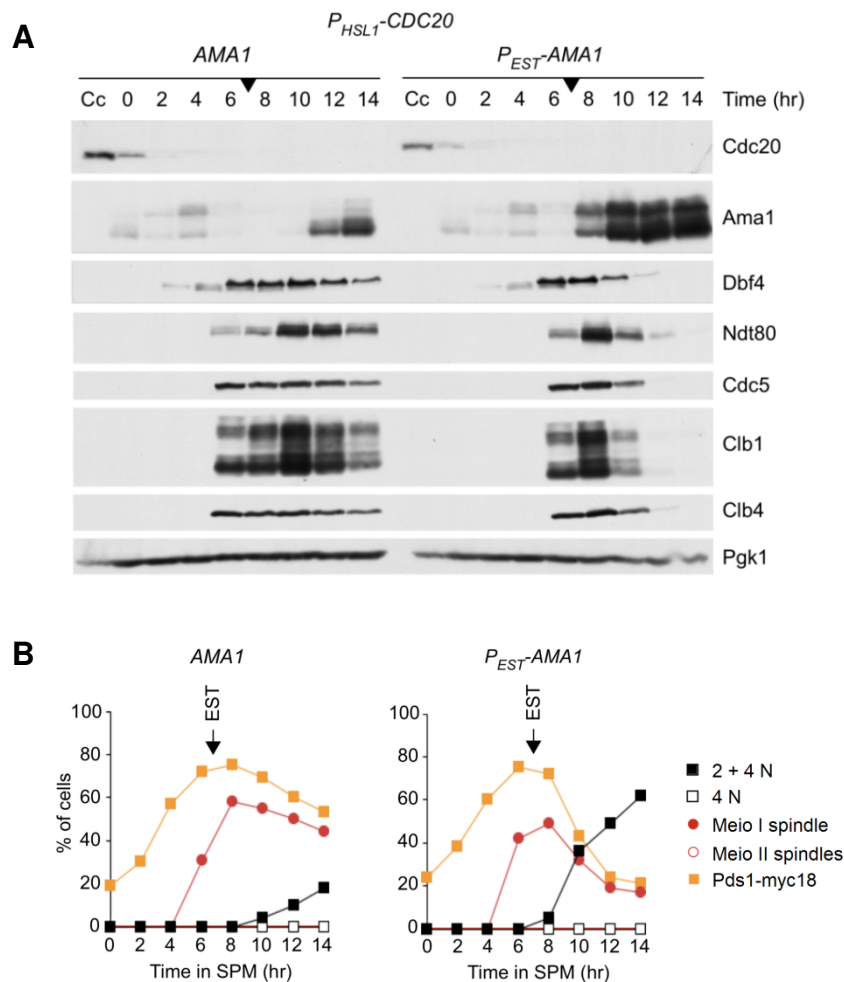


Figure 29. Ama1 activity does not take the role of Cdc20 in the exit from meiosis I. Cells were arrested in metaphase I by depletion of Cdc20 from meiosis by expressing P_{HSL1} -*CDC20*. 10 μ l of estradiol (EST) was added at $t = 7$ hr to the cultures expressing WT *AMA1* (Z34661) or WT *AMA1* with an additional inducible copy P_{EST} -*AMA1* (Z34662). **(A)** Immunoblot detections of proteins. Black arrowhead indicates addition of EST. Cc means proliferating cells. **(B)** Quantification of meiotic progression by IF detection of nuclear division (2+4N is at least one division, 4N is two divisions), meiosis I (Meio I) and -II (Meio II) spindles, and nuclear Pds1-myc18.

Next, we tested *in silico* the possibility of Ama1 taking the role of Cdc20 at the exit from meiosis II. For this purpose, we simulated the inactivation of Cdc20 during metaphase II. We did not induce the expression of Ama1, but allowed WT accumulation of the protein using **Equation 45** for Ama1_T. We inactivated Cdc20 at 7 hr during the time when cells enter metaphase II. Cells with active Cdc20 at meiosis II exhibit lower levels of Clb1 and Clb4 than at metaphase I (**Figure 30A**). They degrade cyclins and Ndt80 abruptly, disassembling metaphase II spindles within <20 min. However, cells with inactivated Cdc20 at meiosis II accumulate higher levels of cyclins and maintain high Ndt80 and Cdc5 levels for ~3 hr (**Figure 30B**). Strong accumulation of cyclins in metaphase II indicates the inability of Ama1 to limit the levels of its own inhibitors, unlike Cdc20. Inactivation of Cdc20 leads to a delay in Ama1 accumulation and

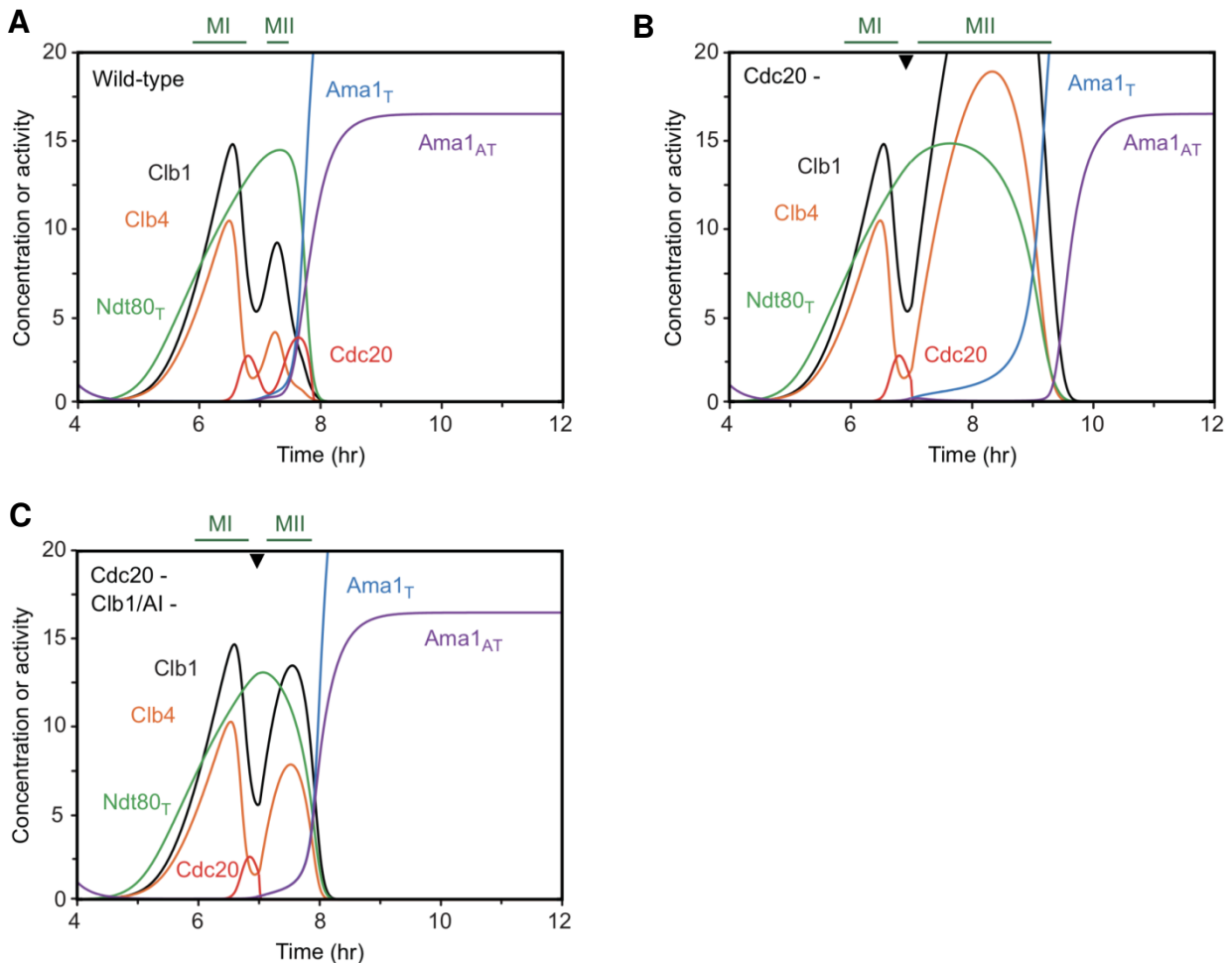


Figure 30. Cells exit from meiosis II with a delay in the absence of Cdc20 activity during meiosis II. Simulations present concentration or activity of proteins in the presence (Wild-type) (A) or absence (Cdc20 -) of activity of Cdc20 in meiosis II ($k_{Cdc20a1} = 0$ at $t = 7$ hr) (B-C). (A-B) Cells with WT inhibition of Ama1 activity mediated by Clb1 and AI. (C) Cells without Clb1- and AI-dependent inhibition of Ama1 (Clb1/AI-) ($k_{Ama1i2} = k_{AIs1} = 0$). Black arrowheads indicate change of the parameters. MI and MII are metaphase I and -II spindles indicating the consecutive divisions.

a significant delay in its activity due to the persistence of the Ama1 inhibitors, namely Clb1 and AI. Metaphase II spindles are stabilized for ~2 hr. Simulations of cells without the Clb1- and AI-dependent inhibition of Ama1 shows that this inhibition is necessary for keeping proper time of metaphase II-arrest. In cells with inactivated Cdc20 in meiosis II, the metaphase II is shortened from ~3 hr to ~45 min (**Figure 30C**).

Cells evolved a mechanism that inhibits the premature activation of APC/C in order to have sufficient time for proper segregation of chromosomes. The SAC usually inhibits Cdc20 activity during metaphase, thus extending the time necessary to attach the chromosomes to the spindle poles. In the absence of Cdc20, additional machinery is necessary to inhibit premature exit from meiosis II. Our simulations suggest that this machinery is based on Clb1- and AI-dependent inhibition of Ama1. Although in the absence of Cdc20 cells lacking this inhibition break from the metaphase II-arrest faster than cells with inhibited Ama1, they are still unable to exit meiosis on time.

Simulations of the model show that Cdc20 activity is important for the timely exit from meiosis II and Ama1 is not able to perform the same role as Cdc20 in its absence. We tested this prediction biologically. We developed a new method that allows to inactivate Cdc20 in meiosis II without affecting the exit from meiosis I. We made advantage of a *CDC20* allele sensitive to high temperature, *cdc20-3*, for inactivation of APC/C^{Cdc20} (Shirayama et al., 1998). We modified the *CDC20-mAR* system by mutating *P_{CUP1}-CDC20* to create *cdc20-3-mAR*. This approach allows to inactivate Cdc20 in highly synchronized meiotic culture precisely at metaphase II. We used as a control the unmodified *CDC20-mAR* system with active Cdc20. We arrested *CDC20-mAR* and *cdc20-3-mAR* cells with WT *AMA1* in metaphase I and released them from the arrest at 8 hr. At 50 min, we inactivated Cdc20 in *cdc20-3-mAR* cells by shifting the temperature from 25 °C to 36 °C. At this time, the meiosis I-specific protein Spo13 is degraded in both strains, indicating the completion of the first division (**Figure 31A**). Although *cdc20-3-mAR* cells enter meiosis II at the same time as the control, as indicated from accumulation of meiosis II-specific cyclin Clb3, they accumulate higher levels of cyclins and Pds1-myc18. In contrast to the control strain that activates Ama1 at ~100 min and degrades Ndt80 and Cdc5, the strain with inactive Cdc20 maintains high levels of these proteins for longer period of time. Additionally, as Clb3 and Clb5 are degraded around 140 min, Clb1 and Clb4 exhibit high levels until the end of the time course. These results indicate a long delay in the exit from meiosis II in the absence of Cdc20 activity. Similarly as predicted by the model, cells arrest in metaphase II for ~1 hr with high

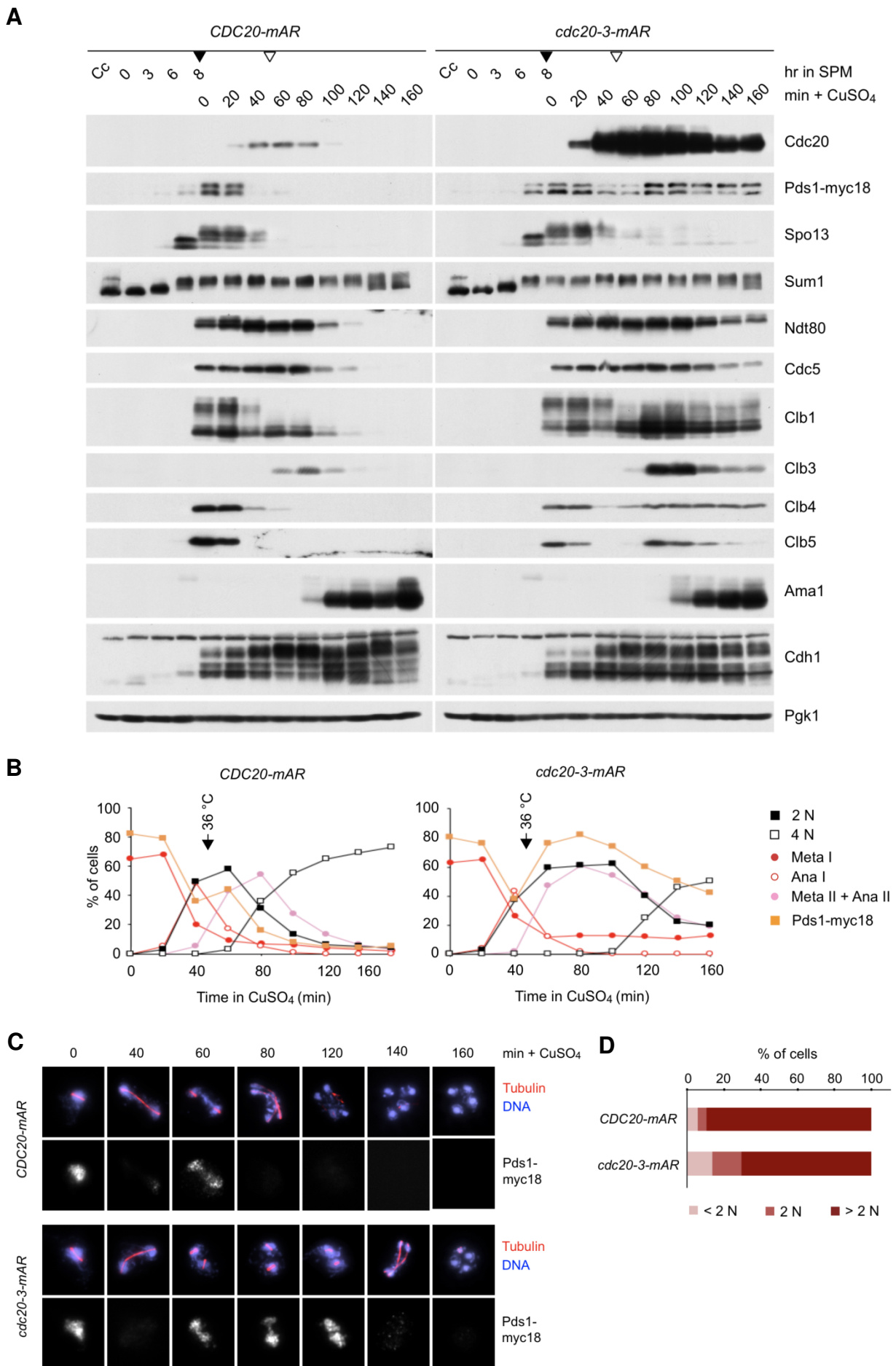


Figure 31. Cells do not exit from meiosis II on time in the absence of Cdc20 in meiosis II. (Figure legend on the next page 71)

accumulation of cyclins and Pds1-myc18 (**Figure 31B**). Individual cells contain visibly higher intensity of Pds1-myc18 nuclear signal in meiosis II than the control cells at the same time (60-120 min) (**Figure 31C**). In addition to strong accumulation of Clb1, Clb4 and Pds1-myc18 in meiosis II, cells re-accumulate Clb5, which is not observed in the control strain. This indicates a basal activity of Cdc20 in wild-type cells during metaphase II that does not allow re-accumulation of the S-phase cyclin in meiosis II. Although the exit is visibly delayed, after 24 hr in SPM, the majority of cells complete two meiotic divisions (**Figure 31D**). Thus, the arrest in metaphase II is not stable in the presence of active Ama1. Eventually, in the absence of Cdc20 cells break out from the arrest, but with a significant time delay. We conclude that Cdc20 is required for timely degradation of cyclins and the exit from meiosis II. In its absence, Ama1 is unable to perform the same role as Cdc20.

Due to the instability of the metaphase II-arrest in the absence of Cdc20, we asked whether for stabilization in metaphase II-arrest cells have to be depleted of both Cdc20 and Ama1. We simulated a scenario, in which we inhibited Cdc20 activity in metaphase II in the absence of Ama1. In the absence of both APC/C co-activators, cells are unable to degrade cyclins, disassemble meiotic spindles and exit from meiosis II (**Figure 32**). They maintain high level of cyclins and metaphase II spindles due to inactivation of Cdc20 and stabilization of Ndt80, which continues to synthesize Clb1 and Clb4.

To verify the stability of metaphase II-arrest in the absence of the activities of both Cdc20 and Ama1 in meiosis II, we used the *cdc20-3-mAR* system. We arrested *ama1Δ P_{DMC1}-AMA1* cells in metaphase I and released them from the arrest at 8 hr in SPM. 50 min after the release, we shifted the temperature to 36 °C, which led to inactivation of Cdc20 in the *cdc20-3-mAR* strain. The control *CDC20-mAR* strain and the *cdc20-3-mAR* strain enter meiosis II at the same time with accumulation of Clb3 at 60 min

Figure 31. Cells do not exit from meiosis II on time in the absence of Cdc20 in meiosis II. Cells from *CDC20-mAR* culture (Z21260) and *cdc20-3-mAR* culture (Z31711) in the presence of WT *AMA1* were arrested in metaphase I and released from the arrest at $t = 8$ hr by the addition of 10 μ M of CuSO_4 at 25 °C. At $t = 50$ min, temperature was shifted to 36 °C to inactivate Cdc20. **(A)** Immunoblot detection of proteins. CC means proliferating cells. Black arrowheads mean addition of CuSO_4 ; white arrowheads mean temperature shifts. **(B)** Quantification of meiotic progression by IF detection of nuclear division (2N is one division, 4N is two divisions), metaphase I (Meta I), anaphase I (Ana I) or meiosis II (Meta II + Ana II) spindles and nuclear Pds1-myc18 signal. **(C)** Representative IF pictures of cells at the given time after the release from metaphase I-arrest ($t = 0$). **(D)** Bar plots indicating percentage of cells with one nucleus (<2N), two nuclei (2N) and more than two nuclei (>2N) 24 hr in SPM.

(**Figure 33A**) and formation of metaphase II spindles at the same time (**Figure 33B-C**). Cells with active Cdc20 complete both meiotic divisions within 2 hr after the release from metaphase I-arrest. In contrast, cells with inhibited Cdc20 stabilize Cdc20 substrates. At 120 min, ~60% of cells maintain metaphase II spindles in comparison to control cells, which disassemble meiotic spindles at this time. After 24 hr in SPM, ~70% of cells remain bi-nucleated in contrast to cells with active Cdc20 (<5%) (**Figure 33D**). Based on the morphology of the spindles and the persistence of metaphase II proteins, we conclude that cells with inhibited activities of both Cdc20 and Ama1, but not Cdh1, arrest in metaphase II. Thus, APC/C activity is required for cells to exit from the second meiotic division.

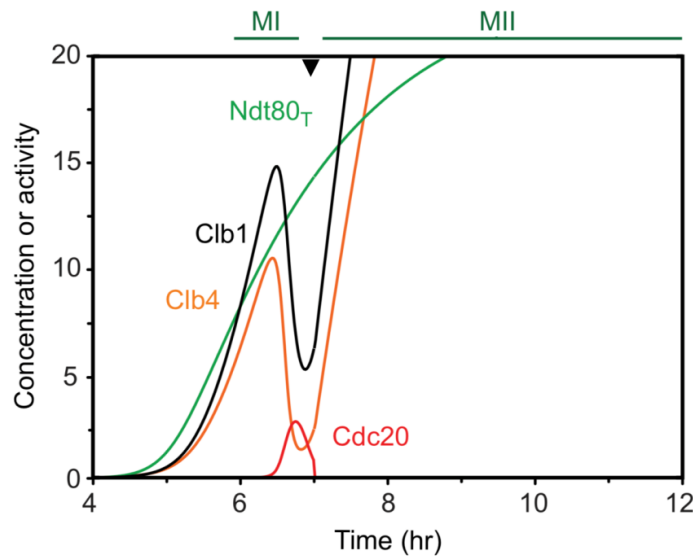


Figure 32. Cells arrest in metaphase II in the absence of Cdc20 and Ama1 in meiosis II. Simulation presents concentration or activity of Clb1, Clb4, Cdc20 and Ndt80_T in the absence of Ama1 ($Ama1_T = Ama1_{AT} = 0$, $k_{Ama1s1} = 0$). Cdc20 was inactivated at metaphase II ($k_{Cdc20t1} = 0$ at $t = 7$ hr), what is indicated by black arrowhead. MI and MII are metaphase I and -II spindles indicating the consecutive divisions.

Figure 33. Cells arrest in metaphase II in the absence of Ama1 and Cdc20 activity in meiosis II. Cells from *CDC20-mAR* culture (Z27968) and *cdc20-3-mAR* culture (Z31712) in *ama1Δ P_{DMC1}-AMA1* background were arrested in metaphase I and released from the arrest at $t = 8$ hr by the addition of 10 μ M of CuSO₄ at 25 °C. At $t = 50$ min, temperature was shifted to 36 °C to inactivate Cdc20. **(A)** Immunoblot detection of proteins. CC means proliferating cells. Black arrowheads mean addition of CuSO₄; white arrowheads mean temperature shift. **(B)** Quantification of meiotic progression by IF detection of nuclear division (2N is one division, 4N is two divisions), metaphase I (Meta I), anaphase I (Ana I) or meiosis II (Meta II + Ana II) spindles and nuclear Pds1-myc18 signal. **(C)** Representative IF pictures of cells at the given time after the release from metaphase I-arrest ($t = 0$). **(D)** Bar plots indicating percentage of cells with one nucleus (<2N), two nuclei (2N) and more than two nuclei (>2N) 24 hr in SPM.

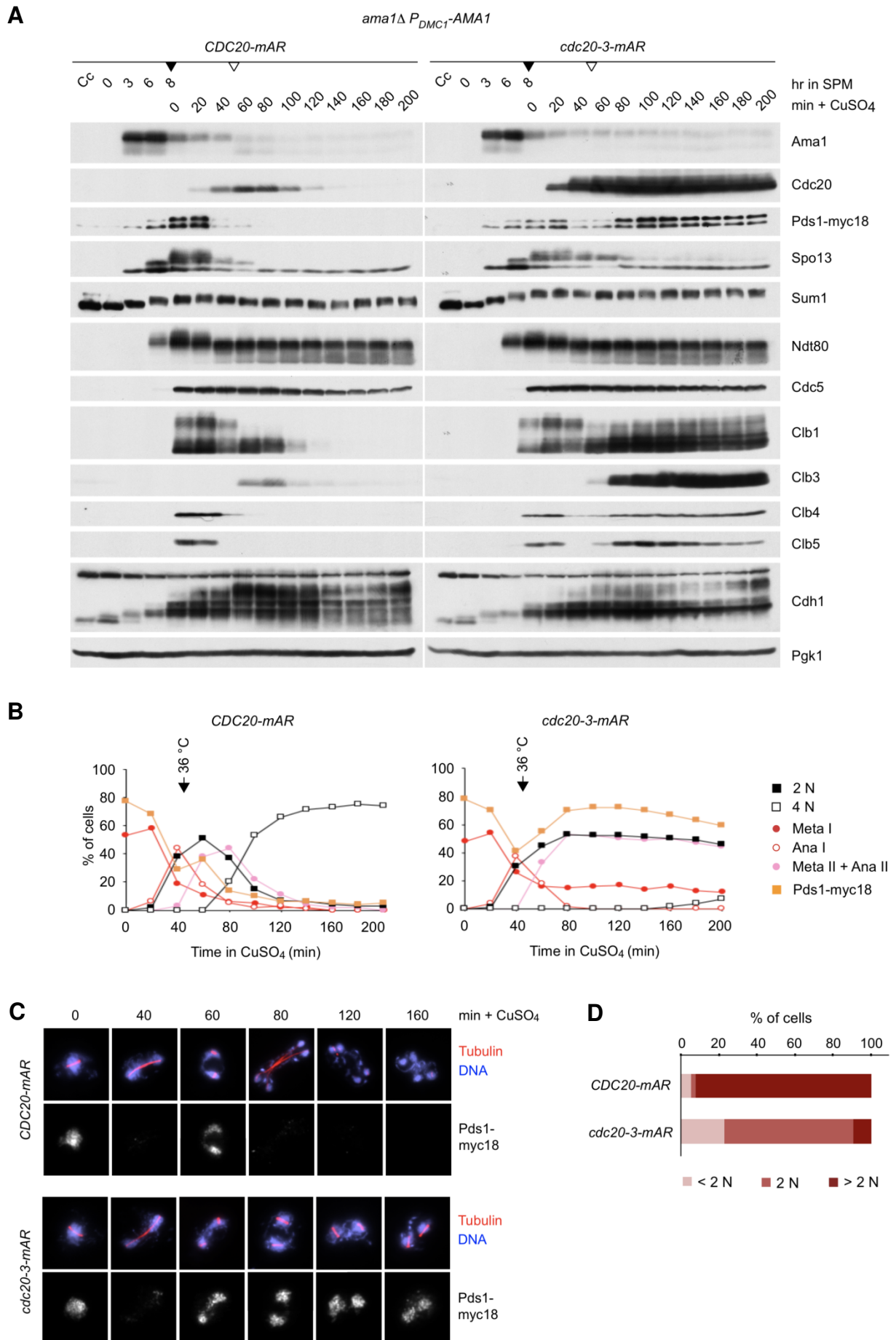


Figure 33. Cells arrest in metaphase II in the absence of Ama1 and Cdc20 activity in meiosis II. (Figure legend on the previous page 72)

2.5.3. Cells do not enter a third division after inactivation of Cdc20 and Ama1 at the exit from meiosis II

We showed that the activity of Cdc20 is required for the timely exit from meiosis II. We speculated that Cdc20 takes the role of the terminator of meiotic oscillations in the absence of Ama1. To test the hypothesis of Cdc20 terminating the oscillations, we performed computational and biological experiments that allowed us to shed light on this process. We used the advantage of mathematical modeling and *cdc20-3-mAR* system allowing manipulation of Cdc20 activity after the exit from meiosis II to test whether inactivation of Cdc20 may lead to re-accumulation of cyclins for a third division.

Cells arrested at metaphase II accumulate high levels of cyclins and Pds1-myc18. In addition, they exhibit elevated levels of Ndt80 and Cdc5. We speculated that high levels of meiotic regulators in meiosis II that mimic or exceed the levels at meiosis I may lead to the possibility of a third division after restoration of Cdc20 activity. Firstly, we performed simulations, during which we arrested cells in metaphase II for ~1 hr by inactivating Cdc20 in the absence of Ama1, and then reactivated Cdc20 for the release from the metaphase II-arrest. This reactivation causes immediate degradation of cyclins and spindle disassembly within 30 min (**Figure 34A**). Unphysiological and long metaphase II-arrest and excessive amount of cyclins do not cause defects in the exit from meiosis and completion of two divisions even in the absence of Ama1. Restoration

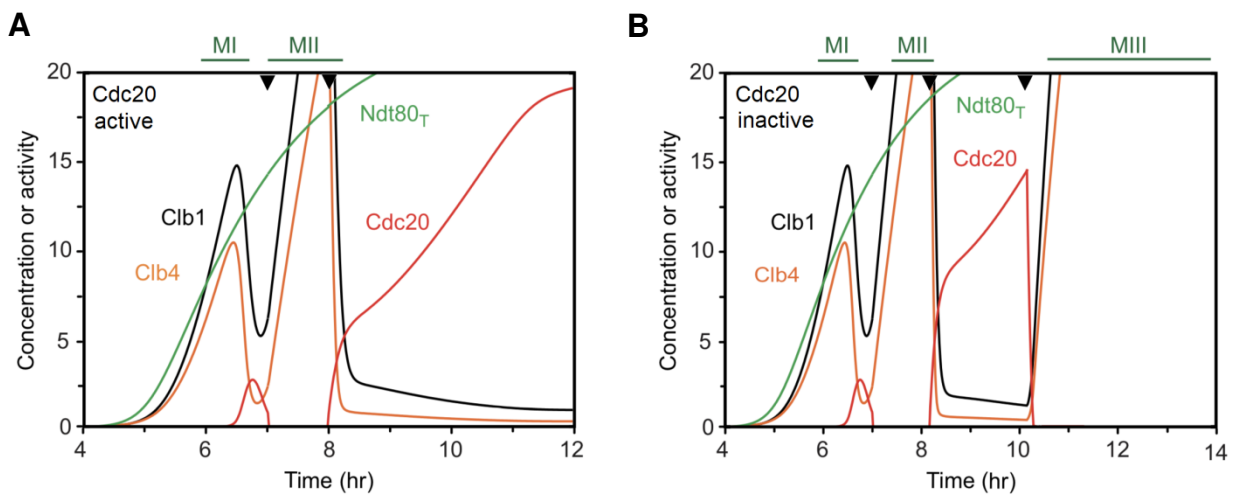


Figure 34. Model predicts the entry meiosis III after complete inactivation of APC/C. Simulations presents concentration or activity of Clb1, Clb4, Cdc20 and Ndt80_T in the absence of Ama1 ($Ama1_T = Ama1_{AT} = 0$, $k_{Ama1s1} = 0$). Cdc20 was inactivated at metaphase II ($k_{Cdc20a1} = 0$ at $t = 7$ hr). **(A)** Cdc20 reactivated after 1 hr ($k_{Cdc20a1} = 2$ at $t = 8$ hr). Cdc20 is active after the exit from meiosis II causing irreversible exit. **(B)** Cdc20 is reactivated after 1 hr in the arrest ($k_{Cdc20a1} = 2$ at $t = 8.15$ hr) and inactivated after 10 hr ($k_{Cdc20a1} = 0$ at $t = 10.15$ hr) causing the entry into meiosis III. Black arrowheads indicate change of the parameters. MI, MII and MIII are metaphase I, -II and -III spindles indicating the consecutive divisions.

of Cdc20 activity does not lead to waves of Cdk1 activity repeated periodically after the exit from meiosis II. Instead, cells exit from meiosis similarly as in the presence of WT Cdc20. These results imply that manipulation of Cdc20 activity does not change its general behavior and function. Cells exit from meiosis II with termination of meiotic oscillations even after recreation of the levels of metaphase I proteins during metaphase II. Thus, we tested whether inactivation of Cdc20 after the exit from meiosis II may overcome the termination machinery of the oscillations. Indeed, our simulations confirmed that cells lacking Cdc20 activity after the exit from meiosis II re-accumulate cyclins for the third time and create metaphase III-like spindles (**Figure 34B**). This is achieved due to persistent Ndt80 that counteracts degradation of cyclins and in their absence boosts the synthesis of Clb1 and Clb4.

We next tested experimentally whether cells with inactivated Cdc20 after the exit from meiosis II re-accumulate cyclins for a third meiotic division. In order to prevent any APC/C-dependent degradation, we used *ama1Δ P_{DMC1}-AMA1* and *P_{HSL1}-CDH1* genetic background to inactivate both Ama1 and Cdh1, respectively. Using the *cdc20-3-mAR* system, we arrested cells in metaphase I and released them from the arrest at 8 hr. To accumulate high levels of metaphase proteins, Cdc20 was inactivated by the temperature shift to 36 °C at 50 min. To release cells from the metaphase II-arrest, the temperature was shifted back to 25 °C 70 min later. We observed that cells with reactivated Cdc20 degrade cyclins and disassembly meiotic spindles within 40 min (**Figure 35**). We allowed the control cells ("Cdc20 active") to continue with active Cdc20 after the release from metaphase II-arrest. In order to inactivate Cdc20 in the experimental strain ("Cdc20 inactive"), we shifted the temperature of the culture at 240 min to 36 °C. We did not observe additional strong accumulation of M-phase proteins for a third time. Thus, we conclude that cells do not attempt to enter a third division. We confirmed these results with experiments performed with another marker of meiotic progression, Clb1-myc9, to address the Ndt80-dependent accumulation of component of meiotic oscillator in IF staining. Similarly as in cells with Pds1-myc18, we did not observe a third wave of accumulation of Clb1-myc9 in tetra-nucleated cells (data not shown). We conclude that inactivation of Cdc20 after the exit from meiosis II does not cause re-accumulation of its substrates and reassembly of metaphase spindle. Consequently, additional, APC/C-independent mechanisms exist that are required for terminating meiotic oscillations by maintaining low Cdk1 activity and preventing any additional division after completion of meiosis II.

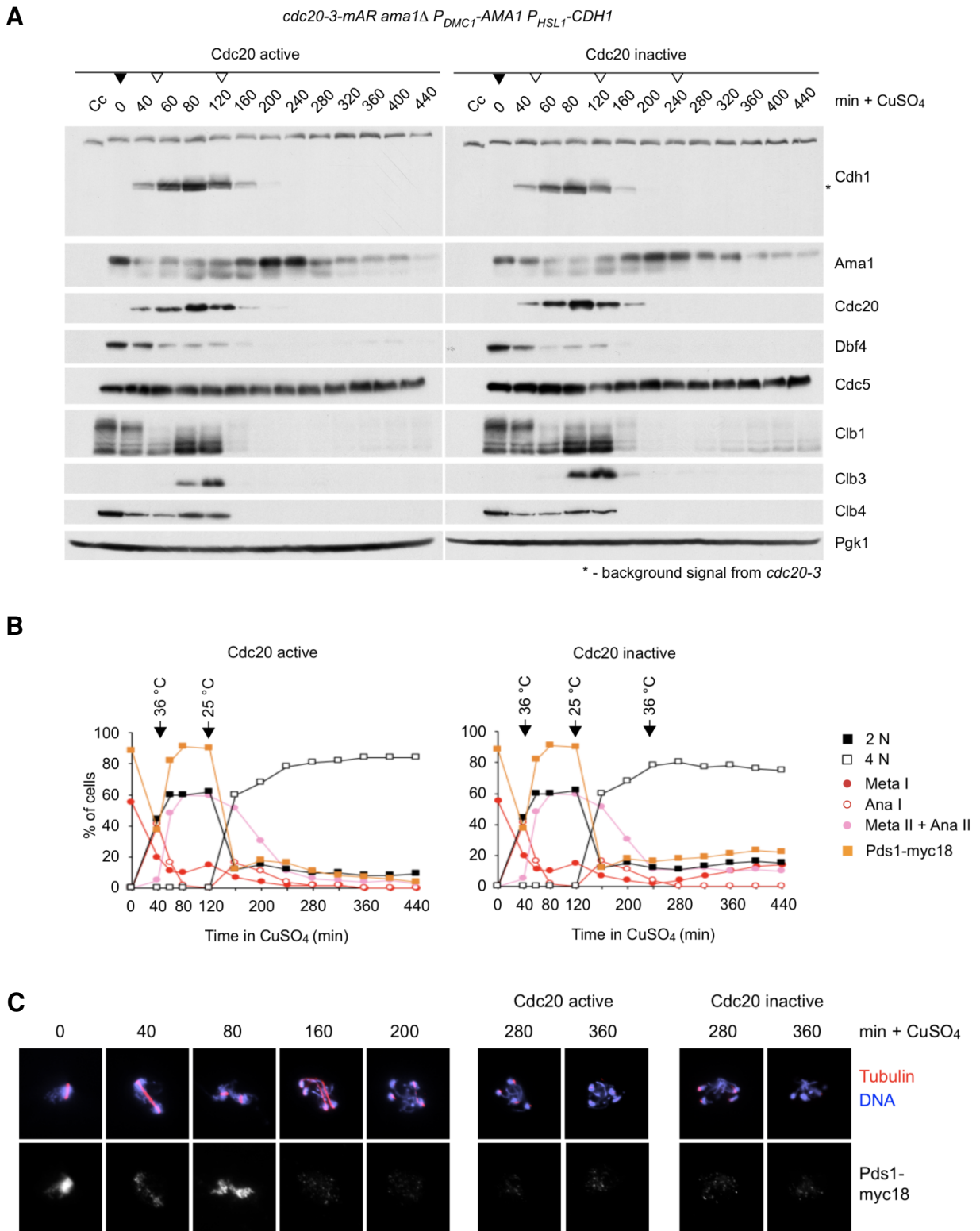


Figure 35. Cells do not enter meiosis III in the absence of Cdc20 and Ama1 activity after the exit from meiosis II. (Figure legend on the next page 77)

A nuclear protein has to be transported to the nucleus after its synthesis in the cytoplasm to perform its function. We speculated that inability of a cell to perform the nuclear import may as a consequence limit the ability to synthesize M-phase proteins after the exit from meiosis II. One possibility of limiting the nuclear import may be due to the process of formation of prospore membrane that engulfs the haploid nuclei, resulting in generation of spores. To prevent possible restriction of protein synthesis by the mechanical barrier, we deleted one of a gene required for the formation of the prospore membrane, namely *MPC70* (Bajgier et al., 2001). As previously, we arrested cells in metaphase I and released them from the arrest at 8 hr. We let them progress synchronously to meiosis II and arrested them for 1 hr in metaphase II to accumulate metaphase I-like levels of meiotic regulators. We released cells from metaphase II-arrest in permissive temperature and after complete degradation of cyclins we inactivated Cdc20 once again. We observed that cells with *mpc70Δ* progress through meiotic divisions with similar kinetics as cells with WT *MPC70* (**Figure 36**). Cells from both strains exit meiosis II at the same time with degradation of cyclins and disassembly of meiotic spindles. Although we suspected that inability to observe the third wave of accumulation of cyclins may be due to the prospore membrane formation, we could not verify these assumption. Similarly as in cells with active Mpc70 protein, *mpc70Δ* cells keep low levels of cyclins after complete inactivation of APC/C at the exit from meiosis II. Thus, we conclude that the formation of the prospore membrane does not prevent re-accumulation of M-phase proteins in the absence of APC/C. Nonetheless, it is important to note that the system of metaphase II-arrest/release used in this work requires strong manipulation of Cdc20 activity and therefore may affect the general conclusion.

Figure 35. Cells do not enter meiosis III in the absence of Cdc20 and Ama1 activity after the exit from meiosis II. Cells in *ama1Δ P_{DMCI}-AMA1 P_{HSL1}-CDH1* background in *cdc20-3-mAR* system (Z33491) were arrested in metaphase I and released from the arrest at t = 8 hr by the addition of 10 μM of CuSO₄ at 25 °C. At t = 50 min, temperature was shifted to 36 °C to inactivate Cdc20. At t = 120 min, temperature was shifted back to 25 °C to reactivate Cdc20. The control strain ("Cdc20 active") was incubated at 25 °C until the completion of the experiment, while the experimental strain ("Cdc20 inactive") was shifted to 36 °C at t = 240 min for inactivation of Cdc20 after the exit from meiosis II. **(A)** Immunoblot detection of proteins. CC means proliferating cells. Black arrowheads mean addition of CuSO₄; white arrowheads mean temperature shifts. **(B)** Quantification of meiotic progression by IF detection of nuclear division (2N is one division, 4N is two divisions), metaphase I (Meta I), anaphase I (Ana I) or meiosis II (Meta II + Ana II) spindles and nuclear Pds1-myc18 signal. **(C)** Representative IF pictures of cells at the given time after the release from metaphase I-arrest (t = 0).

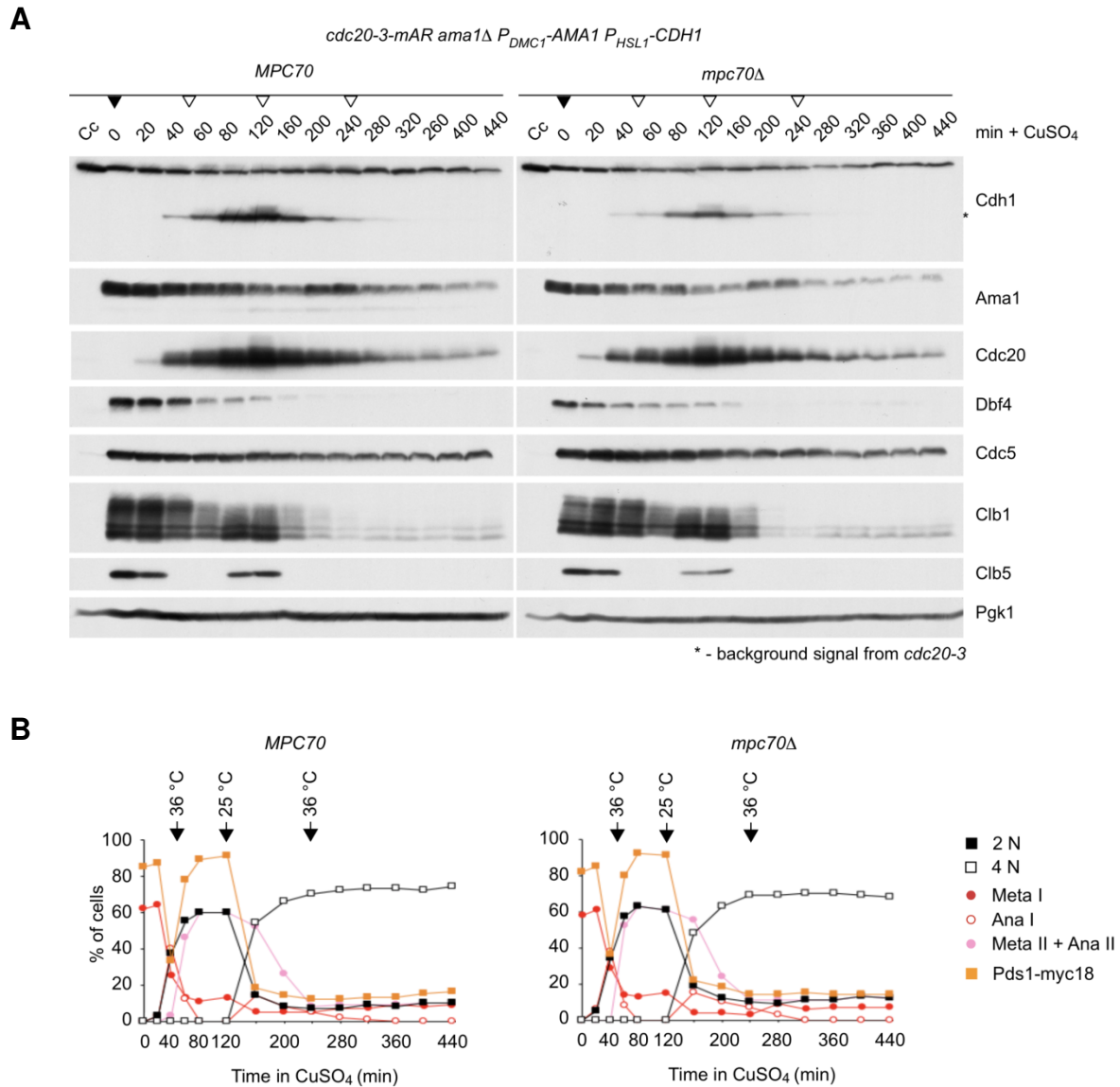


Figure 36. Cells do not enter meiosis III in the absence of prospore membrane and APC/C activity. Cells in *ama1Δ P_{DMC1}-AMA1 P_{HSL1}-CDH1* background in *cdc20-3-mAR* system containing WT *MPC70* (Z34121) or *mpc70Δ* (Z34122) were arrested in metaphase I and released from the arrest at $t = 8$ hr by the addition of $10 \mu\text{M}$ of CuSO_4 at 25°C . At $t = 50$ min, temperature was shifted to 36°C to inactivate Cdc20. At $t = 120$ min, temperature was shifted back to 25°C to reactivate Cdc20. To inactivate Cdc20 after the exit from meiosis II, temperature was shifted to 36°C at $t = 240$ min. **(A)** Immunoblot detection of proteins. CC means proliferating cells. Black arrowheads mean addition of CuSO_4 ; white arrowheads mean temperature shifts. **(B)** Quantification of meiotic progression by IF detection of nuclear division (2N is one division, 4N is two divisions), metaphase I (Meta I), anaphase I (Ana I) or meiosis II (Meta II + Ana II) spindles and nuclear Pds1-myc18 signal.

2.6. Role of phosphatases in termination of meiotic oscillations

Activities of kinases, such as Cdk1 and Cdc5, are driving both mitotic and meiotic divisions. In meiosis, kinases are required for proper progression through two divisions, being important for spindle formation, APC/C activation or general regulation of Ndt80-dependent synthesis. As the events of synthesis of cyclins, and thus activity of Cdk1, are counteracted by Ama1- and Cdc20-dependent degradation, the activities of kinases are counterbalanced by the activities of phosphatases. Therefore, we tested whether some of the well-known cell cycle phosphatases may contribute to the termination of meiotic oscillations together with APC/C.

2.6.1. Phosphatases might inhibit the synthesis of proteins after the exit from meiosis II

Ndt80 activity strictly depends on the activities of three kinases: Cdk1, Ime2 and Cdc5. Both Cdk1 and Ime2 are required for inhibition of the repressor of Ndt80 transcription, namely Sum1. Cdc5 and Ime2 activate Ndt80 through phosphorylation (Schindler and Winter, 2006; Sopko et al., 2002). Therefore, dephosphorylation counteracting Ndt80 phosphorylation may lead to inactivation of Ndt80 and, as a result, decrease in synthesis of other M-phase regulators. Inactivation of such phosphatases may create yet another situation of a gain of function of a protein that usually is not involved in a particular process, such as termination of the oscillations. Here, we studied whether a hypothetical phosphatase activated at the exit from meiosis II may be important for the termination of meiotic oscillations along with Cdc20. Firstly, we simulated a model, in which a component of the termination machinery, called a protein phosphatase PP, inhibited the Ndt80-dependent synthesis at the exit from meiosis II. For simplicity, we assumed that the activity of PP is inhibited by a meiosis I-specific inhibitor (initial value of PP was set to 0) (**Equation 50**).

$$[PP] \frac{d}{dt} = k_{PPa1} \cdot \frac{J_{PI}}{J_{PI} + [Inh]} \cdot \frac{[PP_T] - [PP]}{J_{PP} + [PP_T] - [PP]} - k_{PPi1} \cdot \frac{[PP]}{J_{PP} + [PP]} \quad (50)$$

We assumed direct consequences of the activity of the phosphatase on Ndt80-dependent synthesis (**Figure 37A**). Thus, we modeled a PP-dependent inhibition of Ndt80 activation:

$$[Ndt80] \frac{d}{dt} = (k_{Ndt80a1} + k_{Ndt80a2} \cdot [Cdc5]) \cdot \frac{J_{NPP}}{J_{NPP} + [PP]} \cdot ([Ndt80_T] - [Ndt80]) - (k_{Ndt80i1} + k_{Ndt80d1} + k_{Ndt80d2} \cdot [Ama1] + k_{Ndt80d3} \cdot [Ama1_T]) \cdot [Ndt80] \quad (51)$$

Table 9. Parameter values of the model with a possible phosphatase.¹

Equation number	Parameters and their values
50	$J_{NPP} = 0.001$
51	$k_{PPa1} = 1, k_{PPi1} = 0.8, J_{PI} = 0.1^{-4}, J_{PP} = 0.05, PP_T = 10$

¹Only newly introduced parameters are presented.

With inactivation of Ndt80 after the exit from meiosis II, the levels of the transcription factor and its substrates decrease (**Figure 37B-C**). The activity of PP can be replaced by the activity of either Ama1 or Cdc20, leading to the exit from meiosis II and limitation of the number of divisions. In cells with inactive Cdc20 and Ama1 in meiosis II exit, the phosphatase, or other machinery inhibiting the Ndt80-dependent synthesis, is important to keep the low levels of cyclins and prevent re-entry into the high Cdk1 state of a third meiotic division (**Figure 37C**).

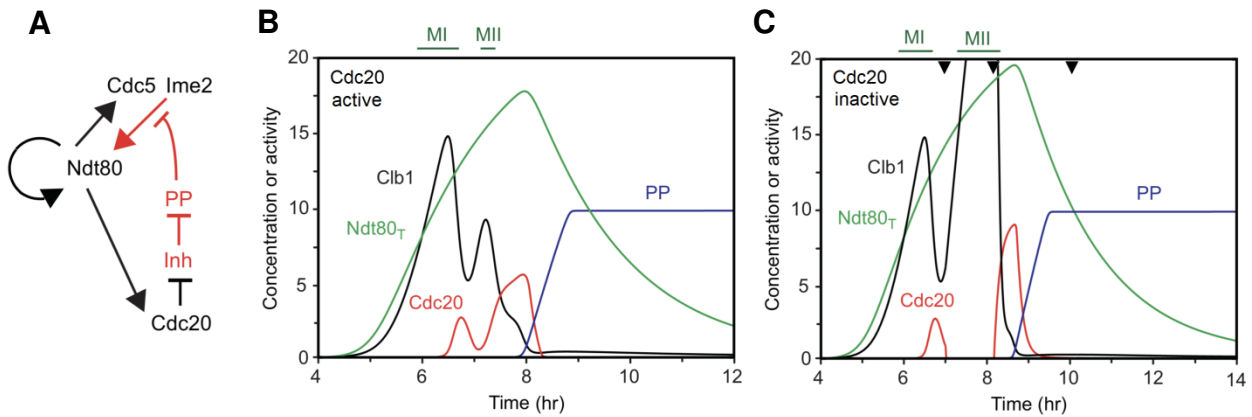


Figure 37. A meiosis II-specific phosphatase may be involved in termination of meiotic oscillations. (A) Simplified wiring diagram with PP module depicted in red. For simplification only interactions between Ndt80 and PP are presented. \downarrow is positive interaction; \perp is negative interaction. (B-C) Simulations depicting concentration or activity of Clb1, Cdc20, Ndt80_T and PP. Simulations were performed in the absence of Ama1 ($Ama1_T = Ama1_{AT} = 0, k_{Ama1s1} = 0$). (B) Simulation in the presence of active Cdc20. (C) Simulation of cells with inhibited Cdc20 activity after the exit from meiosis II ($k_{Cdc20a1} = 0$ at $t = 7$ hr; $k_{Cdc20a1} = 20$ at $t = 8.15$ hr; $k_{Cdc20a1} = 0$ at $t = 10.15$ hr). Black arrowheads indicate change of the parameters. MI and MII are metaphase I and -II spindles indicating the consecutive divisions.

2.6.2. PP2A^{Cdc55} and PP1^{Gip1} modify proteins at the exit from meiosis II

From previous studies, we conclude that Cdc14 activity is not important for the exit from meiosis II (Argüello-Miranda et al., 2017). Cells degrade M-phase regulators, disassemble meiotic spindles and enter a low Cdk1 state in the absence of this phosphatase. Thus, we studied the importance of two other phosphatases known to be involved in the exit from mitosis: PP2A^{Cdc55} and PP1. Firstly, we tested the effect of PP2A^{Cdc55} on the progression through meiotic exit. Cdc55 is known to be required for proper regulation of mitosis and meiosis I (Queralt et al., 2006; Kerr et al., 2011). Thus,

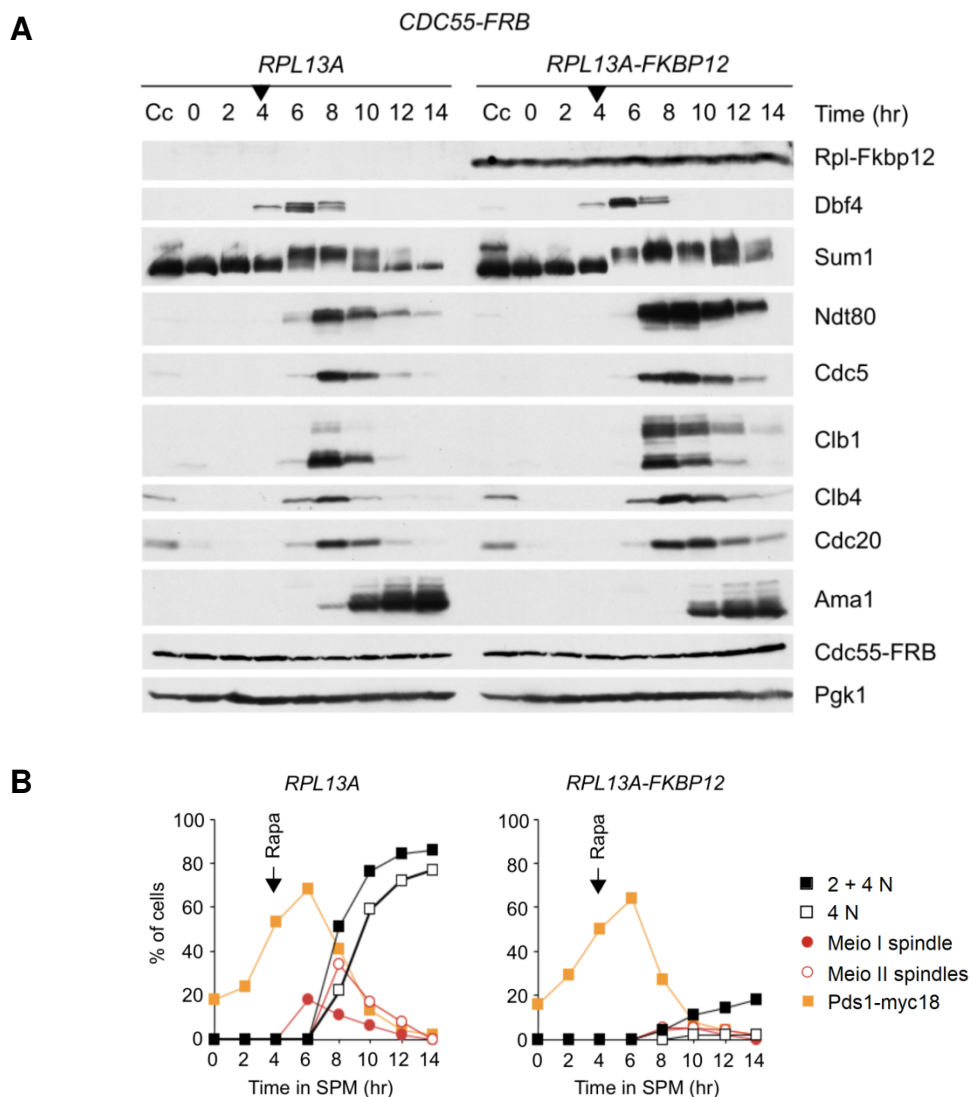


Figure 38. Early inhibition of Cdc55 activity affects the exit from meiosis II. A conventional meiotic time course was performed using anchor-away system with Cdc55 tagged with FRB in control cells *RPL13A* (Z34012) and in experimental strain *RPL13A-FKBP12* (Z34013). For inactivation of Cdc55, 10 μ g/ml of rapamycin (Rapa) was added at $t = 4$ hr. **(A)** Immunoblot detection of proteins. Black arrowhead means addition of rapamycin. Cc means proliferating cells. **(B)** Quantification of meiotic progression by IF detection of nuclear division (2+4N is at least one division, 4N is two divisions), meiosis I (Meio I) and -II (Meio II) spindles, and nuclear Pds1-myc18.

we created a version of Cdc55, which allowed us to inhibit the nuclear activity of the phosphatase at a precise time without interfering with its function in earlier stages. We used an anchor-away (AA) system, in which a nuclear protein of interest is inactivated through its forced export to the cytoplasm (Haruki et al., 2008). The studied protein is tagged with a FRB domain and binds to an anchor, which is a ribosome subunit Rpl13a tagged with FKBP12, in the presence of rapamycin. The complex of the tagged protein and Rpl13a-FKBP12 moves to the cytoplasm. Therefore, the protein fails to exert its nuclear function. The system is implemented with *fpr1* Δ and *tor1-1* mutation, interfering with the binding of rapamycin to Tor1 and its rapamycin-dependent inhibition. We

tagged with FRB the C-terminus of Cdc55 and performed a conventional meiotic time course to test the effect on the phosphatase on the progression through meiotic divisions. Upon inactivation of Cdc55 at 4 hr, cells from the experimental strain (*RPL13A-FKBP12*) accumulate M-phase proteins at the same time as the control strain (*RPL13A*), indicating proper entry into the first division (**Figure 38A**). Cells with inhibited Cdc55 fail to form meiotic spindle (**Figure 38B**), which is in agreement with previous works (Bizzari and Marston, 2011; Kerr et al., 2011). The meiotic oscillator is not disrupted and cells degrade meiosis I-specific protein Dbf4 and accumulate meiosis II-specific Clb3 at the same time as the control strain. Interestingly, a visible delay is observed at the exit from meiosis II. Upon inactivation of Cdc55, cells accumulate Ama1 later, resulting in a delay in degradation of its substrates. These results indicate that Cdc55 is involved in regulation of the exit from meiosis II. Later experiments with inhibition of Cdc55 activity precisely in meiosis II indicated that this regulation strictly depends on the activities of meiosis I-specific proteins, as cells with Cdc55 absent in meiosis II do not exhibit any visible differences in the activity of APC/C and the exit from the second division (data not shown).

Next, we tested another phosphatase known to play a role during mitotic exit, namely PP1. We used a mutant of the meiosis-specific regulatory subunit of PP1, Gip1, which has a defect in sporulation (Tachikawa et al., 2001). We used the *CDC20-mAR* system for better resolution and observed that in the presence of active Ama1 in meiosis II, *gip1Δ* cells fail to dephosphorylate some of the Ime2 substrates, such as Sum1 and Cdh1 (**Figure 39A**). Notwithstanding, cells still degrade Cdc20 and Ama1 substrates and divide the second time, thus performing undisrupted exit from meiosis II (**Figure 39B**). We confirmed this result by using a temperature-sensitive mutant of a catalytic subunit of PP1, Glc7, inactivated precisely in meiosis II (data not shown). These results prompted us to speculate that PP1 may be involved in the exit from meiosis by regulation of Ime2 substrates and thus possibly Ndt80-dependent synthesis of M-phase regulators.

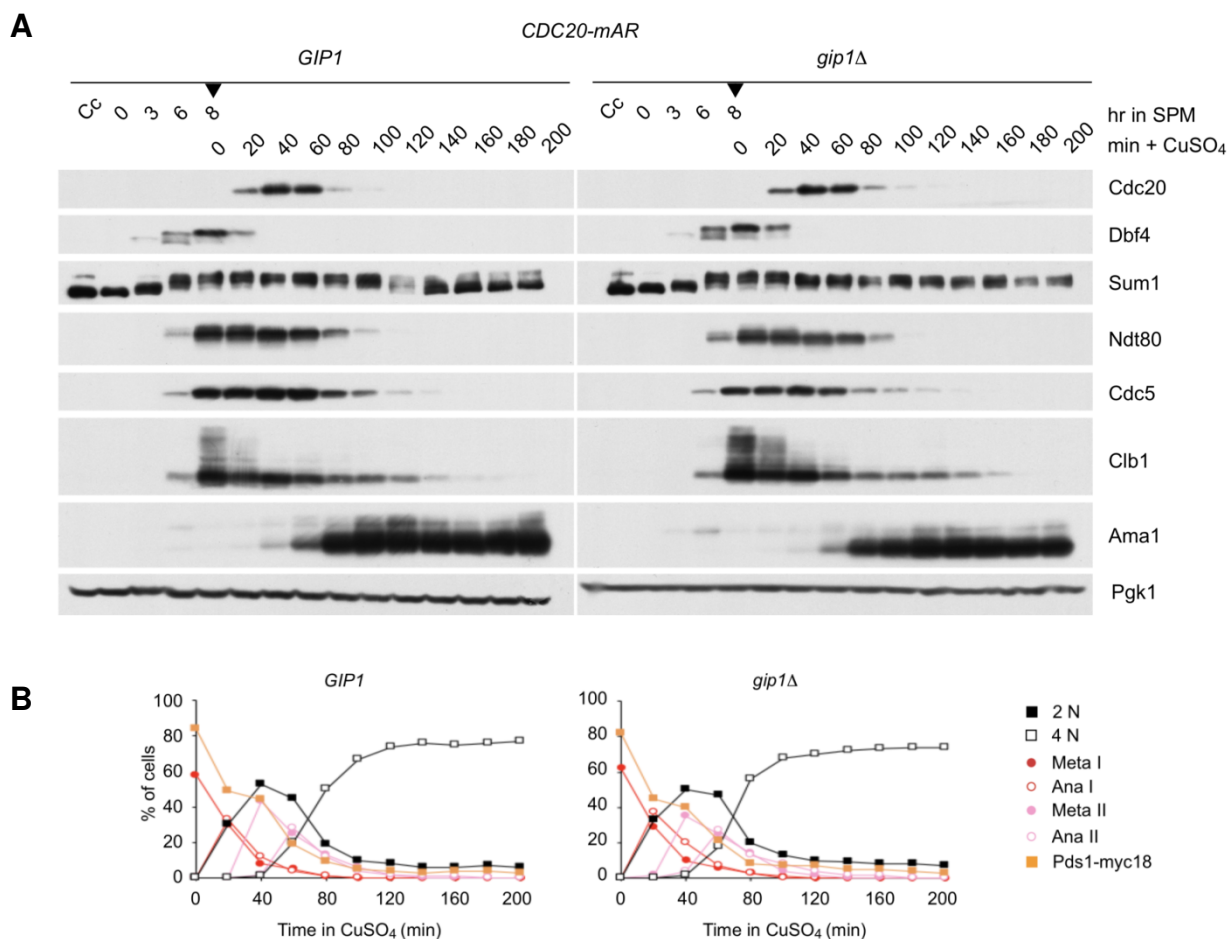


Figure 39. Deletion of *GIP1* causes defects in dephosphorylation of some of the *Ime2* substrates, but not the exit from meiosis II. *CDC20-mAR* system was used. Cells expressing *GIP1* (Z32710) or *gip1Δ* (Z32711) were arrested in metaphase I and released from the arrest at $t = 8$ hr by the addition of $10 \mu\text{M}$ of CuSO_4 . **(A)** Immunoblot detection of proteins. Cc means proliferating cells. **(B)** Quantification of meiotic progression by IF detection of nuclear division (2N is one division, 4N is two divisions), spindles and nuclear Pds1-myc18.

2.6.3. Inhibition of PP1^{Gip1} or $\text{PP2A}^{\text{Cdc55}}$ in the absence of *Ama1* activity does not cause defects in the exit from meiosis

We were interested whether the phosphatases of interest are involved in regulation of the Cdc20-dependent exit from meiosis II in the absence of *Ama1* activity. This would shed light on their involvement in the regulation of the termination machinery of meiotic oscillations independent of *Ama1*. Thus, we inhibited the activities of PP2A and PP1 in the absence of *Ama1* activity in meiosis II. Firstly, we tested the effect of $\text{PP2A}^{\text{Cdc55}}$. We carried out an experiment in a system that allowed us to inhibit Cdc55 activity precisely in meiosis II. We did not use the *CDC20-mAR* system due to a disruption in Cdc14 release in meiosis I in cells with tagged Cdc55 during long metaphase I-arrest (data not shown). Thus, we adopted the Ndt80-arrest/release system (Carlie and Amon, 2008; Matos et al., 2008), in which cells arrest reversibly in prophase I due to deletion of *NDT80*. The release from the arrest is triggered by the expression of

NDT80 from an estradiol-inducible promoter (Benjamin et al., 2003; Picard, 1999). We arrested cells of the *ama1Δ P_{DMC1}-AMA1* background and released them from the arrest at 7 hr in SPM by addition of estradiol. We added rapamycin at metaphase I-to-anaphase I transition to inhibit the activity of Cdc55 in meiosis II. We noticed that the strain lacking Cdc55 in the nucleus progresses through meiotic divisions with similar kinetics as the control strain, degrading Dbf4 ~120 min and accumulating Clb3 at ~150 min (**Figure 40**). Cells from both strains degrade cyclins in meiosis II at similar time and disassemble meiotic spindles, resulting in completion of meiosis and termination of meiotic oscillations.

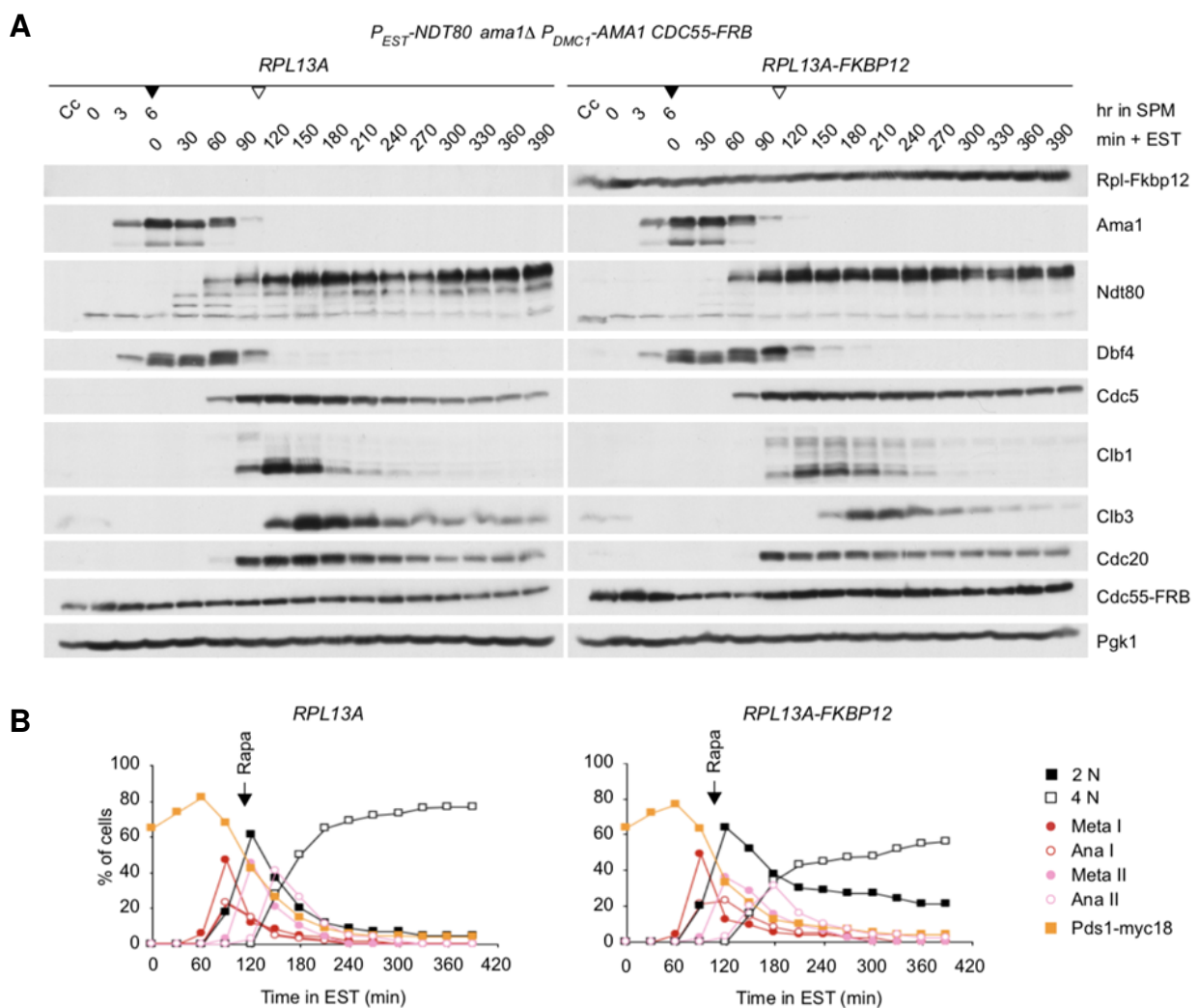


Figure 40. Inhibition of Cdc55 activity in meiosis II does not affect the exit from meiosis II in the absence of Ama1. Ndt80 arrest/release system was used for synchronizing meiotic culture. Anchor-away system was used in *ama1Δ P_{DMC1}-AMA1* background in *RPL13A* strain (Z34712) and *RPL13A-FKBP12* strain (Z34713). Cells were arrested in prophase I and released from the arrest at t = 7 hr by addition of 10 μ M of estradiol (EST). At t = 100 min, Cdc55 activity was inhibited by addition of 10 μ g/ml of rapamycin (Rapa). **(A)** Immunoblot detection of proteins. Black arrowhead means addition of rapamycin. Cc means proliferating cells. **(B)** Quantification of meiotic progression by IF detection of nuclear division (2N is one division, 4N is two divisions), spindles and nuclear Pds1-myc18.

We next tested whether inactivation of PP1^{Gip1} has an effect on the activity of Ime2 kinase, and possibly Ndt80-dependent synthesis, in the absence of Ama1. We used the *CDC20-mAR* system in *ama1Δ P_{DMC1}-AMA1* background. We observed that *gip1Δ* cells progress through meiotic divisions with similar kinetics as the control strain containing *GIP1* (**Figure 41**). Cells degrade cyclins at the similar time at ~100 min and disassemble meiotic spindles, completing two meiotic divisions. Notice that cells degrade cyclins completely after the exit from meiosis II and do not attempt their re-accumulation. Additionally, *gip1Δ* cells in the absence of both Ama1 and Cdc20 in the *cdc20-3-mAR* system keep low levels of cyclins after the exit from meiosis II (data not shown). Taken together, we conclude that neither PP1^{Gip1} nor PP2A^{Cdc55} are important for the termination of meiotic oscillations after the exit from meiosis II in the presence or absence of APC/C co-activators.

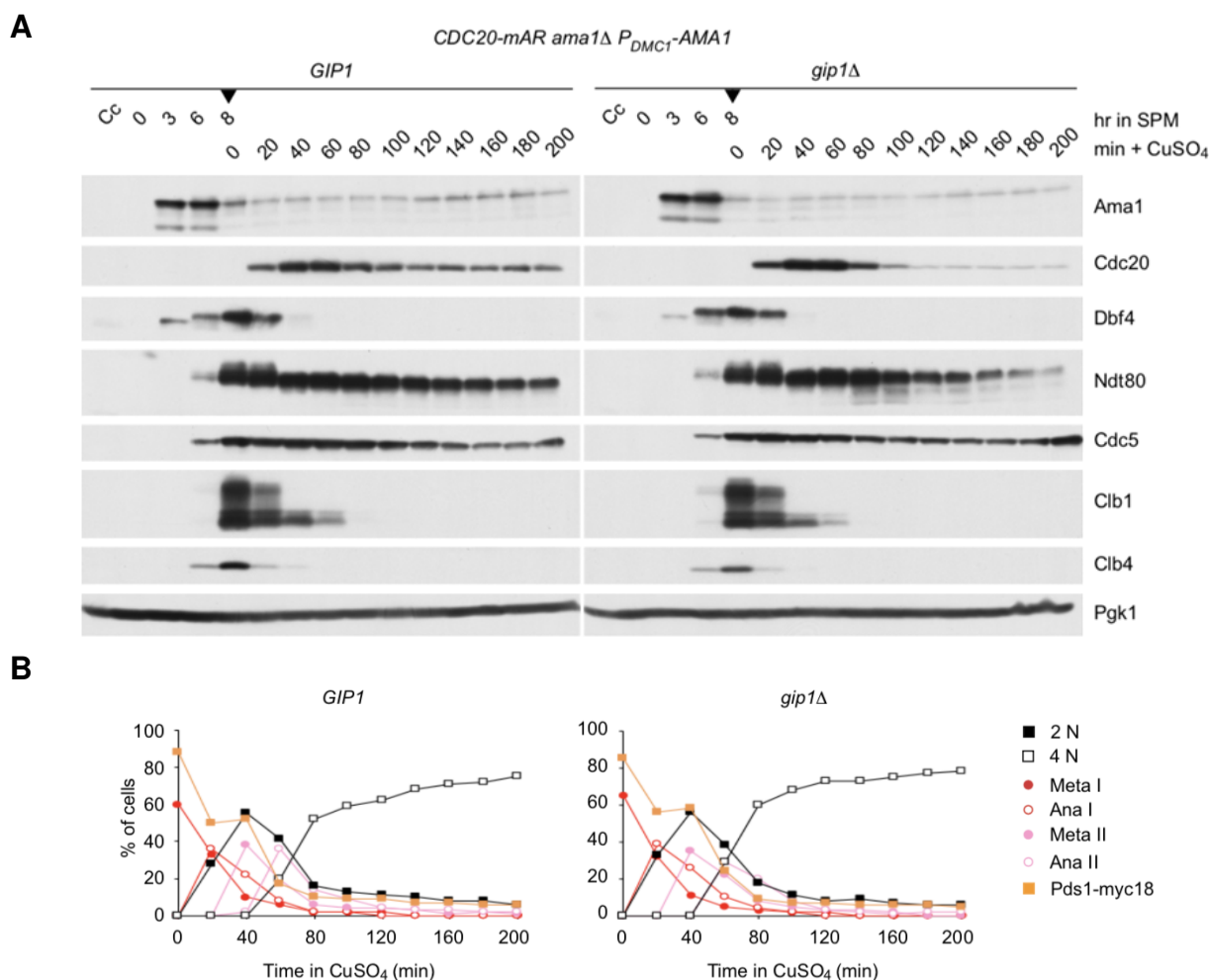


Figure 41. Deletion of *GIP1* does not affect the exit from meiosis II in the absence of Ama1. *CDC20-mAR* system was used. *ama1Δ P_{DMC1}-AMA1* cells expressing *GIP1* (Z24253) or *gip1Δ* (Z34254) were arrested in metaphase I and released from the arrest at t = 8 hr by the addition of 10 μ M of CuSO₄. **(A)** Immunoblot detection of proteins. Cc means proliferating cells. **(B)** Quantification of meiotic progression by IF detection of nuclear division (2N is one division, 4N is two divisions), spindles and nuclear Pds1-myc18.

3. Discussion

3.1. Meiosis consists of two waves of Cdk1-APC/C activity

During meiosis, cells undergo exactly two rounds of chromosome segregation after only one round of DNA replication, resulting in a reduction of the DNA content by half. The two meiotic divisions are followed by a differentiation program, leading to the formation of gametes, such as eggs or sperms. In yeast, four haploid nuclei are engulfed in spores, which allow cells to survive unfavorable environmental conditions (Coluccio et al., 2008). Progression through meiotic divisions is strictly regulated by the periodic activation and inactivation of Cdk1 and APC/C. Unlike in mitosis, during which cells enter a low Cdk1 state to prepare for the next cycle, in meiosis cells reactivate Cdk1 abruptly to enter the second division (Marston and Amon, 2005). Sequential activation of Cdk1 is required for the proper segregation of the genetic material. The exit from meiosis is followed by the sporulation program during which low Cdk1 activity is maintained. Several questions can be asked to unravel how exactly cells regulate this stepwise activation of Cdk1 and the precise exit from meiosis after the second division.

- (i) How is the mitotic engine that consists of waves of Cdk1 and APC/C^{Cdc20} activities modified to perform a two-division meiosis? Meiosis can be viewed as a modified version of mitosis with regard to the regulatory protein network that governs the divisions. Cells require a specific machinery that allows them to modify the mitotic Cdk1-APC/C^{Cdc20} oscillator to segregate chromosomes in two rounds.
- (ii) How do meiotic cells regulate the time of the exit from meiosis? A meiosis II-specific machinery must ensure the completion of two divisions and the immediate exit precisely after meiosis II, preventing any additional meiotic division to occur. In vertebrates, defects in the regulation of the exit result in a third wave of Cdk1 activity and formation of additional spindles, leading to defective gametes (Kubiak, 1989; Dumollard et al., 2011; Pfeuty et al., 2012).
- (iii) How robust is the mechanism that prevents additional divisions? Regulation of the exit from meiosis after meiosis II must not only be precise but also robust to prevent possible re-entry into the third high Cdk1 state after the completion of meiosis II. The exit from meiosis II may be controlled by several different mechanisms that are coupled to meiosis II and create a redundant system for the meiotic exit.

3.2. Mathematical modeling allows to study the multi-component network driving meiotic divisions

The meiotic machinery that orchestrates the events of cell division is based on the Cdk1-APC/ C^{Cdc20} oscillator, well conserved among species, and is complemented by a variety of meiotic regulators. Together, these molecules form a complex protein regulatory network that directs the nuclear divisions. Analyzing the regulation of biological processes, such as meiosis, often requires a mathematical description that takes into account the complexity and the dynamics of the regulatory systems.

Advantages of mathematical modeling

Due to the complexity of dynamical biological systems resulting from a high number of components of the network and their nonlinear responses, it is challenging to study the properties of the system and the behavior of a single cell or the whole population. Mathematical modeling simplifies the biological description of various types of interactions between multiple components of the regulatory network. This approach allows to capture the critical components of the system and helps to understand how it responds to stimuli, perturbations and changes in the regulatory network in mutant cells. Modeling is often used to predict the implications of modifications of the biological system, thus it has a predictive value. In this work, we used a mathematical modeling approach in combination with biological experiments to study the control of the two meiotic divisions in budding yeast.

Unraveling the details of the meiotic regulation in budding yeast is hampered by the fact that the two divisions are very close to each other and the synchrony of meiotic cultures is poor. Describing two divisions using mathematical language allows to perform synchronous *in silico* experiments that do not require manipulation of the network in order to achieve high resolution between particular stages of meiosis. Thus, it is possible to study in more details the properties of transitions in meiosis without interfering with the wild-type properties of the system. Due to the two-division nature of meiosis and the complexity of its regulatory network, no mathematical model describing the two divisions has been developed to date. Tyson and Novak proposed a generic picture of the regulation of meiosis based on the knowledge from mitosis (Tyson and Novak, 2008), which was later adopted as a model to study the regulation of Clb1 during meiosis (Tibbles, 2013). Our model presented here describes in more details the control of progression through meiosis based on the Cdk1-APC/ C^{Cdc20} oscillator with special emphasis on the regulation of the termination of these oscillations precisely after the second division.

Simplification of the meiotic network with mathematical modeling

To understand the crucial components of the regulatory network, mathematical models reduce its complexity. Models containing detailed information about the regulatory network might create difficulties in interpretation of the result of the computation and of the dependences of the particular behavior of the system on a studied mechanism. It is challenging to develop a simplified model of a biological dynamical process that describes the process without impairing the network significantly. The difficulties lie in choosing the most relevant components of the model influencing the process and connecting the assumed simplifications to observed biological phenomena. Although approximations have to be made during model development, the simplified model can be still constructed as quantitative rather than only conceptual, giving a detailed numerical solutions comparable to the biological measures.

We simplified the regulatory network of meiotic divisions by choosing the relevant time scale of the events we wanted to portray. We omitted early events of meiosis, such as DNA replication, and late events, such as sporulation. We focused on reproducing four main transitions between the entry into meiosis I and the exit from meiosis II. To provide the entry into the first division, we used the existing model of the prophase I-to-metaphase I transition (Okaz et al., 2012). We incorporated the Cdk1-APC/C^{Cdc20} oscillator to implement two other transitions: from metaphase I to anaphase I and from anaphase I to metaphase II (**Figure 14**). Lastly, we modified the model by adding a hypothetical regulator of the oscillations that terminates them precisely after meiosis II (**Figure 19**). For further simplification, we chose the nuclear molecules that we identified as most relevant to the progression through the divisions. We tested *in silico* different possibilities of molecules and interactions involved. We simplified some of the interactions, such as complex formation between the APC/C core and Cdc20 activator. For the model of two divisions, we omitted some of the interactions that result from a cross-talk between the chromosomes and protein network. An example is the regulation of Cdc20 activity by the spindle assembly checkpoint (SAC). Its inclusion in future versions of the model might provide additional level of regulation of meiotic divisions that would contribute to the precise timing of the exit from meiosis I and -II. Our model is designed to be extended by additional modules, such as a more detailed network of Ndt80 regulation. Additionally, the model can be further extended to understand events of meiosis I and - II in more details, such as sporulation. **Figure 42** presents a simplified wiring diagram of the final version of the model presented in this work in **Chapter 2.5.**, as well as simulation of wild-type cells recreating the general progression through the divisions and the exit after meiosis II.

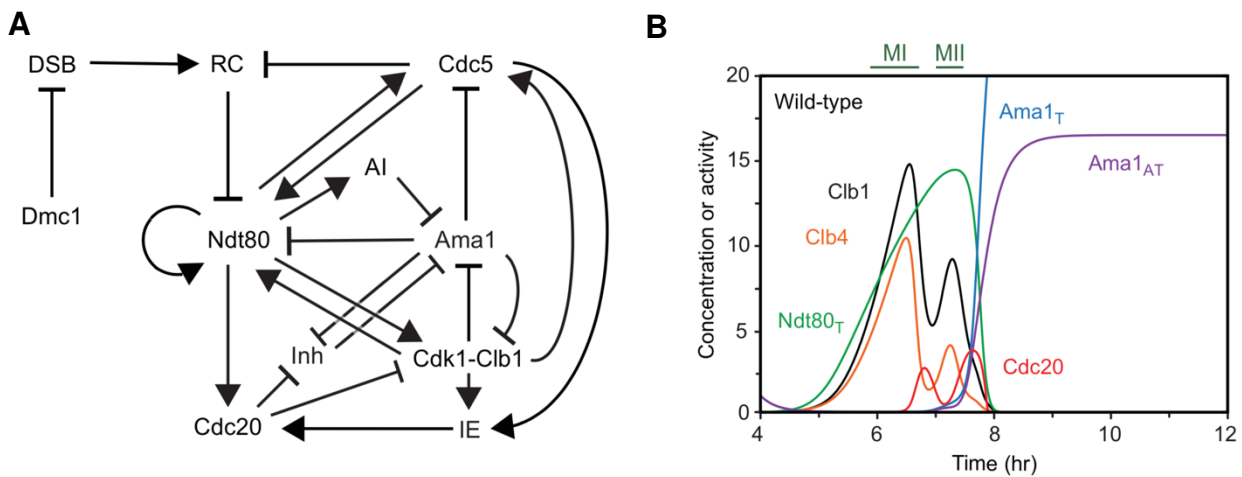


Figure 42. Mathematical model of two meiotic divisions describes regulation of the progression through meiotic divisions and the exit after completion of meiosis II. (A) Simplified wiring diagram of main interactions in the meiotic network included in the model. RC - recombination checkpoint; AI - additional inhibitor; IE - intermediate enzyme; Inh - inhibitor of Ama1. For simplification of the diagram, Sum1, Clb4 and the complex formation between AI and Ama1 are omitted. **(B)** Simulation of progression through meiotic divisions in wild-type cells showing concentration or activity of key regulators of divisions. MI and MII are metaphase I and -II spindles indicating the consecutive divisions.

Relevance of parameter estimation

The properties of the biological system resulting from specific types of interactions between molecules often create more than one type of cellular behavior. The type of the behavior depends directly on the mathematical level of the description of the system based on kinetic laws and values of parameters describing relation between the system components. Small changes in parameter values might result in changes of dynamical behavior. For example, the same set of equations describing negative feedback loop may give an oscillating system or a system that approaches homeostasis. Thus, a crucial step in developing a model is estimation of parameter values. The parameter estimation starts with a guess of the parameter values followed by changes of those values to minimize the discrepancy between the model and the biological data. Kinetic models with nonlinearity have multiple sets of parameters that lead to such minimizations. Given a particular set of biological data, parameterization obtained by a parameter estimation procedure does not mean that all parameters are optimal. Different sets of parameter values might give similar solutions of the equations.

The estimation is usually based on different strategies. For example, in reverse engineering approach parameters are estimated by fitting the model output to available experimental data (Sible and Tyson, 2007). There are different algorithms for computational parameter estimation, but these methods become more complicated with bigger models and higher number of parameters (Ashyraliyev et al., 2009). Therefore, many times a “guessing” method and fitting “by hand” is implemented (Sible and

Tyson, 2007). For development of our model, we combined this approach with our knowledge about experimentally measured values, such as degradation rates of proteins and relative abundance of proteins. This addition results in a more quantitative relation between the dynamics of different components of the network. Other parameters were based on parameters known from previous work on the model of the prophase I-to-metaphase I transition (Okaz et al., 2012) or guessed based on biological observations. All the parameters were adjusted to fit biological observations and to create the most robust system that is able to maintain its behavior in various biological mutant conditions with the introduction of noise and perturbations. A single set of parameters recapitulates the majority of the tested mutant phenotypes.

Robustness of the dynamical system

Dynamical biological systems are usually robust, which means that small changes in the input stimuli or network do not change the general behavior of the system. The chosen values of parameters that describe the interactions, as well as the characteristics of the network ensure robustness of the model and support the complex behavior of the biological system.

As living cells are noisy systems, the regulatory network has to be able to generate the same response for the small perturbations in the activities of molecules. The main challenge in developing a model of meiosis is to ensure that it recreates a two-division meiosis when subjected to small perturbations. At the same time, the model should allow the system to be flexible enough to perform fast changes in the activities of meiotic regulators that result in two sharp waves Cdk1 and APC/C^{Cdc20} activities. The activation of Cdk1-APC/C^{Cdc20} oscillator is a robust characteristic of the meiotic network that cannot change in response to normal biological noise. Thus, for each version of the model presented in this work, we chose the values of the majority of model parameters that maintain the general behavior of the system when subjected to a change of +/- 20% of the initial value in wild-type cells and *ama1Δ* cells.

Robustness of the biological system is a property of this system. The robustness of the oscillations and the exit from meiosis after the second division is preserved in some of the mutant strains, such as *ama1Δ*. Thus, the meiotic network consists of additional machineries that in the absence of one of the component of the network direct the system to perform two undisrupted divisions. The robustness of meiotic divisions depends on the structure of the network. To achieve robustness in the designed model, a set of interactions, equations and parameters have to be carefully selected and tested *in silico* under different conditions.

In summary, the crucial and challenging characteristics of the model of two meiotic divisions that result from the robustness of the model are: (i) the ability for rapid changes in the activities of regulators resulting in sharp and rapid responses; (ii) robustness of the two divisions in response to biological perturbations and changes in the network in mutant cells.

3.3. The Cdk1-APC/C oscillator modulates progression through divisions in meiosis

Progression through the meiotic divisions is ensured by a negative feedback loop between Cdk1 and APC/C^{Cdc20}

Meiotic cells enter the first division after a long period of low Cdk1 activity during prophase I. This transition is a result of cooperation of a set of positive feedback loops and double-negative feedback loops (**Figure 43A**). The entry into metaphase I is mediated by the inactivation of the recombination checkpoint (RC) after the repair of double-strand breaks (DSBs). The components of the positive feedback loops coexist with each other thus amplifying the activation of Ndt80 and Cdk1. On the other hand, the double-negative feedback loop between Cdk1-Clb1 and Ama1 creates two mutually exclusive stable states. After inactivation of the RC and inhibition of Ama1 activity, cells switch irreversibly to the high Cdk1 state of metaphase I. The resulting stability leads to cells being trapped in a high Cdk1 state of metaphase I. In order for cells to progress through the divisions, cells have to escape this stable state. It is known that the addition of a negative feedback loop to a system composed of circuits of positive feedback allows the escape from a stable state by turning a bistable switch into oscillations (Boissonade and De Kepper, 1980; Pfeuty and Kaneko, 2009). A negative feedback operating with a time delay and sharp activation of the inhibitory component allows destabilization of the stable state (Pfeuty and Kaneko, 2009). In the model of meiosis, we created an oscillator by introducing a negative feedback loop between Cdk1 and APC/C^{Cdc20} (**Figure 43B**). APC/C^{Cdc20} activity is responsible for the degradation of B-type cyclins and the escape from the high Cdk1 state of metaphase I. Moreover, the negative feedback loop ensures the presence of the oscillations between Cdk1 and APC/C activities, thus allowing the entry into the second meiotic division. The negative feedback loop allows for a fast and reversible switch resulting in progression through meiosis I and -II.

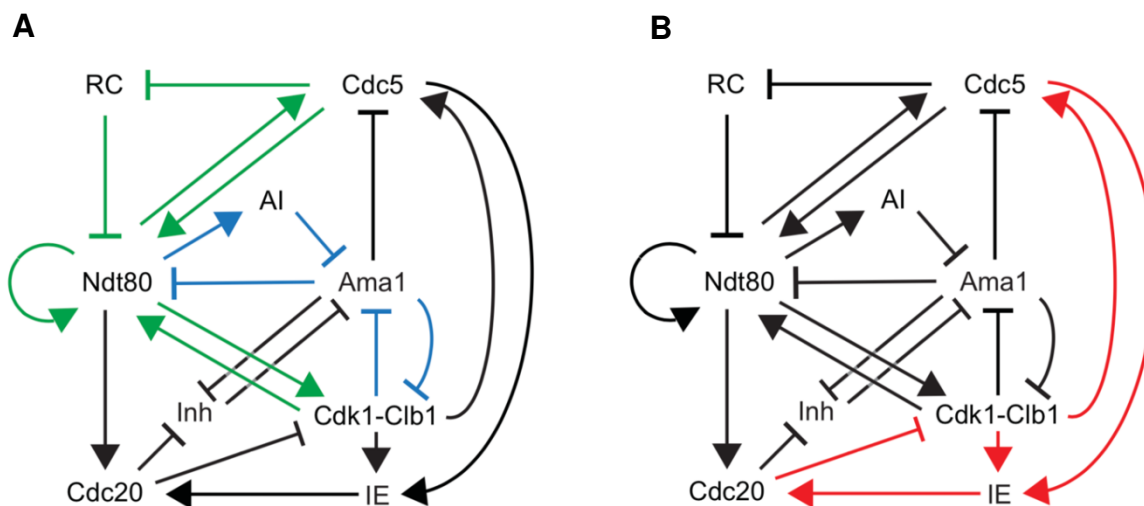


Figure 43. Wiring diagrams presenting feedback loops regulating the progression through meiosis I and II. (A) Positive feedback loops (green) promote the entry into metaphase I, while double-negative feedback loops (blue) offers two mutually exclusive states of prophase I or metaphase I (Okaz et al., 2012). **(B)** Negative feedback loop (red) creates an oscillator allowing rapid and sharp transition from metaphase to anaphase of meiosis I and II.

Modification of mitotic Cdk1-APC/C oscillator in meiosis

We consider that in order to create two, and only two, meiotic divisions cells have to: (i) constantly synthesize cyclins and Cdc20 to be able to activate fast and sharp oscillations resulting in two consecutive divisions; (ii) stop the synthesis of the components of the oscillator precisely after the second division. Thus, strictly regulating the synthesis of cyclins is crucial for progression through two divisions. Budding yeast has three different M-phase cyclins: Clb1, Clb3 and Clb4 (Chu and Herskowitz, 1998). Dahman and Futcher showed that deletion of any two cyclins results in cells executing only one division (Dahmann and Futcher, 1995). We observed that deletions of *CLB1* or *CLB4* leads to defects in progression through meiotic divisions in a majority of cells (**Figure 15**). There are two reasons why Clb1 and Clb4 may be important for proper regulation of the meiotic oscillator: cyclin specificity and general concentration of the proteins. It is known that some of the B-type cyclins have distinct roles during meiosis. The S-phase cyclins, Clb5 and Clb6, are necessary for the execution of DNA replication (reviewed in Bloom and Cross, 2007), while Clb1 inhibits the activity of Ama1 during metaphase I (Okaz et al., 2012). The balance in the levels of cyclins during the two meiotic divisions appears to be a key factor that regulates the activity of Cdk1 and the progression through divisions. Carlie and Amon showed that overexpression of Clb2 or Clb3 in meiosis I, which elevates the overall levels of cyclins, leads to defects in chromosome segregation (Carlie and Amon, 2008). Thus, the proper levels of cyclins have to be ensured to balance the activity of Cdk1 and APC/C for the meiotic oscillator.

For the meiotic system to oscillate, cells have to ensure the re-accumulation of cyclins by persistence of Ndt80 throughout the divisions, until the exit from meiosis II. Switching off Ndt80-dependent synthesis by inactivating one of its activators, Ime2, leads to an inability to re-accumulate cyclins and enter meiosis II (Benjamin et al., 2003). We showed that both Clb1 and Clb4 re-accumulate abruptly after the exit from meiosis I, although with different dynamics (**Figure 16**). Intriguingly, Clb4 exhibits a higher degradation rate than Clb1, leading to complete degradation of this cyclin at anaphase I. By contrast, Clb1 appears to be more stable with a half-life two-fold higher than that of Clb4. Clb1 is not completely degraded between meiosis I and -II, which indicates that Cdk1 activity is not completely abolished between the two divisions. This is in agreement with previous works, suggesting a necessary basal activity of Cdk1 in preventing additional DNA replication between the divisions and ensuring the timely entry into meiosis II (Dahmann et al., 1995; Gerhart et al., 1984; Iwabuchi et al., 2000; Phizicky et al., 2018; Strich et al., 2004). On the other hand, during the exit from meiosis II both cyclins are completely destroyed. To ensure the proper balance between the activity of Cdk1 and APC/C at the exit, we suggested that cells keep a basal activity of APC/C^{Cdc20} during metaphase II. High level of cyclins in the absence of APC/C^{Cdc20} activity causes cells to delay the exit from meiosis II (**Figure 30-31**). We speculate that the basal degradation of cyclins is important for the regulation of the timely exit from meiosis. We have previously shown that prolonged activity of Cdk1 in the absence of Ama1 results in a significant delay in anaphase II spindle disassembly and defects in the exit from meiosis II (Argüello-Miranda et al., 2017). Likewise, increase in cyclins expression in higher eukaryotes leads to improper exit from meiosis II and formation of metaphase III-like spindles (Kubiak, 1989; Verlhac et al., 1996; Dumollard et al., 2011). Thus, robust regulation of the synthesis of B-type cyclins is required for progression to meiosis II and for the proper and timely exit from meiosis.

3.4. Exit from meiosis II and termination of meiotic oscillations are driven by APC/C

At the time of the exit from meiosis II three distinct events happen at the protein regulatory level that are different from the exit from meiosis I: (i) complete degradation of cyclins; (ii) inactivation of Cdk1 and maintenance of a low kinase state after the exit from meiosis; (iii) inactivation of Ndt80-dependent synthesis of the components of the meiotic oscillator. We speculate that in order to limit the number of meiotic divisions, cells require the activity of a meiosis II-specific termination machinery that regulates these events. Inactivation of the termination may lead to re-entering to a high Cdk1 state after meiosis II exit and continuing the oscillations. Due to the importance of the APC/C at the exit from mitosis and meiosis I, we hypothesize that the termination machinery of meiotic oscillations is based on the APC/C co-activators.

The meiosis II-specific activity of Ama1 is responsible for termination of meiotic oscillations

Eukaryotes evolved various methods of triggering the exit from meiosis II based on the activity of APC/C. An example is the adaptation of mitotic regulators, like Cdc20, that control the exit from meiosis in oocytes or development of meiosis-specific Cdc20/Cdh1-related co-activators of APC/C (Chu et al., 2001; Jacobs et al., 2002; Kimata et al., 2011). In fission yeast, Fzr1 has been found to be up-regulated at the exit from meiosis II and it has been speculated that its activity limits the number of meiotic divisions (Blanco et al., 2001; Aoi et al. 2012). Similarly, it has been reported that in plants, APC/C activity is required for proper exit from meiosis II and defects in its regulation lead to the re-establishment of metaphase-like spindles for a third division (Cromer et al., 2012; Cifuentes et al., 2016). Budding yeast evolved a meiosis-specific APC/C co-activator, Ama1, which is closely related to Cdh1 and Fzr1 and, similarly, is up-regulated at meiosis II (Cooper et al., 2000; Diamond et al., 2009). Consistent with our previously published data (Argüello-Miranda et al., 2017), we showed that inactivation of Ama1 in meiosis II causes defects in some of the aspects of meiotic exit (**Figure 22**). Although *ama1*Δ cells are able to exit from meiosis by degrading cyclins and disassembling meiotic spindle, they are unable to degrade Cdc5 and Ndt80. Maintaining strong activity of these regulators provides a possible machinery for the re-accumulation of cyclins and re-introduction of oscillations after the second division. Additionally, *ama1*Δ cells stabilize the phosphorylated forms of the main regulators of meiosis, such as Ime2 and Sum1. This suggests the inability to properly balance the activities of meiotic kinases and phosphatases in the absence of Ama1 in meiosis II.

Ama1 exhibits properties of the hypothetical termination machinery of meiotic oscillations. It is not expressed during mitosis and it is inactive throughout the meiotic divisions, thereby triggering degradation of its substrates only during prophase I (Okaz et al., 2012) and at the exit from meiosis II. Moreover, similar to the hypothetical terminator predicted by our model, Ama1 targets for degradation the components of the meiotic oscillator, as well as other key regulators of meiosis, namely Cdc5 and, indirectly, Ndt80. Such properties make Ama1 a possible terminator of the meiotic oscillations (**Figure 44A**). Premature expression of Ama1 in cells arrested in metaphase I by the depletion of Cdc20 causes degradation of Cdc5, Ndt80 and cyclins, a single nuclear division and, eventually, exit from meiosis after one division (**Figure 28-29**). High activity of Ama1 in meiosis I prevents re-accumulation of cyclins for the second division, thus threatening the progression through meiosis. To be able to perform meiosis II, cells ensure down-regulation of Ama1. One of the methods to prevent early exit from meiosis before the completion of genome haploidization is the control of Ama1 activity through the Cdk1-Clb1-dependent inhibitory phosphorylation (Oelschlaegel et al., 2005; Okaz et al., 2012). Ama1 and Cdk1-Clb1 form a double-negative feedback loop that suppresses the activity of Ama1 during the high Cdk1 state. We showed *in silico* that cells unable to inhibit the activity of Ama1, exhibit a significantly shorter metaphase II, which possibly result in defects in chromosome segregation and meiotic exit (**Figure 30**). Moreover, Ama1 is strictly regulated though its levels. It has been shown that *AMA1* mRNA levels are constant during meiosis I and increase enormously during meiosis II (Chu et al., 1998; Primig et al., 2000). Although Ama1 accumulation depends on Ndt80 (Chu and Herskowitz, 1998; Okaz et al., 2012), it does not accumulate together with other targets of Ndt80 at the beginning of metaphase I. We speculate that *AMA1* mRNA may be down-regulated by a meiosis I-specific inhibitor that prevents the translation of Ama1 protein before the entry into meiosis II. A similar pattern is observed for the meiosis II-specific Clb3 (Carlie and Amon, 2008). Clb3 translation is regulated by the meiosis I-specific inhibitor Rim4, which prevents the synthesis of the cyclin before cells enter meiosis II. Furthermore, strong accumulation of Ama1 in meiosis II is coupled to the activity of APC/ C^{Cdc20} during anaphase I, as in its absence cells exhibit a strong delay in Ama1 accumulation. Due to the fact that Rim4 is regulated in a meiosis-specific manner and is degraded by proteolysis (Carpenter et al., 2018), we speculated that Ama1 may be regulated in a fashion similar to Clb3. Thus, its strong accumulation and activity is inhibited only

during the first division, allowing the entry into meiosis II, but preventing the entry into additional third division.

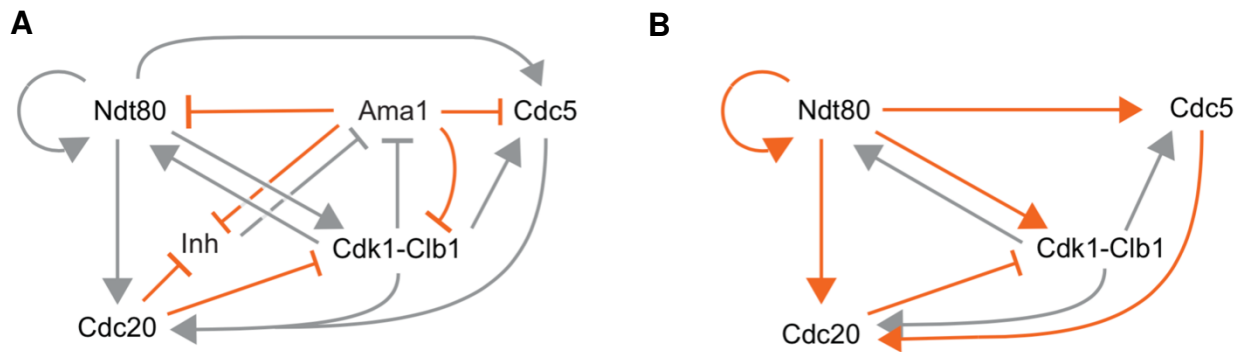


Figure 44. Ama1 and Cdc20 terminate meiotic oscillations at the exit from meiosis II. Orange arrows and bar-headed lines indicate interactions explicit during the exit from meiosis II. (A) Ama1, while freed from the inhibition of its synthesis during meiosis II, triggers rapid degradation of the key meiotic regulators preventing the appearance of additional divisions. (B) Cdc20 in the absence of Ama1 gains the function of the terminator due to persistent synthesis of the protein and Cdc5-dependent activity. Degradation of strongly active Cdc20 in meiosis II exceeds the synthesis level of cyclins thus triggering the exit from meiosis II and preventing additional waves of Cdk1 activity.

In the absence of Ama1, Cdc20 acquires the function of the terminator

In wild-type cells, the exit is characterized by degradation of cyclins, Ndt80, Cdc5 and Cdc20, as well as reactivation of Sum1 and Cdh1. Interestingly, in the absence of Ama1, Ndt80 persists much longer. Despite the maintenance of high levels of the main meiotic regulators, cells continue to degrade cyclins and terminate meiotic oscillations. Although Ama1 is the terminator of the oscillations in wild-type cells, in its absence cells mobilize other proteins to take the function of the missing component of the network, creating a robust exit from meiosis II. How do cells eliminate additional waves of cyclins accumulation in *ama1Δ*? We propose that an additional APC/C co-activator gains the function of the terminator in the absence of Ama1. We showed that one of the main mitotic co-activators present also in meiosis, Cdh1, is not involved in the termination of meiotic oscillations, as depletion of this protein from meiosis does not cause any disruption in the exit from meiosis II (Figure 23). Interestingly, we observed that in *ama1Δ* cells, Cdc20 exhibits different dynamics than in the wild-type cells. The Cdc20 protein persists longer along with Ndt80 and Cdc5. Based on our *in silico* experiments (Figure 26), we showed that Cdc20 acquires the function of Ama1 in its absence as the terminator of the oscillations (Figure 44B). In wild-type cells, Cdc20 is the main degradation mechanism of cyclins that is required for the progression through two divisions. In *ama1Δ* cells, the meiotic network changes the properties of the interactions between its components. With persistence of Ndt80 and Cdc5, Cdc20

presence is maintained long after the exit from meiosis II. This prompted us to speculate that Cdc20 gains the function of the terminator of the oscillations. Thus, Cdc20 activity is tightly controlled during meiotic divisions and changed in the absence of Ama1 at meiosis II. We found that the Cdc20 protein accumulates gradually throughout meiosis (**Figure 17**). However, simulations of the model excluded that strong accumulation of Cdc20 in meiosis II is an important factor for a possible meiosis II-specific activity of Cdc20 (**Figure 27**). We speculate that inhibition of APC/C^{Cdc20} activity rather than accumulation of the protein is necessary for cells to enter meiosis II. On the other hand, lack of inhibition at meiosis II exit is important for maintaining the low Cdk1 state. Other eukaryotes use the strategy of down-regulation of APC/C^{Cdc20} in meiosis I and up-regulation at the meiotic exit. In mammalian oocytes, APC/C^{Cdc20} activity is inhibited at metaphase II by a specific mechanism called a cytostatic factor (CSF) which involves Emi2/Erp1 and/or Emi1 inhibitors of APC/C^{Cdc20} (Wu et al., 2007; Perry and Verlhac, 2008; Schmidt et al., 2005; Tung and Jackson, 2005). Fission yeast evolved a stoichiometric inhibitor Mes1 that binds to the APC/C core and inhibits it from forming an active complex with Cdc20 (Izawa et al., 2005; Kimata et al., 2011). In budding yeast, such an inhibitor has not been found to date.

Cdc20 activity in meiosis II is required for timely exit from meiosis

Although Cdc20 takes the role of Ama1 in its absence, the reverse situation was not observed. Our model predicted that in the absence of Cdc20 in meiosis II, cells delay the exit from meiosis II (**Figure 30**), which was confirmed by biological experiments. Cells that are unable to activate APC/C^{Cdc20} during the second division, accumulate higher levels of Cdc20 substrates during metaphase II and delay their degradation, as well as disassembly of meiotic spindles (**Figure 31**). As predicted by the model, Ama1 is unable to degrade cyclins as efficiently as Cdc20. High levels of Cdc20 substrates during metaphase II in the absence of Cdc20 activity implies that Cdc20 is likely active during metaphase II in wild-type cells. There it prevents the strong re-accumulation of cyclins and a possible delay in the exit from meiosis II. Additionally, Ama1 substrates, such as Ndt80 and Cdc5, persists longer than in the presence of active APC/C^{Cdc20}, indicating a delay in activation of APC/C^{Ama1}. We theorize that Cdc20 is required to maintain low levels of Clb1, which is an inhibitor of APC/C^{Ama1}. With longer persistence of Cdk1-Clb1, Ama1 requires longer time to overcome this inhibition and degrade meiotic regulators resulting in the exit from meiosis II. Such a mechanism of a delay of the exit from the high Cdk1 state resembles regulation of the APC/C^{Cdc20} activity by the SAC. The SAC inhibits APC/C^{Cdc20} activity during metaphase until after all chromosomes are

properly attached to the spindle. In the absence of Cdc20, a delay is not regulated by the feedback from the chromosomes. Thus, cells might have evolved additional machinery that prevents premature exit from the high Cdk1 state. This machinery is possibly based on the Cdk1-dependent inhibition of Ama1 activity in the absence of Cdc20. Eventually, cells break out from the arrest at the high Cdk1 state of metaphase II with the reactivation of APC/C^{Ama1}. We showed that this exit is indeed triggered by Ama1, as in the absence of the activities of both APC/C^{Cdc20} and APC/C^{Ama1} in meiosis II, cells maintain the arrest at the high Cdk1 state (**Figure 32-33**). Based on the persistence of spindles and strong accumulation of Pds1 and Clb1, we concluded that these cells arrest in metaphase II.

3.5. APC/C-independent mechanisms that regulate meiotic exit

APC/C-independent mechanism is likely involved in the termination of the oscillations

We showed that both Ama1 and Cdc20 are important for triggering the exit from meiosis II and for termination of meiotic oscillations after the second division. Ama1 plays the role of the meiosis II-specific terminator in wild-type cells, while Cdc20 acquires its role in its absence. We tested whether inactivation of APC/C^{Cdc20} in the absence of Ama1 creates a third wave of accumulation of cyclins. Such behavior would indicate the reversibility of the exit from meiosis II. The mathematical model implied that inactivation of APC/C^{Cdc20} after the exit from meiosis II in cells lacking Ama1 results in the abrupt re-accumulation of cyclins and in the formation of metaphase III-like spindles due to the persistence of Ndt80 and lack of the degradation machinery. However, the biological experiments did not verify the *in silico* predictions (**Figure 35**). This fact prompted us to speculate about the reason of this discrepancy. We eliminated the possibility of Cdh1 inhibiting re-accumulation of cyclins after the exit from meiosis II, as depletion of this protein does not cause re-accumulation of cyclins. Thus, we investigated whether APC/C-independent mechanisms might contribute to the exit from meiosis II. One of them may be a mechanical barrier between the cytoplasm and the nucleus. Synthesis of nuclear proteins depends on the ability of the cell to maintain nuclear import. Thus, we asked if a prospore membrane formation in yeast meiosis may be responsible for limiting the synthesis of meiotic regulators and thus the number of divisions. It has been reported that in the absence of Ama1 the prospore membrane is formed and remains open (Knop and Strasser, 2000). We tested the involvement of the prospore membrane formation in limiting the nuclear import of proteins using a mutant

of one of the genes required for formation of prospore membrane, namely *MPC70* (Bajgier et al., 2001). However, we did not observe re-accumulation of Cdc20 substrates for the third division or reassembly of metaphase III-like spindles (**Figure 36**). Thus, we conclude that the formation of the prospore membrane does not prevent re-accumulation of M-phase proteins.

Another possibility of the inability of cells to re-accumulate cyclins for meiosis III is the existence of a preventive machinery that controls the translation of proteins or that controls the events of autophagy. Autophagy plays a critical role in the entry into meiosis in budding yeast as a response to starvation signals (Schlumpberger et al., 1997; Sarkar et al., 2014). Additionally, it is known that in higher eukaryotes autophagy is involved in early stages of development, which follows two meiotic divisions (Yin et al., 2016). Thus it might be important to regulate the late events of meiosis, such as the exit (termination of the oscillations) and sporulation.

Regulation of meiotic exit by balancing the activities of kinases and phosphatases

Similar to mitosis, meiosis is driven by the activity of kinases, among others Cdk1, Cdc5 and Ime2. The activity of Cdk1 is essential for DNA replication, formation of meiotic spindles and proper segregation of chromosomes during the two consecutive divisions. It is known that for proper progression through a cell division, cells require the activities of phosphatases that counteract the kinases, thus contributing to the formation of a switch-like response at different stages of mitosis or meiosis (Bollen et al., 2009). Phosphatases are known to be required for the proper entry and exit from mitosis in a variety of eukaryotes (reviewed in Wurzenberger and Gerlich, 2011). We were interested to test whether the well-known phosphatases of the cell cycle are involved in the exit from meiosis II and the termination of meiotic oscillations.

Cdc14 is a major Cdk1-counteracting phosphatase in both mitosis and meiosis in budding yeast (Buonomo et al., 2003; Jaspersen and Morgan, 2000). Although it is required for proper chromosome segregation during both mitosis and meiosis I, the absence of Cdc14 activity during meiosis II does not affect the events of the second division and the exit from meiosis II (Argüello-Miranda et al., 2017). Thus, we studied two other major phosphatases present in yeast meiosis: PP2A and PP1. One of the main phosphatase known to counteract Cdk1 phosphorylation in different species is PP2A^{B55} (PP2A^{Cdc55} in budding yeast). PP2A^{B55} is known to be regulated in a Cdk1-dependent manner through the Greatwall pathway. The Greatwall kinase (Rim15 in budding yeast) inhibits indirectly the activity of PP2A^{B55} during the high Cdk1 state. As cells degrade cyclins and enter anaphase of mitosis, they activate the phosphatase, which

leads to dephosphorylation of Cdk1 substrates (Gharbi-Ayachi et al., 2010). The mutual inhibition of kinases and phosphatases ensures an irreversible switch to the low Cdk1 state (Cundell et al., 2013; Hegarat et al., 2014; Vinod and Novak, 2015). A similar machinery has been found to regulate meiosis in vertebrates oocytes (Li et al., 2013; Yamamoto et al., 2011). Moreover, the activity of the Greatwall- PP2A^{B55} pathway is important in the mitotic cell cycle in budding yeast (Queralt et al., 2006; Sarkar et al., 2014). Also in meiosis, PP2A^{Cdc55} is required for spindle disassembly and chromosome segregation during the first division (Kerr et al., 2011). Thus, PP2A^{Cdc55} is important for the exit from meiosis I. Another phosphatase, PP1, plays a variety of roles during mitosis and meiosis (reviewed in Wurzenberger and Gerlich, 2011). In budding yeast meiosis, PP1/Glc7 is involved in spore wall formation and in the regulation of Aurora B/Ipl1. It is controlled by several different subunits that contribute to the substrate specificity of the phosphatase. Among them is Gip1, which is involved in nuclear localization of the PP1/Glc7 during meiosis (Tachikawa et al., 2001). We showed that inactivation of neither PP1 nor PP2A^{Cdc55} during meiosis II affect the exit from meiosis II. In the absence of the activities of these phosphatases cells progress through the second division undisturbed and degrade cyclins completely at anaphase II (**Figure 38-41**). Cells disassemble meiotic spindles and enter the low Cdk1 state after the meiotic exit. Even in cells with inactivated APC/C after the exit from meiosis II and additional deletion of *GIP1*, we did not observe re-accumulation of cyclins for the third division (data not shown). These results indicate that the activities of the tested phosphatases during the second division are not important for regulation of the exit from meiosis II and termination of meiotic oscillations.

3.6. Regulation of meiosis II-specific terminator by meiosis I-specific inhibitor

Although there are different possibilities for termination of meiotic oscillations, they should all be strictly coupled to the events of meiosis II. Tyson and Novak considered that two waves of Cdk1 activity are controlled by a meiosis-specific protein synthesized in early meiosis I and down-regulated at the exit from the first division (Tyson and Novak, 2008). They proposed a simplified generic model of two meiotic divisions where the meiosis I-specific role is played by an unknown protein Y that activates Cdk1 inhibitors in meiosis II. The protein Y introduced in this generic model has been considered to be the meiosis-specific protein Spo13 (Tyson and Novak, 2008). Spo13 is expressed in early meiosis I and is degraded at anaphase I (Katis et al., 2004). Mutants

of *SPO13* perform only one meiotic division with a delayed exit (Katis et al., 2004; Shonn et al., 2002; Lee et al., 2004), which indicates its role in regulation of the exit from meiosis. Another candidate, which acts in meiosis I but not in meiosis II, is *Dbf4*, a component of the DDK kinase that initiates DNA replication and is important for chromosome segregation at meiosis I (Matos et al., 2008). In the model of two meiotic divisions, we assumed that an inhibitor exists that is specific to meiosis I and does not allow high activity of the terminator, *Ama1* and *Cdc20*, before the exit from meiosis II. We speculate that an inhibitor of *Ama1* is related to high expression of this protein specifically in meiosis II. The meiosis II-specific behavior of *Cdc20* may be dependent on its activity that is possibly inhibited during anaphase I. To date the identities of possible inhibitors of the meiosis II-specific activity of the APC/C remain unknown.

3.7. Is the exit from meiosis II irreversible?

The protein network that regulates the progression through meiotic divisions is composed of circuits of feedback loops. Positive and double-negative feedback loops trigger the transition into metaphase I. A negative feedback loop between *Cdk1* and *Cdc20* triggers the oscillator allowing progression through meiosis I and -II. We propose that the exit from meiosis II is triggered by two double-negative feedback loops that result in strong accumulation of active *Ama1* during the exit from meiosis II. Such behavior resembles the regulation of the transition from prophase I to metaphase I. Both stages of meiosis are characterized by the presence of meiosis-specific events, such as meiotic DNA recombination or sporulation, followed or preceded by the *Cdk1*-APC/C oscillator, respectively. Similar to the exit from meiosis II, at prophase I cells activate APC/C^{*Ama1*}, which inhibits accumulation of M-phase proteins. During the transition to the high *Cdk1* state, APC/C^{*Ama1*} activity is inhibited, allowing strong accumulation of *Ndt80* and its substrates. At the exit from meiosis II, the opposite can be observed. Cells exit from the high *Cdk1* state of metaphase II to the low *Cdk1* state of anaphase II, which is maintained after the completion of meiosis II (**Figure 45**). This transition is triggered by a strong accumulation of *Ama1* due to degradation of the repressor of its synthesis, possibly *Rim4*. Additionally, APC/C^{*Ama1*} is freed from the *Cdk1*-dependent inhibition, which kept it inactive during meiosis I and -II.

In the absence of APC/C^{*Ama1*} activity, the exit is not regulated by two double-negative feedback loops, but rather it is mediated by the activity of APC/C^{*Cdc20*}. The exit from the high *Cdk1* state of metaphase II is based on the negative feedback loop between *Cdc20* and *Cdk1*, as well as surrounding positive feedback loops that amplify the

signal. Sharp activation of APC/C^{Cdc20} and its faster activation in comparison to the speed of the negative feedback, are necessary to restrict the reactivation of Cdk1 to only two waves during meiosis I and -II. APC/C^{Cdc20} is strongly activated in meiosis II possibly due to a change of the properties of the meiotic network in the absence of Ama1. Such negative feedback loop while combined with a set of positive feedback loops in the network, is able to generate a bistable behavior of the system and an irreversible switch (Pfeuty and Kaneko, 2009).

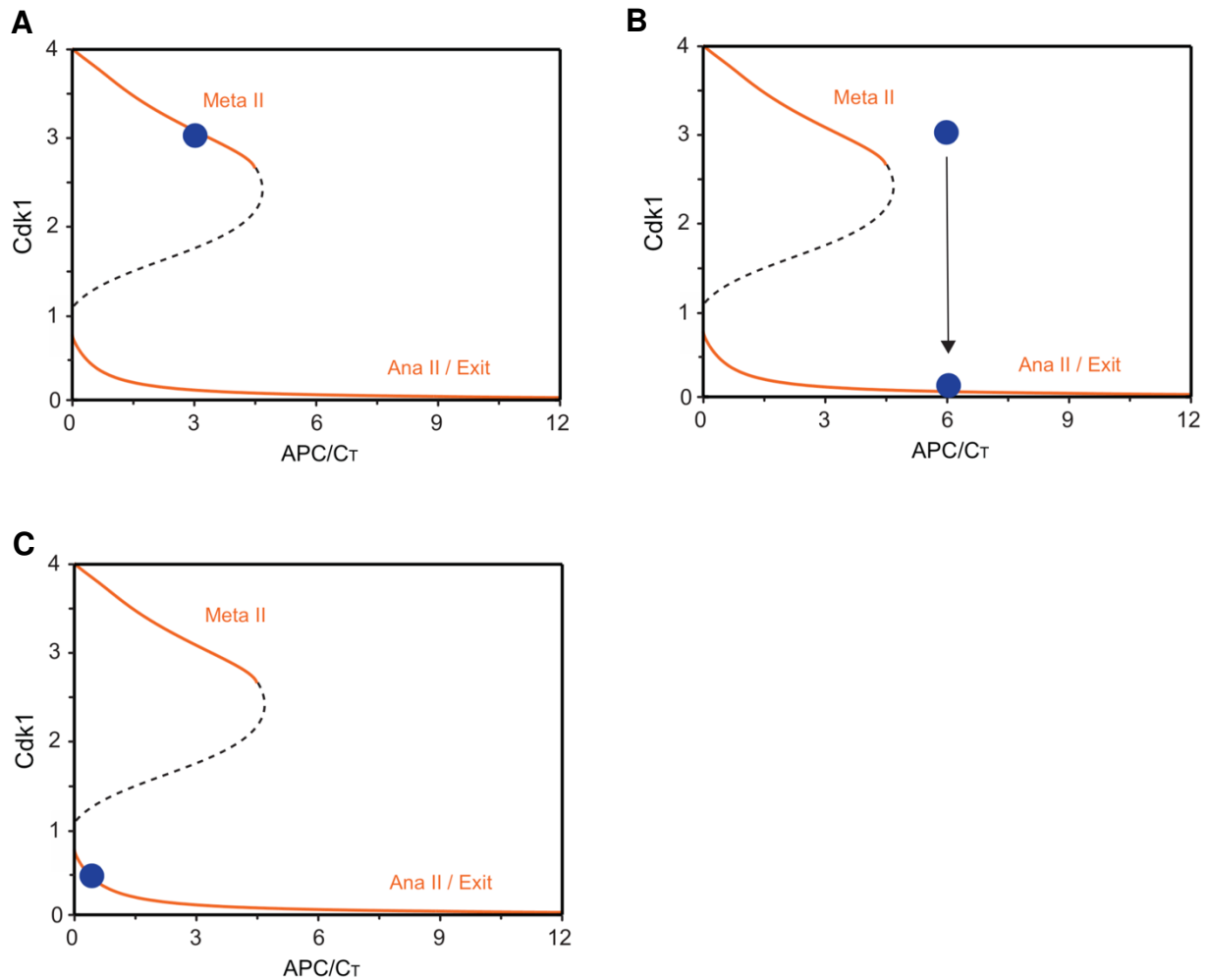


Figure 45. The possibility of an irreversible exit from meiosis II after exceeding the threshold of APC/C activity and cyclin degradation. Graphs present hypothetical bifurcation diagrams of the transition from a high Cdk1 state of metaphase II to a low Cdk1 state at the exit from meiosis II. Orange solid lines represent stable states, while black dashed lines represent unstable state. Blue circle represent a current state of the cell. The signal is presented in form of total activity of APC/C (Ama1/Cdc20) during meiosis II, while the response is presented in form of the activity of Cdk1. Meta II is metaphase II, Ana II is anaphase II, Exit is exit from meiosis II. **(A)** During metaphase II cells are stabilized at the high Cdk1 state with low activity of the APC/C. **(B)** With increase in the APC/C activity, cells jump to the only possible stable state, which is anaphase II. At this point, cells degrade cyclins and exit from meiosis II. **(C)** Artificial inhibition of the APC/C activity after the exit from meiosis II does not cause cells to jump to another high Cdk1 state, creating a possible meiosis III. Instead, it causes cells to stay in a low Cdk1 state preventing them from reactivating Cdk1 and entering additional metaphase-like state.

The exit from meiosis II is probably regulated by a switch that make the transition to the low Cdk1 state irreversible. Thus, instead of re-accumulating cyclins and continuing with oscillations in the absence of their terminator, it is possible that meiotic cells settle in a low Cdk1 stable state after the exit from meiosis II. After exceeding a certain threshold of the activity of the APC/C and degradation of cyclins, cells are not be able to return to a high Cdk1 state. Even after the completion of meiosis, inhibition of any remaining APC/C will not cause the entry into an additional metaphase-like state. This is due to the fact that cells may inactivate APC/C after they stabilize at a low Cdk1 state. Thus, similarly as the transition from prophase I to metaphase I, the exit from meiosis II may exhibit irreversibility due to meiosis II-specific activity of APC/C^{Ama1} or APC/C^{Cdc20} regulated with an additional unknown feedback loop, which allows it to settle in a high activity state and inhibit accumulation of cyclins for meiosis III.

3.8. On studying processes of meiosis II in high resolution

In this work, we presented a newly developed system of metaphase II-arrest/release, *cdc20-3-mAR*, based on the system of the release from metaphase I-arrest developed previously in our lab (Argüello-Miranda, et al., 2017). It allows synchronous release of cells to anaphase I and synchronous arrest in metaphase II by inactivating APC/C^{Cdc20} after its induction in meiosis I. In the presence of Ama1, cells maintain metaphase II arrest for <1 hr (**Figure 31**). After this time, they accumulate high levels of Ama1 and exit from the second division. In the absence of Ama1, cells with inactivated APC/C^{Cdc20} arrest in metaphase II for a long period of time (**Figure 33**). We observed that after 24 hr in the metaphase II-arrest the majority of cells remain bi-nucleated. The system allows manipulation of meiotic regulators precisely during metaphase II, which is normally challenging due to short period spent in metaphase II by non-arrested cells (<40 min). Additionally, cells arrested in metaphase II can be released from the arrest to synchronously enter anaphase II (**Figure 35**). Thus, the system is able to mimic the behavior of vertebrates oocytes which arrest in metaphase II until fertilization, which triggers the activation of APC/C^{Cdc20} for the completion of meiosis. The metaphase II-arrest/release system can be used as a model for studying metaphase II and post-anaphase II events with high resolution.

3.9. Concluding remarks

During meiosis, cells have to perform a set of coordinated events that lead to formation of haploid gametes or spores. One of the biggest challenges is to understand how cells regulate sequential events of meiosis resulting in the exit precisely after meiosis II. To achieve a two-division meiosis, cells implement a set of distinct decisions requiring sharp activation of key regulators of cell division, namely Cdk1 and APC/C. These two regulators create an oscillatory core, which is commonly found in various systems requiring the control on a cell cycle level, from embryonic cell cycle, stem cells development to oocyte maturation. Mathematical modeling helps to understand how, despite the complexity and specificity of biological systems, the Cdk1-APC/C core remains unchanged. It suggests modifications of the network surrounding the core based on complementary feedback loops that regulate process-specific transitions. In budding yeast meiosis, the core that drives the progression through two meiotic divisions is adjusted to be able to complete the divisions precisely after meiosis II. The oscillator is complemented with meiosis-specific regulators that unleash the machinery preventing the appearance of an additional third division. The protein network that regulates meiosis sheds light into an overall regulation of processes based on the Cdk1-APC/C oscillator. General principles of modification of the core to generate two divisions can be applied to various organisms, and be used to describe specific regulation of Cdk1-APC/C core in other oscillatory processes based on a cell cycle machinery.

4. Materials and Methods

4.1. Construction of yeast strains

We used diploid *Saccharomyces cerevisiae* strains of the fast-sporulating SK1 genetic background (*ho::LYS2 lys2 ade2::hisG trp1::hisG leu2::hisG his3::hisG ura3*) (Kane and Roth, 1974). Diploid strains were produced by mating of the correspondent *MATa* and *MATα* haploids. Genotypes of all strains are listed in **Table 10**. The following alleles have been previously characterized: *Myc18-CDC20* (Zachariae et al., 1998), *mpc70Δ::KanMX4* (Knop and Strasser, 2000), *CLB1-myc9* (Buonomo et al., 2003), *P_{CLB2}-CDC20* (Lee and Amon, 2003; Petronczki et al., 2006), *PDS1-myc18* and *ama1Δ::NatMX4* (Oelschlaegel et al., 2005), *P_{GALL}-AMA1*, *clb1Δ::NatMX4*, *clb4Δ::KanMX4*, and *ndt80Δ::NatMX4* (Okaz et al., 2012), *HRR25-HIS3::hrr25::KanMX4*, *P_{DMC1}-AMA1* and *P_{CUP1}-CDC20* (Argüello-Miranda et al., 2017). The strains with estradiol-inducible expression from the *GAL* promoter (called *P_{EST}* herein) contains a plasmid producing a *P_{GDP1}-GAL4⁴⁸⁴-ER* fusion (Benjamin et al., 2003). *GPD1* promoter is a fusion of the Gal4 transcription factor and a hormone-binding domain of the human estrogen receptor ER. The Ndt80 arrest/release system uses *P_{EST}-NDT80* in *ndt80Δ* background (Benjamin et al., 2003; Carlie and Amon, 2008; Matos et al., 2008). The anchor-away (AA) system (Haruki et al., 2008) uses *tor1-1::HIS3*, *fpr1Δ::KanMX4* and *RPL13A-2xFKBP12* (a gift from Andreas Hochwagen; Argüello-Miranda et al., 2017).

For deletion of the genes *CLB3* (*clb3Δ::TRP1*) and *GIP1* (*gip1Δ::NatMX4*), PCR-generated cassettes were used (Goldstein and McCusker, 1999; Wach et al., 1994). For C-terminal tagging with Myc9 and Myc18, PCR-generated cassettes were used (Ciosk et al., 1998; Knop et al., 1999). Tagged proteins are fully functional as verified by testing proliferation and sporulation of the homozygous diploids. For the AA system, *CDC55* was tagged at the C-terminus with a PCR-generated cassette encoding FKBP12-rapamycin-binding (FRB) domain of human mTOR (Haruki et al., 2008). For depletion of Cdc20 and Cdh1 in meiosis, the endogenous promoters were replaced with the mitosis-specific promoter of *HSL1* (Okaz et al., 2012). The temperature-sensitive mutant *cdc20-3* (G360/S) (Shirayama et al., 1998) was generated by PCR-mediated site-directed mutagenesis (Li and Wilkinson, 1997) of *CDC20* integrated behind the copper-inducible *CUP1* promoter in the yeast integrative plasmid YIplac204. The plasmid was integrated into the *trp1* locus by cutting with *Bsu36I* restriction enzyme.

Table 10. List of *Saccharomyces cerevisiae* SK1 strains used in this study.

Figure ¹	Strain	Genotype ²
15	Z30291	<i>PDS1-myc18::KITRP1</i>
15	Z22156	<i>clb1Δ::NatMX4 PDS1-myc18::KITRP1</i>
15	Z30292	<i>clb3Δ::TRP1 PDS1-myc18::KITRP1</i>
15	Z30293	<i>clb4Δ::HphMX4 PDS1-myc18::KITRP1</i>
16, 17A, 20	Z29971	
16A	Z29974	<i>CLB1-myc9::KITRP1</i>
16B	Z5157	<i>CLB4-myc9::KITRP1</i>
17A	Z29973	<i>Myc18-CDC20::TRP1</i>
17B	Z7122	<i>HRR25-HIS3::hrr25::KanMX4</i>
17B	Z19647	<i>HRR25-HIS3::hrr25::KanMX4 PDS1-myc18::KITRP1</i>
20	Z27965	<i>hct1::P_{HSL1}-HCT1::HphMX4</i>
22	Z20217	<i>PDS1/ PDS1-myc18::KITRP1</i>
22	Z20219	<i>ama1Δ::CaURA3 trp1/trp1::P_{DMC1}-cAMA1::TRP1 PDS1/PDS1-myc18::KITRP1</i>
23	Z22388	<i>ama1Δ::CaURA3 leu2::P_{DMC1}-cAMA1::LEU2 PDS1- myc18::KITRP1</i>
23	Z28157	<i>ama1Δ::CaURA3 leu2::P_{DMC1}-cAMA1::LEU2 hct1::P_{HSL1}- HCT1::HphMX4 PDS1-myc18::KITRP1</i>
24	Z29418	<i>cdc20::P_{CLB2}-CDC20::KanMX6 trp1::P_{CUP1}-CDC20::TRP1 ESP1-myc18::TRP1</i>
25A,C	Z31284	<i>cdc20::P_{CLB2}-CDC20::KanMX6 ura3::P_{CUP1}-CDC20::URA3 Ha3-MPS1::LEU2 PDS1-myc18::TRP1</i>
25B-C	Z31285	<i>ama1Δ::NatMX4 leu2::P_{DMC1}-cAMA1::LEU2 cdc20::P_{CLB2}- CDC20::KanMX6 ura3::P_{CUP1}-CDC20::URA3 Ha3- MPS1::LEU2 PDS1-myc18::TRP1</i>
29	Z34661	<i>cdc20::P_{HSL1}-CDC20::HphMX4 ura3::P_{GPD}-GAL4⁴⁸⁴- ER::URA3 PDS1-myc18::TRP1</i>
29	Z34662	<i>cdc20::P_{HSL1}-CDC20::HphMX4 ura3::P_{GPD}-GAL4⁴⁸⁴- ER::URA3 leu2::P_{GALL}-cAMA1::LEU2 PDS1-myc18::TRP1</i>
31	Z21260	<i>cdc20::P_{CLB2}-CDC20::KanMX6 trp1::P_{CUP1}-CDC20::TRP1 PDS1-myc18::HIS3MX6</i>
31	Z31711	<i>cdc20::P_{CLB2}-CDC20::KanMX6 trp1::P_{CUP1}-cdc20-3::TRP1 PDS1-myc18::HIS3MX6</i>

33	Z27968	<i>ama1Δ::NatMX4 leu2::P_{DMC1}-cAMA1::LEU2 cdc20::P_{CLB2}-CDC20::KanMX6 trp1::P_{CUP1}-CDC20::TRP1 PDS1-myc18::HIS3MX6</i>
33	Z31712	<i>ama1Δ::NatMX4 leu2::P_{DMC1}-cAMA1::LEU2 cdc20::P_{CLB2}-CDC20::KanMX6 trp1::P_{CUP1}-cdc20-3::TRP1 PDS1-myc18::HIS3MX6</i>
35	Z33491	<i>ama1Δ::NatMX4 leu2::P_{DMC1}-cAMA1::LEU2 cdc20::P_{CLB2}-CDC20::KanMX6 trp1::P_{CUP1}-cdc20-3::TRP1 hct1::P_{HSL1}-HCT1::HphMX4 PDS1-myc18::HIS3MX6</i>
36	Z34121	<i>ama1Δ::NatMX4 leu2::P_{DMC1}-cAMA1::LEU2 cdc20::P_{CLB2}-CDC20::KanMX6 trp1::P_{CUP1}-cdc20-3::TRP1 hct1::P_{HSL1}-HCT1::HphMX4 PDS1-myc18::HIS3MX6</i>
36	Z34122	<i>mpc70Δ::BleMX4 ama1Δ::NatMX4 leu2::P_{DMC1}-cAMA1::LEU2 cdc20::P_{CLB2}-CDC20::KanMX6 trp1::P_{CUP1}-cdc20-3::TRP1 hct1::P_{HSL1}-HCT1::HphMX4 PDS1-myc18::HIS3MX6</i>
38	Z34012	<i>CDC55-FRB::NatMX6 fpr1Δ::KanMX4 tor1-1::HIS3 PDS1-myc18::HIS3MX6</i>
38	Z34013	<i>CDC55-FRB::NatMX6 fpr1Δ::KanMX4 tor1-1::HIS3 RPL13A-2XFKBP12::TRP1 PDS1-myc18::HIS3MX6</i>
39	Z32710	<i>cdc20::P_{CLB2}-CDC20::KanMX6 trp1::P_{CUP1}-CDC20::TRP1 PDS1-myc18::KITRP1</i>
39	Z32711	<i>gip1Δ::NatMX4 cdc20::P_{CLB2}-CDC20::KanMX6 trp1::P_{CUP1}-CDC20::TRP1 PDS1-myc18::KITRP1</i>
40	Z34712	<i>ama1Δ::NatMX4 leu2::P_{DMC1}-cAMA1::LEU2 CDC55-FRB::NatMX6 fpr1Δ::KanMX4 tor1-1::HIS3 ndt80Δ::NatMX4 ura3::P_{GPD}-GAL4⁴⁸⁴-ER::URA3 leu2::P_{GAL1}-NDT80::LEU2 PDS1-myc18::HIS3MX6</i>
40	Z34713	<i>ama1Δ::NatMX4 leu2::P_{DMC1}-cAMA1::LEU2 CDC55-FRB::NatMX6 fpr1Δ::KanMX4 tor1-1::HIS3 ndt80Δ::NatMX4 ura3::P_{GPD}-GAL4⁴⁸⁴-ER::URA3 leu2::P_{GAL1}-NDT80::LEU2 RPL13A-2XFKBP12::TRP1 PDS1-myc18::HIS3MX6</i>
41	Z24253	<i>ama1Δ::NatMX4 leu2::P_{DMC1}-cAMA1::LEU2 cdc20::P_{CLB2}-CDC20::KanMX6 trp1::P_{CUP1}-CDC20::TRP1 PDS1-myc18::KITRP1</i>
41	Z24254	<i>ama1Δ::NatMX4 leu2::P_{DMC1}-cAMA1::LEU2 gip1Δ::NatMX4 cdc20::P_{CLB2}-CDC20::KanMX6 trp1::P_{CUP1}-CDC20::TRP1 PDS1-myc18::KITRP1</i>

¹Strains are listed for each figure used in this study.

²All strains are diploid *MATa/MATα* in the SK1 genetic background *ho::LYS2 lys2 ade2::hisG trp1::hisG leu2::hisG his3::hisG ura3*. Mutations are homozygous unless stated otherwise.

4.2. Induction of meiosis

Synchronous meiosis of SK1 diploid strains was induced at 30 °C as described before (Oelschlaegel et al., 2005). Healthy zygotes produced by appropriate haploids were streaked to single colonies on yeast extract peptone glycerol (YPG) plates and grown for 36-40 hr. Single colonies were transferred to YP-dextrose (YPD) plates and grown in ~2 cm² patches for 24-28 hr. Cells were plated evenly on YPD plates and grown until they formed a lawn (~24 hr). Cells were inoculated into 250 ml of liquid YP-acetate medium (YEPA; YP plus 2% K-acetate) to OD₆₀₀ ~0.3. The cultures were shaken at 200 rpm for 11-12 hr in an orbital shaker to OD₆₀₀ ~1.6 and budding index <10% (arrest in G1-phase). Cells were concentrated by centrifugation at 3600 rpm for 3 min and washed once with 150 ml of pre-warmed sporulation medium (SPM; 2% K-acetate). Cells were inoculated to OD₆₀₀ ~3 into 90-110 ml of SPM in a 2.8 l-Fernbach flask and shaken at 200 rpm. For meiotic time courses using temperature-sensitive mutants, cells were grown in YEPA at 25 °C for 14-15 hr and transferred to SPM at 25 °C.

4.3. Meiotic time course experiments

For a conventional (unsynchronized) meiotic time course, samples were taken every 2 hr after the transfer into SPM ($t = 0$) for indirect immunofluorescence (IF) and trichloroacetic acid (TCA) whole-cell protein extracts. For inactivation of Cdc55 using the AA system by induction of binding of FRB to FKBP12, rapamycin (10 µg/ml, LC Laboratories R-5000) was added at 4 hr. The AA system uses depletion of a protein from the nucleus, which depends on the heterodimerization of the human FKBP12 to the FRB domain of human mTOR in the presence of rapamycin (Haruki et al., 2008). The FRB-tagged protein interacts with a ribosome subunit Rpl13a tagged with FKBP12 and moves to the cytoplasm, therefore failing to exert its nuclear function.

To induce expression of Aml1 in metaphase I-arrested cells, estradiol (10 µM, Sigma E2758) was added at 7 hr. For the meiotic time course using the *CDC20*-meiotic-arrest/release system (*CDC20-mAR*) cells were released from the metaphase I-arrest after 8 hr with addition of 10 µM CuSO₄ at 30 °C. For the time course using the modified metaphase II-arrest/release (*cdc20-3-mAR*) cells were released from the metaphase I-arrest after 8 hr with 10 µM CuSO₄ at 25 °C. For the arrest in metaphase II, the temperature was shifted to 36 °C at 50 min. For the release from metaphase II, the temperature was shifted back to 25 °C at 120 min. For inhibition of Cdc20 activity after the exit from meiosis II, the temperature was shifted to 36 °C at 240 min. Temperature shifts were carried out with a covered water bath shaking horizontally at 200 rpm. To

measure half-lives of proteins DMSO solvent (0.5%) or cycloheximide (CHX, 0.5 mg/ml, Sigma C7698) was added at the indicated times and TCA samples were collected at $t = 0, 10, 20, 40$ and 80 min. For meiotic time courses using Ndt80 arrest/release system, cells were released from the prophase I-arrest after 6 hr with estradiol (10 μ M, Sigma E2758). For inactivation of the nuclear activity of Cdc55 with the AA system, rapamycin (10 μ g/ml, LC Laboratories R-5000) was added at 100 min after the release from the prophase I-arrest. Additionally, IF samples were collected 24 hr after the transfer into SPM to visualize nuclear divisions.

4.4. TCA protein extraction and SDS-PAGE analysis

Cells from meiotic time course (8-10 ml from SPM) or proliferating culture (cycling cells, Cc) grown to exponential phase in YPD medium (50 ml, $OD_{600} \sim 0.8$, washed once with ice-cold water) were collected by centrifugation at 4000 rpm (4 °C) for 2 min. Pellets were resuspended in 1 ml of 10% TCA. Samples were transferred to 1.5 ml safe-lock Eppendorf tubes and centrifuged for 2 min at 8000 rpm (4 °C). Samples were resuspended in 200 μ l of TCA. The same amount of zirconia beads (0.5 mm diameter, Roth 11079105z) was added to the samples. Cells were disrupted by shaking at 30 Hertz for 6 min at 4 °C with a mixer mill (MM400 Retsch) and collected by low-speed centrifugation (10 minutes at 3000 rpm, 4 °C). The resulting pellet was resuspended in 2x Laemmli sample buffer (62.5 mM Tris-HCl pH 6.8, 10% glycerol, 2% SDS, 0.01% bromophenol blue, 30 mM β -mecaptoethanol) and neutralized with half-volume of 1 M Tris base. Samples were heated to 95 °C for 10 min and centrifuged at 14000 rpm for 10 min. Protein concentrations were measured with a colorimetric Bradford Protein Assay (Bio-Rad). Samples of 60-100 μ g of total protein were loaded on 8% SDS polyacrylamide (SDS-PAGE) gels (for detection of Sum1 and Spo13 7% and 10% gels were used, respectively). SDS-PAGE gels were run at 35-45 V overnight.

4.5. Immunoblot detection of proteins in whole-cell extracts

Semidry western blotting was used to transfer proteins to PVDF membranes (Immobilon P, Millipore). The transfer was conducted for 1 hr at 0.45 mA/cm². Membranes were blocked for 1 hr in phosphate-buffer saline (PBS) with 0.1% Tween 20 (PBS-T) and 4% non-fat milk powder (PBS-T/milk). Membranes were incubated with primary antibody at room temperature for 1-2 hr. The primary antibodies were diluted in PBS-T/milk with 0.01% sodium azide and stored at -20 °C. Membranes were washed

three times for 10 min in PBS-T/milk and incubated for 1-3 hr with the appropriate secondary antibody conjugated to horseradish peroxidase (dilution 1:5000 in PBS-T/milk). Membranes were washed four times with PBS-T and incubated for 20-40 sec with ECL (ECL detection system, GE Healthcare). Membranes were exposed to X-ray film and developed using an Optimax 2010 machine (Protec).

Rabbit polyclonal antibodies were used for detection of the following proteins: Ama1 (dilution 1:2000; Oelschlaegel et al., 2005), Cdc5 (1:5000; Matos et al., 2008), Cdc20 (1:5000; Camasses et al., 2003), Cdh1 (1:5000; Zachariae Lab), Clb3 (1:3000; Zachariae Lab), Dbf4 (1:5000; Matos et al., 2008), mTOR human FRB domain (1:2000; Enzo Life Sciences ALX-215-065-1), Ndt80 (1:10000; a gift from Kirsten Benjamin; Benjamin et al., 2003), Spo13 (1:5000; Matos et al., 2008), β -tubulin/Tub2 (1:20000; a gift from Wolfgang Seufert). Goat polyclonal antibodies from Santa Cruz Biotechnology were used for detection of Clb1 (1:300; sc-7647), Clb4 (1:400; sc-6702), Clb5 (1:100; sc-6704), Fkbp12 (1:200; sc-6174), and Sum1 (1:200; sc-26441). Mouse monoclonal antibodies were used to detect Pgk1 (1:40000; Invitrogen) and Myc 9E10 (1:150; Evan et al., 1985).

4.6. Indirect immunofluorescence microscopy

Samples (1 ml) for indirect immunofluorescence (IF) were fixed overnight at 4 °C in 3.7% formaldehyde (Salah and Nasmyth, 2000). Samples were washed three times with 1 ml of 0.1 M potassium phosphate buffer (pH 6.4) and once with 1 ml of spheroplasting buffer (0.1 M potassium phosphate buffer pH 7.4, 1.2 M sorbitol, 0.5 mM MgCl₂). Cells were centrifuged for 2 min at 4000 rpm and resuspended in spheroplasting buffer. Spheroplasting was carried out with 10% solution of β -mercaptoethanol. Samples were incubated at 30 °C, 700 rpm, for 15 min. To obtain spheroplasts, 10 μ l of zymolase solution (Zymolase 100T from Amsbio 1 mg/ml in spheroplasting buffer) was added. Cells were shaken at 30 °C, 700 rpm, for 20-60 min until the cell wall was removed from ~75% of cells. The appearance of spheroplasts was assessed by checking cells using phase-contrast microscopy. Digestion was stopped by addition of 1 ml of ice-cold spheroplasting buffer. Cells were centrifuged at 4 °C, 2500 rpm, for 2 min and resuspended in 100-150 μ l of spheroplasting buffer. Spheroplasted samples were added to a polylysine-coated 15-well slide and kept on the slide for 5 minutes to adhere to the surface. Excessive liquid was removed and cells were dehydrated by incubating the slides for 3 min in cold methanol and for 10 sec in cold acetone (at -20 °C). The slides were air-dried and incubated for 10 min with 6 μ l per well of filtered PBS for rehydration. Spheroplasts were blocked for 1 hr with 6 μ l per well of PBS containing 1%

bovine serum albumin (PBS-BSA, filtered). The slides were incubated for 2 hr with primary antibodies in a humid chamber. Monoclonal primary antibodies were used: from rat to tubulin (dilution in PBS-BSA 1:300; Serotec YOL1/34) and from mouse to Myc 9E10 (1:5; Evan et al., 1985). Cells were washed for 5 min 4-6 times with PBS-BSA. They were incubated with secondary antibodies in a humid dark chamber for 1.5-2 hr and washed six times with PBS. Affinity-purified, preabsorbed secondary antibodies were used as follows: from donkey conjugated to α -rat Alexa 488 (1:200; Chemicon) and from goat conjugated to α -mouse Cy3 (1:200; Abcam). To detect DNA, the wells were covered with mounting medium: 100 mg p-phenylenediamine and 0.05 μ g/ml DAPI (4',6-diamidino-2-phenylindole) in glycerol. The slide was carefully covered with a cover slip to uniformly spread the mounting medium. Cells were observed using a Zeiss Axioskop 2 epifluorescence microscope with a 100x plan-apochromat 1.40 NA/oil objective. Pictures were captured with a Retiga Exi CCD camera controlled by QCapture 2.9.12 software (QImaging) and processed with Adobe Photoshop. The width of a single image is 10 μ m. At least 100 cells per time point were counted.

4.7. Quantification of signal intensity from immunofluorescence staining

Spheroplasted, formaldehyde-fixed cells covered with DAPI mounting medium were used to quantify the signal intensity of Myc-tagged proteins at different stages of meiosis. Images were taken using a DeltaVision system (Applied Precision) controlled by softWoRx 5.0 software and included Olympus IX-71 inverted microscope equipped with autofocus module (Ultimate Focus), solid state illumination (InsightISS), Olympus UPLSApo 100X/1.40 NA/oil objective, set of DeltaVision filters and CoolSNAP HQ2 CCD camera (Photometrics). Images were acquired in DAPI to visualize cell nuclei, FITC to visualize spindles and TRITC to visualize Myc signal without the neutral density filter. Exposure times of 0.02-0.08 sec were used. %T was set for 10% for DAPI and 32% for FITC and TRITC. Arc lamp was aligned for Koehler illumination. Digital image was acquired with camera binning 2x2 and camera gain 1x. Raw images were saved without data compression. Images were processed with guidelines described in Waters (Waters, 2009). Images were analyzed using ImageJ (W. S. Rasband, U.S. NIH, Bethesda, MD, <http://imagej.nih.gov/ij/>). For each cell from a specified stage of meiosis based on the morphology of the spindle and number of nuclei, a ROI (region of interest) was defined by the border of the cell nuclei (DAPI). The raw intensity Myc signal was measured within the borders of the ROI. Quantification of the signal intensity was performed on 50-160 cells. The nuclear background signal generated from

untagged cells by the α -Myc antibody was measured and averaged for each stage of meiosis. The mean value of the background signal was subtracted from the nuclear Myc signal of individual protein-tagged cells at the corresponding meiotic stage.

4.8. Quantification of ECL signals

For quantification of half-lives and estimation of degradation rates, cultures treated with cycloheximide (CHX) were used. X-ray films with ECL signals were scanned using densitometric scanning. Scanning was performed in 480 dpi in 8-bit grayscale without any adjustment of signal levels. Digital scans were analyzed using ImageJ (W. S. Rasband, U.S. NIH, Bethesda, MD, <http://imagej.nih.gov/ij/>). Intensity of the ECL signal of each protein band was measured using Gel Analyzer. Background surrounding the signals was subtracted.

4.9. Mathematical modeling

Mathematical modeling was performed using a deterministic approach. Change of the concentration or activity of the variables was described using nonlinear ordinary differential equations (ODEs) according to biochemical reaction kinetics. Sets of the equations, parameter values and initial values of the variables were incorporated into XPPAUT software (Ermentrout and Mahajan, 2003) used to solve the ODEs and plot the results in the simulation window. Simulations were run by implementing the Stiff integration method (Hairer and Wanner, 1991; Shampine and Thompson, 2007) as an approximation algorithm to solve the ODEs. The time step for the integrator (Δt) was set to 1. The starting time (T_0) was set to 0. The basic simulation run time integrating the equations was set to 480 or 600 which corresponds to 8 hr and 10 hr of a meiotic time course, respectively. All mathematical models, which simulations are presented in this work are listed in **Table 11**.

Table 11. List of mathematical models.

Figure ¹	Model description	Equations	Tables with model parameters ^{2,3}
12B	Modified prophase I-to-metaphase I model	9-26	1
13B	Minimal Cdk1-APC/C oscillator model	27-30	2
14B-C	Combined model	9-17, 20-26, 31-35	1, 3
18	Combined model with modified levels of cyclins and Cdc20	9-17, 20-26, 31-35	1, 3, 4
19B-C	Model with hypothetical terminator	9-10, 13-17, 20, 23-26, 33-43	1, 3, 4, 5
21B-E	Model with Ama1 as the terminator	9-10, 13-17, 20-22, 24-26, 31-35, 44-48	1, 3, 4, 6
26A-F, 27A-D	Model with Ama1 and Cdc20 as the terminator	9-10, 13-17, 20-22, 24-26, 31-35, 44, 46-49	1, 3, 4, 6, 7
28A-D, 30A-C, 32, 34A-B	Model with Ama1 and Cdc20 as the terminator with adjusted parameters	9-10, 13-17, 20-22, 24-26, 31-35, 44, 46-49	1, 3, 4, 7, 8
36B-C	Model with inhibition of synthesis at the exit from meiosis II	9-10, 13-17, 20-22, 24-26, 31-35, 44, 46-47, 49-51	1, 3, 4, 7, 8, 9

¹Mathematical models are listed for each figure used in this study.

²Table numbers are listed containing parameters used in specified model.

³Only tables containing parameters used to simulate WT conditions are listed. Changes in parameter values in tested mutants are provided in the figure legends.

4.10. Statistical analysis

For calculation of mean, median and 95% confidence interval of IF signal intensity of Clb1-myc9, Clb4-myc9, Pds1-myc18, Myc18-Cdc20 and untagged control, Microsoft Excel was used. BoxPlotR (Spitzer et al., 2014; <http://boxplot.tyerslab.com>) was used for generation of box plots with Tukey whiskers. Box plots display quantified signal intensity (in arbitrary units) of Myc-tagged proteins after subtraction of the background signal from untagged controls. The crosses on the box plots represent the mean value of the signal intensity. The box plot limit displays the 1st and the 3rd quartile (25th and 75th percentile, respectively). The whiskers indicate variability outside the 1st and the 3rd quartiles and extend 1.5 times of the interquartile range. The outliers are represented by empty circles above the upper whisker and below the lower whisker. The notches

represent the 95% confidence interval (CI) for each median displayed as a center line in each box plot. Non-overlapping notches indicate 95% confidence that two medians differ.

For measurement of half-lives of proteins at metaphase I, at anaphase I, and at meiosis II in the presence and absence of Ama1, exponential regression was performed in Microsoft Excel to fit the trend line to the measured data points of ECL signal intensity. Diamonds on the graphs indicate an averaged intensity at a specified time point. Best fit was indicated by the R-squared value. The trend line equation described the line that best fits the data points and was used to calculate half-life of proteins (formula describing exponential decay). Degradation rate was calculated as $\ln(2)$ divided by the value of half life. Background degradation rates of proteins used in the mathematical model were approximated.

Abbreviations

AA	anchor-away
AI	additional inhibitor
APC/C	anaphase promoting complex/cyclosome
BSA	bovine serum albumin
Cdk	cyclin-dependent kinase
CHX	cycloheximide
CSF	cytostatic factor
DAPI	4',6'-diamino-2-phenylindole
DMSO	dimethyl sulfoxide
DSB	double strand break
ER	estrogene receptor
FEAR	cdc14 early anaphase release
FRB	FKBP12-rapamycin-binding
IE	intermediate enzyme
IF	immunofluorescence
mAR	meiotic-arrest/release
MCC	mitotic checkpoint complex
MEN	mitotic exit network
MPF	maturation-promoting factor
OD	optical density
ODE	ordinary differential equation
PBS	phosphate buffered saline
PCR	polymerase chain reaction
PP	protein phosphatase
RC	recombination checkpoint
ROI	region of interest
SAC	spindle assembly checkpoint
SC	synaptonemal complex
SDS	sodium dodecyl sulfated
SPB	spindle pole body
SPM	sporulation medium
TCA	trichloroacetic acid
WT	wild-type

YEPA	yeast extract peptone acetate
YPD	yeast extract peptone dextrose
YPG	yeast extract peptone glycerol

References

- Acosta, I., Ontoso, D., and San-Segundo, P. A. (2011). The budding yeast polo-like kinase Cdc5 regulates the Ndt80 branch of the meiotic recombination checkpoint pathway. *Mol Biol Cell* 22, 3478-3490.
- Adhikari, D., Diril, M. K., Busayavalasa, K., Risal, S., Nakagawa, S., Lindkvist, R., Shen, Y., Coppola, V., Tessarollo, L., and Kudo, N. *et al.* (2014). Mastl is required for timely activation of APC/C in meiosis I and Cdk1 reactivation in meiosis II. *J Cell Biol* 206, 843-853.
- Ahmed, N. T., Bungard, D., Shin, M. E., Moore, M., and Winter, E. (2009). The Ime2 protein kinase enhances the disassociation of the Sum1 repressor from middle meiotic promoters. *Mol Cell Biol* 29, 4352-4362.
- Alon, U. (2006). An introduction to systems biology: design principles of biological circuits. Chapman and Hall/CRC.
- Aoi, Y., Arai, K., Miyamoto, M., Katsuta, Y., Yamashita, A., Sato, M., and Yamamoto, M. (2013). Cuf2 boosts the transcription of APC/C activator Fzr1 to terminate the meiotic division cycle. *EMBO Rep* 14, 553-560.
- Argüello-Miranda, O. (2015). The regulatory network controlling the transition from prophase I into metaphase I. Doctoral dissertation, Fakultät Mathematik und Naturwissenschaften der Technischen Universität ät Dresden.
- Argüello-Miranda, O., Zagoriy, I., Mengoli, V., Rojas, J., Jonak, K., Oz, T., Graf, P., and Zachariae, W. (2017). Casein Kinase 1 Coordinates Cohesin Cleavage, Gametogenesis, and Exit from M Phase in Meiosis II. *Dev Cell* 40, 37-52.
- Ashyraliyev, M., Fomekong-Nanfack, Y., Kaandorp, J. A., and Blom, J. G. (2009). Systems biology: parameter estimation for biochemical models. *FEBS J* 276, 886-902.
- Bailis, J. M., and Roeder, G. S. (2000). Pachytene exit controlled by reversal of Mek1-dependent phosphorylation. *Cell* 101, 211-221.
- Bajgier, B. K., Malzone, M., Nickas, M., and Neiman, A. M. (2001). SPO21 is required for meiosis-specific modification of the spindle pole body in yeast. *Mol Biol Cell* 12, 1611-1621.
- Baliga, B. S., Pronczuk, A. W., and Munro, H. N. (1969). Mechanism of cycloheximide inhibition of protein synthesis in a cell-free system prepared from rat liver. *J Biol Chem* 244, 4480-4489.
- Baro, B., Rodriguez-Rodriguez, J. A., Calabria, I., Hernáez, M. L., Gil, C., and Queralt, E. (2013). Dual regulation of the mitotic exit network (MEN) by PP2A-Cdc55 phosphatase. *PLoS Genet* 9, e1003966.
- Benjamin, K. R., Zhang, C., Shokat, K. M., and Herskowitz, I. (2003). Control of landmark events in meiosis by the CDK Cdc28 and the meiosis-specific kinase Ime2. *Genes Dev* 17, 1524-1539.
- Berchowitz, L., Gajadhar, A., van Werven, F., De Rosa, A., Samoylova, M., Brar, G., Xu, Y., Xiao, C., Futcher, B., and Weissman, J. *et al.* (2013). A developmentally regulated translational control pathway establishes the meiotic chromosome segregation pattern. *Genes Dev* 27, 2147-2163.
- Bhola, T., Kapuy, O., and Vinod, P. K. (2018). Computational modelling of meiotic entry and commitment. *Sci Rep* 8, 180.
- Bizzari, F., and Marston, A. L. (2011). Cdc55 coordinates spindle assembly and chromosome disjunction during meiosis. *J Cell Biol* 193, 1213-1228.

- Blanco, M. A., Pelloquin, L., and Moreno, S. (2001). Fission yeast *mfr1* activates APC and coordinates meiotic nuclear division with sporulation. *J Cell Sci* 114, 2135-2143.
- Bloom, J., and Cross, F. R. (2007). Multiple levels of cyclin specificity in cell-cycle control. *Nat Rev Mol Cell Biol* 8, 149-160.
- Boissonade, J. And De Kepper, P. (1980). Transitions from bistability to limit cycle oscillations. Theoretical analysis and experimental evidence in an open chemical system. *The Journal of Physical Chemistry* 84, 501-506.
- Bollen, M., Gerlich, D. W., and Lesage, B. (2009). Mitotic phosphatases: from entry guards to exit guides. *Trends in cell biology* 19, 531-541.
- Bolte, M., Steigemann, P., Braus, G. H., and Irniger, S. (2002). Inhibition of APC-mediated proteolysis by the meiosis-specific protein kinase Ime2. *PNAS* 99, 4385-4390.
- Borisuk, M. T., and Tyson, J. J. (1998). Bifurcation analysis of a model of mitotic control in frog eggs. *J Theor Biol* 195, 69-85.
- Bowles, J., and Koopman, P. (2010). Sex determination in mammalian germ cells: extrinsic versus intrinsic factors. *Reproduction* 139, 943-958.
- Brar, G. A., Yassour, M., Friedman, N., Regev, A., Ingolia, N. T., and Weissman, J. S. (2012). High-resolution view of the yeast meiotic program revealed by ribosome profiling. *Science* 335, 552-557.
- Breeden, L. (2000). Cyclin transcription: Timing is everything. *Current Biology* 10, R586-R588.
- Brooks, R. F., Bennett, D. C., and Smith, J. A. (1980). Mammalian cell cycles need two random transitions. *Cell* 19, 493-504.
- Buonomo, S. B., Clyne, R. K., Fuchs, J., Loidl, J., Uhlmann, F., and Nasmyth, K. (2000). Disjunction of homologous chromosomes in meiosis I depends on proteolytic cleavage of the meiotic cohesin Rec8 by separin. *Cell* 103, 387-398.
- Buonomo, S. B., Rabitsch, K. P., Fuchs, J., Gruber, S., Sullivan, M., Uhlmann, F., Petronczki, M., Tóth, A., and Nasmyth, K. (2003). Division of the nucleolus and its release of CDC14 during anaphase of meiosis I depends on separase, SPO12, and SLK19. *Dev Cell* 4, 727-739.
- Busygina, V., Gaines, W. A., Xu, Y., Kwon, Y., Williams, G. J., Lin, S. W., Chang, H. Y., Chi, P., Wang, H. W. and Sung, P. (2013). Functional attributes of the *Saccharomyces cerevisiae* meiotic recombinase Dmc1. *DNA Repair* 12, 707-712.
- Camasses, A., Bogdanova, A., Shevchenko, A., and Zachariae, W. (2003). The CCT chaperonin promotes activation of the anaphase-promoting complex through the generation of functional Cdc20. *Molecular cell* 12, 87-100.
- Cappell, S. D., Mark, K. G., Garbett, D., Pack, L. R., Rape, M., and Meyer, T. (2018). EMI1 switches from being a substrate to an inhibitor of APC/C CDH1 to start the cell cycle. *Nature* 558, 313-317.
- Carlile, T. M., and Amon, A. (2008). Meiosis I is established through division-specific translational control of a cyclin. *Cell* 133, 280-291.
- Carpenter, K., Bell, R. B., Yunus, J., Amon, A., and Berchowitz, L. E. (2018). Phosphorylation-mediated clearance of amyloid-like assemblies in meiosis. *Dev Cell* 45, 392-405.
- Charvin, G., Oikonomou, C., Siggia, E. D., and Cross, F. R. (2010). Origin of irreversibility of cell cycle start in budding yeast. *PLoS Biol* 8, e1000284.
- Chen, K. C., Csikasz-Nagy, A., Gyorffy, B., Val, J., Novak, B., and Tyson, J. J. (2000). Kinetic analysis of a molecular model of the budding yeast cell cycle. *Mol Biol Cell* 11, 369-391.
- Chen, K. C., Calzone, L., Csikasz-Nagy, A., Cross, F. R., Novak, B., and Tyson, J. J. (2004). Integrative analysis of cell cycle control in budding yeast. *Mol Biol Cell* 15, 3841-3862.

- Cohen-Fix, O., Peters, J.-M., Kirschner, M. W., and Koshland, D. (1996). Anaphase initiation in *Saccharomyces cerevisiae* is controlled by the APC-dependent degradation of the anaphase inhibitor Pds1p. *Genes and Development* 10, 3081–3093.
- Chou, T. F., and Deshaies, R. J. (2011). Quantitative cell-based protein degradation assays to identify and classify drugs that target the ubiquitin-proteasome system. *J Biol Chem* 286, 16546-16554.
- Chu, S., and Herskowitz, I. (1998). Gametogenesis in yeast is regulated by a transcriptional cascade dependent on Ndt80. *Molecular Cell* 1, 685-696.
- Chu, S., DeRisi, J., Eisen, M., Mulholland, J., Botstein, D., Brown, P. O., and Herskowitz, I. (1998). The transcriptional program of sporulation in budding yeast. *Science* 282, 699-705.
- Chu, T., Henrion, G., Haegeli, V., and Strickland, S. (2001). Cortex, a *Drosophila* gene required to complete oocyte meiosis, is a member of the Cdc20/fizzy protein family. *Genesis* 29, 141-152.
- Chung, E., and Chen, R. H. (2003). Phosphorylation of Cdc20 is required for its inhibition by the spindle checkpoint. *Nat Cell Biol* 5, 748-753.
- Cifuentes, M., Jolivet, S., Cromer, L., Harashima, H., Bulankova, P., Renne, C., Crismani, W., Nomura, Y., Nakagami, H., and Sugimoto, K. (2016). TDM1 regulation determines the number of meiotic divisions. *PLoS Genet* 12, e1005856.
- Ciliberto, A., Lukács, A., Tóth, A., Tyson, J. J., and Novák, B. (2005). Rewiring the exit from mitosis. *Cell Cycle* 4, 4107-4112.
- Ciosk, R., Zachariae, W., Michaelis, C., Shevchenko, A., Mann, M., and Nasmyth, K. (1998). An ESP1/PDS1 complex regulates loss of sister chromatid cohesion at the metaphase to anaphase transition in yeast. *Cell* 93, 1067-1076.
- Coluccio, A. E., Rodriguez, R. K., Kernan, M. J., and Neiman, A. M. (2008). The yeast spore wall enables spores to survive passage through the digestive tract of *Drosophila*. *PLoS One* 3, e2873.
- Cooper, K. F., Mallory, M. J., Egeland, D. B., Jarnik, M., and Strich, R. (2000). Ama1p is a meiosis-specific regulator of the anaphase promoting complex/cyclosome in yeast. *PNAS* 97, 14548-14553.
- Corbi, D., Sunder, S., Weinreich, M., Skokotas, A., Johnson, E. S., and Winter, E. (2014). Multisite phosphorylation of the Sum1 transcriptional repressor by S-phase kinases controls exit from meiotic prophase in yeast. *Mol Cell Biol* 34, 2249-2263.
- Cromer, L., Heyman, J., Touati, S., Harashima, H., Araou, E., Girard, C., Horlow, C., Wassmann, K., Schnittger, A., and De Veylder, L. et al. (2012). OSD1 promotes meiotic progression via APC/C inhibition and forms a regulatory network with TDM and CYCA1; 2/TAM. *PLoS Genet* 8, e1002865.
- Cross, F. R., Archambault, V., Miller, M., and Klavstad, M. (2002). Testing a mathematical model of the yeast cell cycle. *Mol Biol Cell* 13, 52-70.
- Csikász-Nagy, A., Battogtokh, D., Chen, K. C., Novák, B., and Tyson, J. J. (2006). Analysis of a generic model of eukaryotic cell-cycle regulation. *Biophys J* 90, 4361-4379.
- Cundell, M. J., Bastos, R. N., Zhang, T., Holder, J., Gruneberg, U., Novak, B., and Barr, F. A. (2013). The BEG (PP2A-B55/ENSA/Greatwall) pathway ensures cytokinesis follows chromosome separation. *Molecular Cell* 52, 393-405.
- Dahmann, C., Diffley, J. F., and Nasmyth, K. A. (1995). S-phase-promoting cyclin-dependent kinases prevent re-replication by inhibiting the transition of replication origins to a pre-replicative state. *Current Biology* 5, 1257-1269.
- Dahmann, C., and Futcher, B. (1995). Specialization of B-type cyclins for mitosis or meiosis in *S. cerevisiae*. *Genetics* 140, 957-963.

- Diamond, A. E., Park, J. S., Inoue, I., Tachikawa, H., and Neiman, A. M. (2009). The anaphase promoting complex targeting subunit Ama1 links meiotic exit to cytokinesis during sporulation in *Saccharomyces cerevisiae*. *Mol Biol Cell* 20, 134-145.
- Dirick, L., Goetsch, L., Ammerer, G., and Byers, B. (1998). Regulation of meiotic S phase by Ime2 and a Clb5, 6-associated kinase in *Saccharomyces cerevisiae*. *Science* 281, 1854-1857.
- Dumollard, R., Levasseur, M., Hebras, C., Huitorel, P., Carroll, M., Chambon, J. P., and McDougall, A. (2011). Mos limits the number of meiotic divisions in urochordate eggs. *Development* 138, 885-895.
- Ermentrout, B., and Mahajan, A. (2003). *Simulating, Analyzing, and Animating Dynamical Systems: A Guide to XPPAUT for Researchers and Students*. *Appl Mech Rev* 56, B53.
- Evan, G. I., Lewis, G. K., Ramsay, G., and Bishop, J. M. (1985). Isolation of monoclonal antibodies specific for human c-myc proto-oncogene product. *Mol Cell Biol* 5, 3610-3616.
- Ferrell, J. E., and Machleder, E. M. (1998). The biochemical basis of an all-or-none cell fate switch in *Xenopus* oocytes. *Science* 280, 895-898.
- Ferrell Jr, J. E. (2002). Self-perpetuating states in signal transduction: positive feedback, double-negative feedback and bistability. *Curr Opin Cell Biol* 14, 140-148.
- Ferrell, J. E., Pomerening, J. R., Kim, S. Y., Trunnell, N. B., Xiong, W., Huang, C. Y. F., and Machleder, E. M. (2009). Simple, realistic models of complex biological processes: positive feedback and bistability in a cell fate switch and a cell cycle oscillator. *FEBS Lett* 583, 3999-4005.
- Ferrell Jr, J. E., Tsai, T. Y. C., and Yang, Q. (2011). Modeling the cell cycle: why do certain circuits oscillate?. *Cell* 144, 874-885.
- Ferrell Jr, J. E. (2013). Feedback loops and reciprocal regulation: recurring motifs in the systems biology of the cell cycle. *Curr Opin Cell Biol* 25, 676-686.
- Ferrell, J. E., and Ha, S. H. (2014). Ultrasensitivity part II: multisite phosphorylation, stoichiometric inhibitors, and positive feedback. *Trends Biochem Sci* 39, 556-569.
- Fischer, H. P. (2008). Mathematical modeling of complex biological systems: from parts lists to understanding systems behavior. *Alcohol Research & Health* 31, 49.
- Futcher, B. (2008). Cyclins in meiosis: lost in translation. *Dev Cell* 14, 644-645.
- Gerhart, J., Wu, M., and Kirschner, M. (1984). Cell cycle dynamics of an M-phase-specific cytoplasmic factor in *Xenopus laevis* oocytes and eggs. *J Cell Biol* 98, 1247-1255.
- Gharbi-Ayachi, A., Labbe, J. C., Burgess, A., Vigneron, S., Strub, J. M., Brioudes, E., Van-Dorselaer, A., Castro, A., and Lorca, T. (2010). The substrate of Greatwall kinase, Arpp19, controls mitosis by inhibiting protein phosphatase 2A. *Science* 330, 1673-1677.
- Golan, A., Yudkovsky, Y., and Hershko, A. (2002). The cyclin-ubiquitin ligase activity of cyclosome/APC is jointly activated by protein kinases Cdk1-cyclin B and Plk. *J Biol Chem* 277, 15552-15557.
- Goldbeter, A., and Koshland, D. E. (1981). An amplified sensitivity arising from covalent modification in biological systems. *PNAS* 78, 6840-6844.
- Goldbeter, A. (1991). A minimal cascade model for the mitotic oscillator involving cyclin and cdc2 kinase. *PNAS* 88, 9107-9111.
- Goldstein, A. L., and McCusker, J. H. (1999). Three new dominant drug resistance cassettes for gene disruption in *Saccharomyces cerevisiae*. *Yeast* 15, 1541-1553.
- Gonze, D., and Abou-Jaoudé, W. (2013). The Goodwin model: behind the Hill function. *PloS One* 8, e69573.

- Griffith, J. S. (1968). Mathematics of cellular control processes I. Negative feedback to one gene. *J Theor Biol* 20, 202-208.
- Gross, S. D., Schwab, M. S., Taieb, F. E., Lewellyn, A. L., Qian, Y. W., and Maller, J. L. (2000). The critical role of the MAP kinase pathway in meiosis II in *Xenopus* oocytes is mediated by p90Rsk. *Current Biology* 10, 430-438.
- Gruber, S., Haering, C. H., and Nasmyth, K. (2003). Chromosomal cohesin forms a ring. *Cell* 112, 765-777.
- Haase, S. B., Winey, M., and Reed, S. I. (2001). Multi-step control of spindle pole body duplication by cyclin-dependent kinase. *Nat Cell Biol* 3, 38-42.
- Hairer, E., and Wanner, G. (1991). Solving ordinary differential equations II, Stiff and Differential-Algebraic Problems. Springer-Verlag, Berlin.
- Hartwell, L. H., and Weinert, T. A. (1989). Checkpoints: controls that ensure the order of cell cycle events. *Science* 246, 629-634.
- Haruki, H., Nishikawa, J., and Laemmli, U. K. (2008). The anchor-away technique: rapid, conditional establishment of yeast mutant phenotypes. *Molecular Cell* 31, 925-932.
- Hassold, T., and Hunt, P. (2001). To err (meiotically) is human: the genesis of human aneuploidy. *Nat Rev Genet* 2, 280-291.
- Hatzimanikatis, V., Lee, K. H., and Bailey, J. E. (1999). A mathematical description of regulation of the G1-S transition of the mammalian cell cycle. *Biotechnol Bioeng* 65, 631-637.
- Healy, A.M., Zolnierowicz, S., Stapleton, A.E., Goebel, M., DePaoli-Roach, A.A., and Pringle, J.R. (1991). CDC55, a *Saccharomyces cerevisiae* gene involved in cellular morphogenesis: identification, characterization, and homology to the B subunit of mammalian type 2A protein phosphatase. *Mol Cell Biol* 11, 5767-5780.
- Hégarat, N., Vesely, C., Vinod, P. K., Ocasio, C., Peter, N., Gannon, J., Oliver, A., Novák, B., and Hohegger, H. (2014). PP2A/B55 and Fcp1 regulate Greatwall and Ensa dephosphorylation during mitotic exit. *PLoS Genet* 10, e1004004.
- Hohegger, H., Klotzbücher, A., Kirk, J., Howell, M., le Guellec, K., Fletcher, K., Duncan, T., Sohail, M., and Hunt, T. (2001). New B-type cyclin synthesis is required between meiosis I and II during *Xenopus* oocyte maturation. *Development* 128, 3795-3807.
- Holt, L. J., Hutti, J. E., Cantley, L. C., and Morgan, D. O. (2007). Evolution of Ime2 phosphorylation sites on Cdk1 substrates provides a mechanism to limit the effects of the phosphatase Cdc14 in meiosis. *Molecular Cell* 25, 689-702.
- Homer, H. A., McDougall, A., Levasseur, M., Yallop, K., Murdoch, A. P., and Herbert, M. (2005). Mad2 prevents aneuploidy and premature proteolysis of cyclin B and securin during meiosis I in mouse oocytes. *Genes Dev*, 19, 202-207.
- Hopkins, M., Tyson, J. J., and Novák, B. (2017). Cell-cycle transitions: a common role for stoichiometric inhibitors. *Mol Biol Cell* 28, 3437-3446.
- Hoyt, M. A., Totis, L., and Roberts, B. T. (1991). *S. cerevisiae* genes required for cell cycle arrest in response to loss of microtubule function. *Cell* 66, 507-517.
- Hwang, L. H., Lau, L. F., Smith, D. L., Mistrot, C. A., Hardwick, K. G., Hwang, E. S., Amon, A., and Murray, A. W. (1998). Budding yeast Cdc20: a target of the spindle checkpoint. *Science* 279, 1041-1044.
- Ingolia, N. T., and Murray, A. W. (2004). The ups and downs of modeling the cell cycle. *Current Biology* 14, R771-R777.

- Irniger, S., Piatti, S., Michaelis, C., and Nasmyth, K. (1995). Genes involved in sister chromatid separation are needed for B-type cyclin proteolysis in budding yeast. *Cell* 81, 269-277.
- Irniger, S. (2006). Preventing fatal destruction: inhibitors of the anaphase-promoting complex in meiosis. *Cell Cycle* 5, 405-415.
- Iwabuchi, M., Ohsumi, K., Yamamoto, T. M., Sawada, W., and Kishimoto, T. (2000). Residual Cdc2 activity remaining at meiosis I exit is essential for meiotic M–M transition in *Xenopus* oocyte extracts. *EMBO J* 19, 4513-4523.
- Izawa, D., Goto, M., Yamashita, A., Yamano, H., and Yamamoto, M. (2005). Fission yeast Mes1p ensures the onset of meiosis II by blocking degradation of cyclin Cdc13p. *Nature* 434, 529-533.
- Jacobs, H. W., Richter, D. O., Venkatesh, T. R., and Lehner, C. F. (2002). Completion of mitosis requires neither *fzr/rap* nor *fzr2*, a male germline-specific *Drosophila* Cdh1 homolog. *Current Biology* 12, 1435-1441.
- Jaspersen, S. L., Charles, J. F., and Morgan, D. O. (1999). Inhibitory phosphorylation of the APC regulator Hct1 is controlled by the kinase Cdc28 and the phosphatase Cdc14. *Current Biology* 9, 227-236.
- Jaspersen, S. L., & Morgan, D. O. (2000). Cdc14 activates cdc15 to promote mitotic exit in budding yeast. *Current Biology* 10, 615-618.
- Kane, S.M., and Roth, R. (1974). Carbohydrate metabolism during ascospore development in yeast. *Journal of bacteriology* 118, 8-14.
- Kapuy, O., He, E., López-Avilés, S., Uhlmann, F., Tyson, J. J., and Novák, B. (2009). System-level feedbacks control cell cycle progression. *FEBS Lett* 583, 3992-3998.
- Katis, V. L., Matos, J., Mori, S., Shirahige, K., Zachariae, W., and Nasmyth, K. (2004). Spo13 facilitates monopolin recruitment to kinetochores and regulates maintenance of centromeric cohesion during yeast meiosis. *Current Biology* 14, 2183-2196.
- Katis, V. L., Lipp, J. J., Imre, R., Bogdanova, A., Okaz, E., Habermann, B., Mechtler, K., Nasmyth, K., and Zachariae, W. (2010). Rec8 phosphorylation by casein kinase 1 and Cdc7-Dbf4 kinase regulates cohesin cleavage by separase during meiosis. *Dev Cell* 18, 397-409.
- Kerr, G. W., Sarkar, S., Tibbles, K. L., Petronczki, M., Millar, J. B., and Arumugam, P. (2011). Meiotic nuclear divisions in budding yeast require PP2A^{Cdc55}-mediated antagonism of Net1 phosphorylation by Cdk. *J Cell Biol* 193, 1157-1166.
- Kerr, G. W., Sarkar, S., and Arumugam, P. (2012). How to halve ploidy: lessons from budding yeast meiosis. *Cell Mol Life Sci* 69, 3037-3051.
- Kerr, G.W., HueiWong, J., and Arumugam, P. (2016). PP2A^{Cdc55}'s role in reductional chromosome segregation during achiasmate meiosis in budding yeast is independent of its FEAR function. *Sci Rep* 6, 30397.
- Kiburz, B. M., Reynolds, D. B., Megee, P. C., Marston, A. L., Lee, B. H., Lee, T. I., Levine, S.S., Young, R.A., and Amon, A. (2005). The core centromere and Sgo1 establish a 50-kb cohesin-protected domain around centromeres during meiosis I. *Genes Dev* 19, 3017-3030.
- Kimata, Y., Kitamura, K., Fenner, N., & Yamano, H. (2011). Mes1 controls the meiosis I to meiosis II transition by distinctly regulating the anaphase-promoting complex/cyclosome coactivators Fzr1/Mfr1 and Slp1 in fission yeast. *Mol Biol Cell* 22, 1486-1494.
- Kitano, H. (2002). Systems biology: a brief overview. *Science* 295, 1662-1664.
- Klapholz, S., Waddell, C. S., and Esposito, R. E. (1985). The role of the SPO11 gene in meiotic recombination in yeast. *Genetics* 110, 187-216.

- Klein, F., Mahr, P., Galova, M., Buonomo, S. B., Michaelis, C., Nairz, K., and Nasmyth, K. (1999). A central role for cohesins in sister chromatid cohesion, formation of axial elements, and recombination during yeast meiosis. *Cell* 98, 91-103.
- Knop, M., Siegers, K., Pereira, G., Zachariae, W., Winsor, B., Nasmyth, K., and Schiebel, E. (1999). Epitope tagging of yeast genes using a PCR-based strategy: more tags and improved practical routines. *Yeast* 15, 963-972.
- Knop, M., and Strasser, K. (2000). Role of the spindle pole body of yeast in mediating assembly of the prospore membrane during meiosis. *EMBO J* 19, 3657-3667.
- Kohl, P., Crampin, E. J., Quinn, T. A., and Noble, D. (2010). Systems biology: an approach. *Clin Pharmacol Ther* 88, 25-33.
- Kraft, C., Herzog, F., Gieffers, C., Mechtler, K., Hagting, A., Pines, J., and Peters, J. M. (2003). Mitotic regulation of the human anaphase-promoting complex by phosphorylation. *EMBO J* 22, 6598-6609.
- Kraikivski, P., Chen, K. C., Laomettachit, T., Murali, T. M., and Tyson, J. J. (2015). From START to FINISH: computational analysis of cell cycle control in budding yeast. *NPJ Syst Biol Appl* 1, 15016.
- Kramer, E. R., Scheuringer, N., Podtelejnikov, A. V., Mann, M., and Peters, J. M. (2000). Mitotic regulation of the APC activator proteins CDC20 and CDH1. *Mol Biol Cell* 11, 1555-1569.
- Kubiak, J. Z. (1989). Mouse oocytes gradually develop the capacity for activation during the metaphase II arrest. *Dev Biol* 136, 537-545.
- Labit, H., Fujimitsu, K., Bayin, N. S., Takaki, T., Gannon, J., and Yamano, H. (2012). Dephosphorylation of Cdc20 is required for its C-box-dependent activation of the APC/C. *EMBO J* 31, 3351-3362.
- Lee, B. H., Kiburz, B. M., and Amon, A. (2004). Spo13 maintains centromeric cohesion and kinetochore coorientation during meiosis I. *Current Biology* 14, 2168-2182.
- Leu, J. Y., and Roeder, G. S. (1999). The pachytene checkpoint in *S. cerevisiae* depends on Swe1-mediated phosphorylation of the cyclin-dependent kinase Cdc28. *Molecular Cell* 4, 805-814.
- Li, R., and Murray, A. W. (1991). Feedback control of mitosis in budding yeast. *Cell* 66, 519-531.
- Li, S., and Wilkinson, M. F. (1997). Site-directed mutagenesis: a two-step method using PCR and Dpn I. *Biotechniques* 23, 588-590.
- Li, Y. H., Kang, H., Xu, Y. N., Heo, Y. T., Cui, X. S., Kim, N. H., and Oh, J. S. (2013). Greatwall kinase is required for meiotic maturation in porcine oocytes. *Biology of Reproduction* 89, 53-1.
- Lindgren, A., Bungard, D., Pierce, M., Xie, J., Vershon, A., and Winter, E. (2000). The pachytene checkpoint in *Saccharomyces cerevisiae* requires the Sum1 transcriptional repressor. *EMBO J* 19, 6489-6497.
- López-Avilés, S., Kapuy, O., Novák, B., and Uhlmann, F. (2009). Irreversibility of mitotic exit is the consequence of systems-level feedback. *Nature* 459, 592-595.
- Loy, C. J., Lydall, D., and Surana, U. (1999). NDD1, a high-dosage suppressor of *cdc28-1n*, is essential for expression of a subset of late-s-phase-specific genes in *Saccharomyces cerevisiae*. *Mol. Cell. Biol.* 19, 3312-3327.
- MacIsaac, K. D., Wang, T., Gordon, D. B., Gifford, D. K., Stormo, G. D., and Fraenkel, E. (2006). An improved map of conserved regulatory sites for *Saccharomyces cerevisiae*. *BMC Bioinf* 7, 113.
- Malone, R. E., Haring, S. J., Foreman, K. E., Pansegrau, M. L., Smith, S. M., Houdek, D. R., Carpp, L., Shah, B., and Lee, K. E. (2004). The signal from the initiation of meiotic recombination to the first division of meiosis. *Eukaryotic Cell* 3, 598-609.

- Marston, A. L., Lee, B. H., and Amon, A. (2003). The Cdc14 phosphatase and the FEAR network control meiotic spindle disassembly and chromosome segregation. *Dev Cell* 4, 711-726.
- Matos, J., Lipp, J. J., Bogdanova, A., Guillot, S., Okaz, E., Junqueira, M., Shevchenko, A., and Zachariae, W. (2008). Dbf4-dependent CDC7 kinase links DNA replication to the segregation of homologous chromosomes in meiosis I. *Cell* 135, 662-678.
- Mendenhall, M. D., and Hodge, A. E. (1998). Regulation of Cdc28 cyclin-dependent protein kinase activity during the cell cycle of the yeast *Saccharomyces cerevisiae*. *Microbiol Mol Biol Rev* 62, 1191-1243.
- Mitchell, A. P., Driscoll, S. E., and Smith, H. E. (1990). Positive control of sporulation-specific genes by the IME1 and IME2 products in *Saccharomyces cerevisiae*. *Mol Cell Biol* 10, 2104-2110.
- Mocciaro, A., and Schiebel, E. (2010). Cdc14: a highly conserved family of phosphatases with non-conserved functions?. *J Cell Sci* 123, 2867-2876.
- Mochida, S., Rata, S., Hino, H., Nagai, T., and Novák, B. (2016). Two bistable switches govern M phase entry. *Current Biology* 26, 3361-3367.
- Mortensen, E. M., Haas, W., Gygi, M., Gygi, S. P., and Kellogg, D. R. (2005). Cdc28-dependent regulation of the Cdc5/Polo kinase. *Current Biology* 15, 2033-2037.
- Murray, A. W. (2004). Recycling the cell cycle: cyclins revisited. *Cell* 116, 221-234.
- Musacchio, A., and Salmon, E. D. (2007). The spindle-assembly checkpoint in space and time. *Nat Rev Mol Cell Biol* 8, 379-393.
- Musacchio, A. (2015). The molecular biology of spindle assembly checkpoint signaling dynamics. *Current Biology* 25, R1002-R1018.
- Nasmyth, K. (1996). Putting the cell cycle in order. *Science* 274, 1643-1645.
- Nasmyth, K., and Haering, C. H. (2009). Cohesin: its roles and mechanisms. *Annual review of genetics* 43, 525-558.
- Nigg, E. A. (2001). Cell division: mitotic kinases as regulators of cell division and its checkpoints. *Nat Rev Mol Cell Biol* 2, 21-32.
- Novak, B., and Tyson, J. J. (1993). Numerical analysis of a comprehensive model of M-phase control in *Xenopus* oocyte extracts and intact embryos. *J Cell Sci* 106, 1153-1168.
- Novak, B., Pataki, Z., Ciliberto, A., and Tyson, J. J. (2001). Mathematical model of the cell division cycle of fission yeast. *Chaos: An Interdisciplinary Journal of Nonlinear Science* 11, 277-286.
- Novak, B., Tyson, J. J., Gyorffy, B., and Csikasz-Nagy, A. (2007). Irreversible cell-cycle transitions are due to systems-level feedback. *Nat Cell Biol* 9, 724-728.
- Novák, B., Vinod, P. K., Freire, P., and Kapuy, O. (2010). Systems-level feedback in cell-cycle control. *Biochem Soc Trans* 38, 1242-1246.
- Nurse, P. (1990). Universal control mechanism regulating onset of M-phase. *Nature* 344, 503-508.
- Oelschlaegel, T., Schwickart, M., Matos, J., Bogdanova, A., Camasses, A., Havlis, J., Shevchenko, A., and Zachariae, W. (2005). The yeast APC/C subunit Mnd2 prevents premature sister chromatid separation triggered by the meiosis-specific APC/C-Ama1. *Cell* 120, 773-788.
- Okaz, E., Argüello-Miranda, O., Bogdanova, A., Vinod, P. K., Lipp, J. J., Markova, Z., Zagoriy, I., Novak, B., and Zachariae, W. (2012). Meiotic prophase requires proteolysis of M phase regulators mediated by the meiosis-specific APC/C-Ama1. *Cell* 151, 603-618.
- Page, S. L., and Hawley, R. S. (2004). The genetics and molecular biology of the synaptonemal complex. *Annu Rev Cell Dev Biol* 20, 525-558.

- Pak, J., and Segall, J. (2002). Role of Ndt80, Sum1, and Swe1 as targets of the meiotic recombination checkpoint that control exit from pachytene and spore formation in *Saccharomyces cerevisiae*. *Mol Cell Biol* 22, 6430-6440.
- Perry, A. C., and Verlhac, M. H. (2008). Second meiotic arrest and exit in frogs and mice. *EMBO Rep* 9, 246-251.
- Pesin, J. A., and Orr-Weaver, T. L. (2008). Regulation of APC/C activators in mitosis and meiosis. *Annu Rev Cell Dev Biol* 24, 475-499.
- Petronczki, M., Siomos, M. F., and Nasmyth, K. (2003). Un menage a quatre: the molecular biology of chromosome segregation in meiosis. *Cell* 112, 423-440.
- Petronczki, M., Matos, J., Mori, S., Gregan, J., Bogdanova, A., Schwickart, M., Mechtler, K., Shirahige, K., Zachariae, W., and Nasmyth, K. (2006). Monopolar attachment of sister kinetochores at meiosis I requires casein kinase 1. *Cell* 126, 1049-1064.
- Pfeuty, B., and Kaneko, K. (2009). The combination of positive and negative feedback loops confers exquisite flexibility to biochemical switches. *Physical biology* 6, 046013.
- Pfeuty, B., Bodart, J. F., Blossey, R., and Lefranc, M. (2012). A dynamical model of oocyte maturation unveils precisely orchestrated meiotic decisions. *PLoS Comput Biol* 8, e1002329.
- Phizicky, D. V., Berchowitz, L. E., and Bell, S. P. (2018). Multiple kinases inhibit origin licensing and helicase activation to ensure reductive cell division during meiosis. *Elife* 7, e33309.
- Picard, D. (1999). Regulation of heterologous proteins by fusion to a hormone binding domain. *Nuclear receptors: a practical approach*, 261-274.
- Pines, J. (1995). Cyclins and cyclin-dependent kinases: theme and variations. *Advances in cancer research* 66, 181-212. Academic Press.
- Pomerening, J. R., Kim, S. Y., and Ferrell Jr, J. E. (2005). Systems-level dissection of the cell-cycle oscillator: bypassing positive feedback produces damped oscillations. *Cell* 122, 565-578.
- Potapova, T. A., Daum, J. R., Pittman, B. D., Hudson, J. R., Jones, T. N., Satinover, D. L., Stukenberg, P.T., and Gorbsky, G. J. (2006). The reversibility of mitotic exit in vertebrate cells. *Nature* 440, 954-958.
- Primig, M., Williams, R.M., Winzeler, E.A., Tevzadze, G.G., Conway, A.R., Hwang, S.Y., Davis, R.W., and Esposito, R.E. (2000). The core meiotic transcriptome in budding yeasts. *Nature genetics* 26, 415-423.
- Queralt, E., Lehane, C., Novak, B., and Uhlmann, F. (2006). Downregulation of PP2A^{Cdc55} phosphatase by separase initiates mitotic exit in budding yeast. *Cell* 125, 719-732.
- Rata, S., Rodriguez, M. F. S. P., Joseph, S., Peter, N., Iturra, F. E., Yang, F., Madzvamuse, A., Ruppert, J.G., Samejima, K., and Platani, M. et al. (2018). Two interlinked bistable switches govern mitotic control in mammalian cells. *Current biology* 28, 3824-3832.
- Ray, D., Su, Y., and Ye, P. (2013). Dynamic modeling of yeast meiotic initiation. *BMC Syst Biol* 7, 37.
- Reed, S. I. (2003). Ratchets and clocks: the cell cycle, ubiquitylation and protein turnover. *Nature Nat Rev Mol Cell Biol* 4, 855-864.
- Riedel, C. G., Katis, V. L., Katou, Y., Mori, S., Itoh, T., Helmhart, W., Gálová, M., Petronczki, M., Gregan, J., and Cetin, B. et al. (2006). Protein phosphatase 2A protects centromeric sister chromatid cohesion during meiosis I. *Nature* 441, 53-61.
- Roeder, G. S. (1995). Sex and the single cell: meiosis in yeast. *PNAS* 92, 10450-10456.

- Rossio, V., Michimoto, T., Sasaki, T., Ohbayashi, I., Kikuchi, Y., and Yoshida, S. (2013). Nuclear PP2A-Cdc55 prevents APC-Cdc20 activation during the spindle assembly checkpoint. *J Cell Sci* 126, 4396-4405.
- Rudner, A. D., and Murray, A. W. (2000). Phosphorylation by Cdc28 activates the Cdc20-dependent activity of the anaphase-promoting complex. *J Cell Biol* 149, 1377-1390.
- Salah, S. M., and Nasmyth, K. (2000). Destruction of the securin Pds1p occurs at the onset of anaphase during both meiotic divisions in yeast. *Chromosoma* 109, 27-34.
- Sarkar, S., Dalgaard, J. Z., Millar, J. B., and Arumugam, P. (2014). The Rim15-endosulfine-PP2ACdc55 signalling module regulates entry into gametogenesis and quiescence via distinct mechanisms in budding yeast. *PLoS Genet* 10, e1004456.
- Sassoon, I., Severin, F. F., Andrews, P. D., Taba, M. R., Kaplan, K. B., Ashford, A. J., Stark, M.J., Sorger, P.K., and Hyman, A.A. (1999). Regulation of *Saccharomyces cerevisiae* kinetochores by the type 1 phosphatase Glc7p. *Genes Dev* 13, 545-555.
- Sauro, H. M. (2018). *Systems Biology: Introduction to Pathway Modeling*. Ambrosius Publishing.
- Schäuble, S., Stavrum, A. K., Puntervoll, P., Schuster, S., and Heiland, I. (2013). Effect of substrate competition in kinetic models of metabolic networks. *FEBS Lett* 587, 2818-2824.
- Schindler, K., and Winter, E. (2006). Phosphorylation of Ime2 regulates meiotic progression in *Saccharomyces cerevisiae*. *J Biol Chem* 281, 18307-18316.
- Schindler, K., and Schultz, R. M. (2009). CDC14B acts through FZR1 (CDH1) to prevent meiotic maturation of mouse oocytes. *Biology of reproduction* 80, 795-803.
- Schlumpberger, M., Schaeffeler, E., Straub, M., Bredschneider, M., Wolf, D. H., and Thumm, M. (1997). AUT1, a gene essential for autophagocytosis in the yeast *Saccharomyces cerevisiae*. *Journal of bacteriology* 179, 1068-1076.
- Schmidt, A., Duncan, P. I., Rauh, N. R., Sauer, G., Fry, A. M., Nigg, E. A., and Mayer, T. U. (2005). *Xenopus polo-like kinase Plx1* regulates XErp1, a novel inhibitor of APC/C activity. *Genes and Dev* 19, 502-513.
- Schneider-Poetsch, T., Ju, J., Eyler, D. E., Dang, Y., Bhat, S., Merrick, W. C., Green, R., Shen, B., and Liu, J. O. (2010). Inhibition of eukaryotic translation elongation by cycloheximide and lactimidomycin. *Nat Chem Biol* 6, 209-217.
- Schwob, E., Bohm, T., Mendenhall, M.D., and Nasmyth, K. (1994). The B-type cyclin kinase inhibitor p40SIC1 controls the G1 to S transition in *S. cerevisiae*. *Cell* 79, 233-244.
- Sclafani, R. A. (2000). Cdc7p-Dbf4p becomes famous in the cell cycle. *J Cell Sci* 113, 2111-2117.
- Shampine, L. F., and Thompson, S. (2007). Stiff systems. *Scholarpedia*, 2, 2855.
- Sherman, S. L., Allen, E. G., Bean, L. H., and Freeman, S. B. (2007). Epidemiology of Down syndrome. *Mental retardation and developmental disabilities research reviews* 13, 221-227.
- Shields, R., and Smith, J. A. (1977). Cells regulate their proliferation through alterations in transition probability. *J Cell Physiol* 91, 345-355.
- Shin, M. E., Skokotas, A., and Winter, E. (2010). The Cdk1 and Ime2 protein kinases trigger exit from meiotic prophase in *Saccharomyces cerevisiae* by inhibiting the Sum1 transcriptional repressor. *Mol Cell Biol* 30, 2996-3003.
- Shirayama, M., Tóth, A., Gálová, M., and Nasmyth, K. (1999). APC Cdc20 promotes exit from mitosis by destroying the anaphase inhibitor Pds1 and cyclin Clb5. *Nature* 402, 203-207.
- Shonn, M. A., McCarroll, R., and Murray, A. W. (2000). Requirement of the spindle checkpoint for proper chromosome segregation in budding yeast meiosis. *Science* 289, 300-303.

- Shu, Y., Yang, H., Hallberg, E., and Hallberg, R. (1997). Molecular genetic analysis of Rts1p, a B' regulatory subunit of *Saccharomyces cerevisiae* protein phosphatase 2A. *Mol Cell Biol* 17, 3242–3253.
- Sible, J. C., and Tyson, J. J. (2007). Mathematical modeling as a tool for investigating cell cycle control networks. *Methods* 41, 238–247.
- Smith, H. E., and Mitchell, A. P. (1989). A transcriptional cascade governs entry into meiosis in *Saccharomyces cerevisiae*. *Mol Cell Biol* 9, 2142–2152.
- Sneddon, A. A., Cohen, P. T., and Stark, M. J. (1990). *Saccharomyces cerevisiae* protein phosphatase 2A performs an essential cellular function and is encoded by two genes. *EMBO J* 9, 4339–4346.
- Sopko, R., Raithatha, S., and Stuart, D. (2002). Phosphorylation and maximal activity of *Saccharomyces cerevisiae* meiosis-specific transcription factor Ndt80 is dependent on Ime2. *Mol Cell Biol* 22, 7024–7040.
- Spitzer, M., Wildenhain, J., Rappsilber, J., and Tyers, M. (2014). BoxPlotR: a web tool for generation of box plots. *Nature methods* 11, 121.
- Stegmeier, F., and Amon, A. (2004). Closing mitosis: the functions of the Cdc14 phosphatase and its regulation. *Annu Rev Genet* 38, 203–232.
- Strich, R., Mallory, M. J., Jarnik, M., & Cooper, K. F. (2004). Cyclin B-cdk activity stimulates meiotic rereplication in budding yeast. *Genetics*, 167(4), 1621–1628.
- Sudakin, V., Ganoth, D. V. O. R. A. H., Dahan, A., Heller, H., Hershko, J., Luca, F. C., Ruderman, J.V., and Hershko, A. (1995). The cyclosome, a large complex containing cyclin-selective ubiquitin ligase activity, targets cyclins for destruction at the end of mitosis. *Mol Biol Cell* 6, 185–197.
- Sudakin, V., Chan, G. K., and Yen, T. J. (2001). Checkpoint inhibition of the APC/C in HeLa cells is mediated by a complex of BUBR1, BUB3, CDC20, and MAD2. *J Cell Biol* 154, 925–936.
- Sullivan, M., and Morgan, D. O. (2007). A novel destruction sequence targets the meiotic regulator Spo13 for anaphase-promoting complex-dependent degradation in anaphase I. *Biol Chem* 282, 19710–19715.
- Szallasi, Z., Stelling, J., and Periwal, V. (2006). System modeling in cellular biology. From Concepts to nuts and bolts. The MIT Press.
- Szwarcwort-Cohen, M., Kasulin-Boneh, Z., Sagee, S., and Kassir, Y. (2009). Human Cdk2 is a functional homolog of budding yeast Ime2, the meiosis-specific Cdk-like kinase. *Cell Cycle* 8, 647–654.
- Tachikawa, H., Bloecher, A., Tatchell, K., and Neiman, A. M. (2001). A Gip1p–Glc7p phosphatase complex regulates septin organization and spore wall formation. *J Cell Biol* 155, 797–808.
- Thron, C. D. (1996). A model for a bistable biochemical trigger of mitosis. *Biophysical chemistry* 57, 239–251.
- Tibbles, K.L. (2013). Regulation of Clb1 during meiosis in *Saccharomyces cerevisiae*. Doctoral dissertation, University of Warwick.
- Tóth, A., Rabitsch, K. P., Gálová, M., Schleiffer, A., Buonomo, S. B., and Nasmyth, K. (2000). Functional genomics identifies monopolin: a kinetochore protein required for segregation of homologs during meiosis I. *Cell* 103, 1155–1168.
- Tung, K. S., Hong, E. J. E., and Roeder, G. S. (2000). The pachytene checkpoint prevents accumulation and phosphorylation of the meiosis-specific transcription factor Ndt80. *PNAS* 97, 12187–12192.
- Tung, J. J., and Jackson, P. K. (2005). Emi1 class of proteins regulate entry into meiosis and the meiosis I to meiosis II transition in *Xenopus* oocytes. *Cell Cycle* 4, 478–482.

- Tyson, J. J., and Othmer, H. G. (1978). The dynamics of feedback control circuits in biochemical pathways. *Prog Theor Biol* 5, 62.
- Tyson, J. J. (1999). Models of cell cycle control in eukaryotes. *J Biotechnol* 71, 239-244.
- Tyson, J. J., Chen, K., and Novak, B. (2001). Network dynamics and cell physiology. *Nat Rev Mol Cell Biol* 2(12), 908-916.
- Tyson, J. J., Chen, K. C., and Novak, B. (2003). Sniffers, buzzers, toggles and blinkers: dynamics of regulatory and signaling pathways in the cell. *Curr Opin Cell Biol* 15, 221-231.
- Tyson, J. J., and Novak, B. (2008). Temporal organization of the cell cycle. *Current Biology* 18, R759-R768.
- Uhlmann, F., Lottspeich, F., and Nasmyth, K. (1999). Sister-chromatid separation at anaphase onset is promoted by cleavage of the cohesin subunit Scc1. *Nature* 400, 37-42.
- Verlhac, M. H., Kubiak, J. Z., Weber, M., Géraud, G., Colledge, W. H., Evans, M. J., and Maro, B. (1996). Mos is required for MAP kinase activation and is involved in microtubule organization during meiotic maturation in the mouse. *Development* 122, 815-822.
- Vinod, P. K., Freire, P., Rattani, A., Ciliberto, A., Uhlmann, F., and Novak, B. (2011). Computational modelling of mitotic exit in budding yeast: the role of separase and Cdc14 endocycles. *Journal of The Royal Society Interface* 8, 1128-1141.
- Vinod, P. K., Zhou, X., Zhang, T., Mayer, T. U., and Novak, B. (2013). The role of APC/C inhibitor Emi2/XErp1 in oscillatory dynamics of early embryonic cell cycles. *Biophys Chem* 177, 1-6.
- Vinod, P. K., and Novak, B. (2015). Model scenarios for switch-like mitotic transitions. *FEBS Lett* 589, 667-671.
- Visintin, R., Prinz, S., and Amon, A. (1997). CDC20 and CDH1: a family of substrate-specific activators of APC-dependent proteolysis. *Science* 278, 460-463.
- Visintin, R., Craig, K., Hwang, E. S., Prinz, S., Tyers, M., and Amon, A. (1998). The phosphatase Cdc14 triggers mitotic exit by reversal of Cdk-dependent phosphorylation. *Molecular cell* 2, 709-718.
- Wach, A., Brachat, A., Pöhlmann, R., and Philippsen, P. (1994). New heterologous modules for classical or PCR-based gene disruptions in *Saccharomyces cerevisiae*. *Yeast* 10, 1793-1808.
- Wannige, C.T., Kulasiri, D., and Samarasinghe, S. (2015). Regulation of Meiosis Initiation before the Commitment Point in Budding Yeast: A Review of Biology, Molecular Mechanisms and Related Mathematical Models. *Current Bioinformatics* 10, 208-224.
- Waters, J. C. (2009). Accuracy and precision in quantitative fluorescence microscopy. *The Journal Of Experimental Medicine* 206, i15-i15.
- Winter, E. (2012). The Sum1/Ndt80 transcriptional switch and commitment to meiosis in *Saccharomyces cerevisiae*. *Microbiol Mol Biol Rev* 76, 1-15.
- Wu, J. Q., Hansen, D. V., Guo, Y., Wang, M. Z., Tang, W., Freel, C. D., Tung, J.J., Jackson, P.K., and Kornbluth, S. (2007). Control of Emi2 activity and stability through Mos-mediated recruitment of PP2A. *PNAS* 104, 16564-16569.
- Wurzenberger, C., and Gerlich, D. W. (2011). Phosphatases: providing safe passage through mitotic exit. *Nat Rev Mol Cell Biol* 12, 469-482.
- Yamamoto, T. M., Blake-Hodek, K., Williams, B. C., Lewellyn, A. L., Goldberg, M. L., and Maller, J. L. (2011). Regulation of Greatwall kinase during *Xenopus* oocyte maturation. *Mol Biol Cell* 22, 2157-2164.
- Yang, Q., and Ferrell Jr, J. E. (2013). The Cdk1-APC/C cell cycle oscillator circuit functions as a time-delayed, ultrasensitive switch. *Nat Cell Biol* 15, 519-525.

- Yeong, F. M., Lim, H. H., Padmashree, C. G., & Surana, U. (2000). Exit from mitosis in budding yeast: biphasic inactivation of the Cdc28-Clb2 mitotic kinase and the role of Cdc20. *Molecular cell*, 5(3), 501-511.
- Yin, J., Ni, B., Tian, Z. Q., Yang, F., Liao, W. G., and Gao, Y. Q. (2016). Regulatory effects of autophagy on spermatogenesis. *Biology of reproduction* 96, 525-530.
- Yudkovsky, Y., Shteinberg, M., Listovsky, T., Brandeis, M., and Hershko, A. (2000). Phosphorylation of Cdc20/fizzy negatively regulates the mammalian cyclosome/APC in the mitotic checkpoint. *Biochem Biophys Res Commun* 271, 299-304.
- Zachariae, W., Schwab, M., Nasmyth, K., and Seufert, W. (1998). Control of cyclin ubiquitination by CDK-regulated binding of Hct1 to the anaphase promoting complex. *Science* 282, 1721-1724.
- Zachariae, W., and Nasmyth, K. (1999). Whose end is destruction: cell division and the anaphase-promoting complex. *Genes Dev* 13, 2039-2058.
- Zhang, T., Schmierer, B., and Novák, B. (2011). Cell cycle commitment in budding yeast emerges from the cooperation of multiple bistable switches. *Open biology* 1, 110009.
- Zhang, S., Chang, L., Alfieri, C., Zhang, Z., Yang, J., Maslen, S., Skehel, M., and Barford, D. (2016). Molecular mechanism of APC/C activation by mitotic phosphorylation. *Nature* 533, 260.

Acknowledgments

I would like to thank my Ph.D. supervisor, Dr. Wolfgang Zachariae, for giving me the opportunity to work in his lab. I thank for his guidance during my work and support in presenting my results at the scientific meetings. I am grateful for the outstanding scientific training I have received and for the advices in writing my thesis.

I thank all the present and former members of Zachariae Lab for sharing with me their knowledge. I am especially thankful to Dr. Ievgeenia Zagoriy, Dr. Orlando Argüello-Miranda, Dr. Valentina Mengoli, Dr. Julie Rojas and Tugce Oz Yoldas for their intellectual and practical support. I thank our lab technicians, Isabella Mathes and Albena Bergsoy, for their excellent technical assistance.

I thank the members of my thesis advisory committee, Prof. Dr. Christiane Fuchs and Dr. Christian Biertümpfel, for their scientific expertise and support. I thank Prof. Dr. Nicolas Gompel, Prof. Dr. Christof Osman, Prof. Dr. Angelika Böttger, Prof. Dr. Peter Becker, Prof. Dr. Wolfgang Frank and Prof. Dr. John Parsch for reviewing this thesis.

I am grateful to the IMPRS research school for giving me the opportunity to be a part of the excellent graduate program.

I am thankful to my family and friends for their faith in me and their patience. I am especially grateful to my partner, Karol, for his unlimited support, for stimulating discussions and for encouraging me to pursue my dreams.

Curriculum Vitae

Katarzyna Jonak

University Education

- 07/2014–present **Ph.D. candidate**, Max Planck Institute of Biochemistry, Germany
- 09/2012–10/2013 **MSc in Molecular Medicine**, Cranfield University, UK (Erasmus Double Diploma)
- 02/2012–07/2013 **MSc in Biotechnology, major in Bioinformatics**, Silesian University of Technology (SUT), Gliwice, Poland
- 10/2008–01/2012 **BSc in Biotechnology, major in Bioinformatics**, SUT, Gliwice, Poland

Peer-Reviewed Publications and Reviews (selected)

- Jonak, K.**, Zagoriy, I., Oz, T., Graf, P., Rojas, J., Mengoli, V., and Zachariae, W. (2017). APC/C-Cdc20 mediates deprotection of centromeric cohesin at meiosis II in yeast. *Cell Cycle* 16, 1145-1152.
- Argüello-Miranda, O.*, Zagoriy, I.*, Mengoli, V., Rojas, J., **Jonak, K.**, Oz, T., Graf, P., and Zachariae, W. (2017). Casein kinase 1 coordinates cohesin cleavage, gametogenesis, and exit from M Phase in Meiosis II. *Dev Cell* 40, 37-52.
- Jonak, K.***, Kurpas, M.*, Szoltysek, K., Janus, P., Abramowicz, A., and Puszyński, K. (2016). A novel mathematical model of ATM/p53/NF-κB pathways points to the importance of the DDR switch-off mechanisms. *BMC Syst Biol* 10, 75.
- Tuszyńska, I., Magnus, M., **Jonak, K.**, Dawson, W., and Bujnicki, J. M. (2015). NPdock: a web server for protein-nucleic acid docking. *Nucleic acids research* 43, W425-W430.
- Mchedlishvili, N.*, **Jonak, K.***, and Saurin, A. T. (2015). Meeting report-Getting Into and Out of Mitosis. *J Cell Sci* 128, 4035-4038.
- Jonak, K.**, Kurpas, M., and Puszyński, K. (2014). Prediction of the behavior of mammalian cells after exposure to ionizing radiation based on the new mathematical model of ATM-Mdm2-p53 regulatory pathway. *Information Technologies in Biomedicine* 3, 349-362. Springer, Cham.
- Jonak, K.**, Jędrasiak, K., Polański, A., and Puszyński, K. (2012). Application of image processing algorithms in proteomics: automatic analysis of 2-d gel electrophoresis images from western blot assay. *International Conference on Computer Vision and Graphics*, 433-440. Springer, Berlin, Heidelberg.

* Equal contribution

Scientific Awards and Scholarships (selected)

- 07/2014–present PhD candidate at The International Max Planck Research School for Molecular and Cellular Life Sciences, Munich-Martinsried, Germany (3.5% acceptance rate)
- 07/2013 Graduation with Distinction, SUT, Poland
- 06/2013 Advanced Biosciences Program Director's Award, Cranfield University, UK
- 05–08/2013 Summer Studentship, Cancer Research UK Cambridge Institute, University of Cambridge, UK
- 10/2012–09/2013 ERASMUS Scholarship Master Joint Study Program with Double Diploma

Scientific Meetings and Conferences (since 2015)

- 23-27/07/2018 11th European Conference on Mathematical and Theoretical Biology, Lisbon, Portugal (poster presentation)
- 03–05/06/2018 EMBL Symposium Biological Oscillators: Design, Mechanism, Function, Heidelberg, Germany (oral presentation)
- 04–07/09/2015 EMBO Workshop Cell Cycle, Budapest, Hungary (poster presentation)
- 10–13/05/2015 Getting Into and Out of Mitosis, The Company Of Biologists Workshop, Steyning, West Sussex, United Kingdom (poster and oral presentation)